Are *CYCLOIDEA*-like genes involved in the control of floral zygomorphy in *Schizanthus wisotonensis*?

Karine Coenen

Doctor of Philosophy

Institute of Cell and Molecular Biology
University of Edinburgh
September 2004

Contents

Declaration

I hereby declare that the work presented here is my own and has not been submitted in any form for any degree to any other university.

Karine Coenen

Acknowledgements

One more page to write.....and THAT'S IT!!!!!!!!!!!!!!!
I would like to thank all the people who have helped me with an advice, a smile, a handkerchief, a roof, a boat, a pint or just some time.....but precious time.
For their constant support, I am particularly grateful to my parents and brothers (arrière-guarde fidèle au poste) and to my supervisor whose inspiration, enthusiasm, patience and dedication to her difficult mission kept the sun shining above my bench!!!!
To my many co-supervisors, Andrew and Justin, Rico and Michael, I will miss your good advice, comments and feedback on work, and more importantly, on life in general!
I am also very grateful to my friends and colleagues who helped me to really enjoy life and work, Magali and family, Ale, Hélène de France, Xav, Sandrine and Killian, Vero and Renald, and the 4th floor of the Swann building; Hélène, Bruce, Miriam, Cheng Xia, Kathryn, Daniel, Tony, Kim and everyone else in the Ingram, Doerner, Hudson and Goodrich's labs; in Edinburgh (The Fergussons, Lee, Laszlo and Niamh) and on the Forth (Dickie, Maggie, Alister, Bill, Martin, Chris and the rest of the fleet!!!!).
Special thanks to the Gatsby network for their financial, training and moral support, and for magnificent wonders in old colleges....
Thanks to the Sci-Fun team for their most appreciated patience!

Finally, thanks to Quentin for helping me to set up the project, but most of all, I shall be indebted for ever to the University of Edinburgh and its staff, for 8 years of support, enjoyable studies, good fun, and of course, the financing of my project!

Evolution goes in all directions, Smith, P. (2000)

And experimentation is not over!!!!!

Abbreviations

A	Adenine
A 280	Absorbance measured at a wavelength of 280nm
AM	Axillary meristem
BCIP	5-bromo-4-chloro-3-indolyl phosphate
bp	Base pair(s)
BS	Branch support
BSA	Bovine serum albumine
C	Cytosine
°C	Degree Celsius
cDNA	Complementary DNA
cpDNA	Chloroplast DNA
CTAB	Hexadecyltrimethylammonium bromide
dH_2O	Deionised water
DEPC	Diethyl pyrocarbonate
DMF	Dimethylformamide
DMSO	Dimethylsulfoxide
DNA	Desoxyribonucleic acid
DNase	Desoxyribonuclease
dATP	Deoxyadenosine triphosphate
dCTP	Deoxycytosine triphosphate
dGTP	Deoxyguanosine triphosphate
dNTP	Deoxynucleotide triphosphate
dTTP	Deoxythymidine triphosphate
DTT	Dithiothreitol
EDTA	Ethylenediaminetetraacetic acid
EtOH	Ethanol
Fig	Figure
FM	Flower meristem
g	Gram
G	Guanine
HCL	Hydrochloric acid
hrs	Hours
ICMB	Institute of Cell Molecular Biology (Edinburgh, UK)
IM	Inflorescence meristem
kb	Kilobase(s)
L	Liter
m	Meter
mm, mg, ml	Millimetre, milligram, millilitre
M	Molar
min	Minute
mRNA	Messenger RNA
mol	Mole
mv	Millivolt
n	Nano
NaCl	Sodium Chloride

NaOAc	Sodium acetate
NaOH	Sodium chloride
NBT	p-Nitrotetrazolium blue
*ndh*F	Gene encoding a sub-unit of the chloroplast NADH dehydrogenase
NTP	Nucelotide triphosphate
NTR	Non Translated Region
ORF	Open Reading Frame
PCR	Polymerase Chain Reaction
pDP	Primordial of dorsal petal
pDS	Primordial of dorsal stamen
pfu	Plaque forming unit
pLP	Primordia of lateral petal
pLS	Primordial of lateral stamen
pVP	Primordia of ventral petal
pVS	Primordia of ventral stamen
p	Pico
pDS	Primordial of dorsal stamen
PFA	Paraformaldehyde
rDNA	Ribosomal DNA
*rbc*L	Gene encoding the large sub-unit of RUBISCO
RNA	Ribonucleic acid
RNase	Ribonuclease
rpm	Revolution(s) per minute
SAM	Shoot Apical Meristem
SDS	Sodium dodecyl sulfate
SEM	Scanning Electron Micrograph
SVS	Sympodial Vegetative Shoot
SVM	Sympodial Vegetative Meristem
Tris	2-amino-2(hydroxymethyl)-1,3-propanediol
tRNA	Tranfer RNA
U	Uracil
UoE	University of Edinburgh (UK)
v/v	Volume:volume ratio
w/v	Weight:volume ratio
X	Times
X-gal	5-bromo-4-chloro-3-indodyl-_-galacto-pyranosideμ
_	Micro

List of Figures

I. Introduction

III. Morphological characterisation of *S. wisotonensis*

IV. Isolation of *CYC*-like genes in *S. wisotonensis, N. tobaccum* and *Petunia hybrida*

V The molecular genetics of *CYC*-like genes in *Schizanthus wisotonensis*

VI Discussion

List of Tables

III. Morphological characterisation of *S. wisotonensis*

IV. Isolation of *CYC*-like genes in *S. wisotonensis* and study of homology/paralogy relationships and for the newly isolated genes

V The molecular genetics of *CYC*-like genes in *Schizanthus wisotonensis*

List of appendices

III. Morphological characterisation of *S. wisotonensis*

IV. Isolation of *CYC*-like genes in *S. wisotonensis*, *N.tobaccum* and *Petunia hybrida*

I. Introduction

The Solanaceae is a plant family comprising about 2950 species grouped in 94 genera (Maberley, 1997). They have a very wide geographical distribution through tropical and temperate regions, from South America to South East Asia (Knapp, 2002). Half of the species and more than three quarters of the genera are found in South America, suggesting that the family originates from the part of Gondwanaland which became this region (Hawkes, 1999).

Many solanaceous species are used by humans, both for agricultural and medical purposes. For example, potato (*Solanum tuberosum*) and tomato (*Solanum lycopersicum*) are world-wide major crops. Solanaceous species producing alkaloids have been used in both modern and traditional medicine (e.g. *Atropa, Brugmansia, Brunfelsia, Datura, Nicotiana etc*) and as stimulants (e.g. *Nicotiana tabaccum*). The family is also famous for its ornamental species (*Salpiglossis, Petunia, Schizanthus, Datura etc*) (Hawkes, 1999).

In this section, after a brief taxonomic introduction, I will describe the morphological characteristics of inflorescences and flowers in the Solanaceae. I will then introduce the concept of floral symmetry and its evolution. Finally, I will give an overview of floral symmetry in the Solanaceae, and explain the relevance of this family as a new model system to further our understanding of the genetic control of zygomorphy and its evolution.

I.1 The Solanaceae: flowers and symmetry

I.1.1 Classification of the Solanaceae

The Solanaceae (Solanales) are eudicots belonging to the "euasterids I", a sub-group of the Asterids (Soltis, Soltis and Chase, 1999; Olmstead *et al.*, 2000) (Fig I.1).

The Solanaceae used to be classified in two major subfamilies, the Solanoidae and the Cestroidae, and a few satellite genera (Knapp, 2002). A new classification has been recently proposed by Olmstead *et al.* (1992) using data from cpDNA restriction site analysis and DNA sequencing. Consequently, the Solanaceae are now provisionally divided into 7 monophyletic sub-families: the Schwenckioideae, the Schizanthoideae, the Goetzoideae, the Cestroideae, the Petunioideae, the Nicotianoideae and the Solandoideae (Fig I.2).

In this revised classification, the genus *Schizanthus* appears close to the base of the phylogenetic tree (Olmstead *et al.*, 1992).

I.1.2 General diagnostic features of solanaceous inflorescences and flowers

I.1.2.1 Introduction

In plants, post-embryonic growth and differentiation is ensured by the activity of highly regulated groups of stem cells called meristems. In most angiosperms, the above-ground plant architecture is dictated by the relative activity of the shoot apical meristem (SAM) producing the main shoot axis and that of other secondary meristems, usually born on the axil of leaves and referred to as axillary meristems (AM) (Fig I.3a). In many species, AM growth arrests before any outgrowth is produced. The length of their dormancy is determined by environmental and physiological factors, and in most species, auxin acts as a growth inhibitor for the

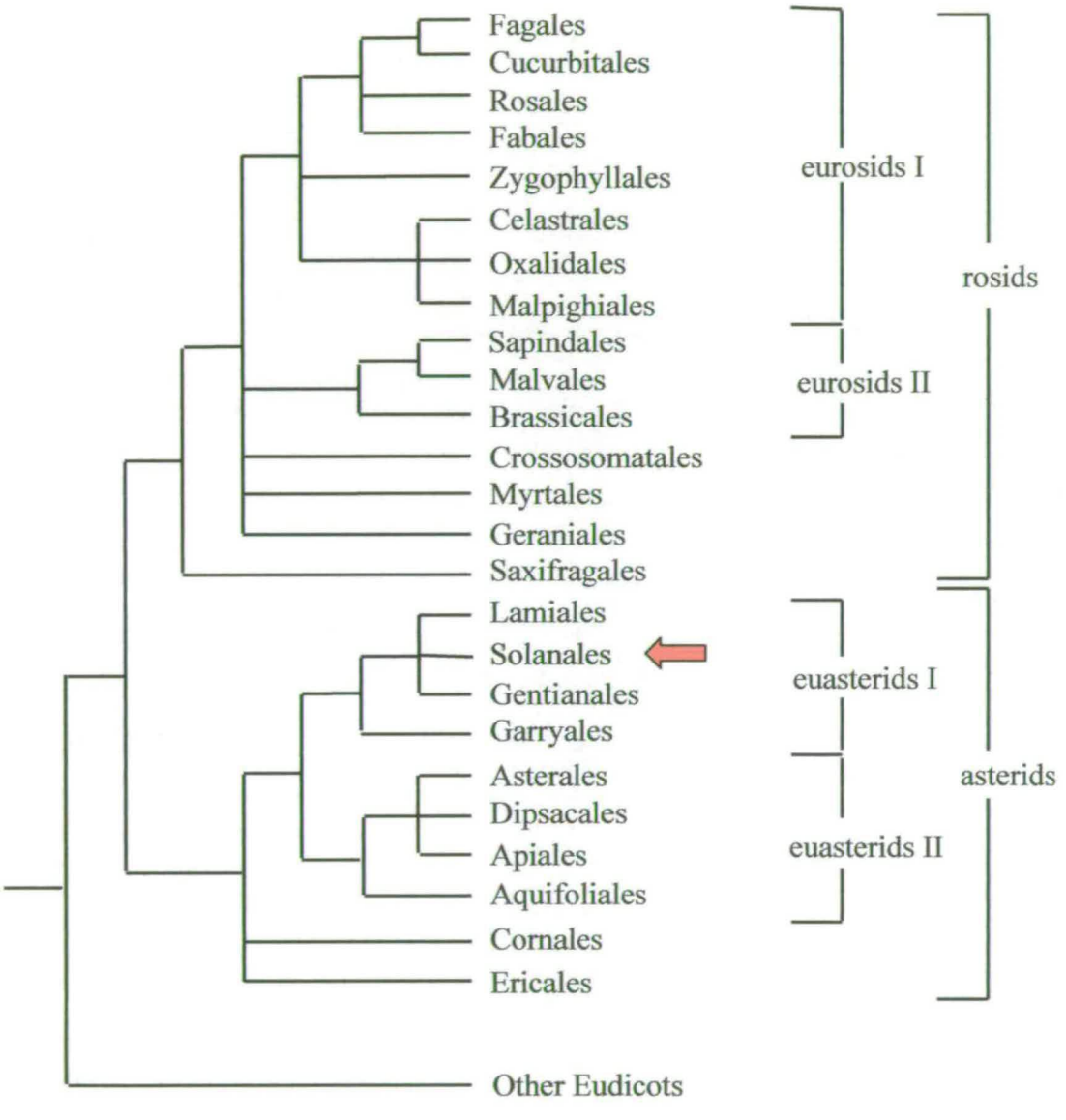

Fig I.1: Partial summary of the phylogenetic relationships in eudicots (after Soltis, Soltis and Chase, 1999)

This tree was inferred from a heuristic parsimony analysis using DNA *rbc*L, *atp*B and 18S rDNA sequences. The red arrow indicates the position of the Solanales, the order comprising the Solanaceae. Branch length is not representative of phylogenetic distance.

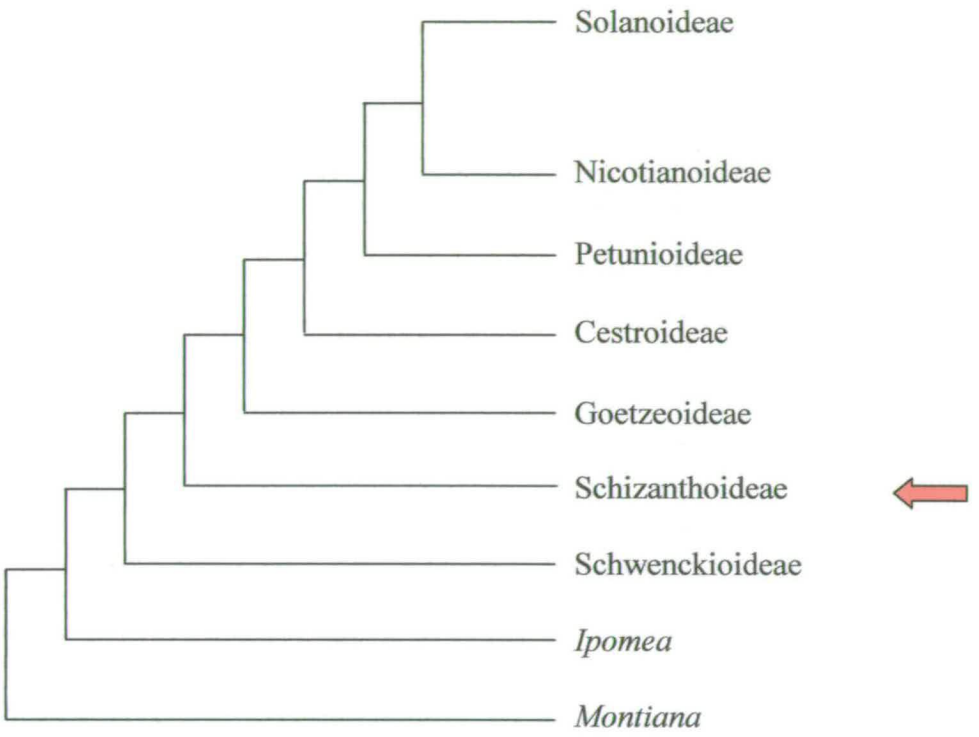

Fig I.2: Summary of the provisional intrafamilial classification of the Solanaceae (After Olmstead *et al.*, 1992)

This phylogenetic tree was obtained using a combination of data from restriction site analysis on the entire chloroplast genome and DNA sequencing of two chloroplasts genes, *rbc*L and *ndh*F. It represents a summary of the strict consensus tree obtained from the 12 equally most parsimonious trees produced by a heuristic analysis. The tree is rooted on *Ipomea* and *Montiana*. The red arrow indicates sub-group comprising *Schizanthus*, branch length is not representative of phylogenetic distance.

development of axillary meristems (Mauseth, 1998). This plant hormone is mainly produced in the SAM, and consequently, the removal of the plant apex during vegetative growth often breaks the dormancy of vegetative AMs (Fig I.3b). Plant growth is subsequently maintained by the resumed activity of these AMs which become SAMs, and produce leaves with AMs (Fig I.3b). During vegetative growth, leaves are usually produced in a repetitive pattern. The region on the main stem where the leaf and its associated vegetative meristem are inserted is referred to as a node, and the internode is the stem axis separating two nodes.

After floral induction, the production of the inflorescence (stem axis bearing flowers) is due to the re-specification of the SAM (and/or the AM) as an inflorescence meristem (IM). The latter either produces a succession of sub-sets of cells destined to form leaf-like organs and flowers meristems (FM) on its flank, or is entirely converted into a unique terminal flower. In many species, leaf-like organs called bracts subtend the IM and the FM.

Recent studies have shown that in a variety of species, related genes have a conserved role in specifying floral meristem identity. This was first demonstrated in *Antirrhinum majus* with a mutant producing indeterminate secondary shoots instead of flowers (Coen *et al.*, 1990). This phenotype was found to be caused by the loss of function of a gene subsequently called *FLORICAULA* (Coen *et al.*, 1990). A similar role was established for its ortholog (*LEAFY*) in *Arabidopsis thaliana* (Weigel *et al.*, 1992). In the past decade, *LEAFY*-like genes with conserved roles in the control of floral identity have been isolated in a range of species including pea (Hofer *et al,* 1997), *Petunia* (Souer *et al.,* 1998) and tomato (Molinero-Rosales *et al.,* 1999, Allen and Sussex, 1996). *FLORICAULA, LEAFY* and *LEAFY*-like genes are now

Fig I.3: Above ground plant architecture during vegetative growth
Fig a&b illustrate the two main types of vegetative growth. (a) In early plant growth, the main vegetative stem axis is produced by the Shoot Apical Meristem (SAM) (in blue). During this phase, axillary meristems (AM) (in red) are borne on the axil of leaves. The SAM negatively regulates growth of AMs, the extent of dormancy being under the control of environmental and physiological factors. (b) In *Arabidopsis thaliana* and many other species, a few AMs resume growth and produce lateral branches when the SAM is removed.
Green arrows indicate the direction of growth.

Fig I.4: Above ground plant architecture during reproductive growth
(a) In the racemose growth habit, upon floral induction, the vegetative SAM of the monopodial vegetative axis (dark green) is converted into an inflorescence SAM (light green), here producing a monopodial indeterminate inflorescence (i.e. growth stops only with senescence). (b) The cymose architecture lacks a main axis, and in this example, growth is determinate, i.e. reproductive growth stops after the production of a fixed number of flowers.

considered to be the earliest known control points in the specification of floral meristems.

The inflorescence can exhibit a great variety of architectures, with flowers often produced in a repetitive pattern. The reiterative production of nodes or flowers may be indefinite (i.e. only stopped by plant death) or pre-programmed to produce definite numbers. These types of growth are referred to as indeterminate and determinate respectively (Fig I.4 a&b). Inflorescences may be classified in different categories depending on their architecture and their mode of growth (i.e. indeterminate or determinate) (Coen and Nugent, 1994).

Racemose inflorescences are monopodial (i.e. one main axis) and cymose inflorescences have a more complex branching pattern lacking a main axis (Fig I.4 a&b) (Coen and Nugent, 1994). The difference between both branching patterns probably depends on the relative activity of the SAM versus the AM.

I.1.2.2 Solanaceous inflorescences

In the Solanaceae, the branching pattern of the reproductive shoot axis has been traditionally described as sympodial, with cymose inflorescences (Child, 1979). In sympodial growth, the growth of the inflorescence is determinate. All subsequent reproductive growth is produced by the development of meristems born in the axils of prophylls (Fig I.5). However, Scanning Electron Microscopy (SEM) has shed a new light on the architecture of at least two solanaceous model species, *Petunia* and tomato (Souer *et al.*, 1998; Molinero-Rosales *et al*, 1999).

In *Petunia,* it was previously thought that the inflorescence stem axis was composed of repeated sets of two nodes called anthoclades (one elongated and one

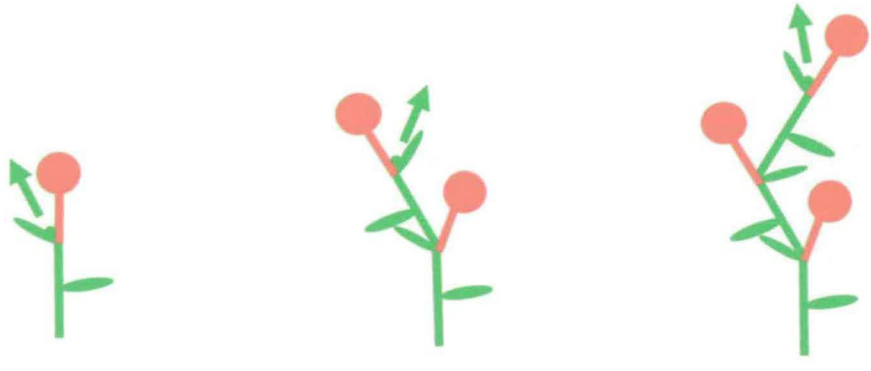

Fig I.5: An example of sympodial growth habit during the reproductive phase
The inflorescence growth (pale green) is not continuous and stops with the production of a terminal flower (red circle). Subsequent inflorescence growth is only taking place through the development of a sympodial (i.e. axilliary) meristem, here in the axil of the floral bract.

compressed) (Napoli and Ruehle, 1996) (Fig I.6a). For each anthoclade, the growth of the inflorescence apical meristem was seen as terminated with its conversion to a flower (compressed node). Subsequent anthoclades would be produced through the activity of the sympodial meristem born on the prophyll axil of the compressed node (Napoli and Ruehle, 1996) (Fig I.6b). The vigour of the sympodial growth was believed to account for the side-ways displacement of the terminal flower (Napoli and Ruehle, 1996) (Fig I.6c). For each anthoclade, a sympodial vegetative meristem (SVM) was described, born in the axil of the leaf belonging to the elongated node (Fig I.6 a, b&c), with a delayed development and the ability to convert to an inflorescence after the production of a few leafs (Napoli and Ruehle, 1996).

However, this traditional classification of *Petunia* as a species with sympodial inflorescences has been challenged by a recent study of the genetic control of branching in *Petunia hybrida* (Souer *et al.*, 1998). This work has shown that in this species, the concept of sympodial branching does not strictly apply because the inflorescence meristem does not terminate with the production of the flower. Instead, Souer *et al.* (1998) discovered that a bifurcation takes place between the on-growing IM and the newly produced flower meristem, resulting in the side-ways displacement of both structures (Souer *et al.*, 1998) (Fig I.6 e&f). The inflorescence meristem undergoes a succession of divisions at right angle to each other and as a result, the inflorescence resembles a "zig zag". In the interpretation of Souer *et al.* (1998), for each node, two bracts are produced simultaneously by the IM, subtending respectively the on-growing IM and the FM. Later in development, new SVMs develop in the axil of both bracts. The growth of SVM is delayed and acropetal (i.e.

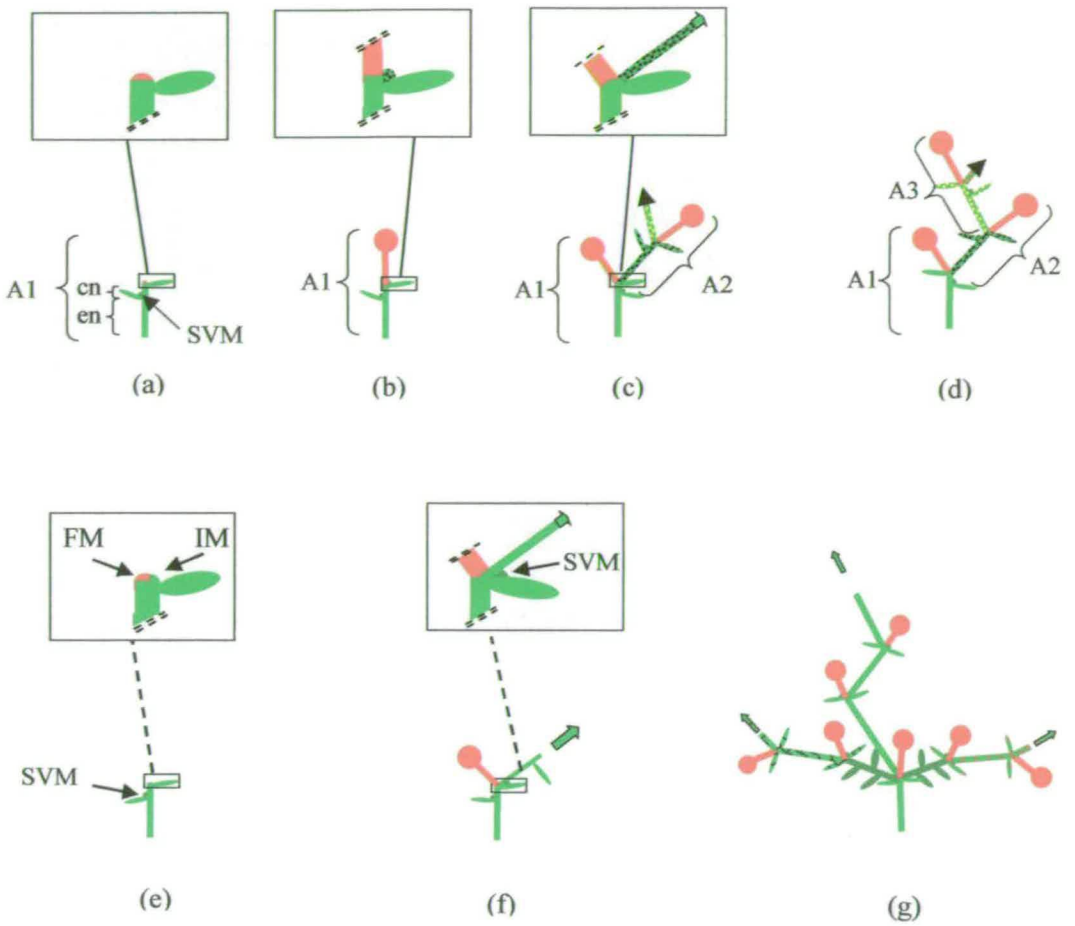

Fig I.6: A simplified diagram of inflorescence architecture in *Petunia* as described by Napoli and Ruehle (1996)

(a-d) In the interpretation on Napoli and Ruehle (1996), the inflorescence (pale green) is composed of one elongated node (en) and one compressed node (cn). The inflorescence meristem terminates by the production of a flower (red circle) and new inflorescence axes (different shades of green) are produced by the activity of sympodial (i.e. axillary) meristems on the axil of the compressed node prophyll. (e-g) Souer *et al* . (1998) have shown that in fact, the inflorescence (IM) does not terminate by the production of a flower and instead, a bifurcation between the IM and the floral meristem (FM) follows initiation of the reproductive phase. As a result of this bifurcation, the FM (the larger half) is situated as a terminal structure and the smaller indeterminate IM is displaced side-ways. (g) Later in development, the growth of sympodial vegetative meristems (SVM) will generate new vegetative axes (dark green) which will produce a few leaves before becoming inflorescences.

the most distal ones relative to the apex develop first). They produce a few vegetative leaves before being converted to IM (Fig I.6g).

Like most members of the Solanaceae, tomato has been traditionally classified as having sympodial growth habit and determinate inflorescences. However, recent studies have similarly demonstrated that in fact, growth of the inflorescence is indeterminate, with a bifurcation between the IM and the FM also taking place (Allen and Sussex, 1996; Molinero-Rosales *et al.,* 1999).

Following floral induction, the differences in body architecture between *Petunia* and tomato are in fact due to the activity of their respective vegetative sympodial meristems. In *Petunia*, sympodial meristems are initially dormant and the production of secondary inflorescences is delayed until the primary axis has produced a few floral nodes. In tomato, growth of the sympodial vegetative meristem is not delayed and is extremely vigorous (Molinero-Rosales *et al.,* 1999; Allen and Sussex, 1996). Consequently, the whole inflorescence is displaced side-ways by the new vegetative axis behaving as a monopodial terminal structure (Fig I.7). After the production of a few leaves, it is converted to an inflorescence and the same pattern is then reiterated.

Therefore, in both *Petunia* and *tomato*, after floral induction, the zig-zag architecture of the inflorescence axis is due to the bifurcation of the inflorescence and the floral meristems. These findings suggest that the branching pattern of the inflorescence in other solanaceous species may have been similarly misinterpreted and further studies are needed to elucidate this question.

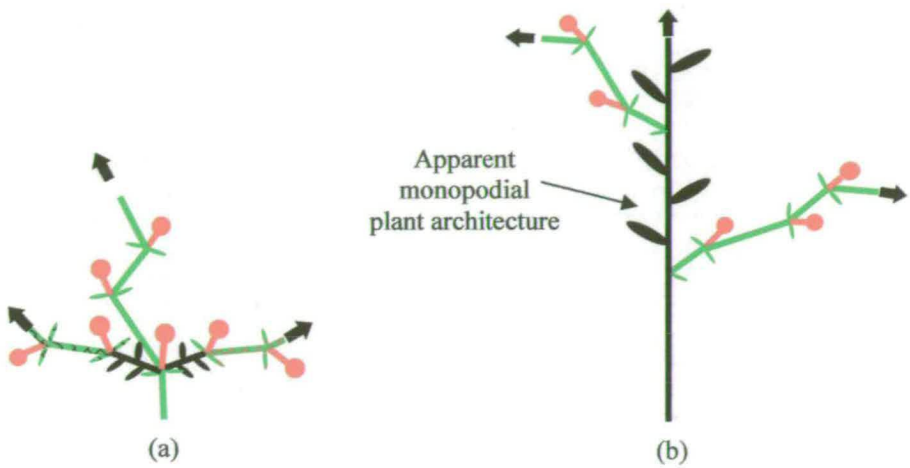

Fig I.7: Comparison between the architecture of *Petunia* and tomato inflorescences
(a) In *Petunia*, the growth of the sympodial vegetative shoot (SVS) in black is not as vigorous as in tomato. As a result, *Petunia* plants retain the sympodial branching pattern. (b) In tomato, the SVS displaces the inflorescence (in pale green) sideways resulting in an apparent plant architecture.

I.1.2.2 Solanaceous flowers

(i) The ABC model in Arabidopsis thaliana and its relevance in the Solanaceae

The identity of floral organs arrayed in a radial symmetrical pattern is thought to be under tight genetic control and determined early in flower development. Organ whorls in *Arabidopsis* are numbered 1-4, from the outer-most to the inner-most domain of the flower, corresponding respectively to sepals, petals, stamens and gynoecium. Over the past fifteen years, studies on genes controlling flower development in *A. majus* (Schwarz-Sommer *et al.*, 1990, Carpenter and Coen, 1990) and *A. thaliana* (Yanofsky *et al.*, 1990) have unravelled the existence and the role of floral homeotic genes in the control of organ identity. The resulting ABC model presents three classes of genes expressed in overlapping rings-like domains and spanning the four whorls of the developing flower (Fig I.8) (Coen and Meyerowitz, 1991). Most of the genes involved ABC model belong to the MADS box family of transcription factors (Becker and Thei_en, 2003). The study of loss and gain-of-function mutants have shown that ABC genes have overlapping domains of expression in whorl 2 and 3, an expression pattern necessary to produce all four organ types (Coen and Meyerowitz, 1991). The co-expression of A and B-genes in whorl 2 is necessary for the production of petals, whereas in whorl 3, both B and C-genes must be co-expressed to form the androecium. However, amongst A, B and C-genes, only class A-genes are required in whorl 1 to produce sepals and C-genes in whorl 4 for carpels (Fig I.8) (Coen and Meyerowitz, 1991).

A lack of expression of any of these genes results in the shifts of organ identity, as predicted by the ABC model (Coen and Meyerowitz, 1991). For example, if the function of B-genes is lost as in the *deficiens* mutant in *A. majus*, the four

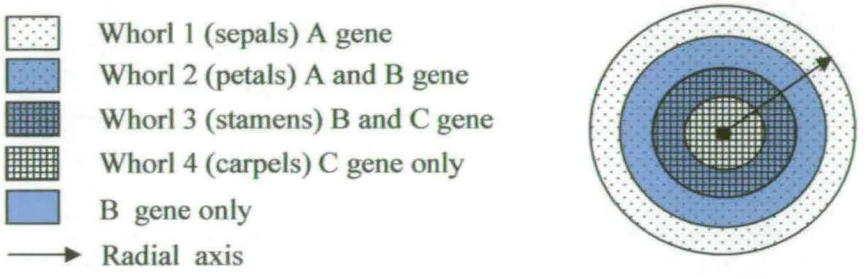

Fig I.8 Concentric radial organisation of floral whorls in a wild-type flower
This model shows the radial arrangement of floral organs in *A. thaliana* in 4 whorls representing sepals, petals, stamens and carpel (1 to 4 respectively). The formation of floral organs requires the following gene activity: class A gene for sepals, A and B genes for petals, B and C genes for stamens and finally, C gene for carpel identity.

whorls (1-4) of the flower will be sepals, sepals, carpels and carpels respectively (Sommer *et al.,* 1990). However, ectopic expression of both B and C genes in vegetative tissue is not sufficient to convert all leaves into petals (Krizek and Meyerowitz., 1996), suggesting that (i) either another factor is required to do so which is not produced out with flowers (ii) or the function of floral homeotic genes is negatively repressed out with flowers. This point was later elucidated, when three newly isolated MADS-box genes in *A. thaliana* (*SEPALLATA 1, 2* and *3*) were found to be required for B and C-gene function (Pelaz *et al.,* 2000). Furthermore, it was later shown that in *A. thaliana,* triple mutant expressing constitutively class B proteins (*PISTILLATA* and *APETALA3*) and *SEPALLATA3* have petaloid organs instead of vegetative leaves (Honma and Goto, 2001).

The sequencing of the genome of *A. thaliana* has allowed the identification of 200 members of the MADS box gene family (Theissen *et al.,* 2000). Therefore, it is very likely that gene redundancy will make the characterisation of other members of this gene family a difficult task.

MADS box genes similar to the ABC class have been isolated in many other species, including in the Solanaceae (Becker and Theissen, 2003). For example, studies in *Petunia,* and *N. tabaccum* and tomato (Mandel *et al.*, 1992, Davies *et al.,* 1996, Vandenbussche *et al.,* 2003, 2004, Gomez *et al.,* 1999, Pnueli *et al.*, 1991) have demonstrated that there is a degree of functional conservation between putative orthologs of this gene family in *Arabidopsis, Antirrhinum* and solanaceous species. This suggests that the organisation of floral organs in radially concentric whorls is at least partially ruled by an ABC-like model in this family too.

(ii) Characteristics of solanaceous flowers

In solanaceous flowers, floral organ number is fixed for each species and four separate whorls can be distinguished. Sepals (whorl 1) and petals (whorl 2) are at least partially fused. Stamens (whorl 3) are partially adnated to the corolla and the order and pattern of anther dehiscence varies amongst species (Robyns, 1931). In addition, many species have shorter or aborted stamens called staminodes. The gynoecium is composed of a bicarpellate superior ovary (whorl 4). However, unlike other asterids, the bicarpellar ovary is always oriented obliquely with respect to the median axis of the inflorescence (i.e. axis of elongation, running through the middle of the IM and the inflorescence bract) except for *Nicandra* (Robyns, 1931) (Fig I.9).

Members of the Solanaceae exhibit a wide range of floral morphology and different types of floral symmetry. This feature is discussed in detail in the next section.

I.1.3 Floral symmetry in the Solanaceae

I.1.3.1 Setting the scene: floral symmetry in the angiosperms

(i) Definition

Floral symmetry usually refers to the type of symmetry displayed in the two-dimensional face-on view of the corolla. Flowers are usually grouped in 4 different types depending on their number of axis/planes of symmetry. The terminology may vary between publications but the following nomenclature is now widely accepted (Giurfa, Dafni and Neal, 1999; Endress, 1999; Luo *et al., 1999*; Clark and Coen, 2002).

(a) Actinomorphic
(e.g. *Nicandra)*

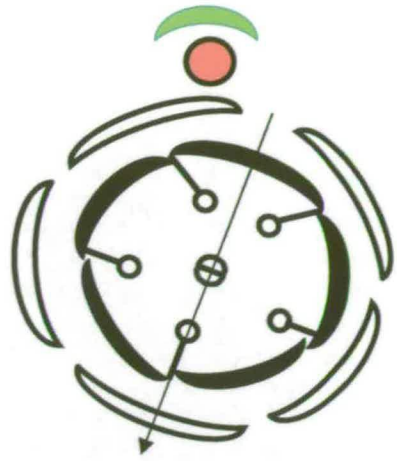

(b) Actinomorphic
(e.g. tomato)

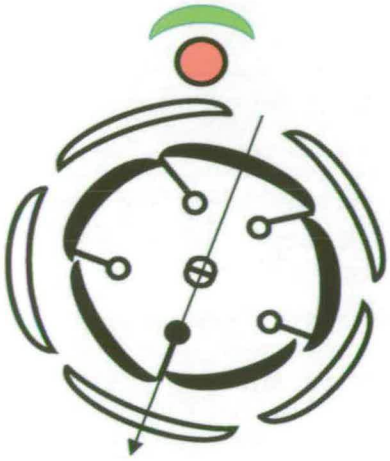

(c) Zygomorphic
(e.g. *N. tobaccum)*

(d) Zygomorphic
(e.g. *S. wisotonensis)*

Fig I.9: Floral diagrams of different types of solanaceous flowers and their classification
(a) Actinomorphic flower, with the gynoecium aligned with the inflorescence axis (*Nicandra* only). (b) actinomorphic flower, albeit oblique orientation of the gynoecium relative to the inflorescence. (c&d) zygomorphic flowers showing both oblique orientation of the gynoecium and various degrees of dorso-ventral asymmetry. (c) moderate zygomorphy in the form of heterandry, with a reduced abaxial stamen in the otherwise actinomorphic *Nicotiana tobaccum*. (d) marked zygomorphy with a bilateral corolla and tridinamum androecium in *Schizanthus wisotonensis*. In the androecium, open circles indicate fertile stamens whereas black circle indicate staminodes. The position of the inflorescence and its bract is indicated by a red circle and a green croissant respectively. The floral axis is shown by the black arrow.

As the name suggests, asymmetrical flowers have no axes of symmetry. Asymmetry may take the form of a spiral organisation of floral organs (e.g. Magnoliaceae) (Fig I.10) or that of a reduced number of organs arranged asymmetrically (e.g. Marantaceae and Cannaceae) (Tucker, 1999).

On the other hand, polysymmetrical flowers have 3 or more axis of symmetry (Fig I.10). They represent the largest category in the angiosperms, many monocotyledonous species bearing 3 axis of symmetry (e.g. Liliaceae). These flowers can also be referred to as regular, actinomorphic or radially symmetrical.

The third category comprises disymmetrical (or bisymmetrical) flowers featuring only two axis of symmetry (e.g. *A. thaliana* (Brassicaceae)).

Finally, monosymmetrical flowers have a unique plane of symmetry along the axis passing by the gynoecium and either (or both) the bract and the inflorescence axis (Fig I.10). They are usually oriented vertically (e.g. orchid, snapdragon), their left and right hand-sides being mirror images of each other along the median plane of symmetry. However, organ shape varies along this axis and two asymmetrical domains may be defined. The upper (dorsal, adaxial) domain is that closer to the axis of the growing inflorescence, and the opposite half is referred to as lower, ventral or abaxial. Often, a third intermediate domain (lateral) is distinguished between the dorsal and the ventral domains.

In the literature, monosymmetry is also referred to as zygomorphy, bilabiate, bilateral or dorso-ventral asymmetry. Sometimes monosymmetrical flowers are called irregular which may lead to confusion as it is also used to describe asymmetry.

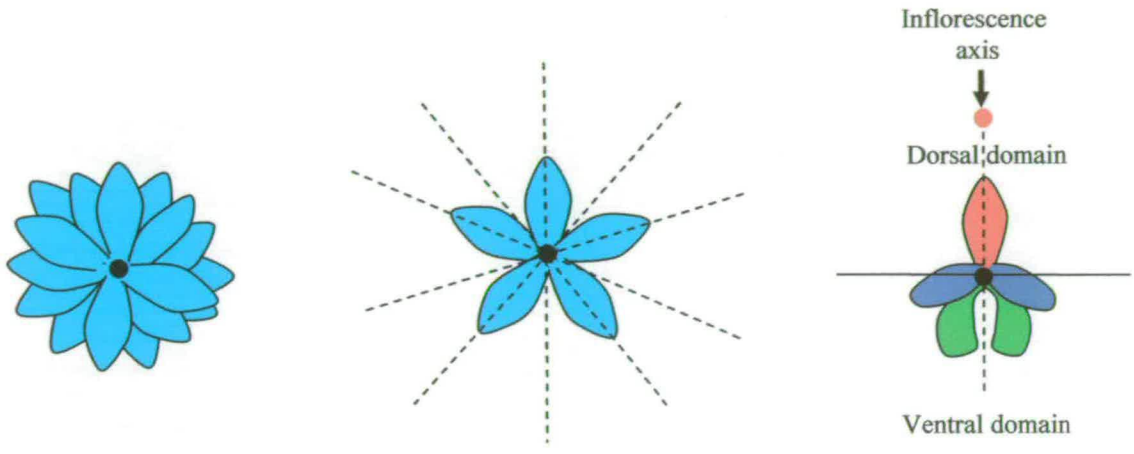

(a) Asymmetry (b) Polysymmetry (c) Monosymmetry

Fig I.10: Simplified diagram of corolla illustrating the three major types of floral symmetry
Differences in colour indicate if organs have morphologies variable within one whorl.
The dotted line indicates axes or planes if symmetry when applicable.

(ii) A broad perspective on the evolution of floral symmetry in the angiosperms

It is generally believed that primitive angiosperm flowers have a spiral phyllotaxy and indeterminate number of floral organs (e.g. *Magnolia*) (Endress, 2001). In more advanced species, spiral phyllotaxy is gradually replaced by the radial organization of floral organs in separate concentric whorls and actinomorphic flowers having a fixed number of organs per whorl. Co-evolution between flowers and types of pollinators, often referred to as pollination syndromes, has been proposed to be the driving force of the evolution of floral symmetry (Giurfa, Dafni and Neal, 1999; Cronk and Möller, 1997). Actinomorphic flowers are open and easy to access, and therefore believed to be visited by generalists (i.e. non-specialised) pollinators. Consequently, the pollen of one species may be wasted during visits to other unrelated species. Flowers with more complex access (i.e. closed and requiring specific physical characteristics and "memory") could be selecting for "skilled" pollinators, providing them with a reliable source of reward (pollen and/or nectar) and less competition. This, in turn, would result in reproductive isolation, a process leading potentially to co-evolution between flowers and their specialised pollinators (Giurfa, Dafni and Neal, 1999).

The polar-coordinate model has been proposed to represent the organisation in concentric whorls and the polarisation of the flower along a median (y) axis in monosymmetrical flower (Coen, 1991) (Fig I.11). From a development view point, the transition from a primitive spiral phyllotactic state reminiscent of vegetative phyllotaxy, to polarised and asymmetric flowers (*sensu* reduced number of organ arranged asymmetrically) can be seen as an increase in floral complexity. In other words, monosymmetry and asymmetry represent an additional developmental

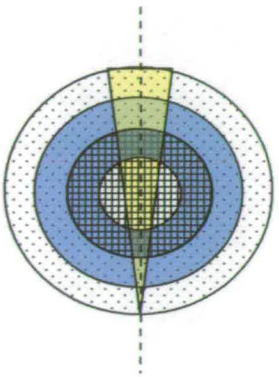

Fig I.11: The polar coordinate model
On the polar coordinate model, the polarisation (yellow triangle) along the dorso-ventral axis (dotted line) is superimposed on the whorled organisation of the flower.

complexity superimposed on the radial pattern, resulting in variation of organ shape and/or size within whorls. The fact that the underlying genetic control of dorso-ventral asymmetry is likely to be more complex than that of regular flower explains why in evolutionary terms, dorso-ventral asymmetry is traditionally considered as more advanced than actinomorphy (Endress, 1999; Tucker, 1999; Cubas, 2004; Rudall and Bateman, 2003).

Stebbins (1974) suggested that zygomorphy has been independently derived (i.e from an actinomorphic ancestor) no less than 25 times in the angiosperms. It is not yet known if some of the supposedly independent gains of dorso-ventral asymmetry are in fact only the independent recruitment of a conserved but "dormant" ancestral zygomorphy (Coen and Nugent, 1994). In developmental terms, this hypothesis translates as a dorso-ventral pre-pattern (i.e. trans-acting factor controlling gene expression) evolved in a common ancestor and recruited independently in related species (Coen and Nugent, 1994; Endress, 1999; Reeves and Olmstead, 2003, Cubas, 2004). Following this scenario, the evolution of floral symmetry could result from changes in cis-regulatory regions determining if, when and how the pre-pattern is interpreted (Doebley and Lukens, 1998). Such questions have recently been the focus of speculations and studies within the Asterids (Coen and Nugent, 1994, Donoghue *et al.,* 1998). This group comprises many examples of changes in floral symmetry which could be interpreted as independent recruitment of either ancestral zygomorphy or ancestral actinomorphy (Coen and Nugent, 1994, Endress, 1999, Donoghue *et al.,* 1998, Cubas, 2004). In the Asterids, the study of actinomorphic mutants in *A. majus* and *Linaria vulgaris* (Scrophulariacae) has already successfully shown that in these two related species (see in I.2.1.2 (iii)),

dorso-ventral asymmetry is indeed under the control of a very similar genetic mechanism. However, to determine if this mechanism is conserved between more distantly related species, it is necessary to extend this research to the next higher taxonomic rank, i.e. to families such as the Solanaceae.

1.1.3.2 Floral symmetry in the Solanaceae

(i) A rule and many exceptions

A wide range of morphological zygomorphies exist in the Solanaceae, affecting usually either or both the corolla and the androecium to varying degrees. For example, in *S. wisotonensis*, a very strong zygomorphy is present in both whorls, and the corolla is often described as papilonaceous (butterfly shape) (Robyns, 1931; Knapp, 2002). In this species, the androecium is heterandrous (i.e. different types of stamens), and more specifically tridynamous (i.e. three different lengths of stamens). It is composed of two fully fertile stamens in a lateral position and three staminodes, two dorsal and one ventral, the latter being the shortest (Fig I.12a). In *Petunia*, the flowers also display zygomorphy in the corolla and in the tridynamous androecium. However, this phenotype is more subtle than in *Schizanthus,* with only a slight asymmetry in the perianth and a tridynamous androecium without staminodes (Fig I.12b). *Nicotiana tabaccum* is a good example of residual zygomorphy, the corolla being polysymmetrical but the androecium sometimes didynamous, sometimes tridynamous (Fig I.12c). Finally, more advanced species often have perfectly actinomorphic flowers (e.g. Solanoideae) (Fig I.12d).

The type of zygomorphy found in *Schizanthus, Petunia* and *N. tabaccum* is the most common in the family, and it is referred to as the Robyns' rule (Knapp,

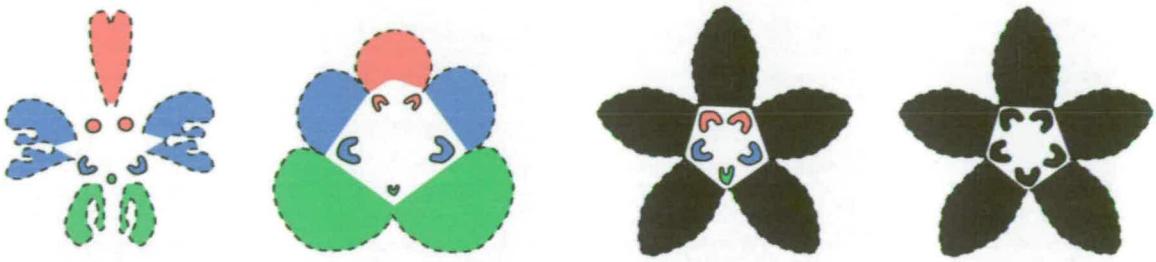

(a) *Schizanthus* (b) *Petunia* (c) *Nicotiana* (d) *Solanum*

Fig I.12: Distribution of dorso, lateral and ventral identity in four solanaceous species
(These drawing are only designed to emphasis the zygomorphic characteristics of the corolla and the androecium). The different domains along the dorso-ventral axis are colour-coded as follows: red for dorsal, blue for lateral and green for ventral. Actinomorphic organs are indicated in grey. The corolla is dashed and the androecium is in full line, circles are staminodes, smi-circle are fertile stamens.

2002). This rule is based on the observation that in many species, the most and sometimes only affected organ is abaxial (Robyns, 1931). For example, in whorl 3, the abaxial stamen may be reduced (e.g. *Nicotiana tabaccum*), lost (e.g. *Brunfelsia*) or enlarged (e.g. *Schultesianthus*) relative to the rest of the androecium (Knapp, 2002). Tridynamous androecia are also frequently observed, with only the abaxial and the adaxial stamens being reduced and/or aborted, the abaxial stamen frequently being shorter than the adaxial pair (e.g. *Petunia, S.wisotonensis*).

(ii) Prevalence, loss and resurgence of zygomorphy, a complex evolutionary picture

Interestingly, recent advances in the study of the phylogenetic relationship in the Solanaceae have shown that, unlike in most other angiosperm families, zygomorphy is mostly confined to basal clades in this family (Olmstead *et al.*, 1992). Therefore, in the Solanaceae, actinomorphy may be regarded as a derived character. It was also shown that zygomorphy can be found in more advanced species evolved from actinomorphic ancestors, so that this trait appears to have multiple independent origins (Knapp, 2002). For example, even within strongly actinomorphic and monophyletic clades such as *Solanum* (Fig I.13a), a few species display a subtle degree of dorso-ventral asymmetry (e.g. *Solanum tridynamum*, Fig I.13b), often solely in the form of heterandry (e.g. *Solanum pennelli*).

The prevalence, loss and resurgence of zygomorphy in the Solanaceae is now shedding new light on the potential of this family to contribute to our understanding of the genetics of zygomorphy and its evolution, both between related species and at a higher level, between related families (i.e. within the Asterids).

Fig I.13a: *Solanum ruberotum*
(Actinomorphic)

Fig I.13b: *Solanum tridynamum*
(Zygomorphic)

I.2 *Schizanthus wisotonensis*, a model species for the study of dorso-ventral asymmetry in the Solanaceae?

The genetic control of floral symmetry has been very well characterised in two species with a strong dorso-ventral asymmetry: *Anthirrinum majus* and *Linaria vulgaris* (Scrophulariaceae). Both species were initially chosen for study on the basis of their existing natural peloric mutants (i.e. mutants with actinomorphic flowers). Interestingly, the genome of *A. majus* harbours a few active transposons providing an invaluable tool to study gene function by both forward and reverse genetics approaches. Consequently, *A. majus* has become the first and best characterised model species for the study of the genetic control of dorso-ventral asymmetry.

In this section, I will first summarize the recent advances in the understanding of dorso-ventral asymmetry in *A. majus*. I will then give an overview of the current knowledge of the genetic control of zygomorphy in other angiosperm species. Finally, I will explain the reasoning underlying the choice of *Schizanthus wisotonensis* as a model species to study the control of dorso-ventral asymmetry in the Solanaceae.

I.2.1 The molecular genetics of dorso-ventral asymmetry in the angiosperms

I.2.1.1 The molecular genetics of dorso-ventral asymmetry in A. majus

(i) Dorso-ventral asymmetry in A. majus

The flower of *A. majus* is pentamerous except for the bi-carpellate gynoecium. Three domains, dorsal, lateral and ventral can be distinguished along a dorso-ventral plane in both the corolla and the androecium (Fig I.14). The two dorsal petals are partially fused and their dorsal-most half is enlarged. The lateral petals have an

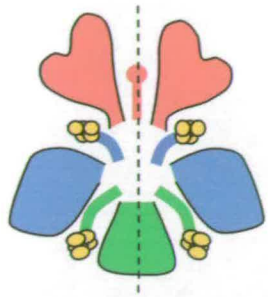

Fig I.14: Simplified diagram of the corolla and the androecium in *Antirrhinum majus*
In *A. majus,* organs from the corolla and the androecium vary in morphology along the dorso-ventral axis (dotted line): in red, the dorsal domain (two dorsal petals and one aborted stamen called a staminode), in blue, the lateral domain (two lateral petals and two intermediate sized stamens) and in green, the ventral domain (one petal, fully grown stamens).

Fig I.15: Simplified diagram of the *cyc* and *cyc;dich* mutant in *Antirrhinum majus*
In the *cyc;DICH* background, the flower is hexamerous and almost completely regular with a residual dorsalisation of the dorsal petals and the dorsal stamen (intermediate size between the staminode and fully grown stamen). In the *cyc;dich* background, the flower is hexamerous and completely regular.

intermediate dorso-ventral shape. They can be divided in a dorsal-most domain resembling the adjacent half of the dorsal petal, and a ventral-most domain similar to the adjacent section of the ventral petal. Therefore, both the dorsal and lateral petals display some degree of internal asymmetry, unlike the ventral petal which is bisected by the dorso-ventral axis and shows internal bilateral symmetry. In the corolla, petals are fused, and a spur-like outgrowth is formed the base of the ventral petal. The androecium is composed of a dorsal staminode (aborted stamen) and 4 fully fertile stamens, with the lateral pair being shorter than the ventral one (Luo *et al*, 1999) (Fig I.14).

(ii) Mutants in dorso-ventral asymmetry in A. majus

By transposon-mutagenesis, Carpenter and Coen (1990) obtained mutants of *Anthirrinum majus* with more regular flowers. Four mutants genetically distinct have been isolated: *cycloidea (cyc), dichotoma (dich), divaricata* (*div*) and *radialis (rad)* (Luo *et al.*, 1996, 1999; Almeida *et al.,* 1997, Cubas, 2004).

The *cycloidea* mutant is almost regular (semi-peloric) (Fig I.15). This mutant shows an increased number of floral organs (six sepals, petals and stamens), and in the androecium, all stamens are fully grown and fertile. In the corolla, all petals resemble the ventral one, except for the dorsal most half of the dorsal petal which is enlarged as in the wild type. In the *cyc* mutant, the increase in organ number suggests that *CYC* has an early role in either the repression of primordium initiation and/or in the regulation of meristem size (Luo *et al.,* 1996). In later stages, *CYC* function is believed to control (i) the reduction in length of the dorsal and the lateral stamens (all fully grown in *cyc*), (ii) the dorsalisation of the lateral petals and that of the dorsal

petal, albeit not completely for the later as a residual internal asymmetry persists in the *cyc* mutant. A study of mutants in floral homeotic genes has shown that the *CYC*-dependent dorso-ventral asymmetry is specific to whorl identity regardless of organ type (Clark and Coen, 2002). However, the B-class gene *DEFICIENS* (sepals instead of petals and carpels instead of stamens in the mutant) has been shown to be necessary for the maintenance of *CYC* expression in whorl 2-3 in later stages of development (Clark and Coen, 2002). This observation suggests a combinatorial interaction between both *CYC* and organ identity genes (Carpenter and Coen, 1990; Clark and Coen, 2002).

In the *dich* mutant, the phenotype is more subtle (Almeida *et al.* 1997, Galego and Almeida, 2002). There is no enlargement of the dorsal most half of the dorsal petals and the divide between the two dorsal petals is deeper than in the wild-type. The dorsal stamen is not aborted, but still shorter than the lateral ones. These phenotypes suggest that *DICH* controls the enlargement of the dorsal-most half of the dorsal petals in the wild type, and therefore the establishment of internal asymmetry in these petals. The intermediate size of the dorsal stamen observed in the *dich* mutant indicates that *DICH* function partially inhibits the growth of the dorsal stamen in the wild type. However, in *cyc* plants, despite functional *DICH,* the dorsal stamen is fully grown suggesting that *DICH* activity is *CYC*-dependent in the androecium (Galego and Almeida, 2002).

In the double mutant *cyc;dich,* the flower is completely ventralised, indicating that the residual dorsalisation observed in the *cyc* single mutant is indeed due to *DICH* function (Galego and Almeida, 2002) (Fig III.15).

In the *divaricata* mutant, the dorsal half of the flower is unaffected whereas the ventral petal resembles the ventral most side of the lateral petal, the later being smaller and rounder than in the wild type. The study of loss-of-function mutants of *div* has shown early effects on organ growth and late effect on cell type (Galego and Almeida, 2002). The earliest phenotype noticed in the *div* mutant is the smaller size of the lateral and the ventral petals through stage 7 and 8. In later stages of development, the shape of the lateral and the dorsal petals is affected, being rounder in the mutant than in the wild type. In stage 9, the furrow at the boundary of the lateral and the ventral domain does not expand in the mutant, whereas is becomes a pronounced fold in the wild type. In addition, the increase in tube length in the ventral petals and adjacent domain of the lateral petal is not observed in the mutant. Therefore, one early effect of *DIV* is an increase in size of the ventral petal and the ventral-most domain of the lateral petals, resulting in the establishment of internal asymmetry in the later.

In later stages, *DIV* is responsible for the shape of the ventral petal and the adjacent domain in the lateral petal, and the formation of a furrow at the boundary between the ventral and lateral petals (Galego and Almeida, 2002). Therefore, *DIV* acts as a determinant of ventral identity, by controlling the ventral-specific morphological traits of the flower (Almeida *et al.*, 1997; Galego and Almeida, 2002).

Finally, the study of the *radialis* mutant revealed that the mutation at this locus is recessive and its phenotype is similar to that of *cycloidea* (Luo *et al.*, 1996).

(iii) *CYCLOIDEA* and *DICHOTOMA: two determinants of dorsal identity*

CYC and *DICH* are two paralogous genes belonging to the TCP gene family of transcription factors (Cubas *et al.,* 1999). This family, only found in plants, was named after the first few genes isolated: *TEOSINTE BRANCHED 1* (*TB1*) in maize, *CYC* in *A. majus* and *PCF1&2* in rice (Cubas *et al.,* 1999). All TCP genes have in common the TCP box, a characteristic basic-Helix-Loop-Helix (bHLH) domain (Cubas *et al.,* 1999). This type of motif is found throughout all kingdoms, in proteins that function in the regulation of transcription during many essential developmental processes (Morgenstern and Atchley, 1999). The bHLH domain of most genes from this family contains a putative nuclear localisation signal, a region for DNA binding and a third domain supposedly necessary for dimerisation (Cubas *et al.,* 1999). In addition, some of the TCP genes have a second conserved domain containing many arginines (R) and called the R box (e.g. *TB1, CYC, DICH, TCP1 & 2*)(Cubas *et al* ., 1999). Recent studies of genes belonging to this family have shown that they are transcription factors involved either directly or indirectly in the control of growth and cell proliferation (Luo *et al.,* 1996, 1999; Cubas, Vincent and Coen, 1999, Doebley, Stec and Hubbard, 1997; Trémousaygue *et al.,* 2003; Kosugi and Ohashi, 2002; Gaudin *et al.,* 2000, Nath *et al.,* 2003, Crawford *et al.,* 2004, Takeda *et al.,* 2003, Hubbard *et al.,* 2002).

The first stage of flower development in *Antirrhinum* is characterized by the emergence of the future floral meristem in the axil of a bract (Carpenter *et al.,* 1995). *CYC* and *DICH* are expressed at the boundary between the inflorescence and the floral meristem during stage 1, *CYC* being expressed slightly later than *DICH* (Luo *et al.,* 1999). This early expression may indicate that, although in *Antirrhinum CYC* and

DICH are not required for the bifurcation of the inflorescence and the flower meristem, they might have had an ancestral function in this developmental process (Luo *et al.*, 1999). In later stages (2-3), before the emergence of petal primordia, the domain of expression of *CYC* and *DICH* expands into the dorsal domain of the floral meristem.

Once organ primordia are visible, *CYC* and *DICH* are expressed in the dorsal sepal (only briefly), in the petal initials and in the staminode (stage 4-5) (Luo *et al.*, 1996, 1999). Although the pattern of expression of *CYC* and *DICH* overlaps, *CYC* expression is confined to sites of primordia initiation whereas *DICH* appears to be evenly expressed througout the dorsal region (Luo *et al.*, 1999).

In the wild-type corolla, *CYC* is expressed in a domain spanning the two dorsal and the dorsal-most half of the lateral petals. *DICH* expression is more restricted and confined to the uppermost part of the two dorsal petals. In the androecium, both genes are expressed in the dorsal staminode.

How is the domain of expression of *CYC* and *DICH* confined to the dorsal half of the flower? The recent study of a mutant named *backpetals* has shed a new light on this question (Luo *et al.*, 1999). This mutant has lateral and ventral petals resembling the lateral side of the dorsal petals. Luo *et al.* (1999) obtained evidence that the dorsalisation of the lateral and the ventral domains in the *backpetals* mutant was caused by ectopic expression of *CYC* in the corresponding domains where it is not normally expressed. Moreover, they found that this abnormal expression of *CYC* was caused by the insertion of a transposon in the promoter region of the *CYC* gene. Therefore, they suggested that in the wild-type, *CYC* is excluded from the ventral side

of the flower through negative regulation involving a cis-acting element in the promoter.

However, this finding does not account for the dorsal expression of *DICH* and it is very likely that the localisation of *CYC* and *DICH* expression to the dorsal domain is controlled by a combination of factors.

In the *cyc* mutant, the ventral domain spreads dorsally in the domain where *CYC* is expressed in the wild type. This suggests that *CYC* function is directly required to repress a ventral identity factor in the dorsal petal and the dorsal most half of the lateral petals

(iv) DIVARICATA: a determinant of ventral identity

DIVARICATA belongs to the MYB family of transcription factors. Interestingly, *DIV* is expressed thorough the whole flower in both the wild-type and the mutant. However, a late ventral asymmetric expression pattern confined to the inner epidermis of the ventral furrow is observed in the wild type flower (Galego and Almeida, 2002). In the *cyc dich* mutant, this pattern of expression is found in the furrow of all petals suggesting that it is linked to the ventralisation of petals. Interestingly, this study also unravelled the role of *DIV* in the self-regulation of its own expression necessary to induce the localised asymmetric expression pattern in the inner cells of the ventral petals (Galego and Almeida, 2002).

(v) RADIALIS: another promoter of adaxial characteristics

The work on *RADIALIS* has not been published yet. This gene, believed to be under the control of *CYCLOIDEA* and *DICHOTOMA*, appears to be also involved in the control of dorsal organ fate (Luo *et al.*, 1996, Cubas, 2004).

In summary, in *A. majus,* the flower can be divided into two zones of influence whose boundary is approximatively in the middle of the lateral petal. The dorsal identity is *CYC* and *DICH* dependent, and the ventral identity is conferred by *DIV* activity. *CYC* expression is confined to the dorsal domain by transcriptional regulation whereas *DIV* expression (as required for the ventralisation of petals) is controlled by the *DIV* protein, itself inhibited post-transcriptionally by *CYC* and *DICH* in the dorsal domain.

I.2.1.2 A role for CYC-like genes in other angiosperms?

In the past few years, many new members of this gene family have been isolated in a variety of angiosperm species, and a few have been thoroughly studied (Cubas, 2004). This has provided an invaluable source of information about the possible role of *CYC*-like genes in the control of dorso-ventral asymmetry in other species (Cubas, 2002, 2004).

(i) Classification of the TCP gene family

This family is traditionally divided in two very distinct classes. Class I comprises the PCF genes initially found in rice, and many of their orthologues, for example in rice (*OsPCF* and in *A. thaliana*) (Cubas *et al.*, 1999). None of these genes

have the arginine-rich (R) domain, and most of them have been isolated by DNA or EST screens.

Class II includes *CYC* and *DICH, TEOSINTE BRANCHED 1* from maize and its ortholog in rice, and about half of the TCP genes found in *A. thaliana* (Cubas, 2002, 2004). In this class, the presence of a second conserved domain (the R box) has provided the sequence information necessary to use PCR-based techniques to isolate new genes from a wide range of species (e.g. Gesneriaceae, legumes, Solanaceae, Boraginaceae and poplar (Citerne, Möller and Cronk, 2000; Citerne *et al.*, 2003, Reeves and Olmstead, 2003).

Usually, a variable number of TCP genes can be isolated from any one species (24 in *A. thaliana*, 6 in rice), suggesting that gene duplication may have played an important role in the evolution of this gene family (Cubas *et al.*, 1999).

(ii) CYC-like genes and dorso-ventral asymmetry in the Lamiales s.l.

The Lamiales s.l. is a group of asterids including families such the Scrophulariaceae and the Gesneriaceae (Olmstead *et al.*, 1992). In this group, most species are zygomorphic, and in the corolla, the petal arrangement is 2/3 (i.e. two dorsal and three ventral) as in *A. majus* (Donoghue *et al.*, 1998). The Lamiales s.l. includes most of the species discovered so far with naturally occurring actinomorphic mutants (e.g. *Ramonda, Sinningia speciosa, Saintpaulia*) (Coen and Nugent, 1994, Cubas, 2004). These set of observations support the hypothesis that the establishment of dorso-ventral asymmetry in related species from the Lamiales s.l. may have recruited a similar pre-pattern (i.e. trans-acting gene regulators) present in a common ancestor.

This hypothesis was initially tested in *Linaria vulgaris,* a related species to *A. majus.* The flowers of *L. vulgaris* have a strong dorso-ventral asymmetry in the corolla (2/3 arrangement) and a dorsal staminode. The study of peloric mutants in *L. vulgaris* has shown that this mutation corresponds to the silencing of the *CYC* homologue (*LCYC*), otherwise expressed in the dorsal domain of the wild-type flower (Cubas *et al.,* 1999). However, in *L. vulgaris,* only one gene controls dorso-ventral asymmetry, and organ number does not change in the peloric mutant (Cubas *et al.,* 1999). These observations suggest that even between two related species, the genetic control of dorso-ventral asymmetry is not completely conserved. A *DICH*-like gene has been isolated in this species has been identified but its role has not yet been characterised (Gübitz, Caldwell and Hudson, 2003; Cubas and Coen, pers. comm.).

In the Gesneriaceae, most species are either regular or weakly zygomophic . It has been suggested that all *CYC*-like genes in this family are derived from a single common ancestor to both the Gesneriaceae and the Scrophulariaceae (Citerne *et* al., Citerne, Möller and Cronk, 2000, Cubas, 2004). The relation between presence/absence of zygomorphy and sequence evolution of two *CYC*-like genes has been addressed in this family but no clear correlation could be drawn between the evolution of these genes and that of floral symmetry (Citerne, Möller and Cronk, 2000).

(iii) CYC-like genes and dorso-ventral asymmetry outwith the Lamiales s.l.

It is not currently possible to estimate how conserved the role of *CYC*-like genes is outside the Lamiales s. l. To test this hypothesis, the role of *CYC* homologues in a more distant species belonging to *Senecio* (Asteraceae), is currently

under investigation. Some encouraging results comprising RNA *in situ* analysis and gene segregation studies suggest a potential role for *CYC*-like genes in the control of zygomorphy in the ray florets of *Senecio radialis* (Gilles, A., pers. comm).

The role of *CYC*-like genes is also currently being investigated in more distantly related species such as *Lotus* (legumes). In this species, a *CYC*-like gene in *Lotus* is expressed at the site of the split in the inflorescence which results in the formation of two flowers with adjacent dorsal domains (Luo, pers. comm). Although, the role of this gene in the establishment of dorso-ventral asymmetry has not yet been shown, its expression pattern is at least similar to that of *CYC* in *A. majus* during stage 1 of floral development. In *Lupinus,* another papilonaceous legume, two homologues of *CYC* have been isolated. Although their function has not yet been elucidated, their overlapping domain of expression in the dorsal domain of the developing flower resembles that of *CYC* and *DICH* (Helene Citerne, pers. comm.).

In *A. thaliana,* TCP1 is the putative *CYC* ortholog. Its expression pattern is reminiscent of that of *CYC* in *A. majus,* albeit more transient (Cubas, Coen and Zapater, 2001). However, *A. thaliana* is dissymmetric and the corresponding loss-of-function mutant is seemingly aphenotypic. Therefore, the function of this gene remains unknown (Cubas, Coen and Zapater, 2001, Cubas, 2002, 2004).

In maize, the putative *CYC* orthologue is *TB1.* In this species, the level of *TB1* transcript controls the development of axillary meristems and stamen abortion in female florets (Doebley, Stec and Hubbard, 1997; Hubbard *et al.,* 2002). A similar study of the rice *TB1* ortholog (*OsTB1*) also demonstrated the role of this gene in the control of axillary growth (Takeda *et al.,* 2003).

These functions are again clearly reminiscent of that of *CYC* and *DICH* in *Antirrhinum* where these two genes control stamen abortion and affect organ growth in the axillary structure (i.e. the flower).

In summary, a degree of conservation in the expression pattern and the function of *CYC*-like genes in the angiosperms is gradually emerging.

Could a similar mechanism to that controlling dorsovental asymmetry in *A. majus* be also present in the Solanaceae?

In the phylogenetic tree of the angiosperms, the Solanaceae are more closely related to the Scrophulariaceae than the Brassicaceae, the Asteraceae, the legumes, rice and maize (Chase *et al.,* 1993). Therefore, it is reasonable to propose that if one or more *CYC*-like genes exist in monosymmetrical solanaceous species, their function might be conserved with that of *CYCLOIDEA* and *DICHOTOMA* in *A. majus*.

I.2.1.3 *S. wisotonensis*, a model species for the study of dorso-ventral asymmetry in the Solanaceae?

(i) Moving away from existing model species

Petunia, tobacco, tomato and potato are the model species belonging to the Solanaceae. They are easily transformable and many genes involved in flowering have been isolated and characterised. Although *Petunia,* tobacco, tomato and potato can be used as stepping stones in the study of the evolution of zygomorphy, they are not well suited for a study of the control of zygomorphy in the Solanaceae. *Petunia* and tobacco exhibit a very moderate zygomorphy with a degree of intraspecific variation. Therefore, even if *CYC*-like genes were isolated in these species, expression patterns might be difficult to interpret due to low level and/or short

window of expression. Instead, *S. wisotonensis* which is highly zygomorphic, was chosen by Marc Chadwick (JIC, UK) to initiate the study of *CYC*-like genes in this family. This species proved to be amenable to molecular genetics, but unfortunately, this project was a small component of his PhD, and despite of a few encouraging results, he did not have the time to complete his work (Chadwick, 1996).

(ii) Origin of S. wisotonensis

Members of the genus *Schizanthus* are found in Chile and the high cordilleras of extreme western Argentina (Walters, 1969). The name is derived from the Greek: *schizo* meaning to split and *anthos*, the flower. This species is named after the apparent split between the two ventral petals and it is also known as the Poor Man's Orchid, the Fringe flower or the Butterfly flower.

S. wisotonensis is a cultivar generally described as a diploid hybrid between *S. pinnatus* and *S. grahamii* produced by plant breeders. However, the nature of its origin remains a matter of debate. In a monograph of *Schizanthus*, Walters (1969) investigated this question by crossing *S. wisotonensis* with its potential parents: *S.grahamii, S. hookeri* and *S. pinnatus*. The result of such crossing experiments showed that some of these species appear to be genetically isolated and did not produce seeds when inter-crossed. Interestingly, *S. wisotonensis* was only producing seeds when backcrossed to *S. pinnatus*. This finding suggests that, unlike what was previously thought, *S. wisotonensis* might not be an interspecific hybrid but more likely the product of crosses between different subspecies of *S. pinnatus*. In support of this hypothesis, Walters (1969) counted the chromosomes and found that both *S. pinnatus and S. wisotonensis* are diploids (n=10) whereas the chromosome number is

different in other *Schizanthus* species. In addition, he carried out a morphological survey of *S. pinnatus* in Chile. He concluded from this study that the characteristic variation of morphology observed in this species could be seen as a geographic cline in the field. Therefore, Walters (1969) concluded that the many variants observed in *S. wisotonensis* are very likely to be the product of crosses between different variants of *S. pinnatus*, possibly reflecting a selection of subspecies by breeders for their commercial attributes.

(iii) Schizanthus wisotonensis: a new model species in the Solanaceae

The advantages of *S. wisotonensis* are numerous. *S. wisotonensis* flowers are strongly zygomorphic, it is easy to cross and to grow, with a generation time of two months. It produces a large number of flowers and lives for almost a year under greenhouse conditions.

During his PhD, Marc Chadwick isolated the partial sequence of two *CYC*-like genes from *S. wisotonensis* and obtained a pattern of expression for one of them. In addition, during a visit to Holland, Anne-Marie Houtbraken (Syngenta, Holland) kindly gave me seeds of a mutant of *S. wisotonensis* which apparently shows a decreased dorso-ventral asymmetry. This mutant, re-named the *rz* mutant (reduced-zygomorphy), offers the possibility of testing the link between the expression patterns and functions of *CYC*-like genes in this species. Therefore, although it is not a classical model species, the data and the plant material available in *S. wisotonensis* provide an interesting technical basis to start a project aimed at investigating the role of *CYC*-like genes in the control of zygomorphy in this species.

From an evolutionnary perspective, *S. wisotonensis* is also interesting at two levels. Firstly, unlike in *A .majus,* it has a 3/2 petal arrangement (i.e. three upper and two lower petals) and the orientation of the flower is oblique relative to the inflorescence. Therefore, although some degree of functional conservation between *CYC* orthologs in both species can be expected, the existing model for *A. majus* cannot be directly used in a solanaceous system (Donoghue *et al.,* 1998). If a new model for the control of dorso-ventral asymmetry is found outside the Scrophulariaceae, this would provide an interesting comparative tool to study the evolution of floral symmetry at a higher taxonomic order, i.e. between the Scrophulariaceae and the Solanaceae.

Secondly, the type of zygomophy characteristic of *S. wisotonensis* complies perfectly with Robyns' rule (see 1.1.3.2 *(i)*). Consequently, the results obtained in this species could be tested in more actinomorphic members of the same family, including species such as *Petunia* and tobacco. Such studies could potentially unravel the genetic mechanisms underlying the gain of actinomorphy from a zygomorphic ancestor.

Therefore, in summary, *S. wisotonensis* provides a promising model system to investigate the role of *CYC*-like genes in a species with cymose (or bifurcating?) inflorescence and a 3/2 arrangement of petals. Furthermore, it can be the foundation of a study on the evolution of floral symmetry in the Solanaceae, and help to test the concept of a conserved pre-pattern in the Asterales.

II. Materials and Methods

All common chemicals were purchased from either SIGMA, Fisher Scientific, AnalaR, Roche or BDH. All steps were carried out at room temperature unless stated otherwise.

II.1 DNA techniques

II.1.1 DNA extraction: small scale

About two leaf disks of the size of the lid of a 1.5µl eppendorf were obtained from fresh plant material (young leaf). They were frozen in liquid nitrogen. The tube was removed from the liquid nitrogen and a plastic mortar was used to break open the plant cells during approximately 15 sec. The tube was then plunged in liquid nitrogen for about 10 sec and the all process repeated once again. 500µl of DNA extraction buffer (50mM EDTA pH8; 0.1M NaCl; 0.1M Tris HCl pH8; 1% SDS) was added to the frozen material and crushed until a homogenous mixture was obtained. The mixture was then plunged again in liquid nitrogen and left on ice until all samples were proceeded (usually about 10 samples at once).

A volume of 500_l of phenol-chloroform (1:1) was added to each sample individually, the sample vortexed for 1 min and left to stand for 5 min. The sample was then centrifuged for 10 min (14000 rpm, room temperature). The upper phase was transferred to a clean tube and the phenol-chloroform extraction repeated once again, and a third time with 500_l of chloroform only. The DNA was then precipitated with the addition of 50µl of 3M NaOAc (pH5.2) and 350µl of isopropanol (propan-2-ol). The sample was centrifuged for 10 min (14000 rpm). The supernatant was discarded, the pellet rinsed in 70% ethanol and left to dry at room

temperature. The DNA pellet was then dissolved in 50µl R40 (10mM Tris-HCL, 1mM EDTA, RNase A at 40µg/ml) and incubated at 65°C for 10 min. The concentration of the DNA sample was estimated by running 1µl in an agarose gel (see II.1.4).

II.1.2 DNA extraction: large scale

Fresh leaf material (2.5g) was grinded in 10ml of DNA extraction buffer (0.1M Sodium diethyldithiocarbonate, 0.1M EDTA pH8, 3X SSC (from 20X SSC (0.3mM NaCl, 30mM Na Citrate stock) using a mortar and pestle. The mixture was then poured in a 50ml falcon tube and 10ml of chloroform was added. The tube was inverted a few times and centrifuged at 3000 rpm for 10 min. The upper phase was collected, poured into a fresh tube and the same procedure was repeated using first 10 ml of phenol-chloroform (1:1) and then finally 10ml of chloroform only. The DNA was then precipitated by adding an equal amount of 96% ethanol to the aqueous phase. The sample was centrifuged at 3000 rpm for 2 minutes, the ethanol was removed and the pellet cointaining the DNA left to air-dry before being dissolved in 0.5ml of 10mM TE (10mM tris_HCl (pH8.0), 1mM EDTA) and 5µl of RNase A (40µg/ml) for 2 hours at 50 °C or O/N at 4°C. Finally, the DNA was again precipitated using 60µl of NaCl (5M) and 500 µl CTAB (2% w/v). The precipitate (i.e. the DNA) was removed from the tube and washed in 70% ethanol and 30% NaCl, and left to air-dry. The concentration of the DNA sample was estimated by running 1µl in an agarose gel (see II.1.4).

II.1.3 Polymerase Chain Reaction (PCR)

PCR reactions were carried out in a maximum volume of 20µl including 2µl of 10X PCR buffer (500mM KCL, 100mM Tris-HCL pH9, 1% Triton X-100), 2µl of 25mM $MgCl_2$, 1µl of 10µM forward primer, 1µl of 10µM reverse primer, 0.4µl 10mM dNTPs (10mM of each, dATP, dCTP, dGTP and dTTP), 0.1µl Taq polymerase enzyme (Promega, Madison, USA), DNA up to 20µl with dH_20. Oligos were ordered from Qiagen Operon (Cologne, Germany). Primers were designed by eye and tested using the program Netprimer (http://www.premierbiosoft.com/netprimer /netprlaunch/netprlaunch.html).

PCR tubes were placed in a T3 Thermocycler (Biometra, Goettingen, Germany) and the following program run: 94°C for two minutes to denature DNA, followed by 30 cycles of [94°C for 30 sec (denaturation), 58° unless stated otherwise for 30 sec (annealing step), 72°C for 30 sec/500bp (elongation step)], 72°C for 7 minutes for complete extension.

For medium stringency PCRs, the annealing temperature was 55°C, and for low stringency 50°C.

A touch-down PCR program was used in the genomic walking and 5' RACE PCR. The first round of the touch-down PCR was done with 2 min at 96°C followed by 5 cycles of (94°C for 5 sec, 70°C for 10 sec and 72°C for 3 min), then 20 cycles of (94°C for 5 sec, 68°C for 10 sec and 72°C for 3 min). The nested round or re-amplification of nested products was done with 96°C for 2 min followed by 20 cycles of (94°C for 5 sec, 68°C for 10 sec and 72°C for 3 min).

II.1.4 Agarose gel electrophoresis of DNA

DNA fragments were separated and quantified by using electrophoresis. 1% (0.8% for Southern blot, 3% to separate fragments <150 bp) agarose gel was made by dissolving agarose powder in 1X TAE buffer (0.04M Tris acetate, 0.001M EDTA pH8, with 0.0005 μg/ml EtBr). DNA samples were loaded in a minimum total volume of 10μl (made up with dH_20) with addition of 1/10 volume of loading dye (30% glycerol in water, 0.25% bromophenol blue). 0.5μg of either 1Kb or 100bp ladder (NEB, Beverly, MA, USA) was used as a size and concentration marker (according to manufacturer's guidelines). Gels were run at 100v for about 40 minutes for diagnostic tests, 70v for isolation of cleaved DNA by gel extraction or at 30v when run overnight for a Southern hybridization. After electrophoresis, using a UV transilluminator, the size and amout of DNA in each band was estimated using the fluorescence of the Ethidium Bromide intercalated in between DNA bases as a guide.

II.1.5 Extraction of DNA fragments from agarose gel after electrophoresis

The QIAEX II Gel Extraction kit (Qiagen, Cologne, Germany) was used and all steps were followed according the manufacturer's specifications. The concentration of the DNA sample was estimated by running 1μl in an agarose gel (see II.1.4).

II.1.6 Purification of DNA fragments

The QIAquick® PCR purification kit (Qiagen, Cologne, Germany) was used and all steps were followed according the manufacturer's specifications. The concentration of the DNA sample was estimated by running 1μl in an agarose gel

(see II.1.4).

II.1.7 Cloning of DNA fragments

The ligation of PCR products or DNA fragments obtained from plasmid digestion in the pGEM©-T easy vector was done using the pGEM©-T easy Vector system (Promega). In an ependorf, 2µl of the PCR mixes or about 200ng of purified DNA fragment, 0.5µl of the pGEM©-T easy vector, 2µl of dH_2O, 5µl of the ligation buffer and 1µl of T4 DNA ligase were added. The ligation was then either left overnight at 16°C or for an hour at room temperature. The cloning was done by transformation of the plasmids in a competent DH5_ strain of *Escherichia Coli* (cell prepared according to Inoue, 1990). The bacterial cells were thaw on ice for 15 min before 5µl of the ligation was mixed with 100µl of competent DH5_ cells and left to stand on ice for 30 mins. The mixture was then heat-choked at 42°C in a water bath for 1 min before being placed on ice for 2 mins. About 1ml of LB (1% tryptone, 0.5% yeast extract, 0.5% NaCl; pH7) was added to the tube and the mixture was left for 45 mins in a 37°C incubator. The mixture was then plated on LB-amp plates (ampicillin (100 µg/ml, 1% bactoagar, Difco) previously spread with 100 µl of X-gal solution (X-gal (20mg/ml) in DMF) to allow for a blue-white screening of colonies. The plates were then incubated overnight at 37°C.

Other routine ligations were done using 1XT4 DNA ligase (NEB) according to the manufacturer's guidelines, using 10-20ng plasmid DNA and 50-60 ng insert DNA, in a total reaction volume of 10µl. Ligations were incubated overnight at 16°C prior to transformation into bacterial cells (*E.* coli, strain DH5_).

II.1.8 Plasmid isolation

Cells were either picked up on plated individual colonies on selective medium or recovered from glycerol stocks. They were incubated in 3ml of LB-amp (ampicillin (100µg/ml) at 37°C overnight. The next morning, 1.5ml of each overnight culture was placed in an eppendorf and centrifuged at 7000 rpm for 3 min. The supernatant was disgarded, and the pellet re-suspended in 350µl of boiling buffer (8% (w/v) sucrose, 0.5% Triton X-100, 50mM EDTA, 10mM Tris•HCl, pH8) with 0.1% lysosyme. The mixture was heated at 100°C for 1 min and placed onto ice for 2 min and centrifuged at 14000rpm for 15 min at 4°C. After centrifugation, the pellet (containing cell debris, bacteria genomic DNA and proteins) was removed using a tooth-pick. 400ml of isopropanol and 40ml of 3M NaOAc (pH5.2) were added to precipitate the plasmid DNA. The tubes were inverted a few times and centrifuged at 14000rpm for 10 min. The supernatant was discarded, the pellet (i.e. containing plasmid DNA) washed with 70% EtOH and centrifuged at 14000 rpm for another 10 min. The supernatant was discarded, and the pellet left to air-dry. The DNA was subsequently dissolved in R40 (see I.1.1). To quantify the amount of plasmid obtained, the plasmids were then digested (*EcoR*I digests for pGEM©-T easy) and the digestion mixture run on an agarose gel (see I.4).

Alternatively, mini-prep or midi-preps of overnight cultures were carried out using the QIAgen Plasmid min or midi prep according to the manufacturer's specifications.

If required, the plasmid DNA was either cleaned up with a phenol/chloroform extraction or cleaned up using the QIAEX II Gel Extraction kit (Qiagen, Cologne, Germany). For the phenol-chloroform extraction, the volume of the sample was

made up to 200µl with dH_20 to which 200µl of phenol/chloroform (1:1) was added. The mix was vortexed (30 sec) and span at 14000rpm for 10 min. The aqueous phase containing the DNA was removed, pipetted into a new tube and precipitated with the addition of 10% (v/v) 3M NaOAC (pH5.2) and 2.2X 96% EtOH. The tube was gently mixed by inversion and left in the freezer at -20°C overnight. The next morning, the tube was centrifuged at 14000 rpm for 10 min at 4°C, the supernatant discarded, the pellet (containing the DNA) washed in 70% EtOH and centrifuged again as before. Finally, the 70% EtOH was removed, the pellet left to air-dry. It was subsequently dissolved in buffer EB (Quiagen) or in TE pH8. When using the QIAEX II Gel Extraction kit, 20µl of DNA from an average mini-prep (approx. 3µg of DNA) and 30µl of dH_20 were mixed. 150µl of QXI yellow buffer was added to the solution together with 10µl of freshly vortexed QIAEXII beads. The mix was incubated at room temperature for 10 min with regular flicking. The same protocol as described in the manufacter's guidelines was followed for the rinses. The DNA was eluted in 20µl of buffer EB.

II.1.9 Sequencing

For plasmid DNA, if required, the Qiaex II Gel Extraction kit (Qiagen) was used to clean mini-prepped vector DNA from *E. coli* in order to remove contaminants as described in II.1.8. DNA was quantified on an agarose gel, with 100 ng used for a 0.25X sequencing reaction. The following was added to a PCR tube: 100ng of DNA, 2µl Big Dye Version 3.1 sequencing mix (Applied Biosystems, Foster City, CA, USA), 1µl 0.8pM oligo. The reaction was made up to 10µl with dH_20 before being overlaid with mineral oil to minimise evaporation and the

following PCR program used: 96°C for 2 min, followed by 30 cycles of [96°C for 30 sec, 50°C for 15 sec, 60°C for four minutes]. After removing the mineral oil, samples were made up to 20µl with dH_20 and processed in-house, within the ICMB sequencing facilities (ABI Prism 3100, Epsom, UK). Sequences were viewed and analysed using DNASTAR.

For PCR amplified DNA, the reaction mixture was purified and 150ng of DNA was used in the sequencing reaction.

II.1.10 BLAST searches

To carry out BLAST searches and find out how related to other known gene the sequences isolated in this project were, the http://www.ncbi.nlm.nih.gov/BLAST/ web site was used with the "translated query versus protein database (blastx)" option

II.1.11 Genomic walking

The genomic walking protocol was adapted from Siebert *et al.* (1995). The advices given in the protocol of Universal Genomic Walker™ Kit User Manual (Clontech) were followed regarding the design of gene specific primers. About 20 µg of genomic DNA (gDNA) was extracted from *S. wisotonensis* (Dr Badger) using the small scale DNA extraction protocol. Five genomic digests of 2.5µg DNA each were set up. Restriction enzymes were chosen to be blunt-end cutters with 6 bp recognition sites not present within the DNA sequences (*Sca*I, *Dra*I, *EcoR*V, *Pvu*II and *Stu*I). Each digest included 5µl of enzyme, 4µl of spermidine, the buffer (according to manufacturer's guidelines) and dH_20 up to 100µl. After 5 hrs of incubation, 1µl of digested DNA from each aliquot was run on a 1% agarose gel

stained with ethidium bromide at low voltage (30 v) and for 5 hours to check the quality of the digestion. The ligation of the adaptors was done in a 10µl reaction including 5µl of the digested DNA, 1µl of 10X ligation buffer, 1µl of T4 ligase (5X) (Biolabs), 2.4µl adaptor (25mM), 0.6µl dH_20. The adaptor was obtained from the annealing of two primers ordered separately (sequence in Fig. IV.2). To do so, the primers were mixed to a final concentration of 25µM, boiled for 10 min and let to cool down at room temperature. The ligation reaction was incubated at 16°C overnight. A touch-down PCR with two rounds as for the 5' race PCR was carried out (see II.1.3).

II.1.12 Southern blotting

DNA was digested, fractionated on an agarose gel, transferred to membrane and hybridised to radioactively labelled DNA probes. DNA samples (5 µg) were fractionated on a 0.8% agarose gel overnight. The gel was then photographed under a trans-illuminator with a ruler, in order to record the positions of the size ladder fragments. The gel was then rinsed consecutively in: depurination solution (0.2M HCL) for ten minutes, dH_20 for 30 sec, twice in denaturation solution (1.5M NaCl, 0.5M NaOH) for 30 min, then twice in neutralization solution (0.5M Tris, 1.5M NaCl pH8) for 30 min. DNA was then transferred to Hybond membrane (Amersham Biosciences, Uppsala, Sweden) which had been pre-wetted in 2X SSC (20X SSC stock: 3M NaCl, 0.3M Sodium citrate; pH7). Capillary transfer was carried out following the instructions described in Sambrook, Fritsch and Maniatis (1989) in 10X SSC buffer overnight at room temperature. After marking the position of the gel wells and air-drying the membrane, DNA was cross-linked to the membrane using a

UV light. The membrane was then baked (to further cross link the DNA) for two hours before being dampened in 2X SSC and rolled into a hybridisation tube. Pre-hybridisation treatment was made by incubating the membrane in 25 ml Church buffer (1% w/v BSA, 0.001M EDTA, 0.5M $NaP0_4$ pH7.2, 7% SDS) for at least five hours at 65°C in a rotary incubator oven.

Radioactively labelled probes were prepared using either random hexamers or specific primers as follows. For random hexamers, 50ng template DNA in 10µl dH_20 was boiled for five minutes then placed on ice for one minute. The following was added: 1µl (1.85µg/µl) random hexamers (Boehringer, Ingelheim, Germany), 5µl 5X buffer/dNTP mix (100mM of: dATP, dTTP, dGTP, 50mM $MgCl_2$, 450mM HEPES solution (0.5g HEPES, 0.8g NaCl, 0.037g KCL, 0.0135g $Na_2HPO_4\_2H_20$, 0.1g dextrose pH6.6), 1µl DNA polymerase I ((Klenow) Gibco/BRL), 5µl $\_^{32}P$ dCTP (Amersham Biosciences), and then the tube incubated at 37°C for one hour. For specific primers, 25ng DNA, 100ng forward primer and 100ng reverse primer together in 14µl dH_20 was boiled for 3 min. The tube was then placed on ice for one minute before adding 5µl 5X buffer/dNTPs, 5µl $\_^{32}P$ dCTP and 1µl Klenow, then incubated at 37°C for one hour. After incubation at 37°C, 30µl of dye (1% Dextran blue, 0.1% Orange G in TE) was added to the labelling reaction. This was then passed over a Sephadex column, in order to remove unincorporated radioisotopes. The radiolabelled probe was collected after fractionation (migrate with the blue dye). Labelled DNA probe fragments were then denatured by heating at 102°C for ten minutes before adding to the pre-hybridised membrane in 10ml Church buffer. Hybridisation was carried out at 65°C for at least five hours. The membrane was then rinsed at high stringency twice in 2X SSC/1% SDS (pH7.2) at 65°C, then twice in

0.2X SSC/1% SDS at 65°C. The first rinses for each were for 30 min, with the second for 15 min. The membrane was air-dried and autoradiography performed using Kodak X-OMAT AR film and intensifying screens, exposed overnight at -80°C inside a cassette. Film was then developed using a Konica developing machine.

II.1.13 Digestion and ligation of DNA

Restriction digestions were carried out according to manufacturer's guidelines (Promega/NEB). Digests were incubated between one and five hours.

II.2 RNA techniques

II.2.1 RNA extraction: small scale

About 30mg of frozen tissue was crushed briefly on dry ice in a 2ml ependorf. Ice cold TRIzol reagent (1ml) (38% H_2O-saturated phenol; 0.8M guanidine thiocyanate; 0.4M ammonium thiocyante; 0.1M of 3M sodium acetate, pH 5; 0.5:10 glycerol) was then added and the mixture homogenised for 2X 30 sec using an electric homogeniser. Chloroform (200µl) was added to result in a phase separation and the mixture was then vortexed for 15 sec. A 2 to 3 min incubation at room temperature followed this step before centrifuging the tube at 6000 rpm at 4°C for 15 min. The supernatant containing the RNA was then transferred to a fresh tube and precipitated by adding (and gently mixing) a volume corresponding to half of the aqueous phase containing the RNA from the previous step of a solution of 0.8M sodium citrate and 1.2M NaCl first, followed by the same volume of isopropanol. The tubes were then left on the bench for about 10 min before being centrifuged at full speed at 4°C for 10 min. After the centrifugation, the supernatant was discarded and

the pellet washed in 75% EtOH. After a brief vortexing, the EtOH was removed and the pellet containing the RNA left to air-dry. Unless stated otherwise, the pellet was then resuspended in 50µl DEPC treated H_2O (1ml/l DEPC, incubation with shaking overnight at 37°C and subsequent autoclaving ensures permanent inactivation of RNases). The quality of the RNA was checked by running it on agarose gele. When two bands corresponding to ribosomal RNA were clearly visible, it was deemed of a good quality. The RNA was quantified with a spectrophotometer by measuring the absorbance of 1µl of RNA solution at a wavelength of 280nm. The purity of the RNA was assessed by comparing the ratio of absorbance at 260nm over absorption at 280nm. If the ratio was below 1.5, the quality of the RNA was deemed unsatisfactory.

II.2.2 5' race PCR

About 100µg of total RNA was obtained from young inflorescences using the TRIzol RNA extraction method (see II.2.1).

An estimated 1µg of Poly A^+ RNA was then isolated from the total RNA using the Oligotex™ mRNA kit (Quiagen).

A 5' race PCR using the polyA^+ RNA isolated was then performed following the instructions of the manufacturer (SMART™ RACE, Clontech). The SMART technology uses the annealing of a SMART II™ oligonucleotide to the 5' tail of the first-stand cDNA which includes several dCs residues added by the reverse transcriptase. This annealed product is then used as a template for a PCR amplification using SMART II™ oligonucleotide specific primers (UPM and NUP, sequence in fig IV.9b) and gene specific primers. Both rounds of PCR were carried out using the TouchAdvantage® 2 PCR kit (Clontech). The PCR was carried out

with a touch-down program (see II.1.3).

II.2.3 RNA *in situ* hybridisation

The following stock solutions were prepared: 20X SSC (0.3mM NaCl, 30mM Na Citrate); 5X NTE (2.5 M NaCl, 50mM Tris pH8, 5mM EDTA); 100mM Tris pH8 and 50mM EDTA; 100mM Tris pH7.5 and 150mM NaCl; Tris pH9.5; 10X PBS (1.3M NaCl, 70mM Na_2HPO_4, 30mM NaH_2PO_4, pH 7); 10X *in situ* Salts (3mM NaCl, 100mM Tris pH8, 100mM NaPhosphate pH6.8, 50mM EDTA), Dextran Sulfate (50% w/v). Buffer 5 (1M tris pH9.5, 1M NaCl, 0.5M $MgCl_2$).

The RNA *in situ* experiment was done over two days. Unless stated otherwise, all reactions were performed at room temperature. All the glassware and the metal rack were oven-baked at 200°C for at least 5 hours prior to the experiment to destroy all RNases. All solutions were prepared using DEPC treated water (see II.2.1) to ensure that all RNases are permanently inactivated.

II.2.3.1 Tissue fixation and sectioning

Ice cold 4% Paraformaldehyde (PFA) pH 7 with 0.1% Twin 20 and 0.1% Triton X-100 was prepared fresh and 5 buds were placed in falcon tubes containing 20ml of this mixture. A vacuum was applied to the samples to ensure that gases were withdrawn from the plant tissue and the fixative was absorbed. The process was carried out for 15 min. Subsequently, the air valve was gradually opened allowing air back in the apparatus. It the tissue was still floating, the same process was repeated until all had sunk to the bottom of the tube. The paraformaldehyde solution was then replaced and the tubes were left to gently shake overnight at 4°C.

All the following steps were carried out at 4°C with gently shaking. The buds

were rinsed twice in 1X PBS for 30 mins, then in 30% EtOH for an hour, followed by 50%, 70%, 85% EtOH also for an hour. Finally, they were left with gentle shaking in 95% EtOH overnight. The next day, all steps were carried out at room temperature with gentle shaking. The first two rinses were done in 100% EtOH and lasted 30 mins each. The tissue was then transferred into glass bottles. All subsequent rinses lasted an hour. These comprised another two rinses in 100% EtOH , then 25% histoclear (Histolene Clearing Agent, CellPath, UK) and 75% EtOH, 50% histoclear and 50% EtOH, 75% histoclear and 25% EtOH, and two rinses in 100% histoclear. Finally, the buds were left overnight in 100% histoclear and _ paraplast chips (BDH) without shaking.

The following day, the bottles were placed in a 42°C incubator until the chips melted. _ of the histoclear was then discarded and replaced by paraplast chips. After a few hours, the temperature of the incubator was increased to 60°C, and once totally dissolved, the mixture was poured out and replaced by freshly melted chips and before being left overnight. For the next 3 days, the wax was changed twice a day. Finally, the tissue was placed in little plastic molds and left to harden at 4°C.

The blocks of wax were sectioned in 7μm thick sections using a Leika rotary microtome. The sections were placed onto ProbeOn Plus slides (Fisher Biotechnology). The slides were then incubated at 42°C with DEPC treated dH_2O to allow the wax ribbons to flatten out for 10 mins. The water was then drained out using a Kimwipe and the slides were left at 42°C overnight.

II.2.3.2 Probe synthesis

The template was purified with a Phenol/ chloroform extraction (1:1) followed by precipitation in 10% v/v 3M NaOAc and ethanol (2.5X). For templates on plasmid, 500ng was needed and for PCR products 350ng. The reaction was set up as follows, DNA in 10.5µl DEPC-treated dH_20, 2.5µl 10X T7 or Sp6 RNA polymerase buffer (Promega, Boehringer or NEB), 1µl RNAase inhibitor (RNAguard™ RNase inhibitor, Amersham Pharmacia Biotech, Inc), 2.5µl dATP, dCTP, dGTP (5mM, Boerhinger Manheim), 2.5µl digoxigenin-11-dUTP (Roche), 1µl RNA polymerase (T7 or Sp6) and left to incubate at 37°C for one hour. After the polymerisation, 75µl H20 and 1µl tRNA (100mg/ml, SIGMA), 1µl RNase free DNase (Boehringer Manheim) were added to the mix to digest any DNA contamination and left to incubate 10 min at 37°C. The mixture was then precipitated by adding 100µl NH_4 Acetate (4M) and 400µl EtOH and left overnight at -80°C. The next morning, after a 15 min spin down, the pellet was briefly rinsed in 70% EtOH 0.5M NaCl, briefly vacuum dried and dissolved in 50µl of DEPC-treated dH_2O.

For the carbonate hydrolysis, the incubation time to obtain 150 bp fragments was calculated as follows: time= Li-Lf/k.Li.Lf where Li : initial length of probe, Lf : final length and k = 0.11kb/minute. Then, 100µl 2X CO_3 buffer was added and the mixture was left to incubate for the calculated time at 65°C. The carbonate hydrolysis was neutralized with 10µl of 10% acetic acid. To precipitate the probe, 1/10 volume of 3M NaOAc (pH5.2) and two volumes of EtOH were added, before being left at -20°C for a few hours. The pellet was subsequently rinsed in 70% EtOH. The probe was dissolved in 50µl of DEPC treated dH_2O.

II.2.3.3 RNA in situ pre-hybridisation

During the first day, the metal rack holding glass slides covered with tissue sections was successively immersed in the following solutions: twice in histoclear for 10 min to dissolve the wax, followed by a re hydration using short incubations (1-2 min) in increasingly dilute solutions of ethanol in DEPC-treated dH_20. The procedure was initiated by two incubations in 96% ethanol, followed by single immersions in solutions of 95%, 90%, 80%, 60% and 30% ethanol. The rack was then briefly plunged in water (1-2 min) before being left for 15-20 min in 2X SSC. In the next step, immediately before immersing the rack, Proteinase K (1µg/ml, Sigma) was diluted into a pre-warmed (37°C) solution of 100mM Tris pH8, 50mM EDTA. This incubation lasted 30 min at 37°C. The reaction was stopped with Glycine in PBS (2mg/ml) for 2 min at room temperature. The rack was then rinsed twice in PBS (2X 2 min) before being left for 10 min in freshly prepared PFA (4% in PBS, pH7). Another two rinses in PBS (2X 2min) preceded a 10 min incubation in 0.1M triethanolamine pH8 with addition of acetic acid (5ml/L) just following the immersion of the rack. This step was followed by another two rinses (2 X 5 min) in fresh PBS before proceeding to a de-hydration. This was done by short incubations (30 sec) in increasingly concentrated solutions of ethanol in water, starting with 30% ethanol, then 60%, 80%, 90%, 95% and finally twice in 96% ethanol. The rack was then stored at 4°C in a dry and closed container with a small amount ethanol to keep moisture away.

II.2.3.4 RNA in situ hybridisation

The hybridisation buffer was prepared, to a final volume of 240µl per slide sandwich (two slides against each other with a solution held by capillarity in the

middle). For a rack of 27 slides, in a 15ml falcon tube, the following components were added: 600µl of 10X *in situ* salts solution, 480µl of DEPC-treated dH_20 , 60µl 100X Denhardts salts [2% BSA, 2% Ficol, 2% Polyvinylpyrrolidone in 3X SSPE (20X SSPE : 3 M NaCl, 0.2 M NaH_2PO_4, 20 mM EDTA, pH7.0], 60µl pre-warmed tRNA (100mg/ml), 2400µl deionized formamide, 1200µl of 50% pre-warmed Dextran Sulfate and 5µl of Triton X-100 per rack. Dampened 4 folded sheets of kitchen roll covered with parafilm were laid in plastic boxes. The probe was diluted in 50% deonised formamide (1:20), denatured by heating at 80°C for 3min and left on ice until addition of the pre-hybridisation buffer (the ration of hybridisation buffer to diluted probe was 4:1). The slides were then removed from the fridge and air-dried. About 250µl of hybridization mix was pipetted onto one slide and two slides destined to be hybridized with the same probe were sandwiched together. The slides sandwichs were then placed on the parafilm, the box hermetically closed and left to stand at 55°C overnight.

II.2.3.5 RNA in situ post-hybridisation

All steps, except when the slides are arranged in sandwiches, were carried out with gentle agitation. After the hybridization, the slides were separated in warm 2X SSC (approx. 50°C), placed in the rack and rinsed in 50% formamide, 2X SSC at 50°C for one hour. This step was repeated once. The slides were then plunged twice for 5 min in NTE at 37°C, followed by a 30min incubation in NTE and RNase (20µg/ml) at 37°C. Another two rinses in NTE (5 min) at 37°C were carried out before a final wash 2X SSC, 50% Formamide. The slides were then incubated for 5 min in PBS, followed by 45 min in 1% blocking reagent (Roche) in buffer 1 (no

BSA, no Triton X-100) and 45 min in 1% BSA in buffer 1 with 0.3% Triton X-100 (BSA buffer). About 7.5 ml of the latter solution was set aside and mixed with 4 µl of the anti-dig antibody (Anti-digoxigenin-AP, Roche). Using capillary force, the antibody solution was sucked in twice in the slide sandwiches and the second time, left to stand for 2 hours at room temperature. Subsequently, the slides were separated and placed in the rack. Four rinses in the BSA buffer were carried out for 15 min each. The rack was then placed in buffer 5 for 10 min whistle the substrate solution was prepared. It consisted of 20µl of NBT (75 mg/ml in 70% DMF), 15µl of BCIP (50 mg/ml in 100% DMF) made up to 10ml with the BSA buffer. The substrate buffer was applied twice and left the second time to incubate in the dark overnight together with wild dreams of Nobel-prize winner signals. The slides were then rinsed in TE pH8 for 10 min to block the enzymatic reaction and finally, rinsed in dH_20. They were then mounted using a few drops of Entellan (Merck) and glass cover slips.

II.2.4 cDNA library

About 700 µg total RNA was obtained from young inflorescences of only one specimen of *S. wisotonensis* using the TRIzol RNA extraction method (see II.2.1). An estimated 5µg of Poly A^+ RNA was then isolated from the total RNA using the Oligotex™ mRNA kit (Quiagen). The construction of the cDNA library was carried out strictly following the manufacturer's guidelines (The Zap-cDNA® Synthesis protocol and Gigapack® III Gold Cloning Kit protocol, Stratagene).

The screening of the cDNA library was essentially following the instructions of the manufacturer's guideline aiming at screening about 1 200 000 pfu. The only modification was the use of larger petra-dishes for the first round (22cm X 22cm), LB agar (bottom agar, see II.1.7) and top agar (Diftoagar (soft) 6g/l) provided by the

institute technicians. The second round was done on square (12cm X 12cm) plates. Plaque lifting and membrane probing was all carried out following a similar technique as for the Southern blot (see II.1.12). When the membrane was resting on the top agar, holes on three corners were carried to remember the orientation. After lifting, the membranes were rinsed for 30 sec in a denaturation solution and 1.5 min in a neutralising solution (see II.1.12). They were then rinsed briefly in 2X SSC, air-dried and baked at 80°C for two hours. The subsequent hybridisation with a radioactively labelled probe was carried following exactly the same protocol as for the Southern blot.

II.2.5 RT-PCR

Reverse transcription PCR was carried on total RNA (II.2.1). The enzyme SUPERSCRIPT™ II, RNase H- Reverse Transcriptase (Life technology) was used and the reaction was carried out following the manufacturer's guideline.

II.3 Phylogenetic analyses

II.3.1 Sample selection and alignment

Protein sequences of the TCP box from a range of angiosperm species were obtained from H. Citerne (legume TCP sequences) and from the NCBI web site (www.ncbi.nihm.nih.gov). Only genes for which the complete DNA sequence of the TCP is known were included in the subsequent analyses.

TCP genes have been isolated in a wide range of species from divergent lineages [e.g. monocots (TB1 in rice and maize) and eudicots (TCP1 in *Arabidopsis*, *CYC* and *DICH* in *Antirrhinum*)]. Therefore, by comparison to the variation expected

between distantly related orthologs, the variation observed between two allelic sequences or closely related orthologs is not expected to help the resolution of a higher scale analysis. Consequently, in the following matrices, only the most relevant sequences have been included. For example, in the Scrophulariaceae, in addition to *CYC* and *DICH*, only the *CYC* ortholog of *Linaria vulgaris* was included (*LvCYC*). In the Solanaceae, one clone per putative locus was randomly selected.

All sequences were aligned manually using the alignment of Citerne *et al.* (2003) as a guide. For all phylogenetic analyses and bootstrapping, the factory settings were used unless otherwise stated. Branch support is indicated as figures on the trees or as « BS » in the text.

Three matrices were assembled. The first one (M1) included the amino-acid sequences of the TCP domain from members of all sub-classes of the TCP gene family in a wide range of species (Appendix IV.37). The second matrix (M2) included the amino-acid sequences of the TCP domain of TCP genes belonging to the sub-group where *CYC* and *TB1* are found (Appendix IV.38). Finally, the third matrix (M3) included the nucleotide sequences corresponding to the second matrix (Appendix IV.39).

II.3.2. Phylogenetic analysis

The program Paup 4.0b10 (Swofford, 2002) was used for parsimony, distance and maximum likelihood (ML) analyses. For all three types of analyses, the branch support was obtained with bootstrapping using the factory settings unless stated otherwise (see corresponding appendices). For the parsimony analysis on M1, M2 and M3, a heuristic search was carried out. For the ML analysis, the following

settings were used to implement the Trn+I+G model as selected by AIC in Modeltest 3.5: Lset Base=(A=0.3159 C=0.2615 G=0.2401 T=0.18250) ; Nst=6 ; Rmat : (1.0000 2.6283 1.0000 1.0000 3.9845) ; Rates=gamma ; Shape=1.3646 ; Pinvar= 0.3248. For distance analyses, neighbor joining (NJ) and UPGMA methods were also applied to all three matrices. For NJ and UPGMA, the ML settings were used as distance settings option for the analysis of M3.

For analyses carried out using Puzzle 5.2 (Schmidt *et al.*, 2002), BS is provided by quartet puzzling tree searches which can be interpreted in the same way as boostrap values (Schmidt *et al.*, 2002). Either *OsPCF1* (M1) or *OsTB1* (M2&3) were chosen as outgroups.

The Bayesian approach was carried out using MrBayes v3.Ob4 (Ronquist and Huelsenbeck, 2003) and following the guidelines suggested in Hall (2001). The following settings were used: Lset; Nst=6; Rates=gamma; set autoclose=yes; mcmcp ngen= 1500 000 print freq=1000; sample freq=100; nchains=4; burnin=1000. A strict consensus tree was computed which provide BS values corresponding to the posterior probability of a clade.

II.4 Plant material

II.4.1 Glasshouse conditions

The plant were grown in glasshouses, with a temperature in the range of 18 - 21°C with 12 hours of light per day.

II.4.2 Crosses

For crosses, *Rz* mutant *S. wisotonensis* plants were grown alongside wild-type specimens (Dr Badger). The lateral anthers of wild-type flowers were removed

manually before anthesis. Mutant pollen was then applied onto stigmas of wild-type flowers (Dr Badger).

II.5 Measurements of floral organs

Measurements of floral organs were done by taking a digital picture of the organ to be measured and measuring either length or surface using UTHSCSA ImageTool Version 3.0, (http://ddsdx.uthscsa.edu/dig/itdesc.html#What).

II.6 Scanning Electron Microscopy

Scanning electron microscopy was carried out at BioSEM, the Electron Microscope facility of the School of Biological Sciences, with the help of Dr. Jeffrey. The sample were dissected from fresh material and immediately frozen in liquid nitrogen (Gatan Alto cryo-preparation system for high-resolution Low-temperature SEM). The scanning electron microscope used at BIOSEM is an Hitachi 4700 II cold Field-emission SEM.

III The development of inflorescence and flowers in *Schizanthus wisotonensis*: a morphological study

III.1 Introduction

Walters, D. R. (1969) described the inflorescence as a terminal panicle with pedicellate flowers born on dense clusters or loosely spaced along the rachis.

The calyx has 5 irregular sepals united at the base. They have entire margins and their outer surface is densely covered in glandular hairs.

The corolla can be sub-divided into three different domains with one dorsal, two lateral and two ventral petals. Petal colour may vary from one plant to another, with a range of cream-white, pink, red and purple tones. In most flowers, the nectar guides observed on the corolla can be described as three overlapping layers of colour. Firstly, there is a wide white area towards the centre of the flower spanning all petals. Usually, a yellow innermost zone is also present on the dorsal petal and the dorsal-most part of the lateral petals, sometimes replaced by a dark purple colour. The outer-most edge of the yellow zone is often bordered by a purple/pink intermediate domain. Finally, small and dark spots are scattered over the yellow layer, usually more concentrated towards the median axis of the dorsal petal (see fig III.1). Any one or all the pattern elements may be absent.

The corolla forms a small tube along the length of the carpel, but petal fusion varies thereafter along the dorso-ventral axis. The dorsal petal is narrow with a nick in the middle of the top margin (Fig III.2a). The dorsal and the lateral petals are partially fused together and a furrow formed along their fused margins (Fig III.2a&b). Therefore, to flatten the dorsal half of the flower, it is necessary to introduce at least two cuts as shown in Fig III.2b. The lateral petals have 4 lobes and

Fig III.1: Specimens of *S. wisotonensis* (WT)

These 5 specimens of wild-type flowers of *S. wisotonensis* illustrate the intra-specific variation in colour and shape characteristic of this species. Colour of petal margin range from white to purple with a majority of pink flowers and rare occurrences of red/salmon flowers. The nectar guides are situated mostly on the dorsal petal and in the dorsal-most part of the lateral petals. In the upper half of the flower, the central background colour is white. Usually, a domain of yellow pigmentation is found in the innermost part of the dorsal petals and the dorsal-most margin of the lateral petals. A dark purple spotty pattern is superimposed on the yellow zone, mostly following the venation of the petal.

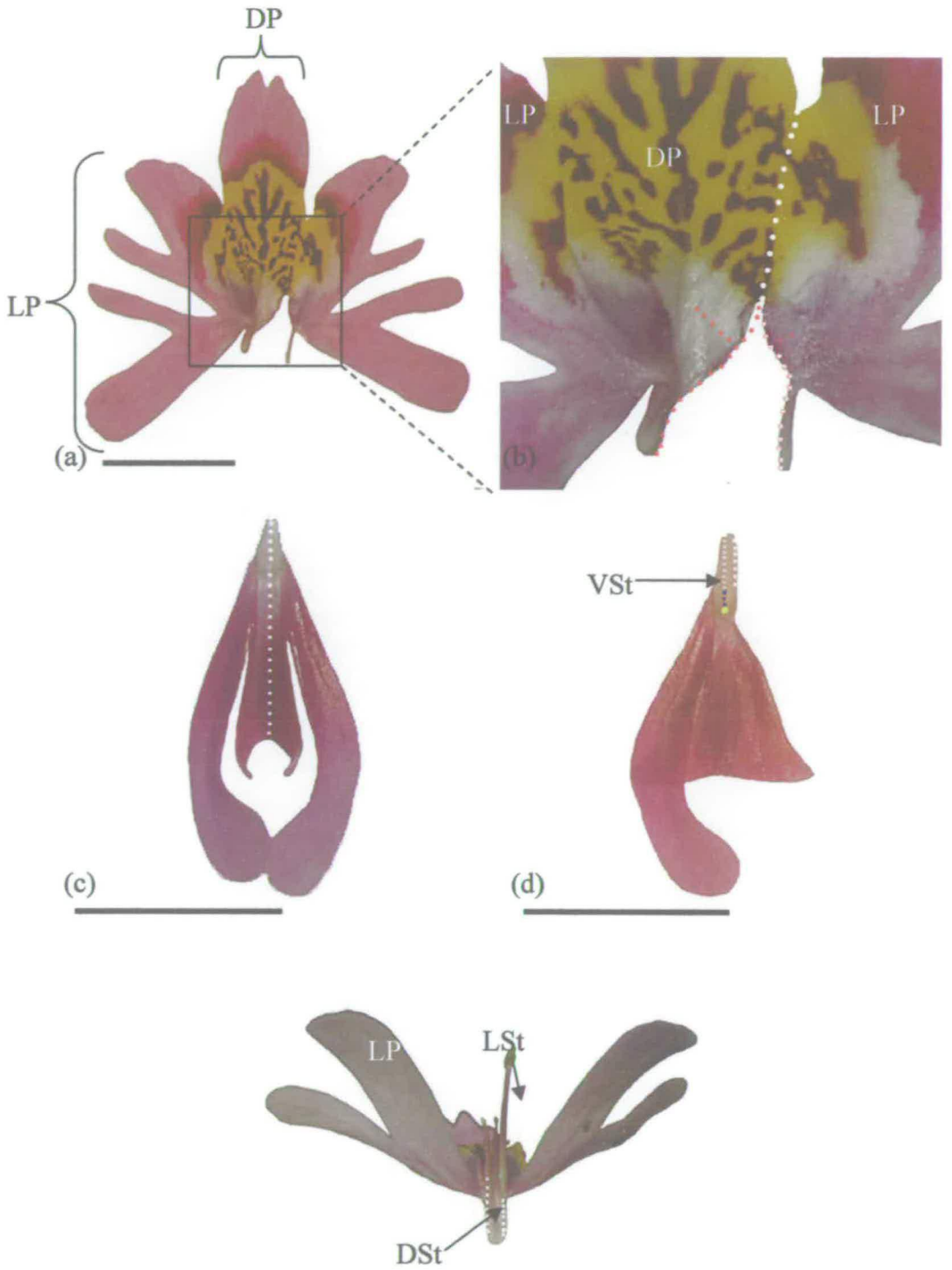

Fig III.2: The corolla and the androecium of *S. wisotonensis* (WT)
(a) Lateral petal (LP) and dorsal petal (DP). (b) Close-up of the region of fusion between dorsal and lateral petal margin (white dots). Dorsal and lateral stamens have been removed. The red dots indicate sites where cuts are required to flatten the dorsal and lateral petals. (c) Ventral petals fused on their ventral margin (white dots). (d) Flattened ventral petals, the upper lobe of the right hand-side petal has been removed. "Vst" indicates ventral stamen (white dots correspond to fused area, blue dots to the free filament). (e) View of the upper half of a flower from below. The ventral petal and the gynodecium have been removed. The white dots indicate area of filaments adnated to the corolla. Vst: ventral stamen; Lst: lateral stamen. Scale bar: 1cm

resemble butterfly wings (Fig III.2a). They are only fused to the ventral petals for the length of the tube (Fig III.2d). The ventral petals are bilobed, the ventral lobes of both ventral petals being fused along their length and with most of the ventral staminode filament (Fig III. 2c&d). The fusion of the ventral lobes results in the formation of a keel (Knapp 2002) (Fig III.2c). The upper lobes of the ventral petals are twisted and longer than their lower counterpart so that they cover the lateral stamens and form a horizontal landing platform for the pollinator (Fig III.2d & III.3).

The tridynamous androecium has three staminodes, two dorsal and one ventral, the later being the smallest (Fig III.3). Fertile pollen is only produced by the lateral stamens. The filaments of dorsal and ventral staminodes are fused to the corolla along most of their length (Fig III.2 d&e) whereas the lateral filaments are mostly free (Fig III.3 & III.2e). As the flower bud develops, the lateral filaments adopt an S shape (Fig III.3). As a result, the fertile anthers are not protruding but held in a protected position within the ventral keel. The application of a pressure on the upper lobes of the keel (e.g. landing of a pollinator) triggers the release of the stamens otherwise held under pressure (i.e. explosive mechanism). This process ensures that the pollen reaches the abdomen of the pollinator where it will be in position to be deposited on the stigma of the next flower (Cocucci, 1989).

As in most other solanaceous species, the gynoecium is bicarpellate and the median axis of the flower (i.e. the dorso-ventral (DV) axis) is oblique relative to the orientation of the IM. In *S. wisotonensis*, the style of the mature flower is longer than the lateral stamens, and its distal end is slightly bent upwards.

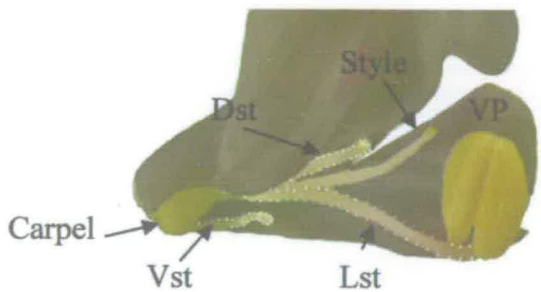

Fig III.3: The androecium of a young flower of *S. wisotonensis* (WT)
Half of a ventral and lateral petal have been removed, the corolla is shaded for clarity . This picture shows the difference in size between the dorsal staminodes (Dst), the lateral stamen (Lst) and the ventral staminode (Vst). The S shape of the lateral stamen (Lst) is holding the anther within the keel formed by the ventral petals (VP). The style is not fully grown, at maturation it will be longer than the lateral stamen.

To our knowledge, a detailed account of the development of the inflorescence and the flower of *S. wisotonensis* has not yet been published.

In this study, I have combined observations from Scanning Electron Microscopy (SEM), light microscopy and measurements on dissected flowers (see material and methods) to characterize the development of the inflorescence and the flowers of *S. wisotonensis*. I also report the development of the *rz* mutant showing decreased dorso-ventral asymmetry kindly provided by Anne-Marie Houtbraken (Syngenta, Holland). A comparison between the wild-type and the *rz* mutant will be carried out. This approach is designed to provide important information on both the expected timing and the localization of developmental changes which may have caused the mutant phenotype.

III.2 Experimental approach and results

III.2.1 Morphological characterization of the development of wild-type *Schizanthus wisotonensis* inflorescences and flowers: from the inflorescence meristem to the adult flowers

III.2.1.1 The developmental dynamics of the inflorescence in S. wisotonensis

The study of the development of inflorescences in *S. wisotonensis* is divided into two sections. First, the comparison between SEMs obtained in *Petunia* and in *S. wisotonensis* helps to understand and describe the developmental dynamics of the inflorescence meristem in *S. wisotonensis*. SEMs of *Petunia* were provided by R Koes (VU, Holland) and Paul Green (Stanford, UK). SEMs of *S. wisotonensis* were obtained both from Coral Vincent (JIC) (indicated by a star) and by using cryofixation at the microscope facilities of UoE with the help of Dr. Chris Jeffrey.

Secondly, the architecture of the inflorescence with its characteristic branching pattern will be described at the whole plant level

(i) Developmental fate and floral meristem: termination or bifurcation?

In the Solanaceae, previous studies have shown that, except for *Petunia* and tomato, the determinate cymose inflorescence terminates with the production of the flower. Growth of the inflorescence is believed to be maintained by the development of sympodial inflorescence meristems born in the axils of floral bracts. In *Petunia,* Souer *et al.* (1998) proposed a model whereby, unlike what has described for most other solanaceaous species, the inflorescence growth in *Petunia* is not terminated by the production of a flower. Instead, the flower meristem is produced by the division of the IM into two halves in a process described as a bifurcation. Successive SEMs obtained on the same inflorescence bud in *Petunia* (from the late Paul Green, Koes, pers. comm.) illustrate convincingly the bifurcating model proposed by Souer *et al.* (1998).

The dynamics of IM growth in *Petunia* from one node to the next can be interpreted as cycles during which two main stages can be distinguished (Fig III.4 a-d). The first stage can be described as the apparition of the groove within the IM (red arrow in Fig III.4), indicating that two meristems originating from the same population of inflorescence stem cells are being separated. The study of fig III.4 (a-d) shows that one meristem adopts a floral fate (FM) and the other retains inflorescence meristematic activity (IM). When both meristems are clearly separated and can be readily identified, the corresponding structure is referred to as the juvenile bifurcating structure. In Fig III.4c, both meristems in the juvenile

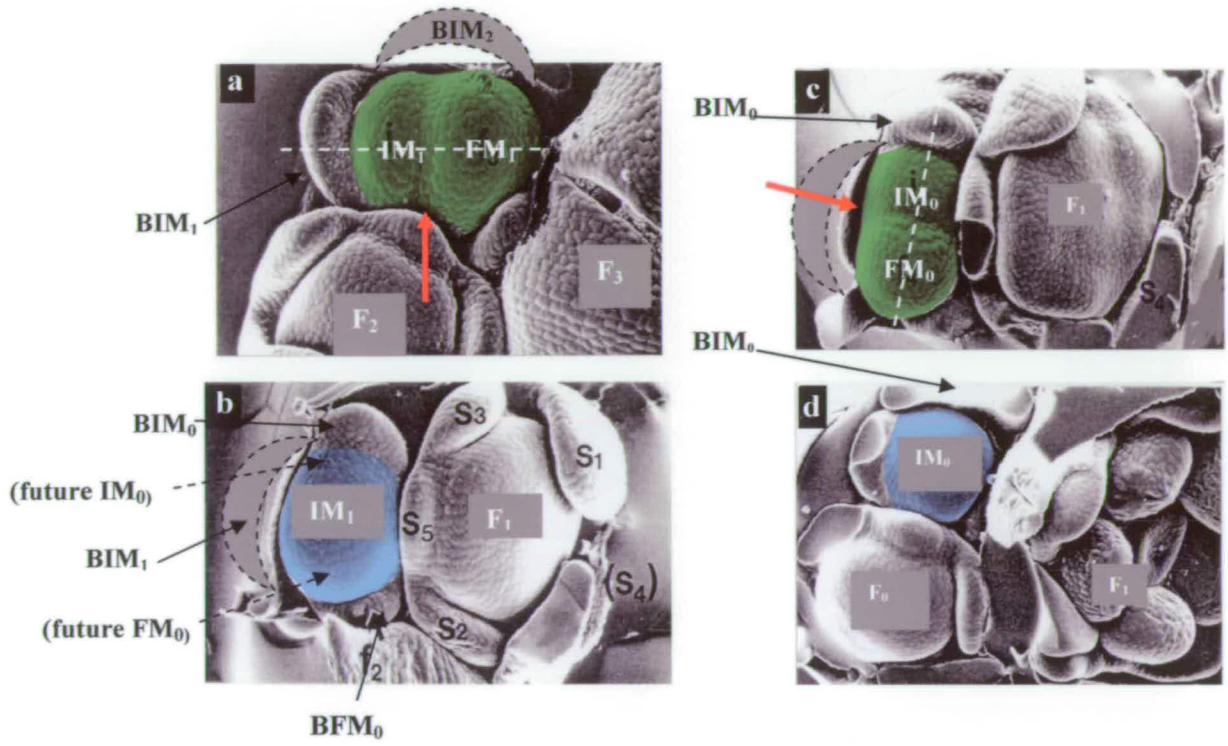

Fig III.4: Succession of SEMs showing the dynamics of the developing inflorescence and young flower in *Petunia* (from Paul Green, Stanford)

This succession of SEM obtained from the same developing inflorescence meristem (IM) spans two successive bifurcations of the inflorescence and the flower meristem (FM) (the red arrow shows groove between the IM and the FM indicative of the site of bifurcation (a&c)). (a&c) The onset of bifurcation can be seen at the stage of the mature IM (here in green, groove visible between the IM and future FM). (b) After the bifurcation, the "juvenile" IM (in blue) is elongating and two bracts initiate on its flank, one next to the half retaining the IM identity (BIM) and the other on the flank of the future FM (BFM). The juvenile IM gradually adopts a pear shape with the largest half destined to become the future FM. (c) A new groove becomes apparent announcing the next bifurcation. This median plane (i.e. axis running through the length shown here as a white doted line) of the future new juvenile IM is at right angle to that of the former mature IM suggesting that successive divisions in the IM are at right angle to each other. All images are on the same scale. S: sepals, S1: ventral sepal. F: older flower.

bifurcating structure appear to have similar sizes. During the second stage, as the structure matures, both meristems adopt characteristic shapes. The FM is bigger and rounder than the IM and once the bifurcation has taken place, the FM is round in shape and the IM is elongated (Fig III.4b) (mature inflorescence meristem). At this stage, the IM can be referred to as the juvenile inflorescence meristem (Fig III.4 b&d). As the juvenile IM matures, it elongates further with one half becoming larger, indicating the onset of the production of a new FM (Fig III.4b). During this stage, two bracts initiate synchronously (Souer *et al.,* 1998) (Fig III.4b). One bract is born at the base of the narrower end (i.e. the half retaining inflorescence identity) and the other bract is initiated at the base of the future FM half, in a "corner" position.

The groove observed across the inflorescence meristem is orientated at right angle to its axis of elongation (median axis) (Fig III.4 a&c). Once this groove can be distinguished, the median axis of the juvenile IM is apparently re-specified to be perpendicular to the former median axis. Therefore, the elongation of the IM and planes of successive bifurcations are at right angles to each other in *Petunia* (Fig III.4 a&c).

The pictures obtained by C. Vincent in *S. wisotonensis* show unequivocally structures reminiscent of the juvenile bifurcating structure (Fig III.5a) and the mature IM (Fig III.5b) observed in *Petunia.* Although pictures in *S. wisotonensis* represent separate IMs rather than snap shots of the same developing structure, the typical characteristics of the two phases described for *Petunia* are clearly recognisable. In Fig III.5b, two domes of cells are separated by a groove. This structure resembles closely the juvenile bifurcating structure described above.

Fig III.5: Developing inflorescence and young flower in *S. wisotonensis* (WT)
See overleaf

Figure (a) shows the structure of a node with the bifurcation between the inflorescence meristem (IM) and the flower meristem (FM) (juvenile bifurcating structure indicated by a yellow bracket). In the bifurcating structure, the half of the IM retaining IM identity is situated next to the former IM bract (BIM_2) and on the same side of the ventral petal (S_1) of the previous flower (F_2). Two bracts are initiated prior to the bifurcation, BFM_0 (the bract of FM_0) and BIM_0 (the bract of the juvenile inflorescence, IM_0). The orientation of the future flower (red dotted line) is indicated by the position of the ventral sepal (S_1, blue arrow) and oblique relative to the orientation of the median axis of IM_0 (i.e. white doted line axis running through the middle of the inflorescence and corresponding bract). SM: sympodial meristem in the axil of BFM_2.
Figure (b) shows an example of an older bifurcating structure. On the mature IM (orange bracket), a groove separates two unequal halves, IM_0 (the smaller half), and FM_0 (the largest half). Both IM_0 and the FM_0 are developing in the axil of a bract as shown in (a). However, the BIM_0 is not visible in b, because it is hidden by BIM_1.
Blue arrows indicate the ventral domain in the FM, red arrows indicate the location of the groove announcing the onset of the bifurcation. F: older flower.
Scale bar: 100μm

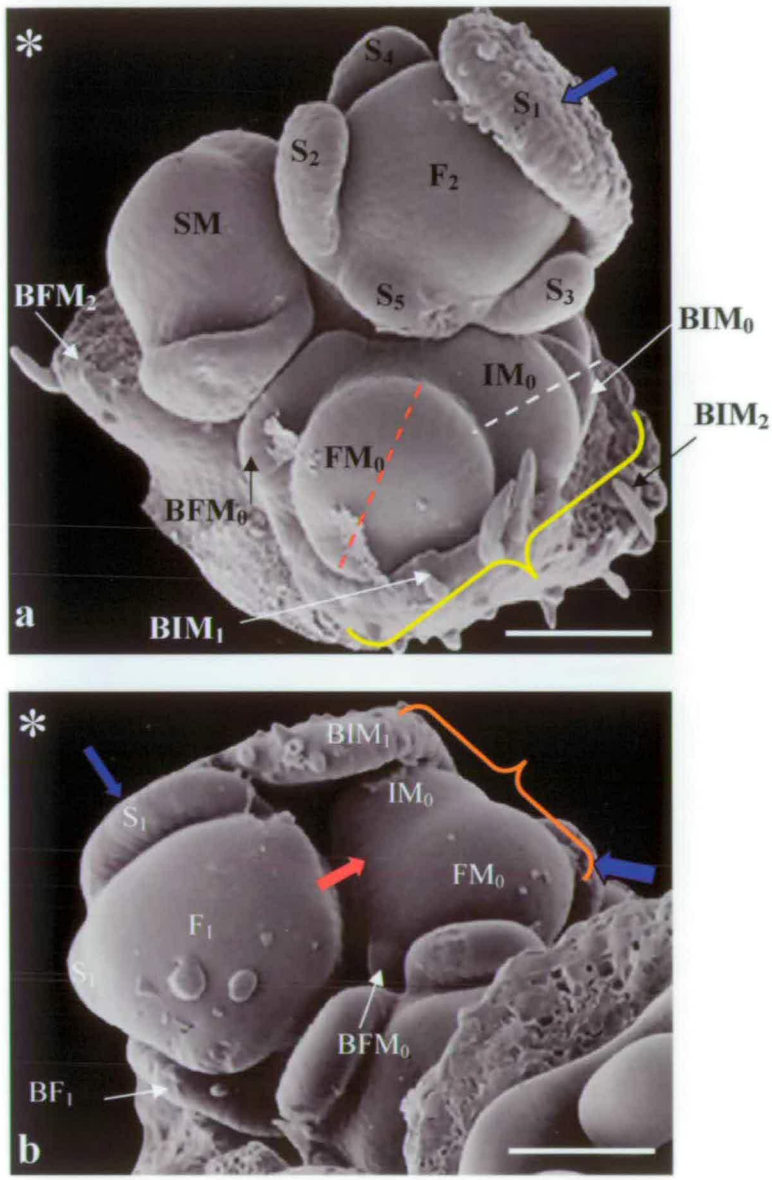
*
S4
S1
S2
F2
SM
S5
S3
BFM2
BIM0
IM0
BIM2
FM0
BFM0
a
BIM1
*
BIM1
IM0
S1
FM0
F1
S1
BFM0
BF1
b

However, unlike in *Petunia,* the two domes of cells have different sizes from the earliest stages of the bifurcation. The identity of each half can be deduced by the fact that for each bifurcation, the ventral side of the flower and the domain of the juvenile IM retaining inflorescence identity are located against the inflorescence bract (Fig III.5a). This reference point is also found in *Petunia* inflorescences (Fig III.4 a-c), supporting the hypothesis that in *S. wisotonensis* too, the smaller half of the juvenile bifurcating structure corresponds to the future juvenile IM. As for *Petunia*, the position of the groove across the juvenile bifurcating structure indicates that in *S. wisotonensis*, successive divisions of the on-growing IM take place at right angles to each other. In Fig III.5a, two bracts are visible, one subtending the flower meristem (BFM), the other subtending the juvenile inflorescence meristem (BIM). They appear to have a similar size suggesting that as in *Petunia,* they are probably initiated simultaneously. For the sake of clarity, the bracts subtending the IM and the FM will be referred to as inflorescence bract and floral bract respectively.

Therefore, in summary, these observations indicate that *S. wisotonensis* does not show cymose branching and a sympodial growth habit. Instead, the growth of the IM is continuous, and flowers are produced by the commitment of more than half the cells of the IM to a floral fate. The splitting of the IM resembles a bifurcation as described for *Petunia* by Souer *et al.* (1998), with both the indeterminate IM and the determinate flower being subtended by their respective bracts. Successive IM divisions take place at right angles to each other. Consequently, the axes of the flowers being oblique relative to that of the inflorescence, flowers are alternatively right and left-handed (model in Fig III.6&7).

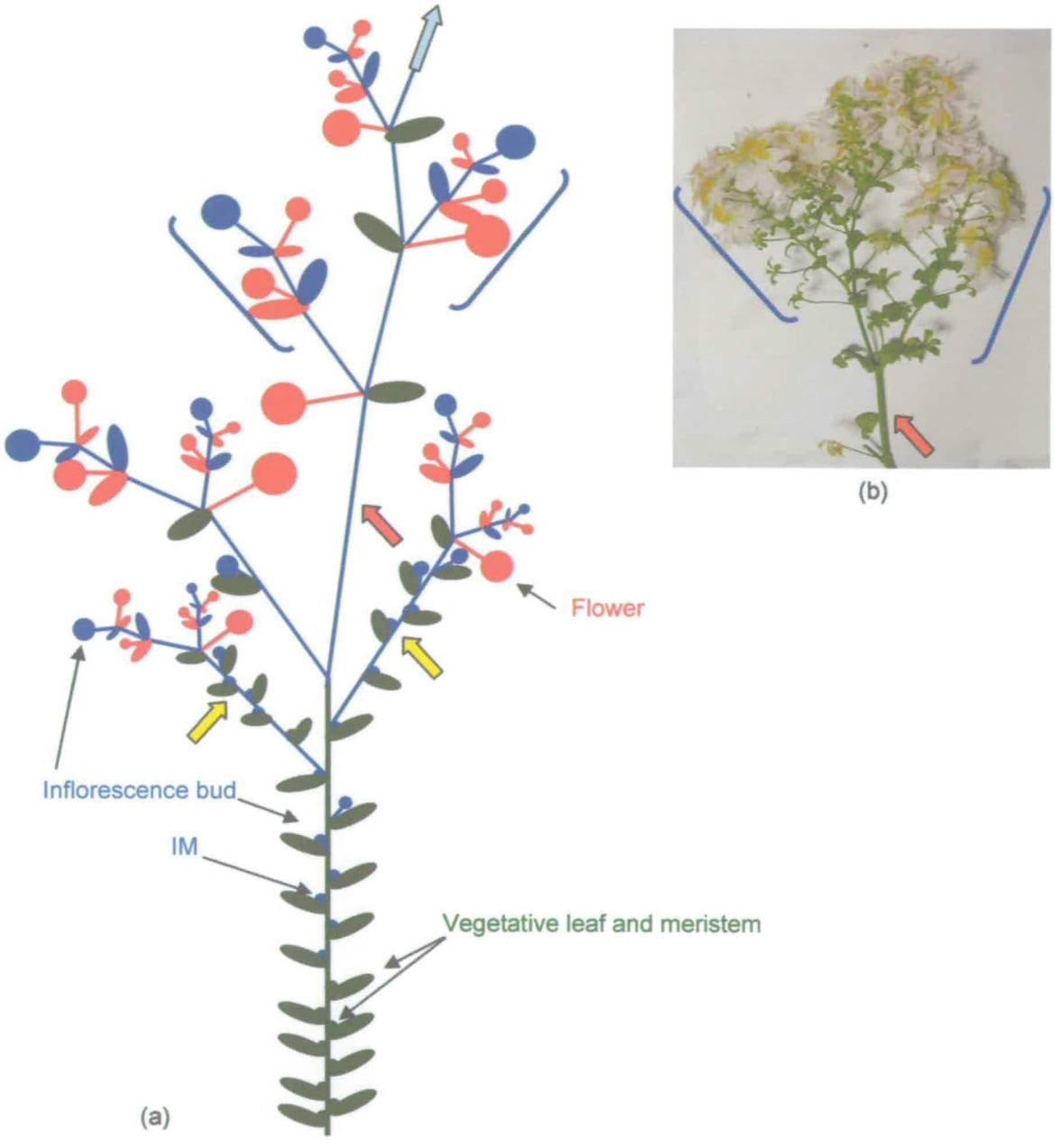

Fig III.6: Whole plant architecture after floral transition in *S. wisotonensis* (WT)
(a) Diagram of a flowering *S. wisotonensis*. Vegetative organs are in green, reproductive organs are in blue (inflorescence buds, IMs and inflorescence bracts). Flowers and flower bracts are in red. The main apical inflorescence shoot is indicated with a red arrow, axial inflorescences with yellow arrows. Blue brackets indicate secondary inflorescences
(b) Photograph of a flowering *S. wisotonensis*. The apical inflorescence shoot with secondary inflorescences is indicated by a blue bracket. The pendulum architecture is clearly visible in the secondary inflorescence. The main apical inflorescence shoot is indicated with a red arrow.

Fig III.7: Model of the bifurcation of the inflorescence in *S. wisotonensis* (WT)
See overleaf

(a, b&c) Model of a developing inflorescence through three successive steps. The dorso-ventral axis of the flower meristem is indicated as a pink line. It is inferred from the position of the ventral sepal (S1), and oblique relative to the median axis of the inflorescence meristem (IM in green). This axis is indicated as a black line and forms an angle with that of the flower. In a&b, the future plane of division of IM_0 which is perpendicular to the median axis of the former mature inflorescence (IM_1) is indicated as a dotted line. The pink stripes on IM_1 show the location of the next FM (FM_0) to be produced. The bract of the flower (BF) and that of the inflorescence (BIM) share the colour coding of the structure they subtend respectively. Sepal primordia are indicated in pale pink.
(d) Inflorescence architecture (pendulum) resulting from the bifurcation pattern of the inflorescence and the oblique orientation of the gynoecium. The flowers are right and left-handed alternatively.

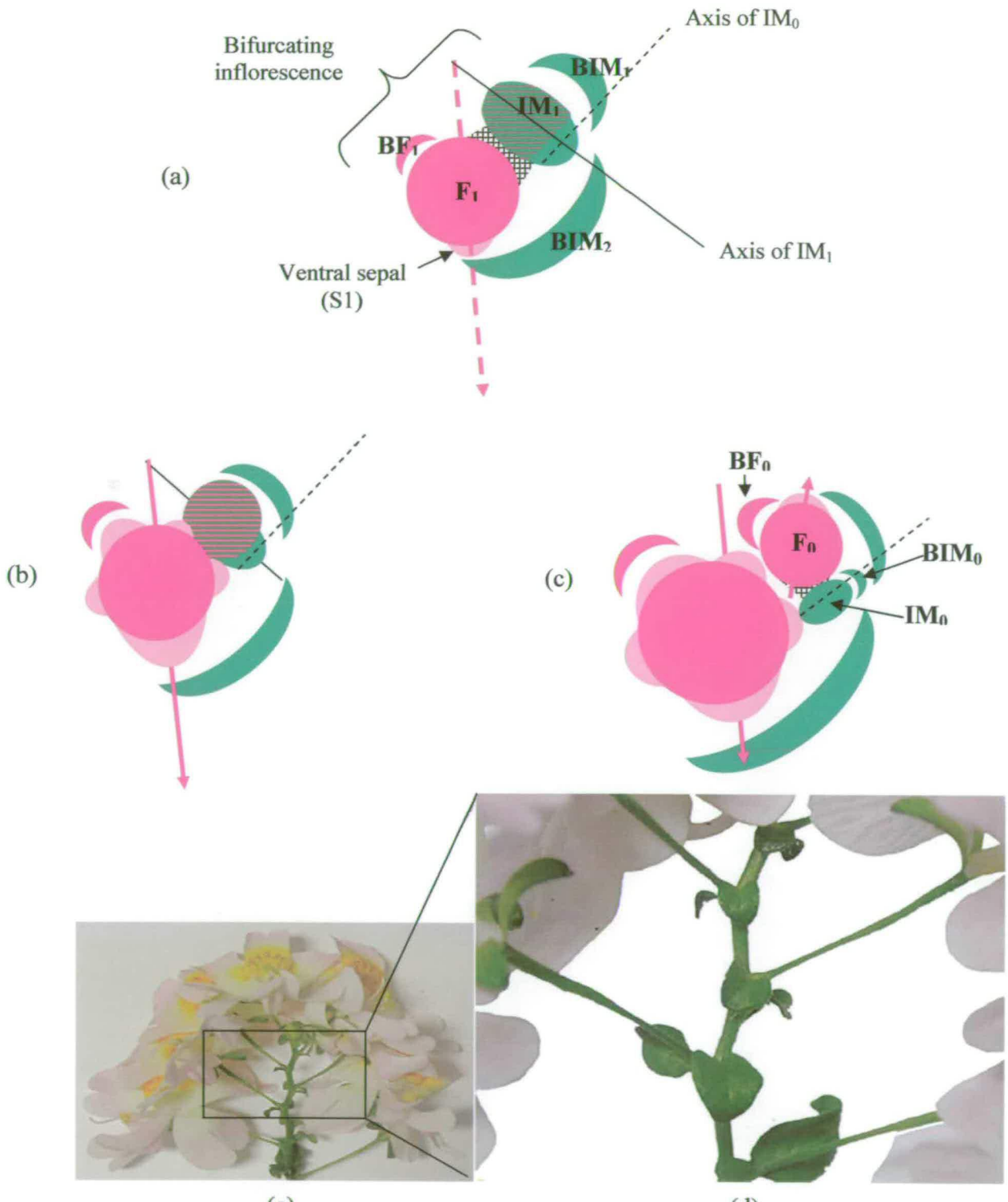
Axis of IM_0
Bifurcating inflorescence
BIM_1
IM_1
BF_1
(a)
F_1
BIM_2
Axis of IM_1
Ventral sepal (S1)
(b)
BF_0
F_0
BIM_0
(c)
IM_0
(c)
(d)

(ii) Branching pattern of the inflorescence at the whole plant level

A detailed study of a mature plant (Fig III.6a) shows that after the transition to flowering, most if not all axillary vegetative meristems below the primary inflorescence become IMs in a basipetal gradient. As new axillary shoots develop, they produce a few vegetative leaves before becoming inflorescences. For both apical and axillary inflorescence shoots, a similar branching pattern can be observed. First a few vegetative leaves are produced on a monopodial stem. In their axils, either vegetative or inflorescence meristems can be recognised. In inflorescence meristems, a bifurcation takes place with the production of the first flower. In the axils of flowers, secondary IMs can be found. However, no axillary meristems develop in the axis of the flowers born on secondary inflorescences.

Regular pendulum architecture, that is with alternating right-handed and left-handed flowers, is expected to result from the division pattern of the inflorescence meristem as described earlier (Fig III.7d). In primary inflorescences, the pendulum is not easily observed due to the displacement of the flowers and the inflorescence axis caused by the growth of secondary inflorescences. This pattern is best observed during the latest stages of flowering, in secondary inflorescences which do not show axial branching (Fig III.6b & III.7d).

III.2.1.2 Initiation of organ primordia in flowers of S. wisotonensis and the establishment of dorso-ventral asymmetry

In this section, the development of the flower from the emergence of the flower meristem to the adult flower is described. Different stages will be defined which represent phases of growth observed with both SEM and light microscopy. Stage 0 (marked by a groove across the elongating IM) corresponds to first visible

signs of the differentiation of the group of cells with a floral fate. After the bifurcation, the flower meristem emerges during the phase referred to as stage 1. The ventral sepal primordium is the first floral organ to develop (Fig III.5a; model in Fig III.7 a-c), and its position is a marker of the dorso-ventral axis of the floral bud (Fig III.5a; model in Fig III.7 a-c). This observation suggests that the oblique orientation of the flower relative to the inflorescence is established before stage 1 in floral development.

After the emergence of the ventral sepal (S_1), the remaining 4 sepal primordia initiate almost synchronously during stage 2 (Fig III.8 a&b). The ventral sepal is markedly larger than the others through these early stages (Fig III.8 a&b). The second largest sepal (S_2) is the dorsal sepal situated on the same axis as the bract. The other three sepals, the two lateral (S_3 and S_4) and the dorsal sepal closest to the inflorescence (S_5) appear to be smaller than S_1 and S_2 up till later stages. Overall, from stage 1, although sepal length is variable, the ventral sepal is bigger than the other 4. On all sepals, hair initials are visible on their adaxial surface from stage 3 (earlier for S1). They will eventually form multi-cellular glandular hairs in the mature flower.

In late stage 2, two large dome-shaped primordia can be distinguished in the central part of the FM, they are the lateral stamens incipients (Fig III.8 b&c). These divide the flowers into 2 asymmetrical halves along the dorso-ventral axis, thereby setting up the first manifestations of zygomorphy.

During stage 3 (Fig III.8d), primordia of staminodes and petals appear synchronously. In late stage 3 (Fig III.8e), the gynoecium forms, resembling a bulging ring in the centre of the flower. The developing petals and stamens are not

Fig III.8: Early stages of floral bud development in *S. wisotonensis* (WT)
See overleaf

(a) Early stage 2: all sepal primordia have emerged, the ventral sepal (S1) is initiated earlier than the other four. (b) Stage 2, all sepal primordia are developing, the difference in their relative sizes is more marked than in (a). (c) Late stage 2, the primordia of the two lateral stamens (pLS) are now visible resembling two domes of cells bulging on the side of the floral meristem (FM), S1 removed. (d) Stage 3, the primordia of the three staminodes and of the petals are emerging synchronously, S1 removed. There is a clear size difference between the staminodes (pVS) and the lateral stamen primordial (pLS), the later being the largest. (e) Late stage 3 (calyx removed), a bulging ring of cells can be distinguished in the centre of the FM, corresponding to the incipient of the gynoecium. A slight dorsoventral asymmetry of the corolla is becoming apparent with a 3/2 arrangement of the petals and the dorsal petal (pDP) being narrower than the other 4, (f) In stage 4 (calyx removed), the middle plane of the bicarpellate gynoecium becomes visible.
S: sepal; pVS: primordial of ventral staminode; pDS: primordia of dorsal staminode; pVP: primordium of ventral petal, pLP: primordium of lateral petal,; pDP: primordium of dorsal petal. Scale bar: 100 μm

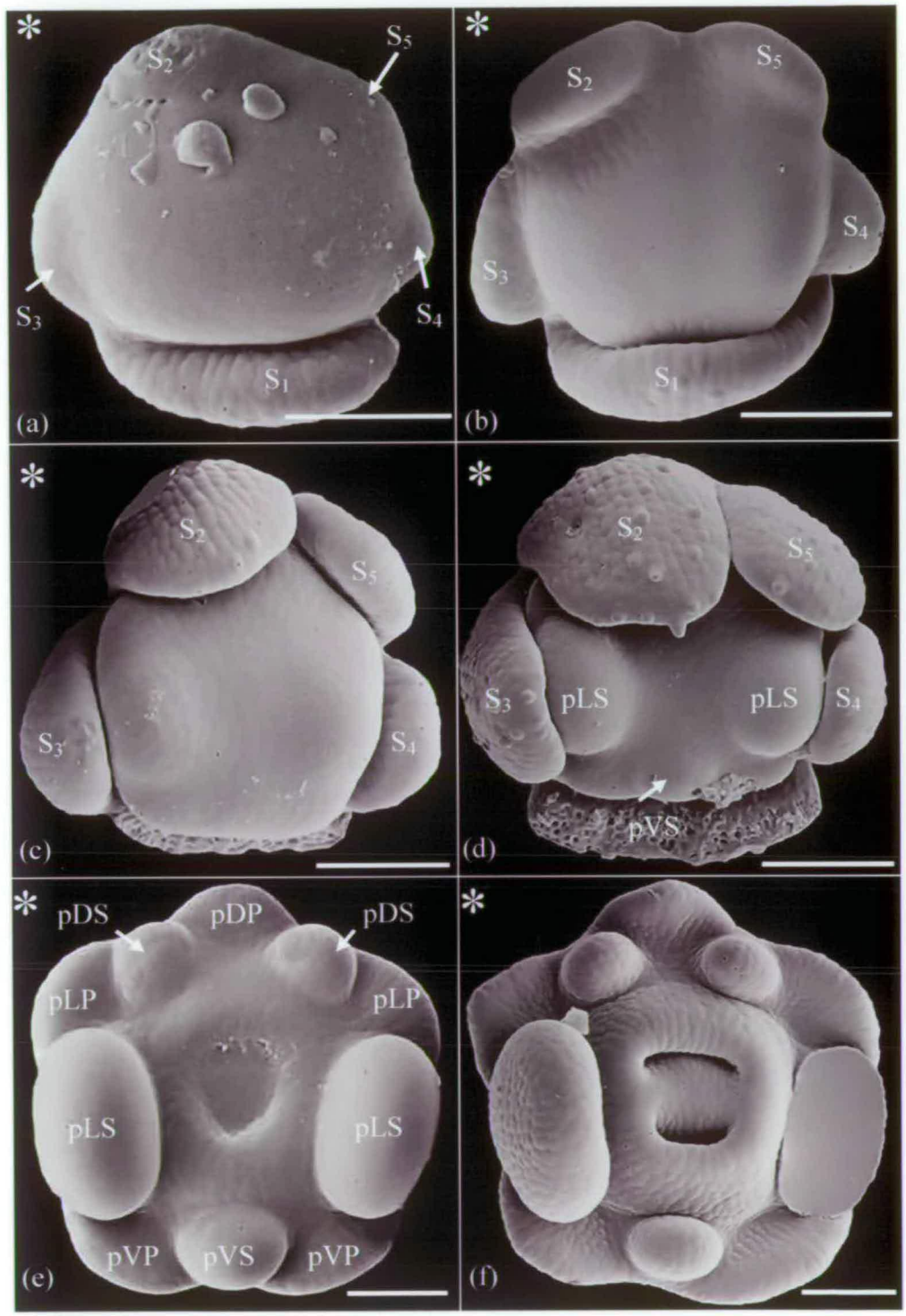
*
S2
S5
S3
S4
S1
(a)
*
S2
S5
S4
S3
S1
(b)
*
S2
S5
S3
S4
(c)
*
S2
S5
S3
pLS
pLS
S4
pVS
(d)
*
pDS
pDP
pDS
pLP
pLP
pLS
pLS
pVP
pVS
pVP
(e)
*
(f)

positioned equidistantly around the central zone due to the massive enlargement of lateral stamen primordia relative to the staminodes.

In stage 4 (Fig III.8f), the middle plane of the bicarpelate gynoecium is apparent.

By stage 5 (Fig III.9), the bicarpellate gynoecium is about to close. The indentation of the lateral and ventral petals is apparent, indicating the onset of lobbing. At this stage, the dorsal petal looks different from the rest of the corolla. It is more elongated, its top margin is not indented, and hairs initials are visible. In the androecium, a central groove becomes visible on the innermost side of the lateral stamen. This structure will later develop to form a bi-lobed anther. At this stage, all staminodes have a similar size.

III.2.1.3 Development of the juvenile flower

In *S. wisotonensis*, the flower can be dissected from late stage 5 onwards, allowing pictures to be taken with a light microscope. In addition, to allow for intra-specific variation, measurements of organ size were taken from juvenile to adult flowers to establish a growth profile along the dorso-ventral axis. The maximum length of the dorsal petal was arbitrarily chosen as the reference to order flowers from the youngest to the oldest. The elongation of the style beyond the tips of the lateral stamen appeared to be the last morphological change prior to flower senescence. Therefore, flowers are considered mature when the length of the gynoecium exceeds that of the lateral stamen.

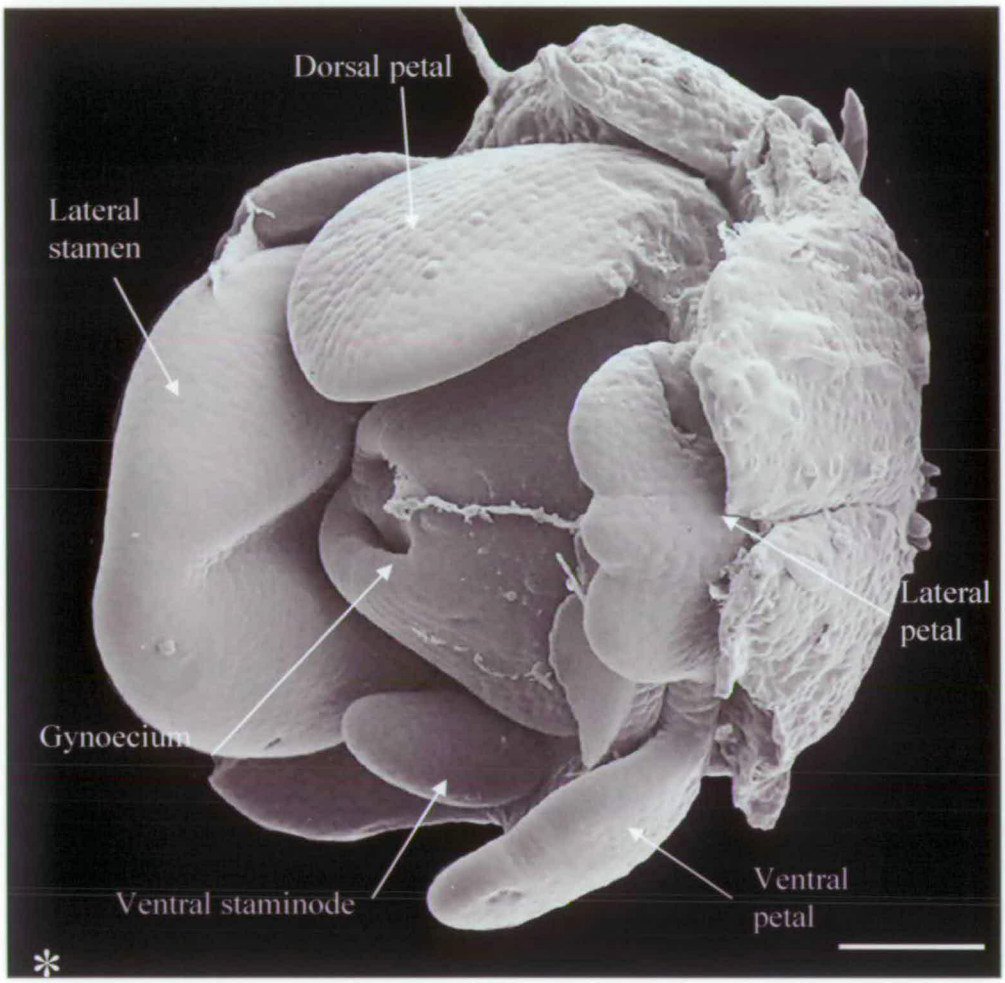

Fig III.9: Stage 5 in the development of *S. wisotonensis* flowers (WT)
In this picture, the calyx and the right stamen have been removed. At stage 5, the bicarpellate gynoecium is about to close. The lobbing of the lateral and the ventral petals is becoming visible, in contrast, the dorsal petal appears unlobed and slightly more elongated at that stage. Scale bar: 100 µm.

From stage 5 onwards, the surface of sepals was measured. On average, it increases regularly as the flower bud develops, and the ventral sepal is almost always larger than the other four (Appendix III. 1&2).

From stage 5 to the mature flower, the morphology of petals changes along the dorso-ventral axis. To describe it more accurately and determine reference points, the growth profiles of the corolla, the androecium and the gynoecium were studied in parallel.

The dorsal petal has a similar shape from late stage 5 onwards; it is un-lobed and elongated, with a notch at the distal margin (Fig III.10).

In late stage 5, for both the lateral and the ventral petals, a difference in size between their respective dorsal and ventral lobes can be observed (Fig III.10a). The dorsal-most lobe of the lateral petal is the largest one, whereas for the ventral petal, it is the shortest.

Stage 6 can be defined as the developmental point at which the 4 lobes of the lateral petals (L1, L2, L3 and L4 from upper to lower) can be clearly distinguished. They form two pairs separated by a central groove. At stage 6, L1 is the largest lobe of all. As the flower develops, the size difference between L1 and L2, 3 & 4 decreases (Appendix III.3).

During stage 6, the dorsal lobe of the ventral petal (V1) is shorter than the ventral one (V2), and in the androecium and the gynoecium, there are no noticeable changes besides organ enlargement and style elongation.

In late stage 6, the anthers of the lateral stamens are green, turgid and translucent. The lateral filaments are mostly free with an opaque epidermis. In contrast, the anthers of the staminodes are markedly smaller, drier and more opaque

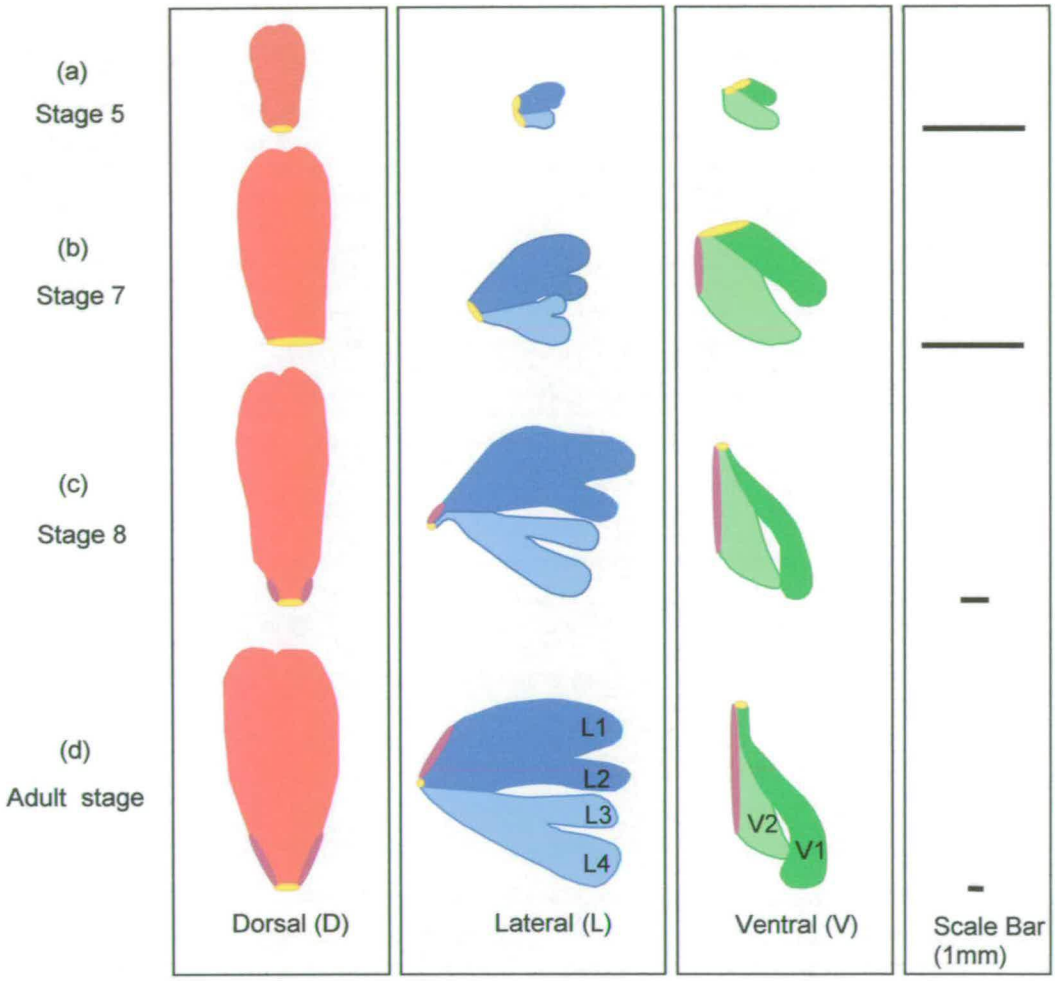

Fig III.10: Diagram of the morphological changes taking place during flower development in the corolla from late stage 5 to adult age in *S. wisotonensis* (WT)
The yellow ellipses indicate sites of attachment to the receptacle, purple ellipses indicate areas of organ fusion between neighbouring petals

than their lateral counterpart. They have a narrower filament covered of cells resembling those of the neighbouring petal epidermis.

The beginning of stage 7 can be defined by the developmental point at which both lobes of the ventral petal have approximately the same size (Fig III.10b). In the three wild-type plants observed, this stage corresponds also to anthesis for the staminodes (Appendix III.4 a&b). Stage 7 is also the earliest stage at which the lateral filaments start to elongate, as shown by the length of their free area compared to that of the dorsal and ventral staminodes (Appendix III.5).

After stage 7, as the flower matures, further changes take place. At the level of the corolla, the areas on both sides of the fused margins of the dorsal and lateral petal further expand. As a result, a furrow develops forming a protruding fold between the two petals (Fig III.11). A comparison of cell size was carried out by comparing SEMs taken in the region of the furrow and its border around stage 6 and in the mature flower (Appendix III.6). This work showed that there is a very similar cell density in the region of the furrow and its border across both stages. This suggests that cell division rather than cell expansion is responsible for the localised growth generating the dorso-lateral furrow.

During maturation, in the ventral petal, the dorsal lobe (V1) becomes longer and appear thinner than the ventral one (V2). The later remains overall larger than V1, with a surface approximately 1.6X that of V1 at maturity (average of WT1, 2 and 3). To determine if the difference in length between V1 and V2 is due to cell elongation or cell division, average cell density was measured by SEM on the proximal and the distal region of V1 and V2 (Fig III.12 & Table III.1). At stage 7, on the proximal region, about twice as many cells per $100\mu m^2$ was found in V1

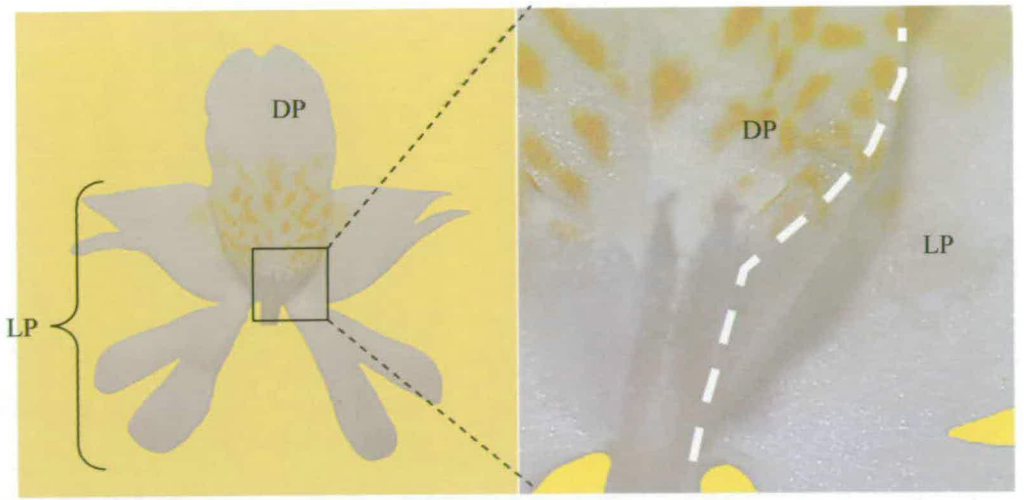

Fig III.11: Detail of the protruding furrow formed along the plane of fusion between the dorsal and the lateral petals in *S. wisotonensis* (WT)
The fused margin of the dorsal and the lateral petals is indicated as a white dotted line. DP: dorsal petal; LP: lateral petal.

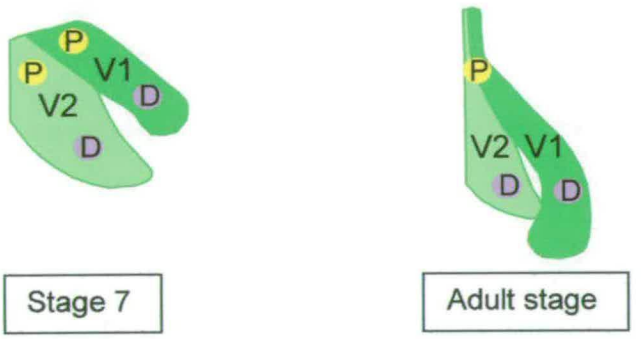

Fig III.12: Area used for cell density measurements on the ventral petal in *S. wisotonensis* (WT)
The proximal region is indicated by a yellow circle and "P" and the distal one by a "D" on a pink background.

		V1/V2
Stage 7	Ratio of lobe surface	0.6±0.1
	Average cell number / 100µm^2 Proximal domain	1.8
	Average cell number / 100µm^2 Distal domain	**7.3**
Adult stage	Ratio of lobe surface	1.4±0.4
	Average cell number / 100µm^2 Proximal domain	2.0
	Average cell number / 100µm^2 Distal domain	**2.7**

Table III.1: Cell density during development in the ventral petal of *S. wisotonensis* (WT)
Cell density was measured from SEM pictures of flowers at different stages of development. V1 refers to the upper half of the petal and V2 to the lower half.

relative to V2. In the distal region, this value increases to about 7 times (Table III.1). In the mature flower, about the same difference in cell density was found in the proximal region, whereas in the distal area, there are only about 2.7X as many cells in V1 relative to V2 (V1 is slightly larger than V2 in the mature flower). Therefore, the vigorous increase in size of V1 observed from stage 6 onwards is mostly accounted for by cell elongation. This in turns indicates that, up until stage 6, cell elongation in V1 is delayed relative to V2 is delayed.

In table III.2, all stages of development described above are summarised.

III.2.1.4 Morphological characterization of adult flowers

A detailed morphological characterization of adult flowers in *S. wisotonensis* is complicated by the intra-specific variation resulting from crosses by breeders. To address this problem, about 30 seeds were planted of which 12 germinated. A series of measurements were taken on individual mature flowers selected from these specimens grown under the same conditions. The surface of both sepals and petals was measured. For the lateral and the ventral petal, the surface of each individual lobe was recorded separately. The maximum length of each petal and their lobes was also measured, together with the size of the fused margins between petals (Fig III.13). In the androecium, the length of the filaments was measured. When possible, the length of their free region and that of the anther were also recorded. For the gynoecium, the length of the carpel and the style was measured.

To allow for intra-specific size variation in the final presentation of the results, relative areas were prefered to absolute ones. The ratio of organ sizes was

Stage 0	Groove in the inflorescence meristem
Stage 1	Emergence of the ventral sepal
Stage 2	Synchronous emergence of all other sepals Late stage 2: two masses of cells emerge, they are the primordia of the lateral stamens.
Stage 3	Primordia of all staminodes and petals visible. Late stage 3: ring of cells at the centre of the floral primordium corresponding to the first signs of the formation of the gynoecium.
Stage 4	The middle plane of gynoecium is apparent.
Stage 5	The gynoecium is about to close. The indentation of the lateral and ventral petals is apparent. Late stage 5: the difference in lobe size is visible for the dorsal and lateral petals.
Stage 6	Lateral petal: 4 lobes can be clearly distinguished. Ventral petal: the upper lobe is shorter than the lower one.
Stage 7	Ventral petal: both lobes have similar length. Androecium: anthesis of staminodes
Stage 8	Maturation of the flower: Corolla: growth of a furrow between dorsal and lateral petal; nectar guides appear; the upper lobe of the ventral petal outgrows the lower one, the keel forms. Androecium: the lateral filaments elongate and anthesis takes place

Table III.2: Summary of the different stages and their respective specific morphological attributes during flower development in *S. wisotonensis* (WT)

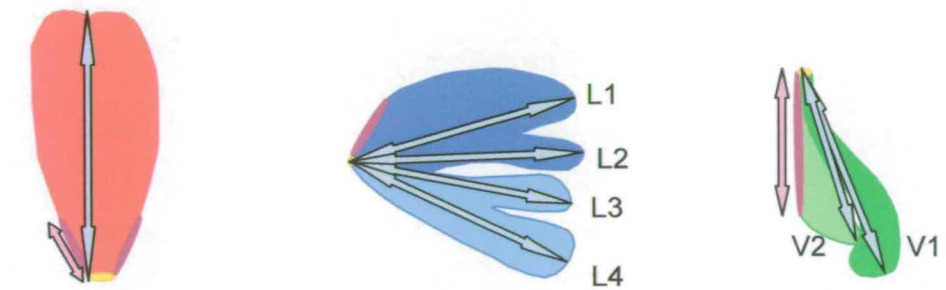

Fig III.13: Regions of the corolla measured on the mature flowers of *S. wisotonensis* (WT)
The blue arrows indicate where the measurements have been taken on the mature flowers for petal and lobe length. The pink arrows have a similar purpose regarding the region of fusion between neighbouring petals. The numbering corresponds to the identification of separate lobes.

therefore calculated individually for each plant and the resulting values were averaged.

(i) The calyx

The results show that for most specimens, the absolute and relative sizes of sepals vary between specimens (Appendix III.7). This observation suggests that the calyx of the mature flower can only be accurately and reliably described as a pentamerous whorl of sepals of variable size. The surface of all sepals features multi-cellular and stalked glandular hairs, with the abaxial surface being more densily covered.

(ii) The corolla

The difference in size between petals along the dorso-ventral axis was quantified by comparing the surface of the dorsal and the lateral petals with their lateral counterpart. The corresponding ratios obatained for each plant were then averaged to produce a value with a standard deviation. It was found that the lateral petal has the largest surface followed by the dorsal and the ventral petals (Fig III.14a). The dorsal petal, which straddles the axis of dorso-ventral asymmetry axis is the only petal to have internal bisecting symmetry. In the lateral and the ventral petals, the dorsal-most lobes are larger than the ventral-most ones (Fig III.14a). The relative extent of fusion between neighbouring petals was also measured. The results show that it is very similar in both the dorsal and the ventral region (the ratio between the averages of these two values is 1.1 ± 0.1).

Fig III.14: Quantitative morphological characteristics of the mature flower of *S. wisotonensis* (WT)
See overleaf

Measurements of organ surface and length were taken from individual flowers chosen in 12 plants of *S. wisotonensis* (WT). The bars correspond to an average of all individual measurements. (a) The first two bars indicate the relative surface of the dorsal and ventral petals compared to their lateral counterparts. The largest petal appears to be the lateral petal followed by the dorsal petal and finally the ventral one. The thirs bar indicates the relative size of the two upper lobes (L1-2) of the lateral petal compared to that of the two lower ones (L2-3). It indicates a decrease in size of lateral petal lobe surface towards the ventral domain. Finally, the last bar the relative size of the upper lobe (V1) of the ventral petal compared to that of the lower one (V2). As for the lateral petal, it indicates a reduction in size of petal lobe towards the ventral-most domain. (b) The theoretical width is the petal surface divided by its length

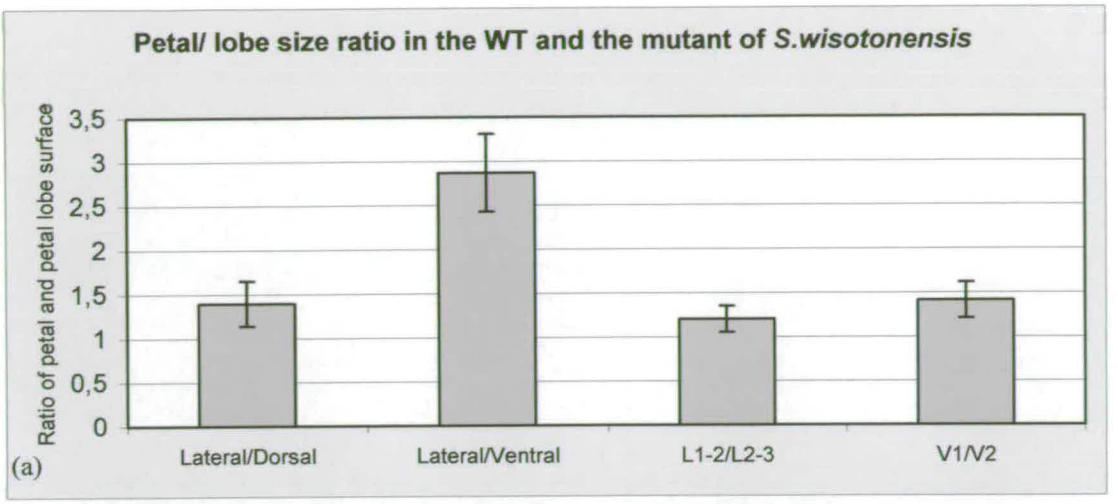
Petal/ lobe size ratio in the WT and the mutant of S.wisotonensis
Ratio of petal and petal lobe surface
3,5
3
2,5
2
1,5
1
0,5
0
Lateral/Dorsal
Lateral/Ventral
L1-2/L2-3
V1/V2
(a)

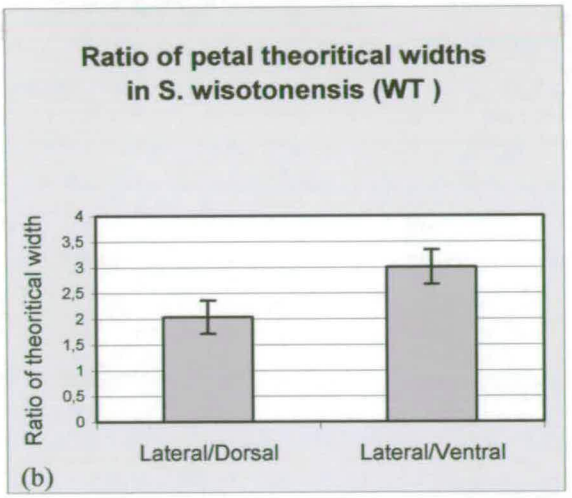
Ratio of petal theoritical widths in S. wisotonensis (WT)
Ratio of theoritical width
4
3,5
3
2,5
2
1,5
1
0,5
0
Lateral/Dorsal
Lateral/Ventral
(b)

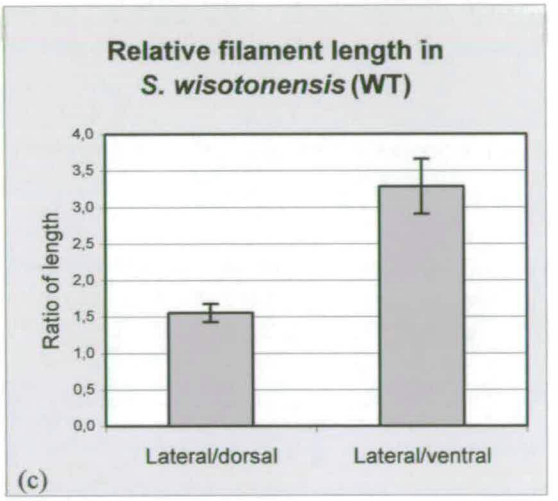
Relative filament length in S. wisotonensis (WT)
Ratio of length
4,0
3,5
3,0
2,5
2,0
1,5
1,0
0,5
0,0
Lateral/dorsal
Lateral/ventral
(c)

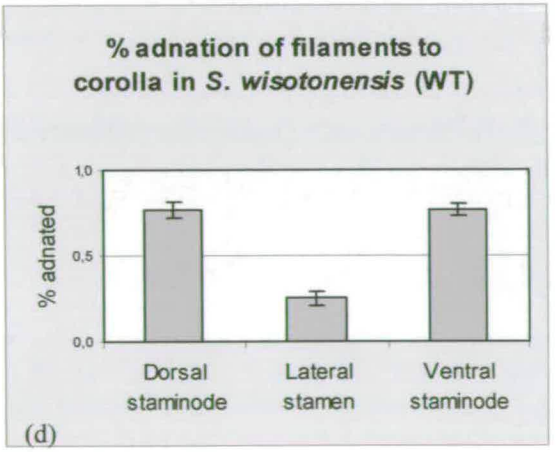
% adnation of filaments to corolla in S. wisotonensis (WT)
% adnated
1,0
0,5
0,0
Dorsal staminode
Lateral stamen
Ventral staminode
(d)

It was not possible to determine a reliable method of measuring petal width due to the changes in petal shape along the dorso-ventral axis. Therefore, a theoretical width was calculated by dividing the surface of each petal by its maximum length (average value of individual lobe measurements for the ventral and lateral petals). The results showed that the theoretical width of the lateral petal is about twice that of the dorsal petal and three times that of the ventral petal (Fig III.14b).

In the corolla, the abaxial side of petals is covered with both uni-cellular and stalked glandular hairs. On the adaxial side of the tube, the surface is increasingly strigosed (i.e. covered in short hairs lying flat against the surface) towards the thoat. In the ventral petal, the inner most domain of the ventral lobe is covered in a dense layer of stalked glandular hairs but otherwise, the rest of the adaxial surface of the corolla is glabrous.

(iii) The androecium

In the androecium, two morphological characteristics were measured: the relative length of the filament and the extent of their adnation to the corolla. The results show that the lateral filaments are about 1.5X longer than the dorsal filaments, and more than three times longer than that of the ventral staminode (Fig III.14c). About 70% of dorsal and ventral filaments are adnated to the corolla whereas the lateral ones are mostly free (only 25% adnated to the corolla) (Fig III.14d).

(iv) The gynoecium

In the mature flower, the style protrudes above the anthers. To quantify this morphological characteristic, the ratio of their respective length was calculated and the gynoecium (ovary plus style) was found to be about 1.2X longer than the filaments of the lateral stamens.

III.2.2 Morphological analysis of the *rz* mutant *S. wisotonensis* with reduced dorso-ventral asymmetry

In this section, the morphology of the *rz* mutant *S. wisotonensis* with reduced dorso-ventral asymmetry (Fig III.15) will be described in detail in compared to that of the WT flower.

III.2.2.1 Morphological characterization of the development of inflorescences and juvenile mutant flowers

When possible, the different stages in the development of the *rz* mutant flower were determined using the same morphological characteristics as for the wild-type. In the absence of the required morphological reference points, the comparison to the wild-type was based on measurements involving organs seemingly unaffected by the mutation at maturity. These included the lateral stamens and the style (Appendix III.10e).

(i) The developmental dynamics of the inflorescence in the mutant of S. wisotonensis

SEM observations of mutant plants showed that there are no apparent differences between the wild-type and the *rz* mutant at the level of the developing and bifurcating IM (Fig III.16 a-c).

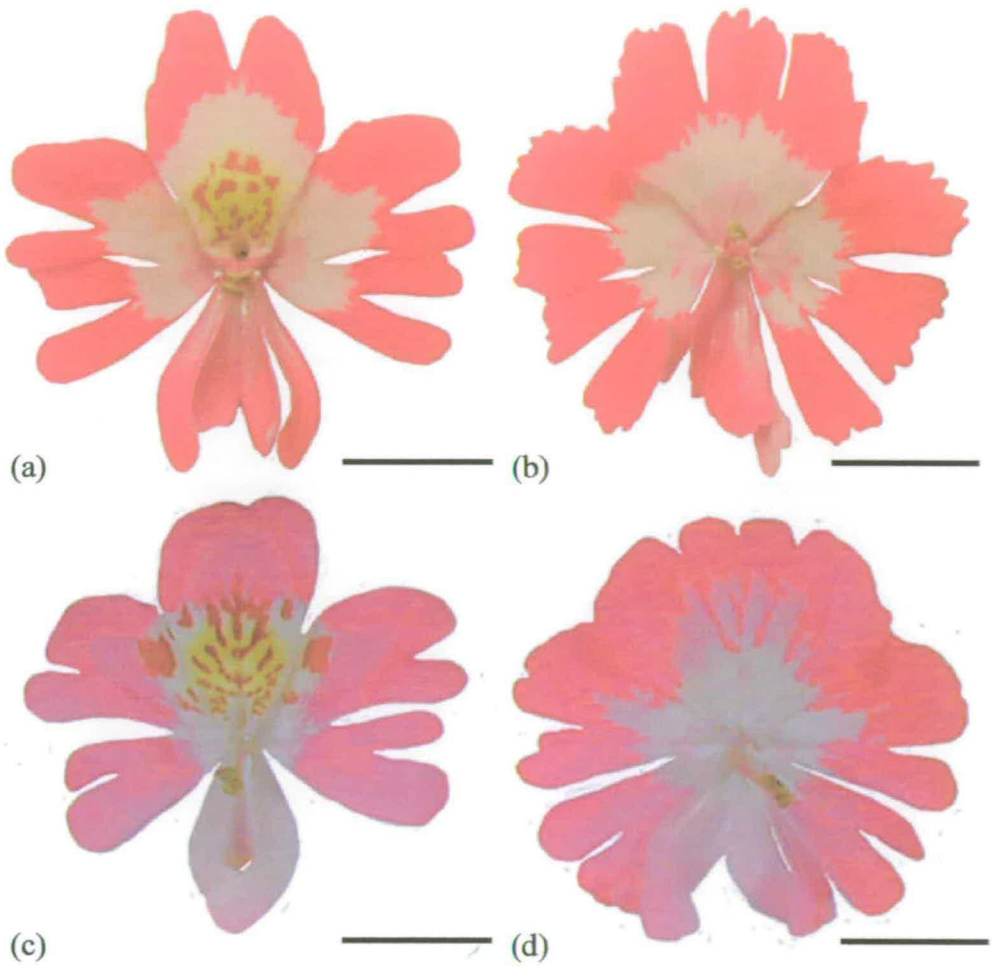

Fig III.15: Two examples of wild-type and mutant flowers developing on the same *rz* mutant plant in *S. wisotonensis*

(a) & (b) and (c) & (d) belong to the same *rz* mutant plants respectively. They grew initially as *rz* mutants (b&d) and produced wild-type looking flowers in later stages of flowering (a&c) respectively. Scale bar: 1 cm.

Fig III.16: Early development of the inflorescence and flower in the *rz* mutant of *S. wisotonensis*
See overleaf

(a) Juvenile bifurcating inflorescence. (b) Juvenile inflorescence. (c) Mature inflorescence. These SEMs show the development of the inflorescence and young flowers in the *rz* mutant. It was noted that a few *rz* mutant plants produced partially fasciated inflorescences with incomplete bifurcation and apedicilate flowers fused to the inflorescence by the calyx. In (a), the fusion of S5 to the juvenile bifurcating structure indicates that this picture might have been taken from an inflorescence undergoing fasciation. In (c), the early signs of a future bifurcation (i.e. boundary between meristems of different sizes) are visible (black arrow). FB: flower bract; F: flower; IM: inflorescence meristem; IB: inflorescence bract; S: sepal. Scale bar: 100μm

(a) Juvenile bifurcating structure (JBS) and older flower (F_3)

(b) Juvenile inflorescence and flower (F_2)

(c) Mature inflorescence and flower (F_2)

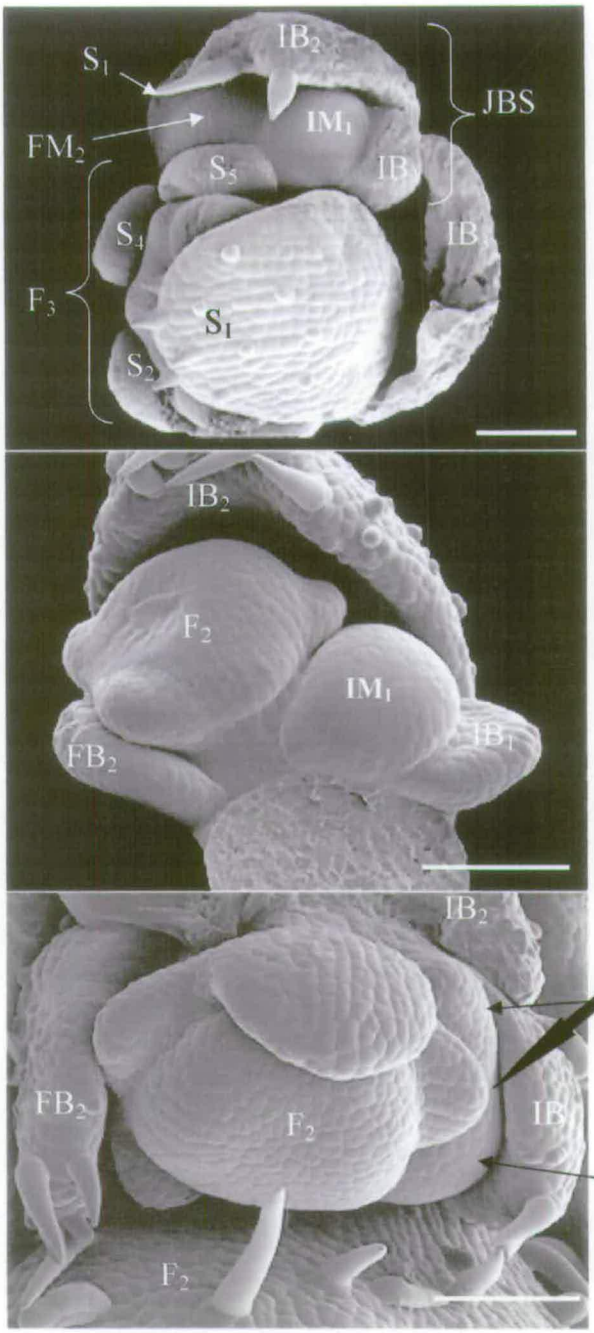

Site of the future bifurcation between the FM_0 and IM_0

At the whole plant level, the branching pattern and the inflorescence architecture of the *rz* mutant is also not different from that of the wild-type. When segregating populations were grown alongside each other, there was no obvious difference in flowering time.

(ii) Organ primordium initiation in mutant flowers of S. wisotonensis until stage 4

SEMs of flowers up till late stage 2/stage 3 indicate that there is no difference between the *rz* mutant and the wild-type flower up until this point in development (Fig III.17). Unfortunately, it was not possible to obtain an SEM picture of the dorsal petal from the *rz* mutant flower at stage 4. Therefore, it is not possible to determine if, as for the wild-type, the dorsal petal incipient of the mutant flower is slightly narrower than its lateral counterparts (Fig III.17). However, this is unlikely because in later stages (see below), the dorsal petal of the *rz* mutant flower is wider than that of the wild-type.

(iii) Development from stage 5 to the adult rz mutant flower

In the *rz* mutant, the pattern of sepal size differences is the same as the wild-type (Appendix III.8). Therefore, during floral development, the calyx appears unaffected by the mutation.

At stage 5, the effect of the mutation on the dorsal petal is clearly visible (Fig III.18). In the wild-type, the dorsal petal is markedly narrower and more elongated than the lateral petal whereas in the *rz* mutant, it is similar in size and shape. At this stage, there are no other obvious phenotypes associated with the mutation.

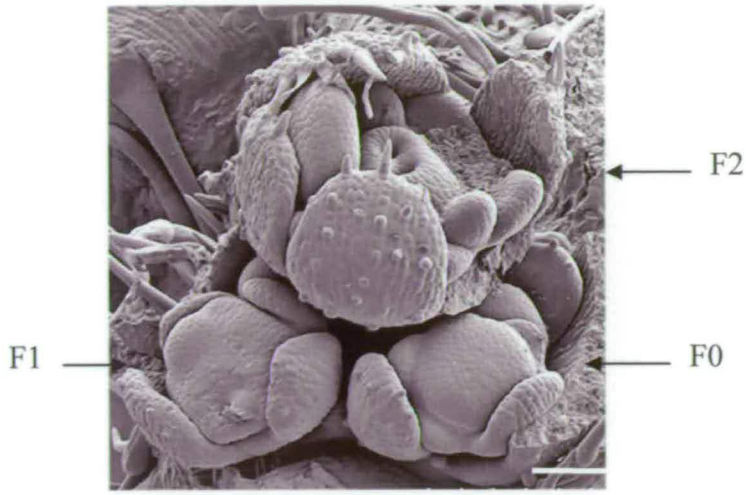

Fig III.17: SEMs showing stage 2 & 4 of flower development in the *rz* rzmutant flower in *S. wisotonensis*

The flower labelled F0 is the youngest, corresponding to stage 2 in the wild-type. In flower F1, one of the lateral stamen initials has been removed and the morphology of all floral organs is clearly reminiscent of a late stage 2 in the wild-type. Finally, in the oldest flower (F3), the middle plane of the gynodecium, the staminodes and petal primordia are visible. These organs have the typical morphological characteristics of stage 4 in the wild-type. A dorsal sepal and a lateral stamen have been removed. Unfortunately, in this picture, it is not possible to visualise the dorsal petal primordium to determine if its shape is different from that of its lateral and ventral counterpart. Scale bar: 100 µm.

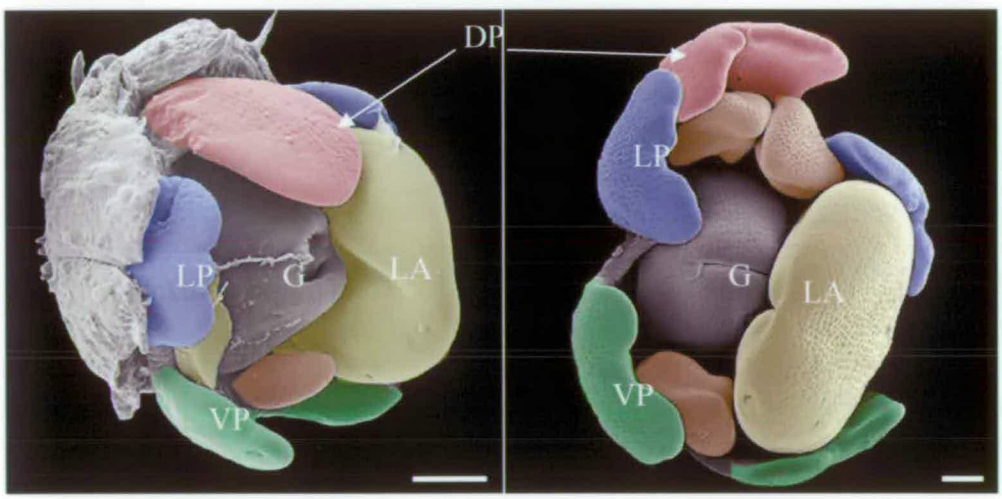

Fig III.18: SEMs showing a comparison between the *rz* mutant and the wild-type flower of *S. wisotonensis* (stage 5)

(a) and (b) are two SEM of flower buds at stage 5 with one lateral anther (LA) removed. The extent of petal lobbing in the mutant flower (b) indicates that it is slightly more advanced in development than the wild-type (a). In the corolla of both flowers, the three domains are clearly distinguishable (Dorsal: red; Lateral: blue; Ventral: green). Although the wild-type flower is less developed than the mutant one, at stage 5, the morphology of the mutant dorsal petal (in red) is clearly different from lateral and ventral petal counterparts. In the mutant, the dorsal petal is very similar to the lateral ones. These SEMs show that except for the corolla where dorsalisation of the dorsal petal is lost, there are no other phenotypes associated to the mutation at stage 5. Scale bar: 100µm.

In the *rz* mutant, both lobes of the ventral petal have very similar length through development (Appendix III.9). In the wild-type, the first main reference point for stage 7 is when the length of V1 equals that of V2. Therefore, for the *rz* mutant, stage 6 and 7 will be grouped together, corresponding to the phase from the emergence of 4 lobes in the lateral petal to the anthesis of the staminodes.

In stage 6-7, the effect of the mutation on petal elongation is obvious for both the dorsal and the ventral petals. In the wild-type, the lateral anther incipients, and to a lesser extent the ventral staminode, are almost entirely covered by the dorsal and the ventral-most half of the ventral petals (Fig III.19a). In the *rz* mutant, neither petals elongate to the same extent so that the lateral anthers protrude from the corolla and the ventral staminode is more visible than in the wild-type (Fig III.19 b-d). Unlike in the wild-type, the dorsal petal looks at least as wide as its lateral counterparts.

Another important morphological difference between the wild-type and the *rz* mutant is that from stage 6-7 to maturity, there are no obvious localised "secondary" outgrowths.

III.2.2.2 Morphological characterization of adult rz mutant flowers and comparison with wild-type in S. wisotonensis

To provide an accurate photographic account for the difference in organ morphology and sizes between the wild-type and the *rz* mutant, pictures were taken from an mutant and wild-type flower produced by the same *rz* mutant plant which displayed a few rare revertants (i.e. wild-type) flowers.

In order to describe more accurately quantifiable changes in petal organ morphology associated with the *rz* mutant phenotype, similar measurements as in

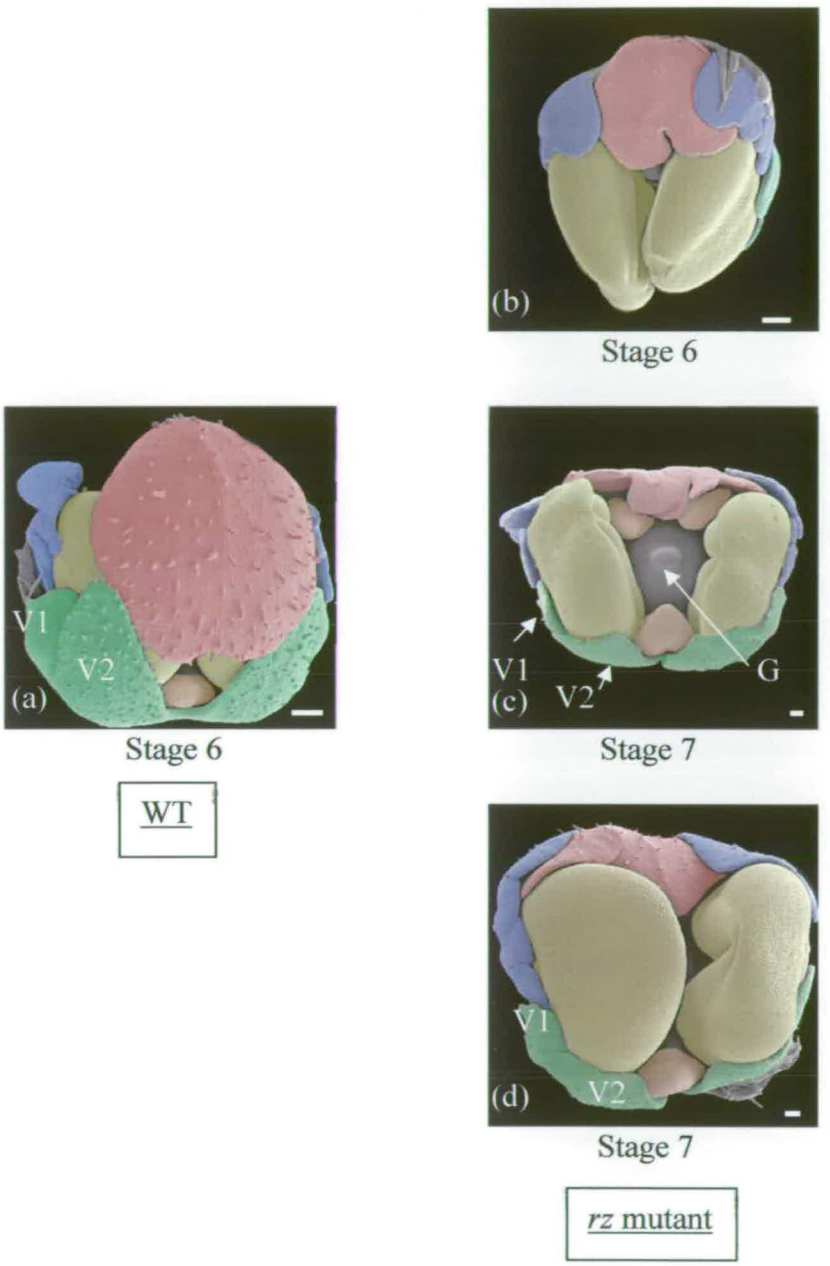

Fig III.19: SEMs showing a comparison between the wild-type and the *rz* mutant flower of *S. wisotonensis* (stage 6-7)

These four pictures show two phenotypes associated with the *rz* mutant. First, in the mutant flower (b, c&d), the dorsal petal (in red) is shorter in length compared to the wild-type (a) where it outgrows the lateral petals (in blue) and covers the lateral developing anthers (in yellow). Secondly, the difference in size of the ventral lobes (V1&V2, in green) in the wild-type is not as marked in the mutant (c&d). Lateral stamens and anthers are coloured in yellow and staminodes in orange. G indicates the gynoecium. Scale bar: 100μm

the wild-type flower were taken on 7 *rz* mutant plants grown under the same conditions. Finally, a study of SEMs in the *rz* mutant will provide the data necessary to describe more subtle effects of the mutation on the gynoecium and on cell shape.

(i) The calyx

In Fig III.20-1, the calyx of the wild-type and the *rz* mutant are similar in morphology further supporting the suggestion that the mutation does not affect sepal development.

(ii) The corolla

In the adult flower, when wild-type and *rz* mutant half flowers are compared side by side, the *rz* mutant dorsal and lateral petals appear similar in size and morphology (Fig III.20-2; Appendix III.10a). The *rz* mutant dorsal petal is bilobed with both lobes being mirror images of the upper lobe of the lateral petal (Fig III.20-2). In addition, this resemblance to the lateral petal is enhanced by the absence of the dorsal specific nectar guides spanning the dorsal and dorsal-most domain of the corolla in the wild-type (Fig III.20). Therefore, one effect of the mutation on the corolla is a loss of dorsalisation, or alternatively, a gain of lateral identity in the dorsal domain. A closer look at cell morphology using SEM shows that cells of the proximal region of the *rz* mutant's dorsal petal are markedly more interlocked than any of the cell types observed in the wild-type (Fig III. 21a). In addition, unlike for the wild-type, the tube is not strigose (covered in unicellular hair) and only a few hairs are visible. In the *rz* mutant, the dorso-lateral furrow is reduced and sometimes absent (Fig III.22), however, the mutation does not seem to have any lateral specific

Fig III.20: Mature half-flowers showing the wild-type* and corresponding *rz* mutant morphology of individual organs

See overleaf

These pictures were obtained from the same *rz* mutant plant which produced a few wild-type looking flowers (WT*). Pictures corresponding to the wild-type are labelled "WT*", and "Mut" for the *rz* mutant. (1) The calyx of the wild-type looking flower looks very similar to that of the *rz* mutant. (2) In the corolla, the dorsal petal is larger and wider in the *rz* mutant than in the WT* flower. The latter has a more pronounced divide than in the true WT. The lateral petal is unchanged and for the ventral petal, V1 is slightly shorter and V2 is longer and wider than its equivalent in the WT*. In the *rz* mutant, all petals have a crenated margin (smooth in WT*) and the dorsal nectar guides are absent. (3) The dorsal staminodes have a similar length for both the WT* and the mutant. However, their adnated region is longer in the WT*. The lateral stamen and filament appear unaffected by the mutation and the ventral staminode has a longer filament in the *rz* mutant. (4) The gynoecium is similar for both the wild-type* and the *rz* mutant.

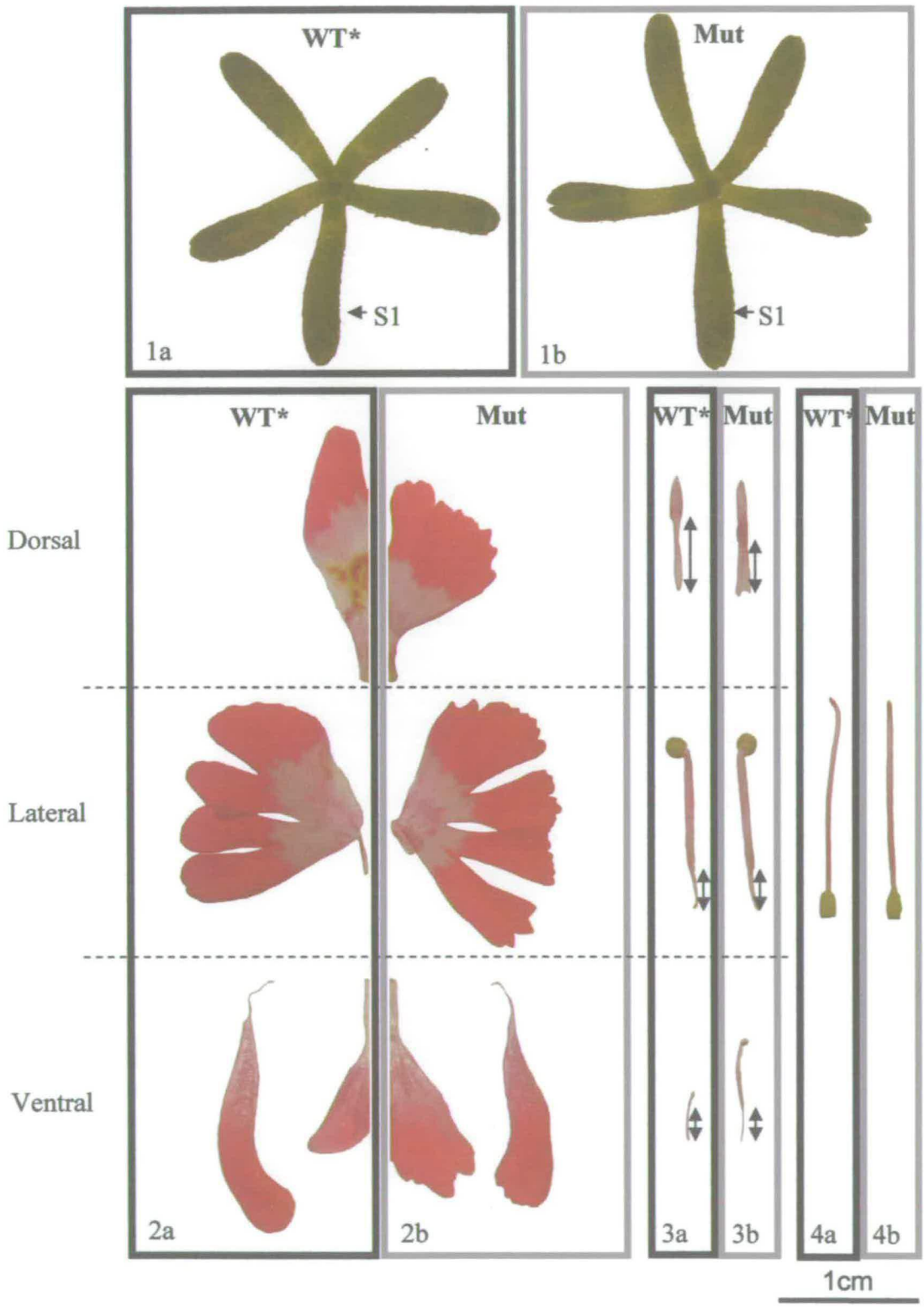
WT*
S1
1a
Mut
S1
1b
WT*
Mut
WT*
Mut
WT*
Mut
Dorsal
Lateral
Ventral
2a
2b
3a
3b
4a
4b
1cm

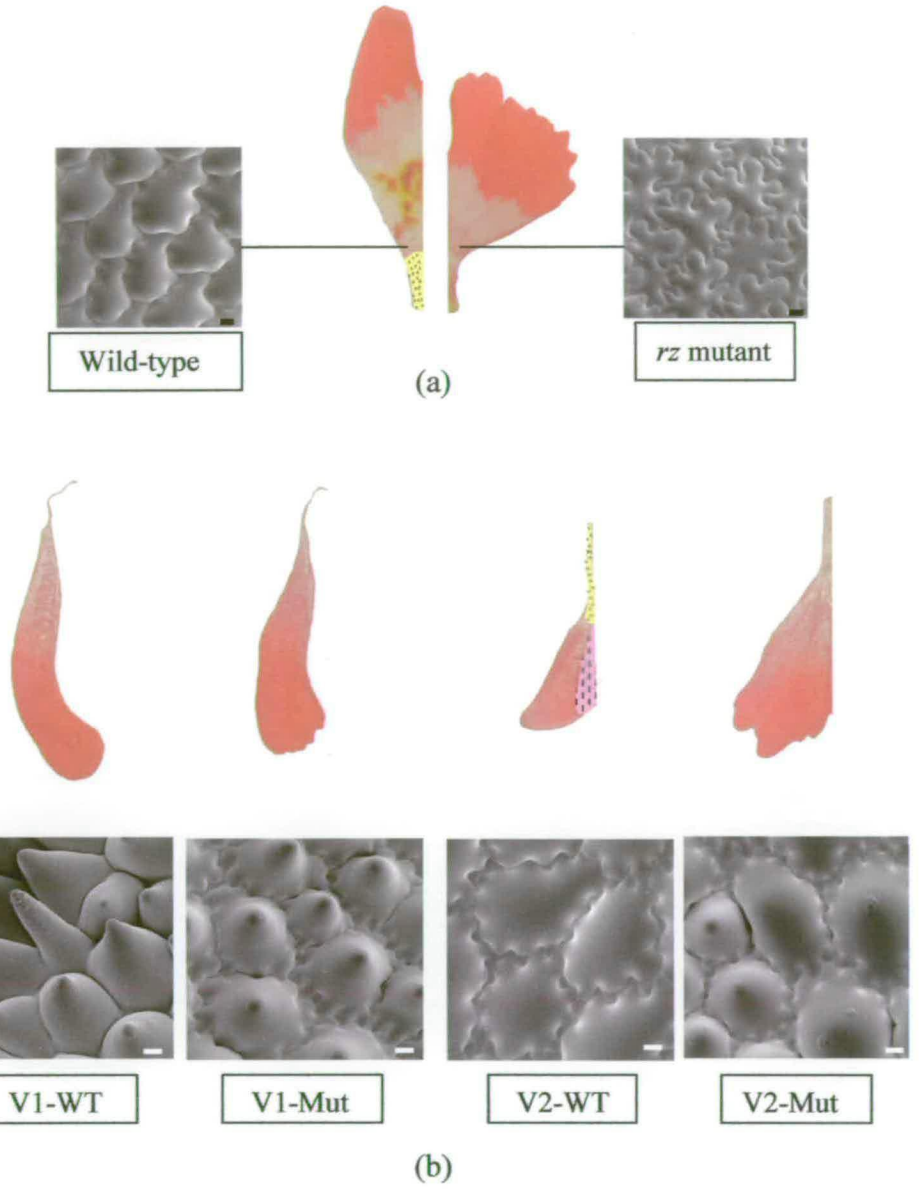

Fig III.21: Differences in cell morphology and petal surface between the wild-type and the *rz* mutant flower of *S. wisotonensis*

(a) Cell morphology of the dorsal petal is similar in the wild-type and in the *rz* mutant except for the proximal region. In the wild-type, the distal domain of the tube is covered in hairs lying flat against the petal surface (yellow background) whereas in the *rz* mutant, only a few isolated hairs can be observed. In addition, within the throat, a region can be found which display cells of morphology differing from the wild-type (crenated) to the *rz* mutant (interlocked). (b) In the wild-type ventral petal, cells from the distal region of the dorsal lobe (V1-WT) have a different morphology than those of the ventral lobe (V2-WT). In the mutant, cells from both lobes are very similar, representing a morphology intermediate between the types found in the wild-type. The staked glandular hairs (pink background) of the ventral petal are absent in the mutant flower.

Cells on the lateral petals have a similar morphology in the WT and the *rz* mutant (Not shown here). WT: wild-type, Mut: *rz* mutant.

phenotype, except for the loss of nectar guides (Appendix III.11). In the ventral domain, V1 is slightly shorter and V2 is longer and wider than in the wild-type flower. Therefore, in the *rz* mutant, there is no keel formation and in addition, V2 has a similar size to V1 (Appendix III.10a) and the stalked glandular hairs present on the ventral petal of the wild-type are absent. However, as for the wild-type, there is a residual reduction in lobe size from the dorsal-most region of the lateral petal to the ventral-most lobe of the ventral petal. Regarding cell morphology, in the ventral petal of the *rz* mutant, cells of the lips are a mixture of the two types of cells found separated on their respective lobes in the wild-type (Fig III.21b).

In appendix III.10b, the variation in relative theoretical width of petals in the corolla between the wild-type and *rz* mutant flowers indicates that in the *rz* mutant flower, the dorsal and the ventral petals are wider and not as elongated as in wild-type. This quantitative result further supports the previous observations regarding petal morphology. In addition to changes in petal size, in the *rz* mutant, the outer petal margin of all petals is crenated whereas in the wild-type, outer edges are smooth (Fig III.20-2).

(iii) The androecium

In the androecium of the mature *rz* mutant flower, the lateral stamens appear to be unaffected by the mutation as their morphology and size is identical to that of the wild-type (Fig III.20-3a&b). For the dorsal staminodes, the overall length is unchanged but in the *rz* mutant, a smaller fraction of the filament is adnated to the corolla (black double headed arrows in Fig III.20-3; Fig III.22; Appendix III.10d). For the ventral staminode, the *rz* mutant ventral filament is often larger than that of

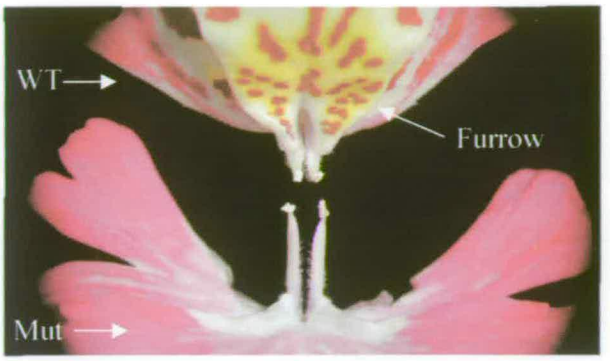

Fig III.22: Comparative view of a wild-type and mutant flower born on the same *rz* mutant plant (*S. wisotonensis*)

This picture shows two flowers obtained from the same *rz* mutant plant which produced a few wild-type flowers. The furrow is visible in the wild-type flower (WT) and not present in the mutant one (Mut).

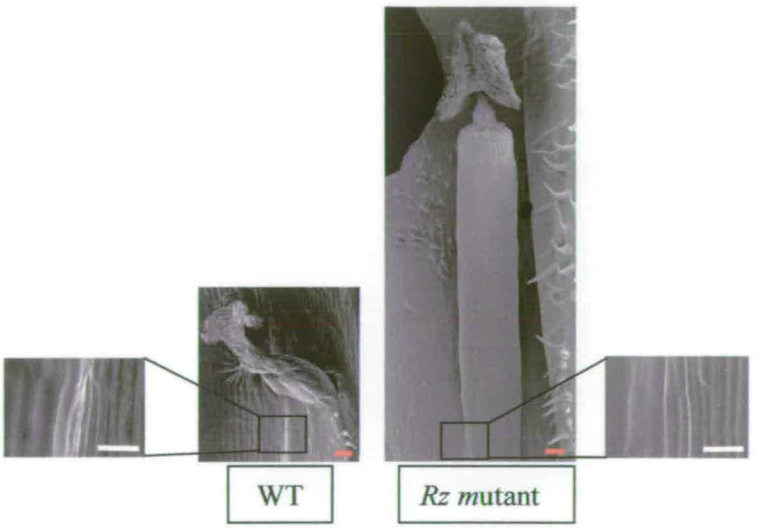

Fig III.23: Comparative view of the wild-type and *rz* mutant ventral staminodes of *S. wisotonensis*

These SEMs show the difference in size and morphology of the ventral staminode in the wild-type (WT) and the *rz* mutant. In both, cell sizes are similar as shown in the enlargements, but the ventral staminode appears overall smaller and drier than in the *rz* mutant. Red scale bar: 100 µm; white scale bar: 40µm.

the wild-type. However, its length never exceeds that of the dorsal staminodes (Fig III.21-3a&b; Fig III.23; appendix III.10c). Consequently, in the *rz* mutant, the androecium often appears didynamous (two lengths of stamen) rather than tridiydnamous.

(iv) The gynoecium

In all *rz* mutant flowers, the bicarpellate gynoecium was found to be rounder compared to that of the wild-type which is oval in cross-section (Fig III.24). In addition, the *rz* mutant has a lower seed set and reduced germination rate compared to the wild type (Anne-Marie Houtbraken, perso. comm.). These observations suggest that the mutation might affect the development of the ovary but not that of the style (Fig III.20-4).

Therefore, in summary, the main effect of the mutation is a loss of dorsalisation and a decreased ventralisation of the corolla. In the androecium, the extent of the adnation of the filaments to the corolla is reduced and the ventral staminode sometimes resembles its dorsal counterpart (i.e. partial loss of ventralisation). In the gynoecium, the compound ovary is rounder in shape in the *rz* mutant than in the wild-type and the seed set is reduced compared to the wild-type.

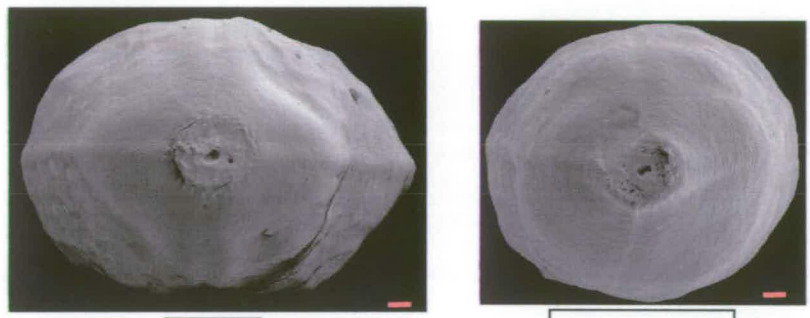

WT

Rz mutant

Fig III.24: Comparative view of the carpel from wild-type and *rz* mutant plants of *S. wisotonensis*

These two pictures of the bicarpellate ovary in the wild-type (WT) and the *rz* mutant show that in the mutant, the ovary is rounder in shape than in the wild-type. Red scale bar: 100µm.

III.3 Discussion

III.3.1 Is the bifurcating inflorescence described in *Petunia* and tomato found in *S. wisotonensis* and other solanaceous species?

The present study of the inflorescence architecture shows convincingly that the bifurcating inflorescence structure is also found in *S. wisotonensis*. A closer look at SEMs produced Hart and Hannapel (2001) suggests that a similar structure exists in *Solanum tuberosum*. Therefore, in both primitive (e.g. *S. wisotonensis*) and evolved solanaceaous species (e.g. *Solanum*), a similar bifurcating inflorescence is present instead of the sympodial inflorescence traditionally described in the literature. Therefore, this work contributes to and further supports the finding that not all solanaceous species have a sympodial growth habit. It suggests that the bifurcating structure could be an ancestral trait in this family and that it is very likely to be present in many, if not all other species in the Solanaceae.

Bifurcating apical meristems have only been described in a few other angiosperm species, in the Palmae and in the Flagellariaceae (monocots, Fisher, 1974, 1975; Tomlinson and Posluszny, 1977), and in *Asclepias syriaca* (Nolan, 1969). Interestingly, this species belong to the Apocinaceae (Gentianales), a family which is nested together with the Solanaceae in the Euasterids I (Fig I.1).

III.3.2 Does the bifurcating structure correspond to a cyme or a raceme?

If solanaceous inflorescences are structurally closer to sympodial cymes, the axillary meristems would have an inflorescence identity. Alternatively, if they correspond to racemes, the floral meristems would be placed in axillary positions.

Obviously, neither definition is well suited for the bifurcating inflorescence structure in the Solanaceae. To clarify further this point, the study of the expression of a floral identity gene called *ALF* in *Petunia* shows that when the transcript of this gene is first detected, it extends over slightly more than half of the dome-like meristematic structure identified as the inflorescence meristem (Souer *et al.*, 1998). This implies that in *Petunia*, the IM is not entirely converted into a floral meristem. The pattern of expression of *ALF* also shows that neither the FM nor the IM are formed by the differentiation of peripheral cells, i.e. neither are axillary.

Surprisingly, the originality and interest of solanaceous inflorescences has been mostly ignored in the recent literature where they are still described as scorpoid cymes with sympodial growth behaviour (Reinhardt and Kuhlemeier, 2002; Schmitz and Theres, 1999, Spichiger, *et al.*, 2002). This can be explained if, following the interpretation of Tucker in pea (Tucker, 1989), one considers that the formation of the bifurcating structure is in fact due to the precocious enlargement of the new axillary IM.

In summary, the bifurcating inflorescence has a main axis but flowers are not born in axillary positions. It is a different type of inflorescence which is *stricto-sensu* neither a cyme nor a raceme.

III.3.3 Floral symmetry and floral development in *S. wisotonensis*

The detailed study of the development of flowers from the incipient to the adult stage provides interesting insights into the mechanisms underlying the establishment of dorso-ventral asymmetry in *S. wisotonensis*. Tucker (1999) proposed that the ontogeny of zygomorphy can take place at different times during

floral development. These included the initial stages of organ formation, differential organ enlargement and late modifications such as glands, spurs and nectar guides.

In *S. wisotonensis*, the calyx shows a pattern of organ formation reminiscent of vegetative leaf phyllotaxis during the initiation of S1, S2 and S3. However, S4 and S5 appear simultaneously. Therefore, it is not possible to clearly distinguish a dorso-ventral pattern in the ontogeny of the calyx.

In most angiosperm species, floral organ primordia appear acropetally (Tucker, 1999) and consequently, petal incipients are normally formed before stamens. The Solanaceae have been traditionally described as a family where acropetal organ initiation prevails (Tucker, 1999). However, in *S. wisotonensis*, a different rule applies. In this species, once the sepal primordia have emerged, the first organ incipients to become visible are those of the lateral stamens. Their growth divides the flower apex in two asymmetric halves, thereby creating the earliest manifestation of zygomorphy in the flower of *S. wisotonensis*. Soon afterwards, the primordia of the three staminodes emerge simultaneously. Until stage 5, they are similar in size and shape along the dorso-ventral axis. However, subsequently, there is differential growth of the dorsal versus the ventral staminodes so that the later is markedly smaller in the adult flower. Once all primordia of the androecium are formed, the petal and gynoecium primordia become visible. As they emerge, petal primordia are all similar in shape. However, their subsequent growth is also clearly differential along the dorso-ventral axis. The dorsal petal has a unique morphology and it is the only petal to have internal bisecting symmetry with both halves being mirror images of each other. In the lateral petal and in the ventral petal, internal

asymmetry prevails so that the flower has three distinguishable domains, dorsal, lateral and ventral.

Finally, organ connation, localised petal enlargement and nectar guides and hairiness can all be grouped as late differentiations of structures contributing to the zygomorphic nature of the *Schizanthus* flower.

Therefore, the morphological analysis has shown that all three types of manifestation of zygomorphy as defined by Tucker (1999) are present in the floral development of *S. wisotonensis*.

III.3.4 Modeling the manifestations of floral symmetry in *S. wisotonensis*

In this section, the information provided by the comparative study of the wild-type and the *rz* mutant flower is used to infer a general model of flower development in *S. wisotonensis* (two alternative models are briefly described in appendix III.12-13).

To simplify the modeling of dorso-ventral (DV) asymmetry in *S. wisotonensis*, the manifestations of dorso-ventral asymmetry (mDV) in the flower will be grouped into separate classes (mDV1, mDV2 and mDV3) based on the localisation of the organ affected and their timing.

As mentioned above, the earliest manifestation of dorso-ventral asymmetry in *S. wisotonensis* is the division of the floral meristem in two unequal halves with respect to the position of the lateral stamen primordia. This mDV will be referred to as mDV1 (Fig III.25). From a developmental view point, the difference in size between the lateral and the dorso and ventral primordia could be interpreted as either growth stimulation of the lateral stamen incipient or growth inhibition on the

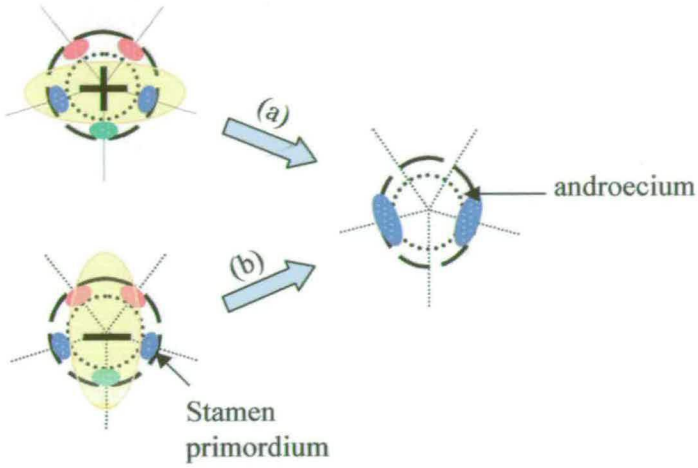

Fig III.25: Putative models for the first manifestation of dorso-ventral asymmetry (mDV1)

Concentric circle represent borders of different whorls. In *S. wisotonensis*, the first manifestation of dorso-ventral asymmetry is the apparition of the lateral stamen incipients before that of the staminodes. (a) The enlargement of the lateral stamen primordia is due to a localised growth stimulation. (b) The enlargement of the lateral stamen primordia is indirectly the consequence of growth inhibition in the central region (along the dorso-ventral axis) of the floral meristem. Yellow: hypothetic zone under localised growth dynamics ((+): growth stimulation;(-): growth inhibition); red for dorsal, blue for lateral and green for ventral.

dorso-ventral axis of the flower. The second model is more plausible since fertile stamens are required for reproduction so that they are more likely to represent the "format" organs.

In later stages, differential growth along the dorso-ventral axis contributes to DV asymmetry by affecting the corolla and the androecium. The observation of the *rz* mutant shows that the mutation affects primarily the growth of organs which are born along or close to the DV axis. These include the corolla, the androecium and the gynoecium (not discussed further as it does not participate in floral zygomorphy in *S. wisotonensis*). In the corolla, my study based on SEMs and mature flowers indicates that in the *rz* mutant, the dorsal petal is wider than in the wild-type and it resembles two dorsal-most halves of the lateral petal. The dorsal petal is the only un-lobed petal in the wild-type flower suggesting that in the latter, its specific morphology could be caused by growth inhibition in the central domain of its prinmordium resulting in a narrower petal.

In the ventral domain of the wild-type flower, the fusion of the two ventral-most lobes which is visible from stage 7 onwards is required for the formation of the keel. Together with the reduced size of V2 with respect to V1 observed in the mature flower, it can be interpreted as growth inhibition in the ventral-most region of the corolla. This hypothesis is supported by the study of the *rz* mutant in which the ventral-most lobes of the ventral petal are less reduced than in the wild-type.

In the wild-type androecium, the staminode born on the DV axis (i.e. ventral staminode) is the smallest. However, in most *rz* mutant flowers, both dorsal and ventral staminodes have approximately the same length (i.e. normal length for a dorsal staminode) even though the ventral staminode is usually thinner (Fig III.20-

3). Therefore, the detailed study of the *rz* mutant shows that the mutation does not affect early organogenesis in the androecium (i.e. the growth repression of the three staminodes) but does affect the later development (i.e. differential growth within staminodes). In the floral meristem, the ventral staminode is located next to the two ventral-most lobes of the ventral petal. Therefore, the study of the *rz* mutant phenotype shows that the growth inhibition of the ventral staminode and the ventral-most domain of the corolla are equally affected and therefore probably controlled by the same genetic mechanism.

In addition, later manifestations of dorso-ventral asymmetry in the upper half of the flower are also lost in the *rz* mutant. These include the late fusion of the latero-dorsal petal margins and expansion of neighbouring tissue (i.e. furrow), the apparition of the dorso-lateral nectar guides during stage 8 and that of different types of hairs along the dorso-ventral axis.

Therefore, this study shows that all the manifestations of DV asymmetry in the corolla and the androecium which affect organs located along or close to the DV axis can be grouped in a single class as mDV2 (Fig III.26). They are very likely to be controlled by the same genetic mechanism which is affected by the mutation.

Another manifestation of dorso-ventral asymmetry during the development of the wild-type flower is the change in lobe size along the DV axis. The larger petal lobe is found closer to the dorsal region (L1 of the lateral petal) and the smaller lobe (V2 of the ventral petal) is in the ventral-most domain of the flower. In the wild-type, this trait is only clearly visible from stage 8 on-wards, once V1 has out-grown V2 in length in the ventral petal. This polarisation of lobe size along the DV axis can be interpreted as a ventralisation (i.e. decrease in lobe size within the flower). It

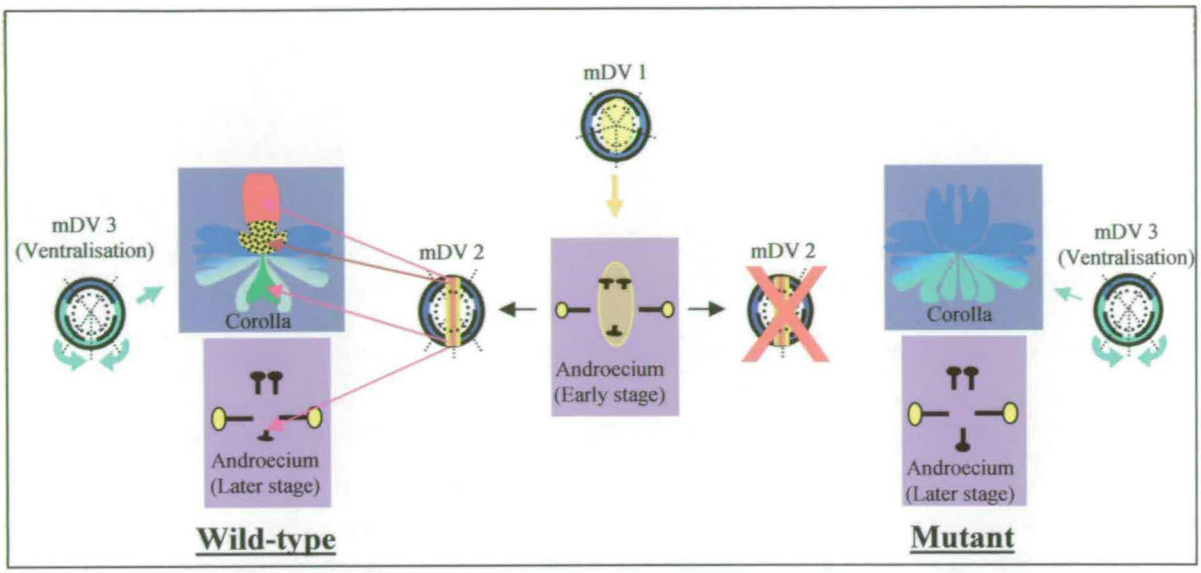

Fig III.26: Model of the establishment of dorso-ventral asymmetry in a wild-type and the *rz* mutant of S. wisotonensis

For clarity, the corolla (purple background) and the androecium (pink background) are represented separately. In the androecium, black stamens correspond to staminodes. The model proposed here corresponds to the simplest developmental pathways (i.e. most parsimonious) inferred from the comparison between wild-type and mutant flowers. The manifestations of dorso-ventral asymmetry are indicated as mDV. mDV1 corresponds to the growth inhibition of the dorsal and the ventral stamens during the enlargement of the lateral stamens which results in the division of the floral meristem into two unequal halves (yellow arrows). mDV2 correspond to the manifestations of dorso-ventral asymmetry affected in the mutant. They are all localised along or close to the dorso-ventral (DV) axis. These comprise early effects such as the growth inhibition of the central zone of the dorsal petal and the ventral-most lobes of the ventral petal and that of the ventral staminode (pink arrow). mDV2 which takes place in later stages include the formation of a furrow at the junction between the dorsal and the lateral petal, the production of nectar guides and changes in cell types (brown arrow). mDV3 is the ventralisation indicated with green arrows (i.e. reduction in petal lobe size towards the ventral domain) which is not affected in the *rz* mutant. The red cross indicates that in the mutant, the floral meristem cannot interpret the pre-pattern (i.e. trans-acting factors) controlling the downstream genetic machinery required to set up mDV2.

will be referred to as "mDV3" (Fig III.26). In the *rz* mutant, mDV3 is still present. Taken together, these observations suggest that the genetic control required for the establishment of mDV2 differs from that governing mDV3.

Until stage 7, both halves of the lateral and the ventral petals closer to the lateral stamens are smaller in size than the rest of their respective petals. This could be due to the vigorous early growth of the neighbouring lateral stamen which may recruit a large number of cells produced by the meristem. Therefore, this trait will not be discussed further in relation to dorso-ventral asymmetry.

As mentioned in the introduction, members of the TCP gene family including *CYC* and *DICH* are generally classified as transcription factors often involved in the control of cell proliferation (Cubas, 2004). This function is well illustrated in *A. majus* where *CYC* and *DICH* control both localised growth arrest and growth stimulation in whorl 2 and 3 of the flower (Luo *et al.*, 1999).

The model proposed for *S. wisotonensis* shows similarities and differences with its equivalent in *A. majus*. In both species, the establishment of dorso-ventral asymmetry involves the setting up of separate domains. The establishment of a pre-pattern (trans-acting factors controlling domains of gene expression) along the dorso-ventral axis is therefore required to establish regional identitites in the floral meristem. In *S. wisotonensis*, the most likely equivalent to what is found in *A. majus* corresponds to the polarisation of the flowers as observed in the wild-type and the *rz* mutant (i.e. mDV3). However, unlike in *A. majus*, additional elements of dorsalisation and ventralisation (i.e. mDV2) which are independent of the polarisation of the flower (i.e. mDV3) are required to produce a wild-type *S.*

wisotonensis flower. Therefore, in this species, the comparative morphological analysis of the wild-type and the *rz* mutant flowers has shown that the genetic control of dorso-ventral asymmetry is likely to require the establishment of two separate pre-patterns. One set of trans-acting elements would control the downstream elements required to produce the morphological changes associated to mDV3 in the corolla. The other pre-pattern would be acting upon target genes along the DV axis, affecting more strongly organs situated closer to the axis (i.e. not the lateral organs). It is very likely that a gene function which is required for the axial pre-pattern is missing in the *rz* mutant. Consequently, downstream genes which control developmental changes associated to mDV2 do not respond in the *rz* mutant flower.

The phenotype of the *rz* mutant indicates that the early interpretation of this additional pre-pattern can be summarized as the growth inhibition of organs from whorl 2 and 3 along the DV axis. Later interpretations of the pre-pattern along the DV axis are more complex, they include effects on cell division and cell type. Therefore, the similarities between the establishment of floral dorso-ventral asymmetry in whorl 2&3 in *A. majus* and *S. wisotonensis* support the initial hypothesis proposing a role for *CYC*-like genes in the control of zygomorphy in the latter.

If *CYC*-like genes control differential cell division in the floral meristem of *S. wisotonensis*, it is reasonable to expect them to be expressed early in development, both in the primordia of staminodes (mDV1), along the dorso-ventral axis in the central region of the floral meristem (early mDV2) and either in the dorsal or the ventral domain (mDV3). Later on in development, members of this

gene family could be expressed in the dorsal half of the flower where they may control the changes in cell division taking place in late mDV2. In the *rz* mutant, only patterns of expression of *CYC*-like genes controlling mDV2 would be expected to be affected.

III.3.5 Can other traits help to determine which model is the most likely?

The study of cell shape indicates that in the *rz* mutant, the dorsal petal features a cell type at the base of the throat which is found in no other location in the wild-type or the *rz* mutant. Therefore, the mutant dorsal petal is not an exact copy of the dorsal half of the lateral petal. This could be explained if a residual dorsal specific factor is acting upon cell morphology in this petal. Alternatively, a lateral specific factor could remain excluded from the dorsal domain. Unfortunately, none of the three models can be favoured based on our results.

III.3.6 The development of the inflorescence and the flower of *S. wisotonensis* in the evolutionary context

In the most recent published phylogenetic tree of the Asteridae, the Solanaceae have been grouped in the Solanales together with the Convolvulaceae, the Boraginaceae, the Montianiaceae and the Hydroleaceae (Olmstead *et al.*, 2000). Both the Boraginaceae and the Convolvulaceae have inflorescences traditionally described as variable cymes (Spichiger *et al.*, 2002; Walters and Keil., 1996). However, a more detailed study of *Heliotropium* (Boraginaceae) has revealed the existence of bifurcating meristem structures in the inflorescence, as in the Solanaceae (Frohlich, perso. comm.). In addition, in a related order (Gentianales), bifurcating inflorescences were also reported (*Asclepias syriaca*, Apocinaceae,

Nolan, 1969). Therefore, it is not possible to determine if the bifurcating structure has evolved independently in the Solanaceae or if this type of structure could be derived from a common ancestor to the Solanales and possibly, to the euasterids I.

The early organogenesis of *S. wisotonensis* described here agrees with what has been previously mentioned in a poster (Ampornan and Armstrong, 1988). In the Solanaceae, heterandry at inception is also observed in *Schwenkia* (Ampornan and Armstrong, 1990) and *Salpiglossis* (Ampornan and Armstrong, 1989). In the later, unlike for *S. wisotonensis,* the larger stamens are dorsal and all stamen primordia initiate simultaneously. Both *Schwenkia* and *Salpiglossis* are closely related to *S. wisotonensis*. *Schwenkia* is also a basal species in the Solanaceae (Olmstead and Reeves, 2000) suggesting that this trait (precocious development of lateral stamen incipients) might be ancestral rather than having been recruited twice independently. In *Petunia,* the petal and stamen incipient appear simultaneously and heterandry is the product of differential growth later in development (Angenent *et al.*, 1993). Interestingly, in tobacco, organ initiation follows the "normal" acropetal sequence (Mandel *et al.*, 1992). Therefore, zygomorphy as a trait first manifested with the apararition of organ incipient (mDV1) is likely to be an ancestral trait in the Solanaceae. As for the development of the inflorescence, it would be interesting to obtain SEMs from other species in the Solanales to pursue further this line of investigation.

IV. Isolation of *CYC*-like genes in *S. wisotonensis*, *N. tabaccum* and *Petunia hybrida*

IV.1 Introduction

Mark Chadwick, a PhD student working under the supervision of Prof. Coen at the John Innes Institute in Norwich investigated the existence and the role of *CYC*-like genes in *S. wisotonensis* and in *N. tabaccum.*

By carrying out RT-PCR on young inflorescence buds with degenerate primers against the TCP and R box of *CYC* and *DICH*, he isolated and cloned two partial complementary DNA (cDNA) sequences of *CYC*-like genes in *S. wisotonensis* (*SCHCYC1m & 2m*) (fig IV.1) and in *N. tabaccum* (*NICYC1m & 2m*). In addition, he obtained the 3' end of these genes and part of the 5' end of *SCHCYC1m* by race PCR (Fig IV.1). The comparison of the similarity in DNA sequence in the variable region for the two clones isolated in each species indicated unambiguously that each gene corresponded to a separate locus (34% for *SCHCYC1m & 2m*; 40% for *NICYC1m & 2m*).

In this chapter, the isolation of new sequence data for *SCHCYC1 &2* and *NICYC1 & 2* will be described, followed by that of new members of the TCP gene family in both *S. wisotonensis* and *Petunia*. In addition, the sequence data obtained from *S. wisotonensis*, *Petunia* and *N. tabaccum* will be integrated to a data matrix comprising a representative sample of the known TCP genes sequences across the angiosperms. This matrix will then be used for phylogenetic analyses to find the most likely *CYC* ortholog in *S. wisotonensis*.

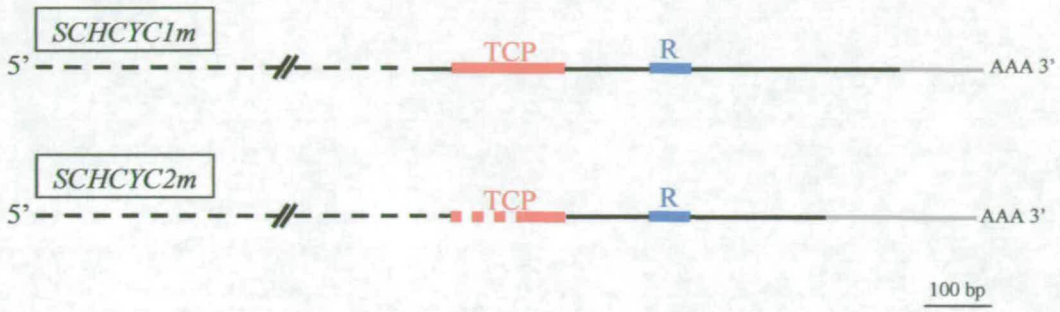

Fig IV.1: Map of the partial *CYC*-like cDNA sequences obtained by Marc Chadwick in *S. wisotonensis*

The full line indicates known cDNA sequence, the black section corresponds to ORF and the red and the blue sections correspond to the region of DNA incoding the TCP and the R domain respectively. The dashed line indicates unknown 5' region including the start codon and 5' Untranslated Region (UTR). The 3' UTR is indicated in grey.

IV.2 Experimental approach and results

IV.2.1 Isolation of new TCP genes in *S. wisotonensis, N. tabaccum* and *P. hybrida*

In this project, the new sequences isolated are provisionally labelled with the first letters of the generic name followed by the epithet *CYC*, e.g. *SCHCYC, NICYC, PETCYC*. This nomenclature was chosen to reflect the fact that all genes are isolated on the basis of their TCP and R domains. These features are shared by many members of the class II, a sub-group comprising *CYCLOIDEA* and all *CYC*-like genes isolated so far.

IV.2.1.1 Isolation of full length DNA sequences for SCHCYC1 & SCHCYC2

(i) Isolation of the 5' end for SCHCYC1 & 2 by genomic walking on genomic DNA

The genomic walking (GW) protocol comprised the ligation of an adaptor to the restricted gDNA followed by a PCR amplification of ligated fragments (including 5' DNA sequence) using gene and adaptor specific primers (See Fig IV.2). A touch-down nested PCR with adaptor and gene specific primers was used to amplify upstream 5' sequences from each gene. For both *SCHCYC1* and *SCHCYC2*, the primers were designed against the non-conserved region of their DNA sequence, i.e. out with the TCP and the R domain (Fig IV.2). For *SCHCYC1*, the nested primer (S1-R3) was originally designed for another purpose and includes a 5' *EcoR*I site.

The PCR mixes were run on a gel and a Southern blot was carried out at low stringency using a DNA fragment comprising the cDNA encoding for the TCP box from *NICYC1* as a probe (see IV.2.1.3) to confirm that the bands on the gel were not artefactual. In all digests, more than one band hybridized to the probe suggesting

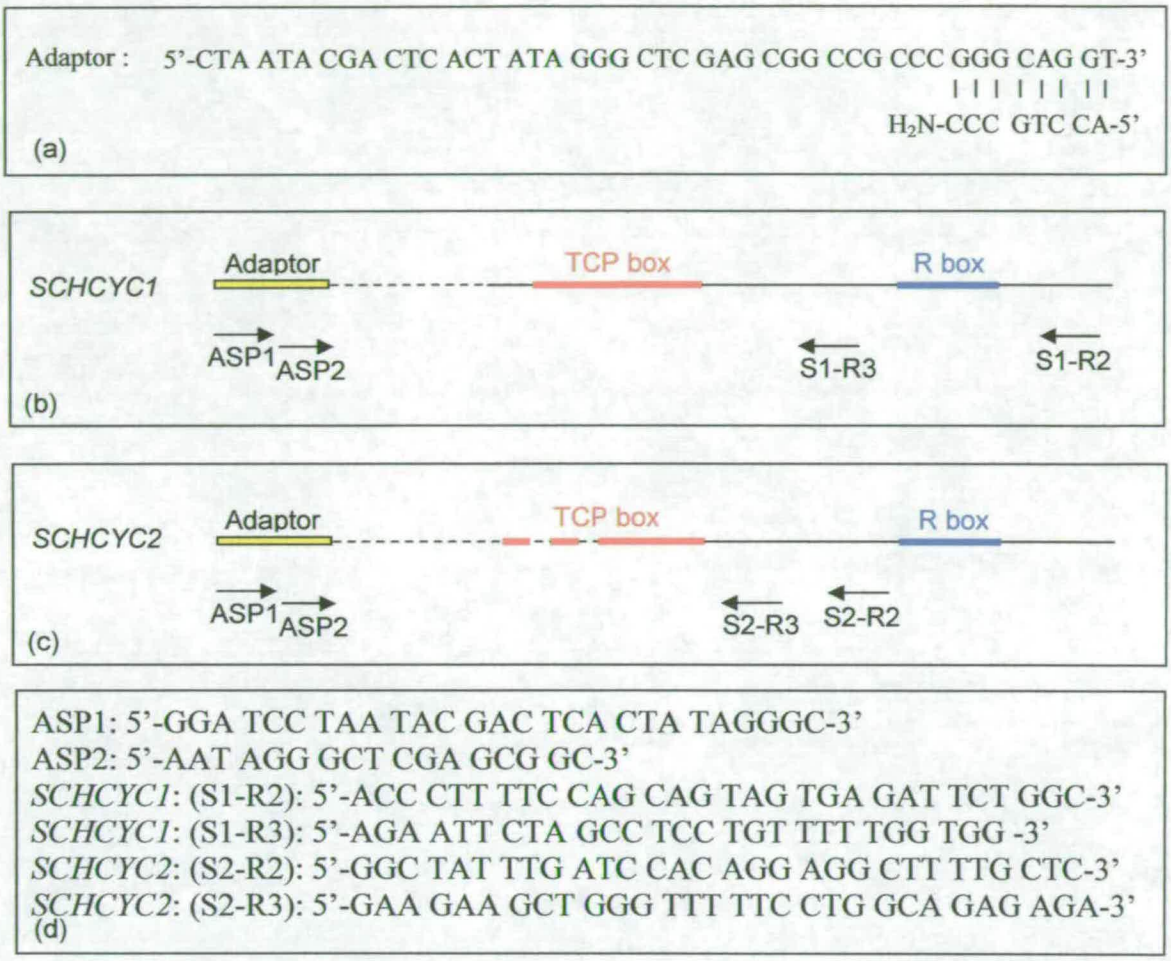

Fig IV.2: Summary of the PCR strategy (genomic walking) for the isolation of unknown 5' DNA sequence in *SCHCYC1 & 2*

Gene specific primers were designed against the DNA sequence of *SCHCYC1*(a&d) and S*CHCYC 2*(b&d) which is not conserved between both genes. After the ligation of an adaptor (a), two round of PCR were carried out. The first round of PCR included ASP1 (adaptor specific primer, (d)) and either S1-R2 or S2-R2 and the second nested PCR was carried out using ASP2 and either S1-R3 or S2-R3. This strategy enabled the isolation of unknown 5' sequence for both *SCHCYC1 & 2*.

(a) Sequence and structure of the adaptor, (b&c) strategy for genomic walking for *SCHCYC1* and *SCHCYC2* respectively, (c) sequence of all primers.

incomplete digestion or unspecific breaking of the DNA during the manipulation. For each gene, the PCR mix with the longest product (around 1kb) (*SCHCYC1gw* and *SCHCYC2gw*) and showing the strongest signal on the Southern blot was cloned in pGEM®-T Easy Vector (KC 23 for *SCHCYC1gw* and KC 24 for *SCHCYC2gw*). After plasmid isolation and digestion with *Eco*RI, for *SCHCYC1gw*, one plasmid with an insert of about 950 bp was identified (KC 23-1) and for *SCHCYC2gw*, one with an insert of about 1.1 kb (KC24-1).

For both *SCHCYC1gw* and *SCHCYC2gw*, the gDNA sequence recovered by GW included the unknown 5' region of the ORF with a putative start codon. In addition, about 175 bp of the 5' NTR for *SCHCYC1gw* and 621 bp of 5' NTR for *SCHCYC2gw* were recovered. For each gene, the overlapping domains of the cDNA and the gDNA sequences were translated and their respective overlapping amino-acid region compared manually to *SCHCYC1m* and *SCHCYC2m* to confirm their identity. However, the comparison of their DNA sequences revealed a degree of divergence higher than what can be attributed to PCR errors (Table IV.1). Consequently, they were grouped provisionally as putative alleles.

Clone identity	*SCHCYC1m*	*SCHCYC2m*
SCHCYC1gw	98.8 %	-
SCHCYC2gw	-	92%

Table IV. 1: DNA sequence similarity in percentage found in overlapping region of clones isolated by Marc Chadwick (m) and by genomic walking (gw) in *S. wisotonensis*

For the rest of the project, new sequences will be likewise identified and grouped together as provisional loci based on the similarity of their amino-acid sequence in the variable regions.

(ii) Additional sequence information for SCHCYC1 & 2

Using the sequence data obtained by GW, a new set of gene specific primers were designed to obtain a full length genomic DNA sequence including the open reading frame (ORF) and some additional 5' and 3' NTR sequence for both *SCHCYC1* and *SCHCYC2*. The forward primers were designed against the gDNA sequence of the 5' NTR of *SCHCYC1gw* & *SCHCYC2gw* (S1-F1 and S2-F1), and the reverse primers were designed against the 3' NTR cDNA sequence of *SCHCYC1m* and *SCHCYC2*m (S1-R1 and S2-R1) (Fig IV.3). Two separate PCRs at high stringency were then carried out and one band per PCR reaction was observed on the corresponding gel. For *SCHCYC1*, the length of this band was found to be of about 1.1 kb, and for *SCHCYC2*, about 1.3 kb. Both mixes were cloned in pGEM®-T Easy Vector and transformed in *E. Coli* (KC 39 for *SCHCYC1* and KC40 for *SCHCYC2*). For *SCHCYC1,* plasmid isolation and screening by digestion with *EcoR*I enabled the identification of one insert of the expected length (KC39-12). For *SCHCYC2*, two clones with inserts of different lengths were found. The shorter, KC40-10 (*SCHCYC2B*) was about 1.1kb long and the longer insert, KC40-11 (*SCHCYC2A*) was about 1.3kb in length. The three plasmids were purified and sequenced to confirm their identity as putative alleles of *SCHCYC1* and *SCHCYC2* respectively. For KC 39-12, the translated DNA sequence was clearly very similar to that of *SCHCYC1m*. This sequence was renamed *SCHCYC1* (Fig IV.4a, Appendix IV.1a&b). The 5' end and the 3' of this clone were sequenced thereby confirming its identity as a putative allele of *SCHCYC1m* (86.2% DNA sequence similarity). In addition, the presence of a putative 3' intron (107bp) between the R box and the stop codon (Fig IV.3) was identified (Fig IV.4a, appendix IV.1a&b).

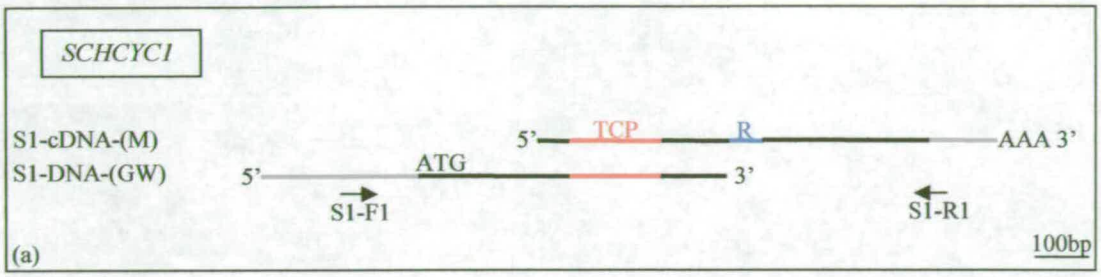

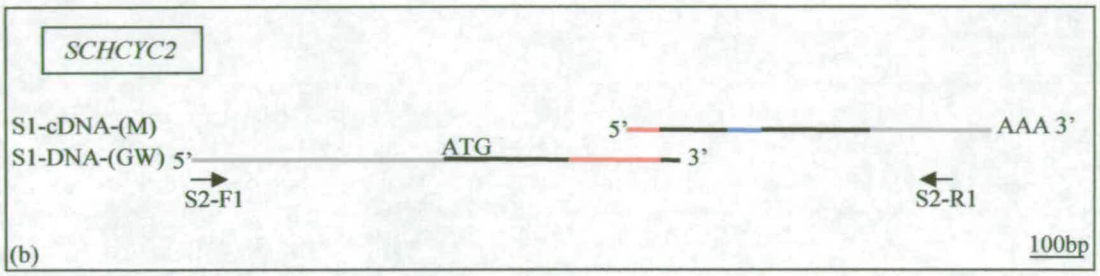

S1-F1 : 5'-GAA ACC GCA TCG TTT ACT TTGCCT TCC AC-3'
S1-R1 : 5'-CAG TAA GGT AAG TTT AGC TTA CAC TGT CAC-3'
S2-F1: 5'-ACA CTC AGT GCA AAC ATA AAG CTC ACG GAG-3'
S2-R2 : 5'-ATG AGT ATA GGA CAA CTG ACA ATT CTG G-3'

(c)

Fig IV.3 : Map of partial sequences for *SCHCYC1* and *SCHCYC2* including data obtained by M. Chadwick (M) and with the genomic walk (GW)

The grey line indicates putative 5' Untranslated Region (UTR) and 3' UTR, the black line the open reading frame, the red and blue section correspond to the sequence coding for the TCP and R domain respectively. The sequence obtained by Marc was isolated from cDNA and the genomic walk from genomic DNA.(a) Map of *SCHCYC1* indicating the location of the primers (S1-F1 and S1-R1) designed to amplify a full length sequence, (b) same as in (a) for *SCHCYC2* (S2-F1 and S2-R1), (c) Primers sequences.

Fig IV.4: Summary of all partial and complete sequences available for *SCHCYC1* and *SCHCYC2*-like genes in *S. wisotonensis*
See overleaf

(a) Map of all partial and complete sequences corresponding to putative alleles of *SCHCYC1* and *SCHCYC2*. The sequence nomenclature is as follows: *m* is for sequences obtained by Marc Chadwick; *gw* by genomic walking; the red arrow is indicating full length open reading frame (ORF) isolated by PCR on gDNA, *lib* identifies products obtained from the screening of the cDNA library. The full line indicates coding sequence, the red and the blue sections correspond to the region of DNA coding the TCP and the R domain respectively. The 3' and 5' Untranslated Region (UTR) are indicated in grey, and the triangle indicates the position and size of introns.
(b) Alignment of DNA sequence corresponding to the region directly upstream to the putative start codon for *SCHCYC2*. The shadowing indicates 100% identity with *SCHCYC2B*. The sequences of *SCHCYC2A* and *B* can only be aligned for a stretch of 48 bp directly upstream of the putative start codon of *SCHCYC2B*, albeit 94% sequence identity for the ORF region.
(c) Alignment of the protein sequence corresponding to the 5' region of the ORF.

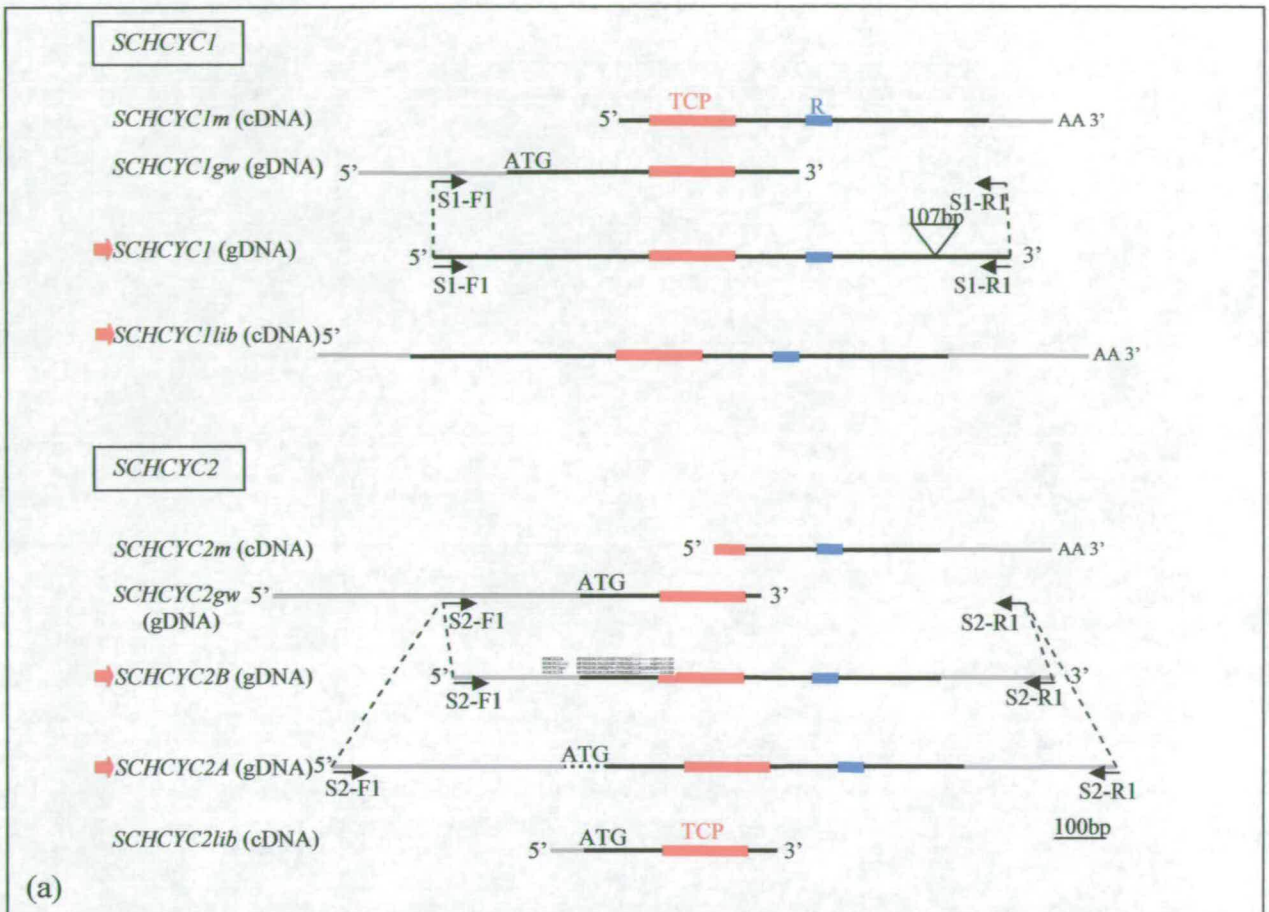

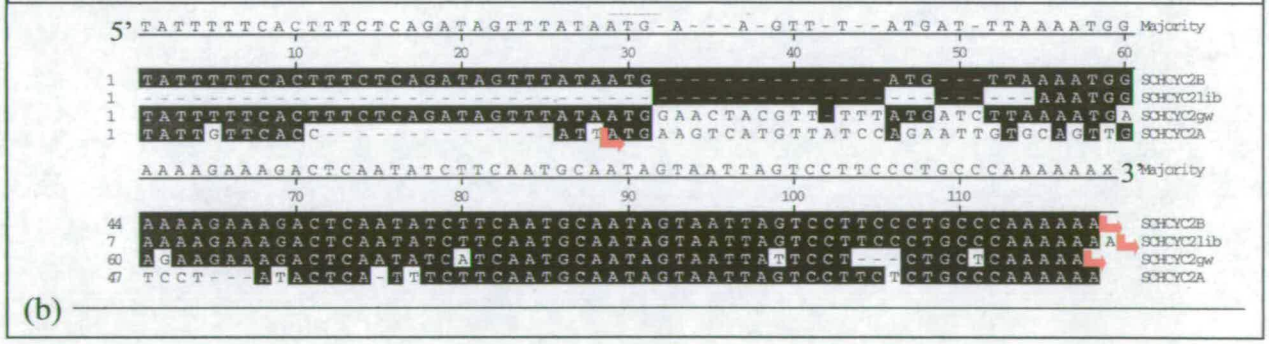


```
SCHCYC2B     MFSSGDPLPSIHISSTFNDNQILLH----HQNVLPIDN
SCHCYC2lib   MFSSGDPLPSIHISSTFNDNQILLH----HQNVLPIDN
SCHCYC2gw    MFSSGDPLPSNQFS-TFTGNEILLHQQHQHQNAIRIDN
SCHCYC2A     MFSSGDPLPSIHISSTFNDNQILLH--------LPIDN
```

(c)

For *SCHCYC2*, the full gDNA sequence was obtained for both products thereby confirming their identity as putative alleles of *SCHCYC2*. Consequently, they were renamed *SCHCYC2A* (KC40-11) and *SCHCYC2B* (KC40-10).

The degree of identity between *SCHCYC2A* and *SCHCYC2B* was high within the alignable ORF domain and 3' UTR (94% for the DNA sequence). However, the putative start codon of *SCHCYC2A* was found to be 78 bp upstream of that of *SCHCYC2B*, within a region where the DNA sequences of both genes are not alignable (Fig IV.4b). A further comparison of *SCHCYC2A* and *SCHCYC2B* sequences obtained with GW revealed that their respective 5' region upstream of the putative start codon corresponded to two fragments of different length. For *SCHCYC2A*, this region of the clone was 471 bp long, whereas for *SCHCYC2B*, it was 254 bp (Appendix IV.2 and 3). Within this 5' region, the sequences of *SCHCYC2A* and *SCHCYC2B* are not alignable, except for sequence corresponding to that of the 5' primer (S2-F1) and a 48bp stretch directly upstream of the putative ATG for *SCHCYC2B* (Fig IV.4b). The eventual presence of an intron within the 5' region of *SCHCYC2A* could explain their difference in length and sequences. This hypothesis was tested manually by searching for a putative splice site consensus sequence (ref: http://www.arabidopsis.org./splice_site.html), but no obvious intron splicing site was found in this region of *SCHCYC2A*. When the partial ORF sequence of *SCHCYC2gw* was compared to that of *SCHCYC2A* and *2B*, the alignment of all three sequences revealed a region of high variation between the start codon and the start of the sequence encoding for the TCP domain (fig IV.4b). From the pattern of variation, and from their sequence similarity (Fig IV.4b&c) at the DNA and the protein level, it is not possible to determine which gene (*SCHCYC2A* or *SCHCYC2B*)

is more similar to *SCHCYC2gw*. It is very likely that the latter correspond to either another locus or a pseudogene.

To determine the location of the first stop codon, the following strategy was followed. The gDNA sequences of *SCHCYC2A* and *B* were aligned and the first stop codons were found to be situated 716 bp after the putative start codon for *SCHCYC2A* and 720 bp for *SCHCYC2B*. However, when both sequences were aligned with *SCHCYC2m*, this stop codon was not found as the cDNA sequences is unalignable with the gDNA sequence from a few base pairs upstream of the putative stop codon. This indicates the presence of an intron and when all sequences were aligned, a putative intron of 255bp was found for *SCHCYC2A* and one of 252 bp for *SCHCYC2B*. However, there was no clear splicing site present at the border of the putative introns, neither in *SCHCYC2A*, nor in *SCHCYC2B*. Moreover, an RT-PCR approach showed the presence of an intron of about 100bp, suggesting that the sequence difference between *SCHCYC2A, B* and *SCHCYC2m* was not only due to the intron. To clarify this point, the RT-PCR reaction mixture was cloned and sequenced. This experiment was repeated twice but failed both times. It was not repeated a third time as it was not deemed essential for the project. The putative stop codon indicated in these sequences is the first one to appear in the gDNA. The alignment of the 3' end of *SCHCYC2A, 2B* and *SCHCYC2m* is presented in appendix IV.4.

In an attempt to clarify this situation and provide an additional tool for the isolation of new TCP genes in *S. wisotonensis*, a cDNA library was constructed using a bank of cDNAs isolated from young floral and inflorescence tissue (See Material and methods). The cDNA library was then screened at high stringency, using

successively the same nitrocellulose filters with probes specific to *SCHCYC1* and *SCHCYC2*.

The template used for the *SCHCYC1* probe was obtained by the *EcoR*I digestion of KC39-12, and for *SCHCYC2*, by the PCR amplification of the KC40-10 insert using the oligo S2-F1 and S2-R1. For *SCHCYC1*, a few positive candidates were isolated and the phagemid with the longest insert was excised and re-ligated resulting in a pBluescript® vector with a 1453bp insert (CK4). When translated, the corresponding cDNA sequence confirmed that it was *SCHCYC1*. It includes the entire ORF, 203bp of the 5'UTR and 297bp of the 3' UTR and was named *SCHCYC1lib*. For *SCHCYC2*, a positive clone was also isolated from the screening of the cDNA library. The sequencing of the corresponding plasmid (CK9) confirmed that it comprised 458 bp of the 5' end of *SCHCYC2* (*SCHCYC2lib*), including 393 bp of ORF with the complete TCP domain (Fig IV.4a). However, the second part of the sequence (from position 459 onwards) presented no similarity with that of *SCHCYC2* indicating that a recombination had most likely occurred during the making of the cDNA library. In the region corresponding to a *SCHCYC2* gene, 100% similarity with *SCHCYC2B* was found (Fig IV.4b&c). Another screen of the cDNA library using the same conditions as above was again unsuccessful in obtaining a full length cDNA for *SCHCYC2*.

IV.2.1.2 Isolation of new CYC-like genes in S. wisotonensis using a PCR approach

This section is initially reporting the isolation of the partial sequence (i.e. between the TCP and the R domain) of 3 new *CYC*-like genes using a PCR approach with the primers provided by H. Citerne (RBGE, Edinburgh, UK)(Fig IV.5). These

degenerate primers were designed against sections of the DNA region encoding for the TCP box and the R domain of *CYC*-like genes in the legumes and in the Gesneriaceae. This set of new sequences was further completed by another partial sequence of a *CYC*-like gene in *S. pinnatus* originally discovered by Patrick Reeves (Olmstead and Reeves, 2003; Genbank AY168170). To obtain the DNA sequence corresponding to the TCP box, a screening of the cDNA library and a genomic walk were carried out.

LEGCYC-F: 5'-CTT YGA TCT HCA RGA CAT GYT RGG RTT YGA YAA-3'
LEGCYC-R: 5'-GTY CKY TCC CTS GCY CKY GCT CTY GC-3'

Fig IV.5: Sequence of primers provided by Helene Citerne designed to amplify the DNA sequence from within the TCP domain to the within the R box in legumes
LEGCYC-F: forward primer (TCP box), LEGCYC-R: reverse primer (R box), Y: C,T; H: A,T,C; R: A,G; K: G,T

A PCR at low stringency was carried out using the degenerate primers provided by Helene Citerne (Fig IV. 5). When the PCR mix was run on a gel, a smear resembling products of lengths varying between 250 and 350 bp was observed. The mix was then ligated into pGEM®-T Easy Vector (KC47), and five plasmids (KC47-8, 12, 15, 22 and 23) were purified and sequenced.

For KC 47-8 and 23, the translated DNA sequence situated next to the forward primer (TCP domain) and next to the reverse primers (R box) did not show any similarity to corresponding sections of the TCP and the R box in other TCP genes. In addition, for both products, the sequence was interrupted by many stop-codons indicating that these clones were likely to be PCR artefacts produced by the low annealing temperature used for the experiment.

The protein sequence of KC 47-12, 15 and 22 indicated that the gDNA amplified was most likely to correspond to partial gDNA sequences of new *CYC*-like genes in *S. wisotonensis*.

To obtain the full length sequence of these three new genes, the cDNA library was screened using their partial gDNA sequences as template for probes. For KC47-12 renamed *SCHCYC3p*, the screening was successful and a 1.2 kb long cDNA was isolated and sequenced from the corresponding Bluescript® vector (CK4) (Appendix IV.5). This cDNA comprised the entire putative ORF, 84 bp of the 5'UTR and 183 bp of the 3'UTR. The ORF between the TCP and the R box was found to be almost identical to that of *SCHCYC3p* with 97.5% similarity at the DNA level. CK4 was renamed *SCHCYC3lib*. Interestingly, when compared visually with other *CYC*-like genes isolated in the Solanaceae, the unconserved region of the predicted protein sequence of *SCHCYC3lib* was found to be partially alignable with that of *NICYC2*. The screening of the cDNA library for *SCHCYC4p* (KC47-15) and *SCHCYC5* (KC47-22) was unsuccessful. In parallel to this work, Patrick Reeves (University of Washington, USA) used a similar PCR approach with an array of degenerate primers to isolate members of the TCP gene family in *S. pinnatus* (Reeves and Olmstead, 2003). By doing so, he obtained the partial sequences of 4 different TCP-like genes in *S. pinnatus* (*SpTCP1, 3, 5&7*). Amongst them, only one new gene could be identified, *SpTCP3* (Reeves and Olmstead, 2003). *SpTCP7* was visually identified as a putative ortholog of *SCHCYC3* (*PRSCHCYC3*), *SpTCP1* as a putative ortholog of *SCHCYC4* (*PRSCHCYC4*) and *SpTCP5* as a putative ortholog of *SCHCYC5* (*PRSCHCYC5*). In this report, for the sake of clarity, *SpTCP3* will be called *PRSCHCYC6*. To obtain the entire TCP box and the 5' end of *SCHCYC4*, *SCHCYC5*

and *SCHCYC6*, a new screening of the GW banks was done. For each gene, two specific primers were designed against the known gDNA sequence (Fig IV.6(a&b)) and after a second round of the touch down PCR, products were run on a gel. The PCR mix containing to the strongest band on the gel was cloned in a pGEM®-T Easy vector.

For *SCHCYC4*, the product was 1.1 kb long and corresponded to the *Stu*I GW bank, for *SCHCYC5*, the product was 700 bp (*Dra*I GW bank) and for *SCHCYC6*, the product was 400bp long (*Stu*I GW bank). For all three genes, the cloning was successful (KC 61, 62 and 63 respectively). The sequencing of the inserts revealed that when translated, their corresponding uninterrupted protein sequence included the recognisable 5' half of the TCP domain and a putative start codon for *SCHCYC4* and *SCHCYC5*. It was therefore deemed likely that for *SCHCYC4* and *SCHCYC5*, the complete 5' coding DNA sequence had been recovered (Fig IV.6a). In addition, 710 bp of the 5' non-coding region for *SCHCYC4* and 86 bp for *SCHCYC5* were isolated (Fig IV.6a). For *SCHCYC6*, 265 bp upstream of the start of the DNA sequence coding for the TCP box were recovered (Fig IV.6a), however, this fragment did not include a putative start codon.

Finally, a new set of primers was designed for each gene in the 5' domain of the GW products, about 100bp upstream of the putative ATG, and within the 3' most domain (i.e. close to/within the R box) of the partial sequences (Fig IV.6 (a&b)). PCR products were then cloned in pGEM®-T Easy vectors and sequenced, confirming the results described above (Fig IV.6a)(Appendix IV.6,7 and 8).

Fig IV.6: Summary of all partial and complete sequences available for *SCHCYC4*, *SCHCYC5* and *SCHCYC6* in *S. wisotonensis* and the corresponding primers sequences
See overleaf

Fig (a) shows the earliest stage (stage 3) at which the expression of *SCHCYC1* was detected in a staminode primordia. Fig (b) and (d) are two sections obtained from the same flower bud at stage 4. In (c) and (e), the red line indicates the plane of sectioning on a SEM of a flower bud at a similar stage of development. G: gynoecium; LP: lateral petal; VP: ventral petal; DS: dorsal sepal; VS: ventral sepal; Lst: lateral stamen; Dst: dorsal staminode; Vst: ventral staminode.

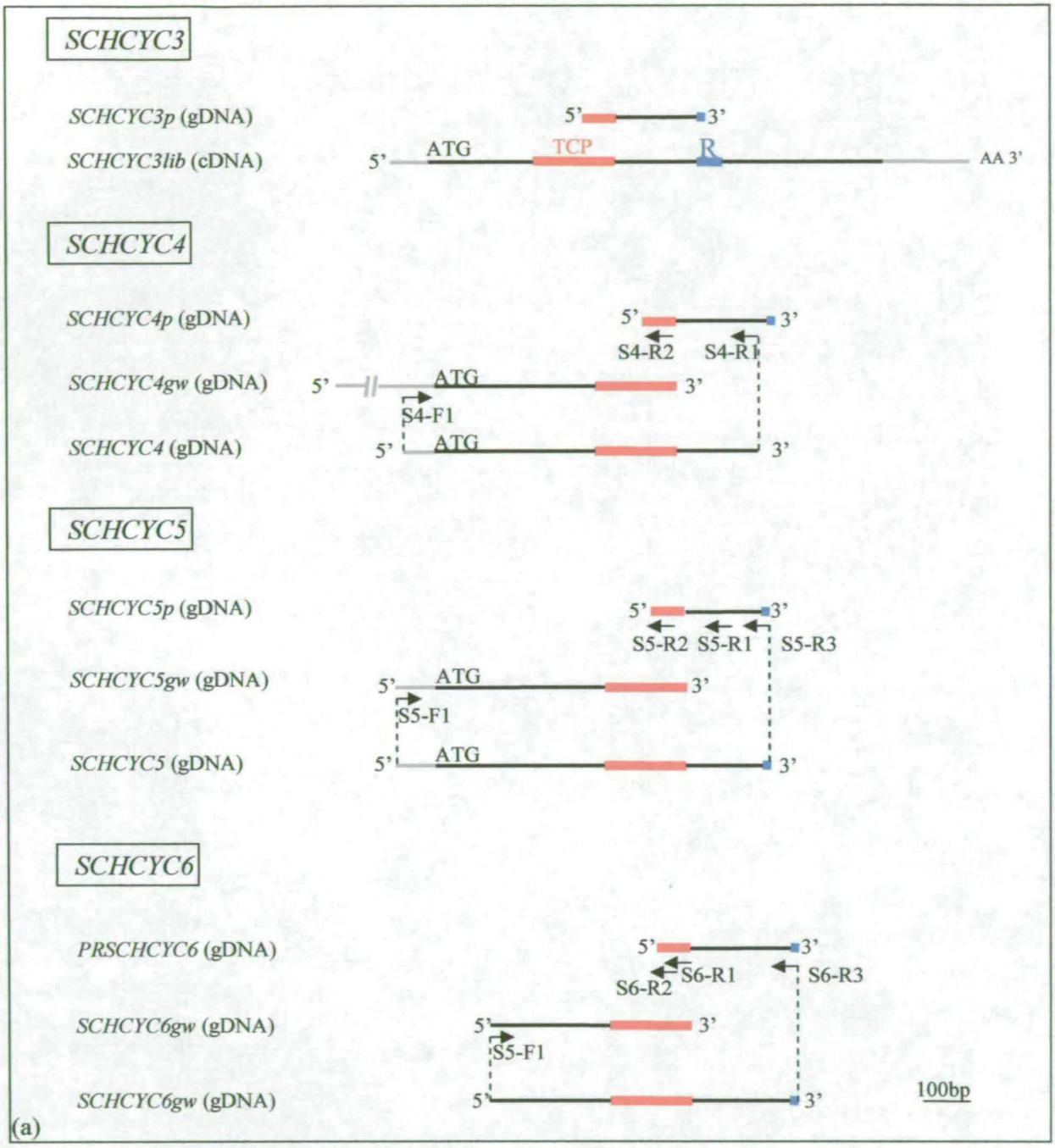

(a)

S4-R1: 5'-CGATTTAGCCTTCTTCTCCTCGTTTGAGC-3'
S4-R2: 5'-GTCTCATTCTTCGGTCTCGTGGACC-3'
S4-F1: 5'-AAAAGAAGTATCAGTCTTCCTCAAG-3'
S5-R1: 5'-TCGAGTGTGTGATGTTTCCGGAGAGCTC-3'
S5-R2: 5'-CCGGTCTCTTATGCCTTGAGCCGTGC-3'
S5-F1: 5'-TTTCTTGAGAGCTCATCATGAAGCT-3'
S6-R1: 5'-CTTACGCGCTGTTTGAAGCGATAGCC-3'
S6-R2: 5'-CTCATTCTTCGATCTCTCACGCCTTGAGC-3'
S6-F1: 5'-CATCATCAAAACCCTAGTTCATCTT-3'

(b)

In summary, the full coding sequence was obtained for *SCHCYC1* and *SCHCYC2*. In addition, three new CYC-like genes have been isolated, namely *SCHCYC3*, *SCHCYC4* and *SCHCYC5*. The full coding sequence of *SCHCYC3* was obtained, and for *SCHCYC4* and *SCHCYC5*, the 5' coding region was isolated including the TCP domain and a fraction of the R box. In addition, part of the 5' coding region of a new *CYC*-like gene, *SCHCYC6*, was found, with the help of the partial DNA sequence provided by P. Reeves. Using the full length of the TCP domains, a protein matrix and its corresponding gene tree was assembled using Megalign and its phylogenetic tree option (Fig.IV.7(a&b)). The topology of the resulting tree confirms that at least 6 putative sub-groups possibly corresponding to 6 loci can be distinguished (Fig.IV.7b).

Therefore, this work has resulted in (i) the isolation of new members of the TCP gene family in *S. wisotonensis* (ii) the obtention of their full TCP box and additional sequence information. This data will provide both the information necessary to determine how similar/related these genes are to *CYCLOIDEA* and *DICHOTOMA*, and provide the sequence data necessary for further molecular experiments.

IV.2.1.3 Isolation of new cDNA and gDNA sequences information for NICYC1 & NICYC2 in N. tabaccum and new CYC-like genes in Petunia

The work carried out by M. Chadwick in *N. tabaccum* aimed to produce RNA *in situ* hybridization probes for the comparison of the pattern of expression of *CYC*-like in *N. tabaccum* (weakly zygomorphic) with that of *CYC*-like genes in *S. wisotonensis* (strongly zygomorphic). Mark used the same degenerate primers and the same experimental procedure in *N. tabaccum* as he did for the isolation of *SCHCYC1*

```
SCHCYC1       KDRHSKIVTAQGQRDRRVRLSIGVARKFFDLQDMLGFDKPSKTLDWLFTNSKLAIDDL
SCHCYC2A      KDRHSKIITAKGPRHRRVRLSIDAARKFFDLQEMLGFEKPSKTLDWLFTNSKLAIDDL
SCHCYC2B      KDRHSKIITAKGPRHRRVRLSINAARKFFDLQEMLGFEKPSKTLDWLFTNSKLAIEDL
SCHCYC3       RDKHSKILTAQGPRDRRVRLSIAIARKFFDLQDTLGFDKPSKTLDWLFSNSKIAIDEL
SCHCYC4       TDRHSKINTAKGPRDRRMRLSLDIARKFFNLQDMLGFDKASKTVDWLIIQSKSAINEF
SCHCYC5       KDRHSKICTAQGIRDRRMRLSLQIARKFFDLQDMLGFDKASKTIEWLFTKSKNAIKEL
SCHCYC6       KDRHSKICTAQGVRDRRMRLSLQIARKFFDLQDTLGFDKASKTIEWLFSKSKNAIKEL
PRSCHCYC1     -------NTAKGPRDRRMRLSLDIARKFFNLQDMLGFDKASKTVDWLLIQSNSAINEF
PRSCHCYC2     -------NTAKGPRDRRMRLSLDIARKFFNLQDMLGFDKASKTVDWLLIQSNSAINEF
PRSCHCYC3     ---------AQGVRDRRMRLSLQTARKFSDLQDTLGFDKASKTIEWLFSKSKNAIKEL
PRSCHCYC4     -------CTAQGVRDRRMRLSLQIARKFFDLQDTLGFDKASKTIEWLFSKSKKAIKEL
PRSCHCYC5     -------CTAQGIRDRRMRLSLQIARKFFDLQDMLGFDKASKTIEWLFTKSKNAIKEL
PRSCHCYC6     -------CTAQGIRDRRMRLSLQIARKFFDLQDMLGFDKASKTIEWLFTKSKNAIKEL
PRSCHCYC7     -------LTAQGPRDRRVRLSIAIARKFFDLQDTLGFDKPSKTLDWLFSNSKIAIDEL
```

(a)

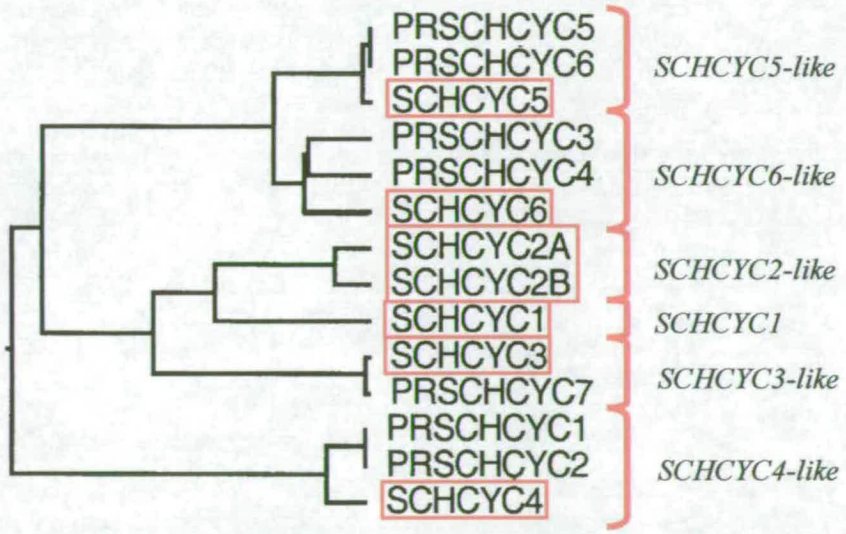

(b)

Fig IV.7: Aligned matrix and corresponding phylogenetic tree showing the relation between *CYC*-like genes obtained in *S. wisotonensis* and these obtained by P. Reeves in *S. pinnatus*

(a) Alignement of the sequences obtained in *S. wisotonensis* and in *S. pinnatus*. The partial TCP sequences obtained by P. Reeves in *S. pinnatus* are labelled PRSCHCYCx. (b) The sequence of the complete TCP boxes obtained by M. Chadwick and me are highlighted in red boxes. In *S. wisotonensis* and *S. pinnatus*, all sequences obtained so far can be grouped in 6 sub-groups shown in red brackets.

and *SCHCYC2* in *S. wisotonensis* (section IV.2.1). He obtained two partial cDNA sequences, *NICYC1m* and *NICYC2m*, comprising the cDNA sequence encoding the 3' most domain of the TCP domain to the R box (Fig IV.8). It is not possible to align the protein sequence of *SCHCYC1m* and *SCHCYC2m* with either *NICYC1* or *NICYC2* in the variable region between the TCP and the R box indicating no obvious orthologous relationship between the two sets of CYC-like genesIn addition, Mark Chadwick also carried out a 3' race PCR and obtained the cDNA sequence for the 3' end of these two genes. Unfortunately, he did not obtain any meaningful pattern of expression using these partial sequences as RNA *in situ* probes.

My project initially aimed at pursuing the work of Marc Chadwick. To do so, I used PCR-based techniques to obtain additional sequence information for *NICYC1* and *NICYC2*. After a preliminary PCR amplifications of the gDNA sequence corresponding to *NICYC1m* and *NICYC2m* in *N. tabaccum*, my first aim was to obtain the full amino-acid sequence of the TCP box for both genes and run a phylogenetic analyses. My second aim was to produce specific RNA *in situ* probes to obtain the pattern of expression of *NICYC1* and *NICYC2* in *N. tabaccum*. These probes were designed to include only the unconserved 5' or the 3' regions of the genes. Therefore, to achieve both aims, I needed to isolate the 5' cDNA sequence upstream of the TCP box for both *NICYC1* and *NICYC2* and to do so, a 5' race PCR approach was chosen. Finally, during the PCR amplification of 3' specific cDNA fragments, amplification of gDNA as positive controls revealed the presence of a 3' intron in both genes. The corresponding gDNA sequences were cloned and sequenced. To complete this work, the isolation of cDNA and gDNA spanning the entire ORF was attempted but could

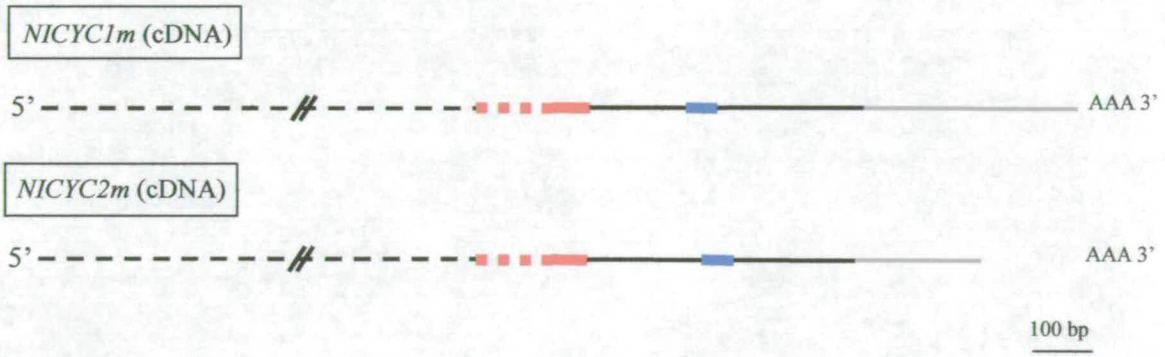

Fig IV.8: Map of the partial cDNA sequences of *NICYC1* (*NICYC1m*) and *NICYC2* (*NICYC2m*) obtained by M. Chadwick

The full line indicates coding sequence, the red and the blue sections correspond to the region of the cDNA incoding the TCP and the R domain respectively. The 3' Untranslated Region (UTR) is indicated in grey and the unknown part of the DNA sequence, including upstream open reading frame and 5' UTR is in dashed line.

only be successfully amplified, cloned and sequenced for the gDNA sequence corresponding to *NICYC1*.

(i) Amplification of gDNA corresponding to NICYC2m

A DNA extraction (small scale protocol) was carried out on young leaves of *N. tabaccum*. A set of two degenerate primers was designed to amplify both *NICYC1* and *NICYC2* (N1-F1 and N1-R1) (Fig IV.9(a&b)). A PCR at high stringency using the gDNA as a template was carried out and when the reaction was run on a gel, two bands were visible, one around 250bp and the other around 600bp. However, the analysis of the cDNA sequences obtained by M. Chadwick predicted two bands of approximatively equal length, around 200bp. This result suggested the presence of an intron between the TCP and the R box in either *NICYC1* or *NICYC2*. The PCR products were cloned (KC51) and only one plasmid was recovered with an insert of about 600bp. Its sequencing revealed that a 392 bp intron was located between the TCP and the R box (Fig IV.9a) of what was identified as a *NICYC2*-like sequence (95% sequence identity with *NICYC2m*). The absence of intron in *NICYC1* suggested by the banding pattern was later confirmed by sequencing (see below).

(ii) Isolation of 5' end of the cDNA sequence corresponding to NICYC1m and NICYC2m using race PCR

The sequence information provided by Mark Chadwick was used to design a new degenerate primer (N-R2) within the cDNA sequence of both *NICYC1m* and *NICYC2m* encoding the TCP domain (Fig IV.9b). The first round of race PCR was with N-R1 and UPM, and the second round was a nested PCR with N-R2 and NUP (Fig IV.9a). When both reaction mixes were run on an agarose gel, no bands were

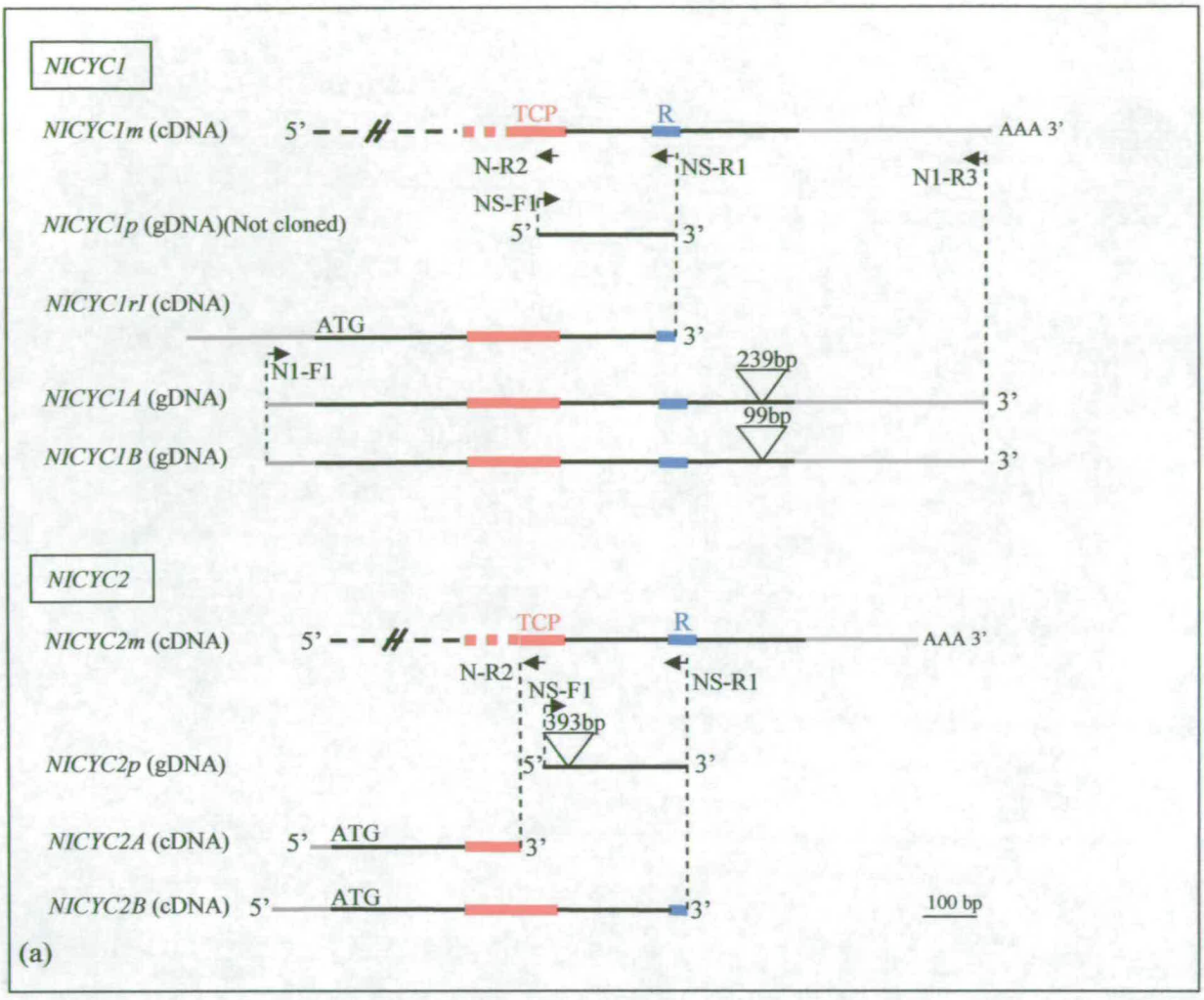

NS-F1: 5'-AA(AG) ACG CTG GAT TGG CT(ACT) TTC-3'
NS-R1: 5'-T(GC)T TGA TTG TTC TTT C(CT)C TAG CTC TTG CTC-3'
N-R2: 5'-GA(GC) TT(AT) GTG AA(AT) AGC CAA TCC AGC-3'
N1-F1: 5'-TTC CCT TCT GGA AAC AGT AGT GG-3'
UPM(long): 5'- CTA ATA CGA CTC ACT ATA GGG CAA GCA GTG GTA ACA ACG CAG AGT-3'
UPM (short): 5'- CTA ATA CGA CTC ACT ATA GGG C-3'
NUP: 5'-AAG CAG TGG TAA CAA CGC AGA GT-3'

(b)

Fig IV.9: Map of the partial cDNA and gDNA sequences obtained for *NICYC1* and *NICYC2* and primers used for PCR amplification

(a) Map of the partial cDNA and gDNA sequences. The full line indicates coding sequence, the red and the blue sections correspond to the region of the cDNA incoding the TCP and the R domain respectively. The 3' Untranslated Region (UTR) is indicated in grey and the unknown part of the DNA sequence, including upstream open reading frame and 5' UTR is in dashed line.

(b) Primer sequences

visible. Following this first attempt, the reaction of the first round PCR was diluted in dH_2O by a factor of 50 and re-amplified using normal PCR conditions and high stringency. The re-amplification of the first round PCR reaction was then run on a gel and revealed bands ranging from 300bp to 1.2kb. A new nested PCR (high stringency, primers: N-R2, NUP) was then performed on this mix and produced a similar banding pattern on a gel, albeit with products of a smaller length. The difference in lengths between the strongest bands from the two reaction mixes was about 300 bp, indicating that the 5' race was likely to have been successful. Consequently, both reactions were cloned in pGEM®-T Easy vectors, KC 18 for the first round and KC13 for the second (nested) round. The cloning was expected to recover separate products corresponding to each individual gene as the degenerate primers were designed to amplify cDNA sequences from both *NICYC1* and *NICYC2* during the same PCR reaction. For both genes, the sequence upstream of the nested primer was unknown and the sequence information provided by the cloning of the first round of 5' race PCR (including the domain between the TCP and the R box) helped to ensure that the cDNA sequences obtained in the nested PCR could be correctly identified.

For *NICYC1*, the longest cDNA (879bp) isolated from the first round of PCR (*NICYC1r1*) was identified by comparing the sequence between its TCP and R box with that of *NICYC1r1* and *NICYC1m* (96% similarity at the DNA level). This partial cDNA spanned the coding region from the start codon to the R box, including the whole TCP domain and 243 bp of the 5' UTR (Fig IV.9, appendix IV.9a&b).

When the protein sequence of other partial cDNA obtained in the nested 5' race PCR were compared to that of *NICYC1*, 4 products were isolated which had

100% sequence similarity with that of *NICYC1r1* along their alignable sections. However, a few clones were found to be non-alignable with *NICYC1* for most of their length, except for the partial 5' domain of a TCP-like box. This suggested that these non-*NICYC1* clones corresponded nevertheless to the 5' end of TCP genes. Within this group of non-*NICYC1* sequences, two sub-classes of cloned partial cDNAs could be distinguished (*NICYCx*A and B) with about 94% similarity at the DNA level between *NICYCx*A and *NICYCx*B. To determine if these clones corresponded to the 5' end of *NICYC2* or that of other *CYC*-like genes, more clones from the first round of the 5' race PCR were characterised. This screen did not allow the isolation of other partial cDNAs than these corresponding to *NICYC1* and the reaction mix was cloned again in a pGEM®-T Easy vector (KC14). This time, a clone was sequenced which revealed an uninterrupted ORF spanning a region from 57 aas upstream of the TCP domain, to the beginning of the R box (Appendix IV.10). The variable domain between the TCP and the R box was aligned with that of *NICYC2m* and showed 87% sequence similarity at the DNA level (including a 4 aas deletion in *NICYC2m* compared to the race clone). The comparison of the alignable 5' cDNA sequence of this clone with that of *NICYCxA* and *NICYCxB* revealed 100% sequence similarity between with *NICYCxB*. The partial cDNA sequences of *NICYCxA* and *NICYCxB* being very similar (94% at the DNA level), this finding suggests that both genes are putative allelic copies of *NICYC2m*. Consequently, *NICYCxA* and *NICYCxB* were re-labelled *NICYC2A* and *NICYC2B* respectively (Fig IV.9, appendix IV.10).

(iii) Isolation of other sections of the cDNA and gDNA sequence corresponding to NICYC1 and NICYC2(A &B) using PCR

Two sets of new primers were designed against the cDNA sequence of *NICYC1m* (N1-F2 and NI-R3) and *NICYC2m* (N2-F2 and N2-R3) to isolate a 3' specific fragment (Fig IV.10b). A PCR at high stringency was carried out, and when the reaction was run on a gel, it revealed a unique band for *NICYC1* (580bp) and two bands for *NICYC2* referred to as *NICYC2(3'x)*(538 bp) and *NICYC2(3'y)*(392bp)(Fig IV.10a). When both cDNA sequences were aligned, the difference in sequence length between *NICYC2(3'x)* and *NICYC2(3'y)* appeared to be mostly due to a 144 bp (43 aas) in frame addition in *NICYC2(3'y)* before the putative stop codon, and their sequence identity was found to be 83% at the DNA level. To determine if one of the new sequences was likely to correspond to *NICYC2m*, all three DNA sequences were aligned. *NICYC2(3'x)* had 97% similarity with *NICYC2m*, including the same 43 amino acids deletion compared to *NICYC2(3'y)*(Appendix IV.11). When the DNA sequence of *NICYC2(3'y)* was compared to that of *NICYC2m*, 86.4% identity was found between the two partial sequences. During the amplification of the 3' end cDNA sequence, a gDNA control was run alongside and two bands were observed on the corresponding gel: one band of about 1.1kb and another one of about 800bp. Comparison with the bands produced by the amplification of cDNA sequences and that produced by the amplification of gDNA suggests the presence of an intron in both *NICYC2(3'x)* and *NICYC2(3'y)*. The pile up of the cDNA and the gDNA sequences using megalign confirmed that the largest band corresponded to the gDNA of *NICYC2(3'y)* (100% DNA sequence similarity) and the smaller band to *NICYC2(3'x)* (100% DNA sequence similarity)(Appendix IV.11). However, although the DNA sequence similarity between *NICYC2(3'x)* and *NICYC2(3'y)* in the coding

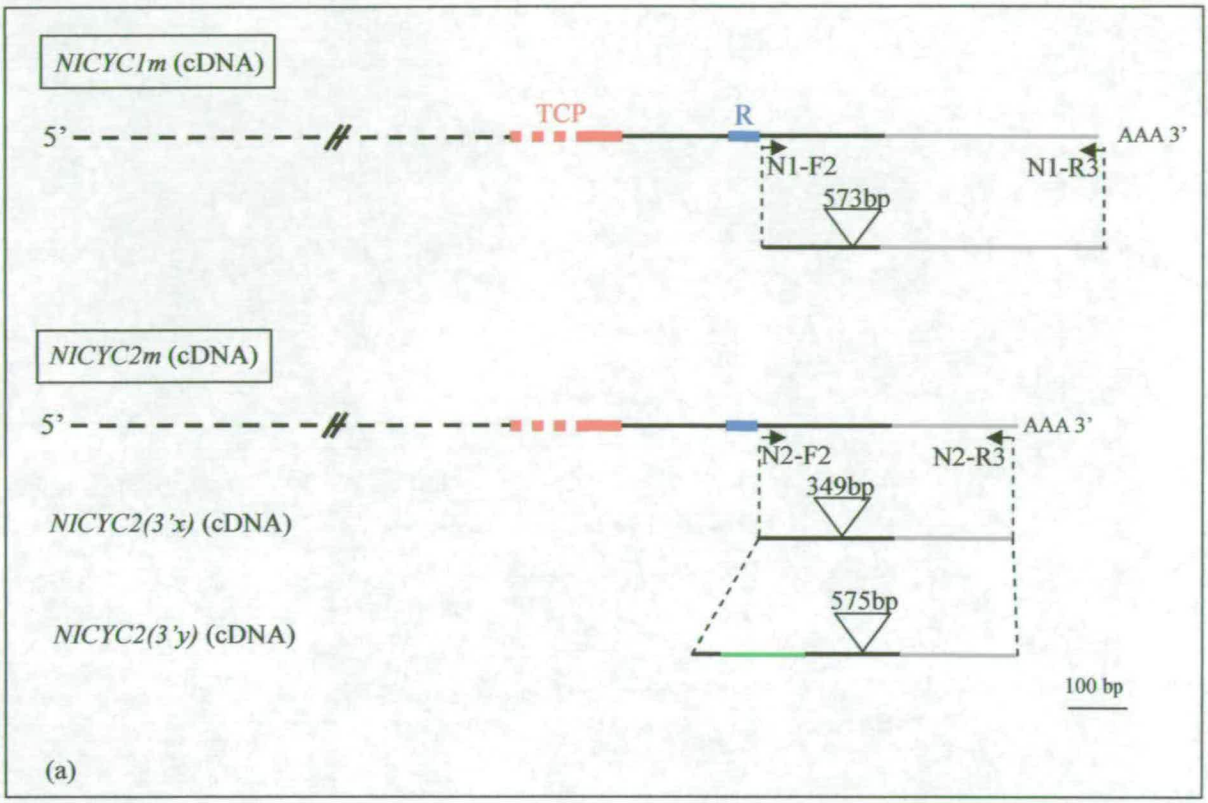

N1-F2: 5'-CCC AAA TTG AAG CCA AAC TTA ACT CAT C-3'
N1-R3: 5'-CTT GTA ATA CAG TAC TAC ACC AAA AAC TCC-3'
N2-F2: 5'-GAG TAG AAT TGA AAC TAG CCA GAG GTC-3'
N2-R2: 5'-GCA AAA GTC TAA TAG TTC ATC GGT G-3'

(b)

Fig IV.10: DNA sequence and map of the primers designed to amplify the 3' end of *NICYC1* and *NICYC2*

(a) Map of the partial cDNA and gDNA sequences. The full line indicates coding sequence, the red and the blue sections correspond to the region of the cDNA coding the TCP and the R domain respectively. The 3' Untranslated Region (UTR) is indicated in grey , the intron is symbolized as a triangle and the green line corresponds to an addition of 144bp in *NICYC2y*

(b) Primer sequences

region is of 83%, that of their respective introns is overall only 58.6%, with 72% identity in the last 97bp (3' end).

The variation between the different putative alleles in *N. tabaccum* observed for *NICYC1* and *NICYC2* is likely to be caused by allelic variation between the two sets of genes inherited from each parents. Unfortunately, due to time constraints, this question was not further investigated.

(iv) Isolation of full gDNA sequences for NICYC1 and NICYC2

For *NICYC1*, a PCR on gDNA was carried out to isolate a full gDNA sequence for this gene (using N1-F1 and N1-R3 primers) (Fig IV.9). The PCR reaction produced two bands later cloned in pGEM®-T Easy vector (KC38). The two products were successfully cloned, sequenced and named *NICYC1A* and *NICYC1B* (sequence of *NICYC1A* in appendix IV.9a). When their sequence was aligned with *NICYCm* (cDNA), the difference in size between *NICYC1A* and *NICYC1B* could be explained by the presence of an intron of variable length (Appendix IV. 9c).

Finally, PCR were carried out on cDNA and gDNA using either N2A-F1 or N2B-F1 and N2-R3 (Fig IV.9) to amplify the cDNA or the gDNA section including the entire ORF corresponding to *NICYC2A* and *NICYC2B*. Unfortunately, despite several attempts, the PCR failed to amplify these sequences judged by the absence of bands on the corresponding gel.

In summary, partial sequences including the TCP domain, the 5' end and the 3' region of putative alleles of *NICYC1m* and *NICYC2m* were successfully isolated,

thereby potentially providing additional information on the evolution of *CYC*-like genes in the Solanaceae.

IV.2.1.4 Isolation of CYC-like genes in Petunia using a PCR approach

With its moderate zygomorphy and its intermediate position between *Schizanthus* and *Nicotiana* in the phylogenetic tree of the Solanaceae, *Petunia* can be considered as an interesting stepping stone in the evolution of floral symmetry in this family.

At the beginning of the project, in addition to *S. wisotonensis* and *N. tabaccum*, I tried to isolate *CYC*-like genes from *Petunia*, using PCR based techniques. Firstly, I isolated a partial gDNA sequence of one *CYC*-like gene (*PETCYC1*) using primers against the TCP and the R box. I then obtained the 5' end of this gene using 5' race PCR. Finally I obtained the partial gDNA sequences (between the TCP and the R box) of two new TCP-like genes (*PETCYC2 & 3*).

Petunia hybrida (W138) was grown from seeds provided by Erik Souer (VU, Amsterdam, Holland). Genomic DNA was extracted from young leaves using the small scale DNA extraction protocol. A PCR at medium stringency was carried out using the pair of degenerate primer (NS-F1 and NS-R1) designed against the cDNA sequence encoding for the TCP and the R box domains of *N. tabaccum* and *S. wisotonensis* (Fig IV.9). A unique band of about 700bp was observed on the corresponding gel. The PCR product was cloned in a pGEM®-T Easy vector (KC 31) and the insert was sequenced.

The predicted protein sequence encoded by DNA downstream of the 5' primer (NS-F1) was found to be similar to the 3' end of a TCP domain suggesting that this

gene (*PETCYC1p*) is a TCP-like gene. The rest of the cDNA sequence was translated in all three frames. All possible protein sequences were interrupted by a few stop codons suggesting the presence of one or more introns. Supporting this hypothesis, putative intron splicing sites were identified. Only one combination of splicing sites corresponding to single 409 bp intron resulted in a potentially continuous protein sequence once the intron is removed (Fig IV.11a). To obtain the 5' end of this gene including the entire TCP domain, a 5' race PCR was carried out using the same experimental procedure as described for *N. tabaccum.* A new 3' reverse primer was designed (P1-R1) against the gDNA sequence comprised between the 3' splice site of the putative intron and the beginning of the R box (Fig IV.11a). The first round of race PCR was carried out with the primers UPM and NS-R1 (degenerate 3' reverse primer situated within the R box) (Fig IV.11a). An aliquot of the products from the first round of race PCR was run on an agarose gel, but no bands were visible. These products were diluted in water by factors 10 and 50, and the pure reaction plus its diluted aliquots were used as templates for the nested PCR in three separate touch–down PCR using P1-R1 and NUP, and the same polymerase as for the first round. When the nested PCR reactions were run on a gel, two bands (500 bp and 600 bp) were visible. To test if the products really included the 5' end of *PETCYC1p*, a second nested PCR was carried out on a dilution of the nested products using the primer NS-R2 (reverse primer within the TCP box) and normal PCR conditions and reagents. As expected, the banding pattern of the corresponding gel showed two smaller products. The products of the nested race PCR were cloned into pGEM®-T Easy vector (KC 47). The digestion with *EcoR*I of 36 isolated plasmids revealed inserts of three different lengths (450bp, 500bp and 600bp).

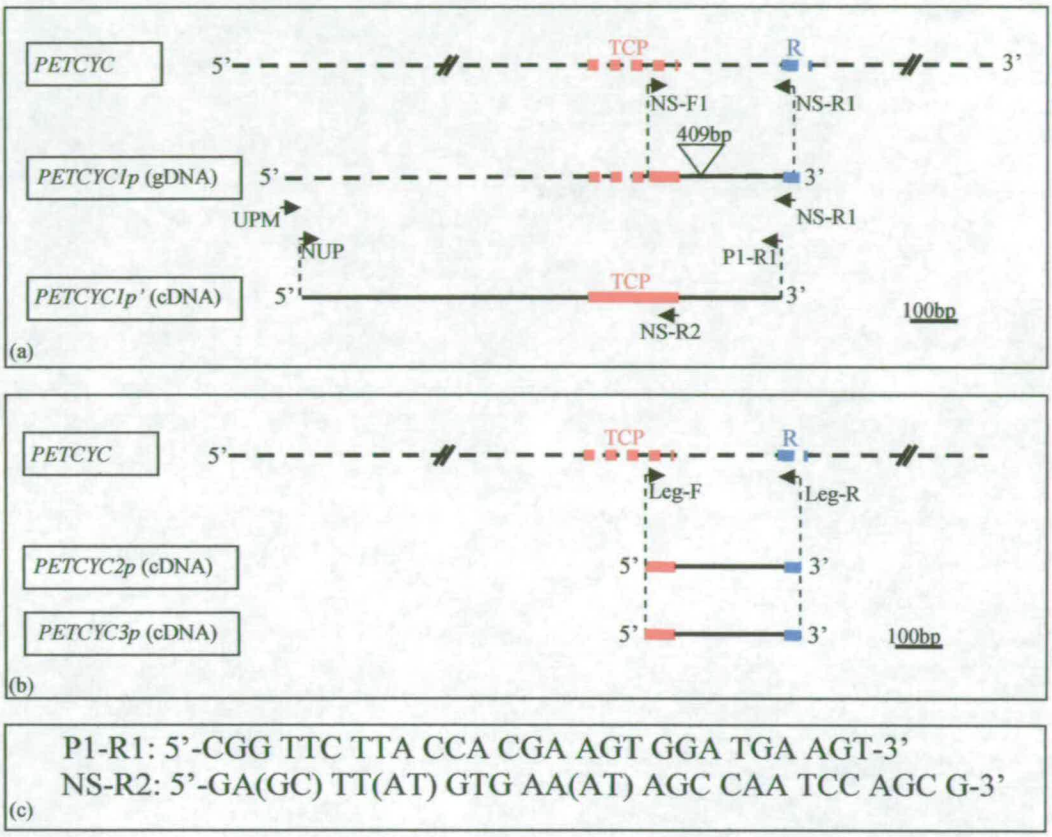

Fig IV.11: Map of partial cDNA and gDNA sequences obtained in *Petunia* and sequences of corresponding PCR primers

(a) Map of the steps required to obtain the 5' end of *PETCYC1*. First, the gDNA sequence of *PETCYC1p* was obtained by PCR and its corresponding cDNA region amplified by 5' race (*PETCYC1p'*). The doted line indicates unknown DNA, the full line indicates coding sequence, the red and the blue sections correspond to the region of the cDNA coding for the TCP and the R domain respectively. The intron is symbolized as a triangle, the primer sequences are in Fig IV.9.

(b) Isolation of two novel partial sequences of *CYC*-like genes in *Petunia* labelled *PETCYC2p* and *PETCYC3p*. Both sequences were obtained using different primers as for *PETCYC1p* (primer sequences in Fig IV.5).

(c) Primers sequences used for the 5' race PCR.

One plasmid representative of each band was sequenced (KC 47-24, 25 and 35). It showed that 47- 25 was an artefact whereas 47-24 and 35 corresponded to two clones of the same 5' cDNA sequence, 47-35 being 98 bp longer than 47-24. The translated sequence of KC47-35 revealed an uninterrupted protein sequence including 106 amino-acid upstream of the TCP box and most of the region between the TCP and the R box (Appendix IV.12). The first "in frame" methionine was found at position 47. The alignment of KC47-35 and *PETCYC1* gDNA (after the removal of intron sequence) revealed 100% DNA sequence identity indicating that KC47-35 was the 5' end of *PETCYC1*. When the protein sequence of *PETCYC1* was aligned with that of other *CYC*-like gene in the Solanaceae, it was found to have 78.1% identity with that of *NICYC2B*. The comparison between these putative orthologs suggests that the methionine in position 47 is not likely to correspond to the start codon and that therefore, the 5' end of the ORF was missing (Fig IV.12).

```
NICYC2B  MFPASNSTGNPPPHPSLSFHSSSPFLGLNGNQILLHHYQNQLSSHHFA
PETCYC1  ---------NPLPHPSSIFHSSSPFLGLNGNQILLHRYQDQFSTHYKD
```

Fig IV.12: Alignment of the 5' end of *NICYC2B* and *PETCYC1*

To isolate new *CYC*-like genes in *Petunia*, a cDNA library from *Petunia hybrida* (W138) provided by Dr. Erik Souer was screened using *PETCYC1* as a probe. This screening failed to identify potential positive plaques, and instead, a PCR approach was taken. The experimental procedure was identical to that of the isolation of new *CYC*-like genes in *S. wisotonensis* using a PCR amplification at low stringency and the primers provided by Helene Citerne. The PCR was carried out on

the first strand cDNA mix obtained during the 5' race. On the corresponding gel, a smear of several bands was observed around the 200-400 bp region. The products were cloned into the pGEM®-T Easy vector (KC 50) and the *EcoR*I digestion of 24 plasmids revealed inserts with different length.

Four representative plasmids of were sequenced (KC50-2, 4, 7 and 12). The translated DNA sequence directly downstream of the 5' primer was used to identify putative TCP genes. For KC 50-4 and KC 50-12, a TCP box-like protein sequence could be recognized downstream of the 5' primer. For KC 50-2 and 7, no TCP box-like domain could be recognised suggesting that the two later inserts were PCR artefacts. KC 50-4 and KC50-12 were renamed *PETCYC2p* and *PETCYC3p* respectively (Fig IV.11, appendix IV.13a&b). Unfortunately, due to time constraints, no further work was done to obtain additional sequence information for these 2 putative genes.

In summary, in *Petunia*, the partial sequences of three TCP genes have been isolated. The sequence data obtained for *PETCYC1p* includes most of the coding 5' end, the whole TCP box and the gDNA corresponding to the section comprised between the TCP and the R boxes. For *PETCYC2p* and *PETCYC3p*, the sequences obtained are derived from PCR amplification of gDNA using primers against the TCP and the R box. Therefore, these partial sequences do not include the whole DNA sequence coding for the TCP domain.

IV.2.2 Characterisation of the new TCP genes isolated in S. wisotonensis

The TCP gene family is defined by the presence of the TCP box (Cubas,1999). This domain is the only conserved region found in all members of the TCP gene family. Therefore, it contains the sole data available to be used for sequence comparison and phylogenetic analysis of these proteins across the angiosperms.

In the course of this project, 6 TCP genes with their complete TCP domain have been isolated in *S. wisotonensis*, 2 in *N. tabaccum* and 1 in *Petunia.*

In this section, I will first report the study of allelic/paraloguous relationships between the different TCP genes in *S. wisotonensis*. Secondly, the protein sequence of the TCP domain will be used to determine in which class the genes isolated in this project belong, and to identify the most likely putative orthologs of *CYCLOIDEA* and *DICHOTOMA*.

IV.2.2.1 Alleles or paralogues in S. wisotonensis

The cloning of partial and entire cDNA and gDNA sequences during the course of the project has unravelled the existence in the population of more than one sequence for each TCP gene in *S. wisotonensis*. Are these sequences representative of allelic variation or gene duplication?

To clarify this point, a Southern hybridization approach was undertaken to determine how many copies of each TCP gene were present in the genome of *S. wisotonensis*. Genomic DNA was extracted from a few specimens using the large scale DNA extraction protocol. For *SCHCYC1, 4, 5&6*, one clone per locus was chosen to provide the template for the synthesis of radioactive labelled probes. They were carefully selected so that, when possible, they did not comprise highly variable

regions such as introns (Fig IV.13). For *SCHCYC2* and *SCHCYC3*, a PCR approach was required to obtain suitable templates (Fig IV.13). For each gene, the restriction enzymes were then chosen to be 6bp cutters with no restriction sites within the known region of the DNA sequence. The probes were synthesized using ^{32}P dCTP and gene specific primers, and the radioactive hybridization was carried out following the normal protocol (see material and methods).

To infer gene copy numbers, Southern hybridization is easier to interpret when there are no or little polymorphisms affecting (i.e. creating/abolishing) enzymes recognition sequences. Therefore, if the genetic background is heterogeneous (e.g. hybrid), the interpretation of the data is expected to be rendered more complex by this consideration.

If a gene is present as a single copy and the genetic background is homogenous, only one band should be observed, providing the restriction enzyme does not cut within the region hybridized by the radioactive probe. If more than one locus is present, two bands of similar intensity should be found in all digests. In both scenarios, the same banding pattern should be found in all digests, unless some of the DNA has not transferred to the nitrocellulose paper during the blotting process (e.g. very large fragments). However, if the genetic background is heterogeneous (e.g. hybrid), the spacing of restriction sites in a given plant may differ between the two genomes, so two bands of different length might be observed even when only one locus is present. The only two possible ways to determine if the frequent occurrence of a double band represents duplicated or allelic copies is to look at their inheritance or compare their intensity. In the context of this project, it was not possible to study their inheritance. Therefore, the second approach was chosen instead.

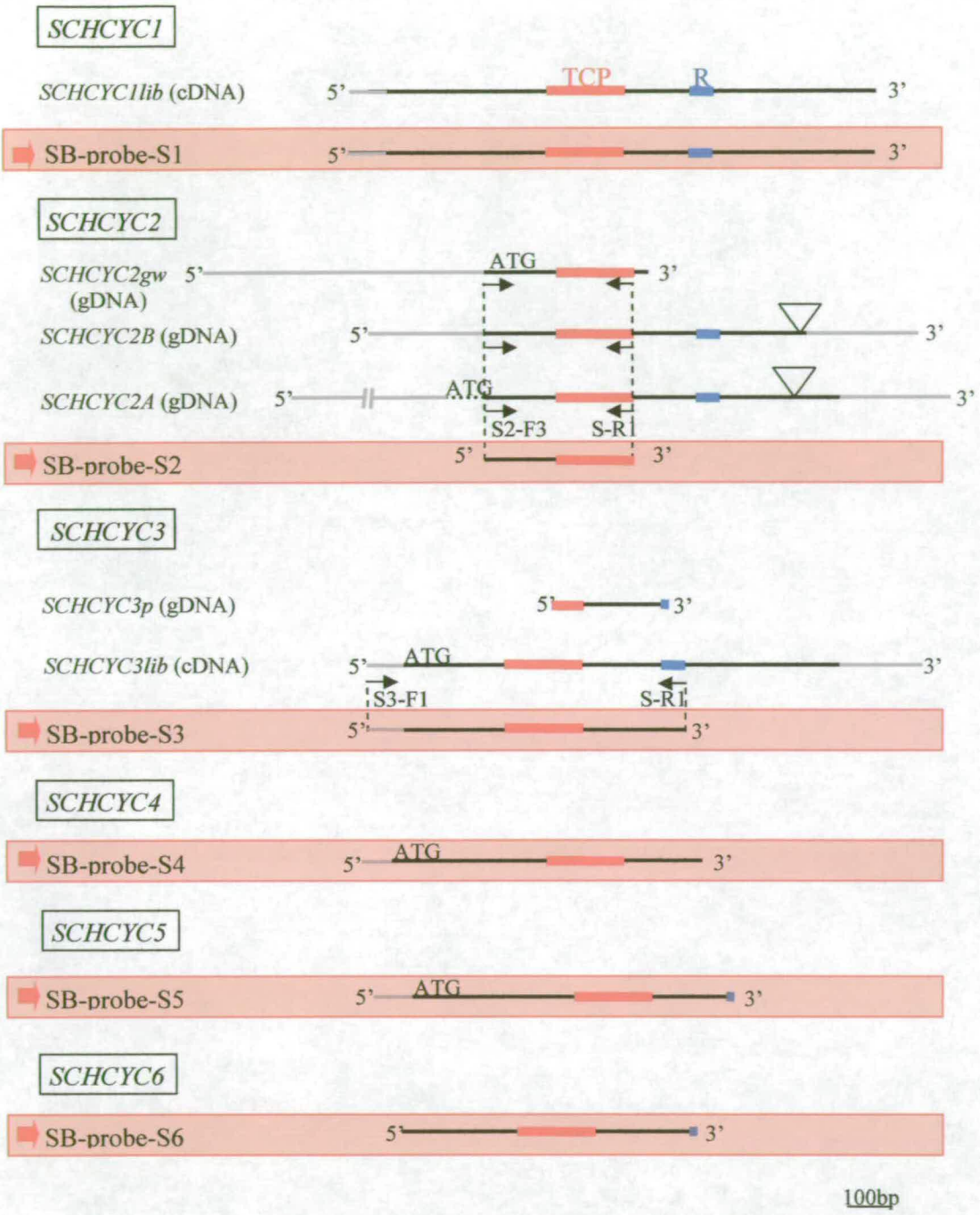

Fig IV.13: Map of gene sections used as template for Southern blotting probes in *S.wisotonensis*

Map of the partial cDNA and gDNA sequences form *SCHCYC1-6*. The full line indicates known coding sequence, the red and the blue sections correspond to the region of the cDNA coding the TCP and the R domain respectively. The red arrow indicates the region of the gene used as a template for the production of radioactive labelled probes.

If two genes are duplicated, and only one band in one digest can be observed because some of the DNA has not been transferred, then this single band should have the same intensity as any of the double bands. Assuming equal loading on the gel, if two alleles are picked up by the radioactive probe as two bands, then these two bands should be half as intense as single bands on the same blot. For each blot, the result of the radioactive hybridization is described as strong when the signal is the strongest, medium when its intensity is about half of a strong band and weak when the signal is clearly weaker than that of a medium band.

For *SCHCYC1*, the template used to produce a radioactive probe was the full length cDNA fragment obtained by a double digestion (*EcoR*I, *Hun*II) of the plasmid CK4 (Fig IV.13). In a first Southern blot, the gDNA was digested with *EcoR*I, *EcoR*V, *Dra*I, *Hind*III and *Nco*I (Fig IV.14(a&b)). The resulting hybridization pattern shows two lanes with a single band (strong) and two with a double band of similar strength (medium) and no bands for the *Dra*I digest (Fig IV.14a). On this blot, the difference in band intensities between the first two digests (*EcoR*I and *EcoR*V) and two last (*Hind*III and *Nco*I) is difficult to interpret. For *Hind*III and *Nco*I digests, the bands are of higher molecular weight which might account for the observed difference in intensity (less efficient transfer). A second Southern hybridization was done using the same probe, a different plant sample and the enzymes *EcoR*I, *EcoR*V and XbaI (Fig.IV.14b). Four bands were found in the *EcoR*I digest, two for EcoRV and one for XbaI, although the later was possibly due to incomplete digestion of the gDNA. When the patterns obtained with *EcoR*I are compared from one plant to the other, they appear different. However, both have in common band (i) and (ii). The presence of two more bands in (b) cannot be explained by the existence of additional

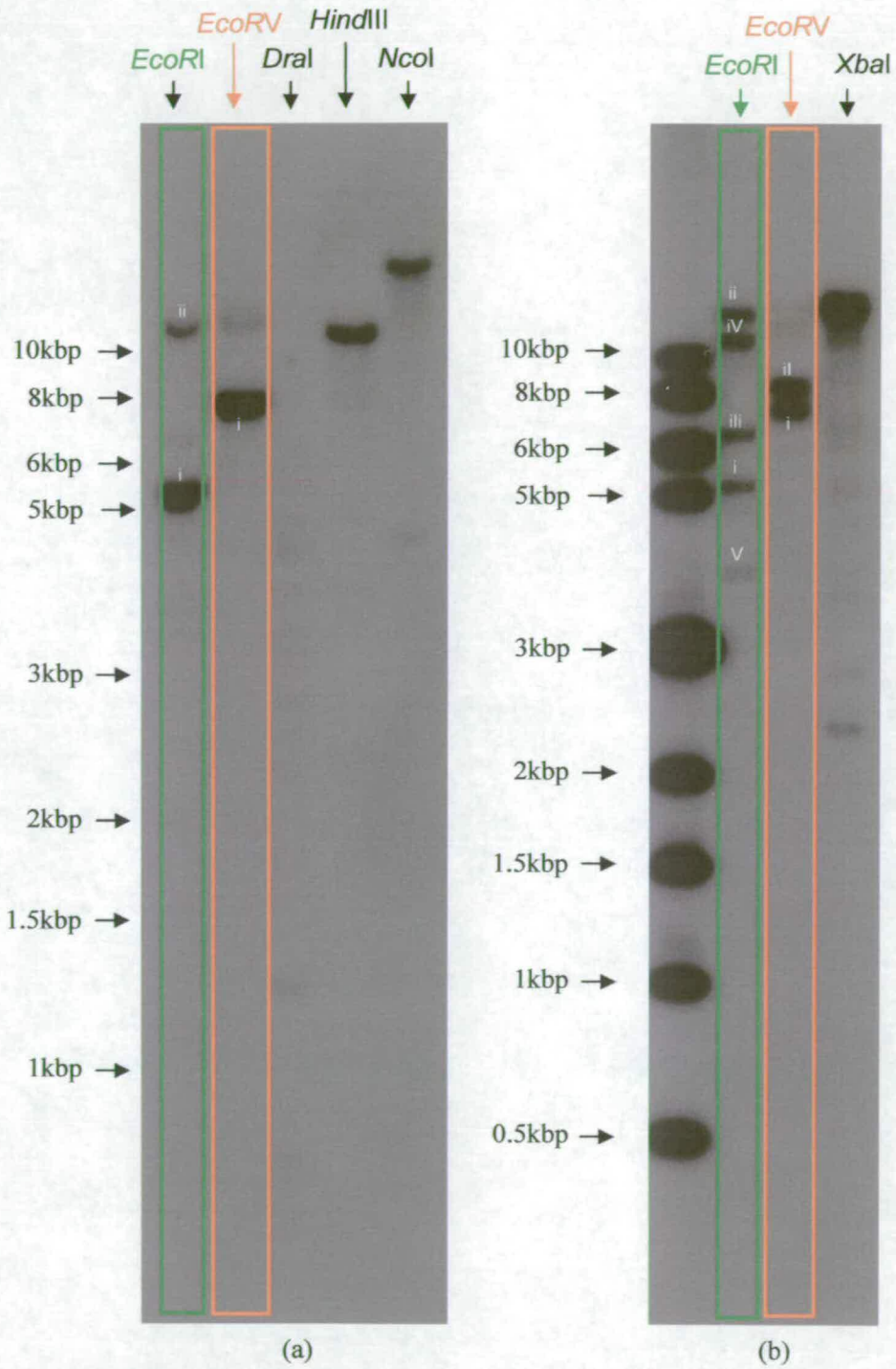

Fig IV.14: Southern hybridisation with a *SCHCYC1* radioactive probe in *S. wisotonensis*
Each blot corresponds to a different plants, polymorphism in band patterning can be observed for *EcoR*I and *EcoR*V (for the latter, it is likely that band (i) is a double band) . The line corresponding to *Xba*I has a pattern indicating that digestion might have been incomplete.

*EcoR*I sites within the region hybridized by the probe because the new bands would then be expected to have smaller molecular weight than about 5 kb. Therefore, it is very difficult to interpret these results because neither the allelic variation, nor the gene duplication hypotheses can account for the observed variation in banding pattern.

For *SCHCYC2*, a short probe was designed so that it would only hybridize to a small region of known DNA sequence in all known putative alleles. In the first instance, gDNA was extracted from 5 wild type plants, and from the progeny of a cross segregating for the *rz* mutant phenotype (two wild-types and two *rz* mutants). The gDNA of these 9 plants was digested with *EcoR*I and with *EcoR*V. The resulting hybrisation pattern obtained with *EcoR*I shows that, except for two lines (c&i), there are always at least two bands of equal intensity, with recurrent banding patterns (Fig IV.15a). When a third band is present, it is markedly weaker than the other two, suggesting that it is produced by the presence of an *EcoR*I restriction site within the radioactively labelled region. This type of pattern suggest that the variation is allelic (recurrent patterns reminiscent of segregation, lines with a unique band) and not due to gene duplication. Moreover, to support this hypothesis, two wild type and two *rz* mutant plants obtained from the same cross between a female wild type and a heterozygote *rz* mutant are also represented in this blot. The wild type plants are in line g&h and the *rz* mutant in line i&j. Overall, their banding pattern is not what would be expected from a diploid (only one major band in g,h&i). Instead, their respective banding pattern shows variation in band length and intensity, suggesting a change in location of *EcoR*I restriction sites, an outcome expected from a cross between parents plants supplied by different seed breeders.

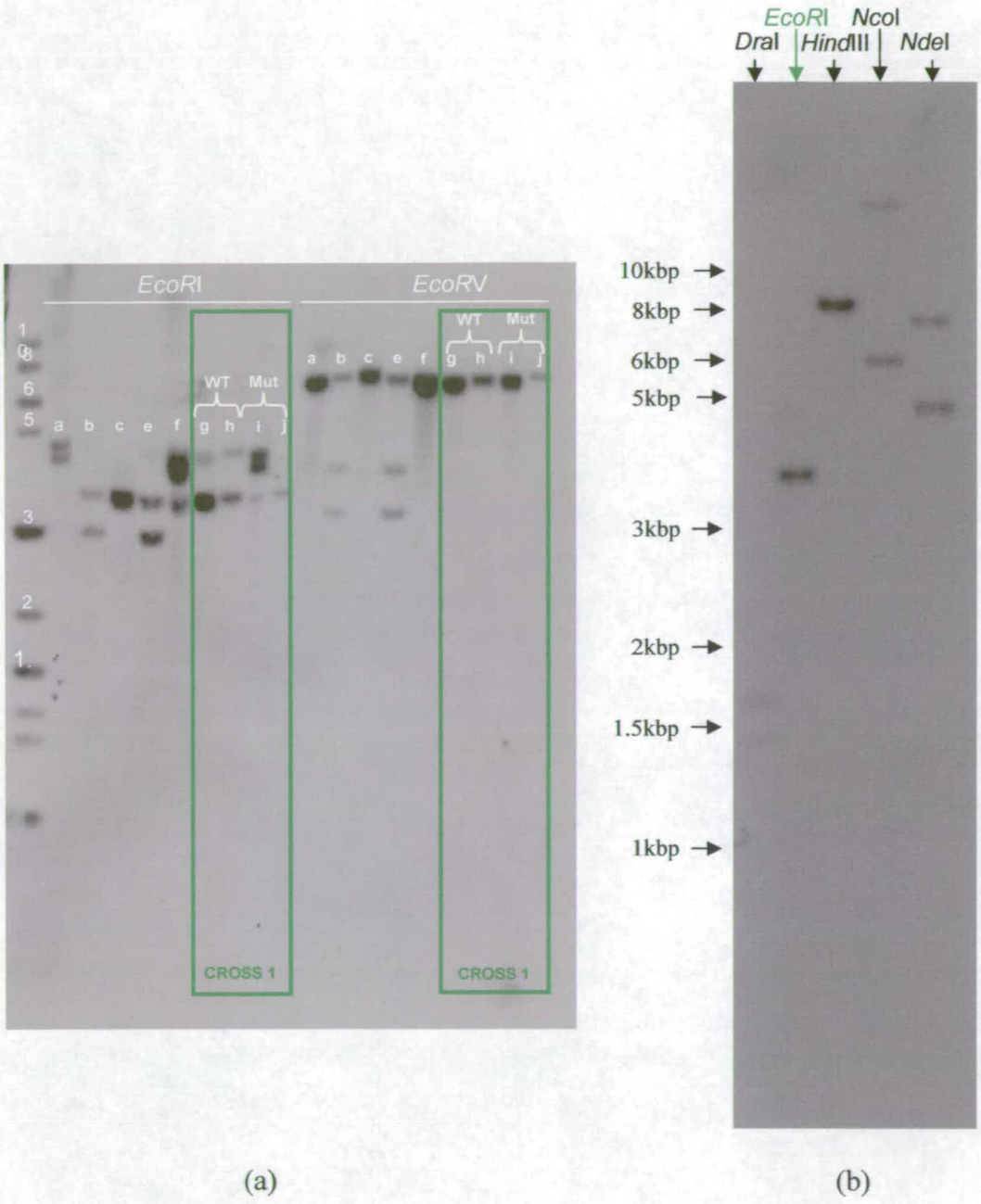

Fig IV.15: Southern hybridisation corresponding to *SCHCYC2* in *S. wisotonensis*
(a) Southern hybridisation based on using two enzymes and 9 plant samples, including two wild type (g&f) and two mutant plants (i&j) segregating from a single cross. The polymorphism observed between g,f,I and j strongly supports the hypothesis that allelic variation and not gene duplication is causing the variation in banding of pattern.
(b) Southern hybridisation with three enzymatic digestions on gDNA extracted from a single plant.

When digested with *EcoR*V, the pattern of hybridization shows only one band except for two lines where three bands are present, with the two weakest bands being of equal intensity. Interestingly, when added together, the lengths of the two weaker bands roughly add up to that of the larger band, suggesting that the weaker could be the product of *EcoR*V cutting within the area of the probe.

Therefore, although the results observed with *EcoR*I are difficult to interpret, the single band present in two lines for *EcoR*I digests and in most lines for *EcoR*V digests indicates that it is likely that *SCHCYC2* is single copy in *S. wisotonensis*. An additional Southern blot was done using the same probe and the following restriction enzymes (*Dra*I, *EcoR*I, *Hind*III, *Nco*I and *Nde*I) (Fig IV.15b). The corresponding autoradiograph shows two lines with a strong band, and two lines with two bands of medium intensity, the line corresponding the *Dra*I digestion being blank. These results further support that there might be only one locus for *SCHCYC2* and that the two bands observed for *Nco*I and *Nde*I could be due to allelic variation around the same locus. However, further experiments would be required to clarify this question.

For *SCHCYC3,* two separate Southern hybridizations were done using a short probe designed to only hybridize to the region of the gDNA which do not contain the intron. Overall, the resulting banding pattern shows two lanes with a unique band, two lanes with bands of equal intensity and a third lane with three bands (Fig III.16 (a&b)). Unfortunately, the single bands have a similar intensity to the double band present on the same blot, therefore it is not possible to conclude from this data if there are one or two copies of *SCHCYC3* in the genome of *S. wisotonensis*.

For *SCHCYC4*, the probe corresponded to the ORF up till the R box and about 60 bp of the putative UTR. The gDNA was digested with *EcoR*I, *EcoR*V and *Xba*I. In

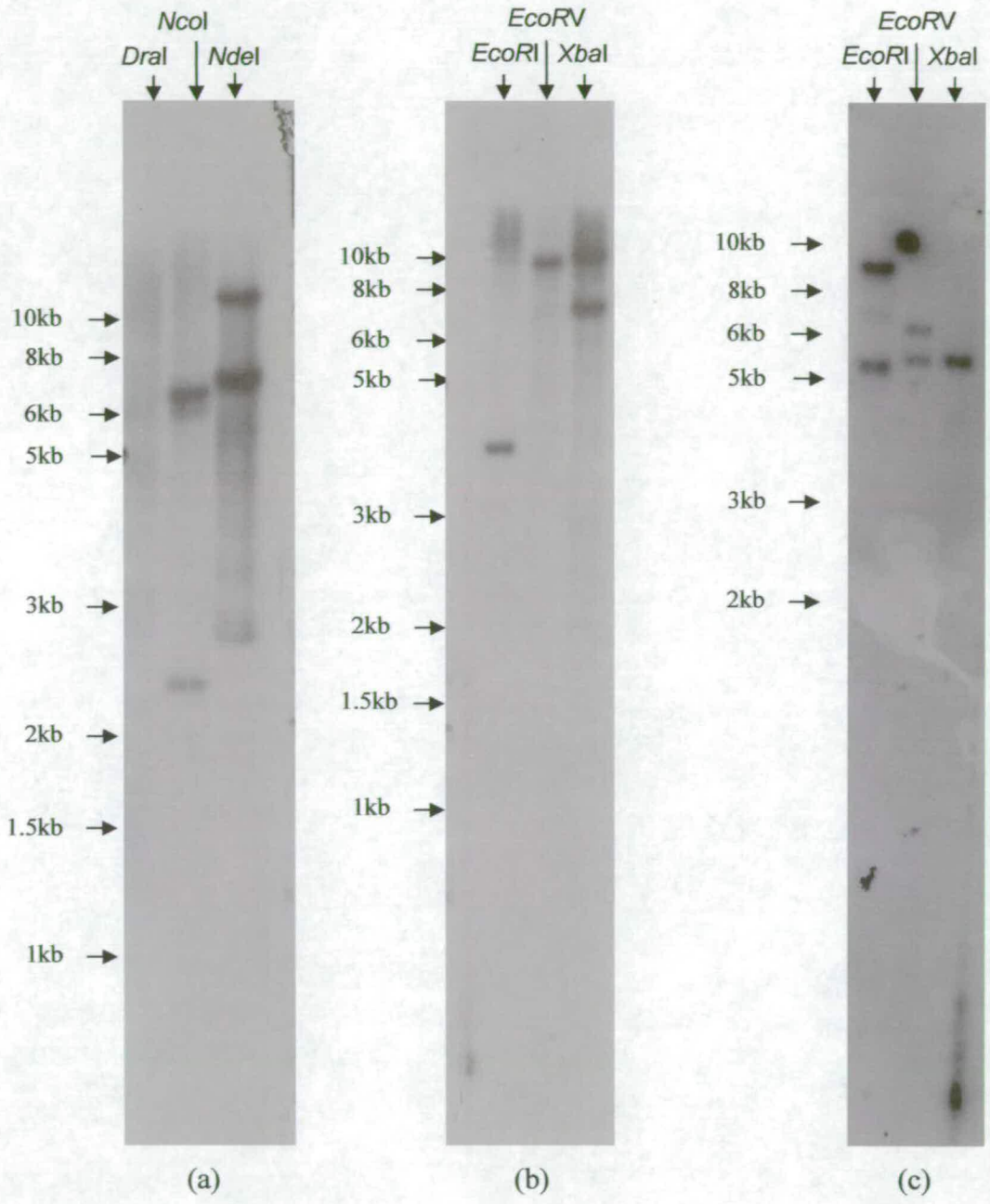

Fig IV.16: Southern hybridisation corresponding to *SCHCYC3* and *SCHCYC4* in *S. wisotonensis*

(a&b) Southern hybridisations corresponding to *SCHCYC3* on two different plants.
(c) Southern hybridisation corresponding to *SCHCYC4*.

the lane corresponding to the *EcoR*I digest, three bands, two strong and one weak were present; for *EcoR*V, two strong bands were observed, and for *Xba*I, one strong and one weak band hybridized with the radio-active probe (Fig IV.16c). It is therefore not possible to conclude from this result on how many copies of *SCHCYC4* are present in the genome of *S. wisotonensis*.

For *SCHCYC5* and *6*, a similar Southern hybridization as for *SCHCYC4* was carried out but failed to produce a clear hybridization pattern. There was no time to reproduce these experiments.

In summary, the results obtained using a Southern blotting are overall inconclusive. However, for *SCHCYC2*, these preliminary results indicate that, despite the variation in DNA sequence of the putative alleles, the possibility of only one locus being present cannot be ruled out.

IV.2.2.2 Determination of the putative CYCLOIDEA orthologs in S. wisotonensis

To determine the relationship of the genes isolated in this project with other TCP genes, a set of phylogenetic analyses were carried out. The sampling selection and phylogenetic analyses are reported in detail in material and methods. M1 is a matrix including the amino acid sequence of the TCP box from a wide range of angiosperm species (see II.3.1). M2 is a subset of M1, focussing on more related species to the Solanaceae. M3 corresponds to the same sampling as M1 but it features DNA rather than amino-acids sequences.

(i) SCHCYC1-6, NICYC1-2 and PETCYC1 in the TCP gene family

All analyses suggest that major groups can be distinguished in the TCP family (97-100% branch support, table IV.2). The first group corresponds to class I genes as described in the introduction. It includes all the PCF genes and *AtTCP*11 to 22. The second group corresponds to class II genes and includes *CYC* and *TB1*. Furthermore, the results suggest that in the latter, two well supported clades are present, one of which includes *CYC, DICH* and *LvCYC*, *OsTB1* and *MaizeTB1* (appendix IV. 14 to 20).

In all analysis, *SCHCYC1*-6, *NICYC1-2* and *PETCYC1* were found to belong to the same clade as *CYC* and *TB1* with varying branch support (74-100% BS, Table IV.2 and appendix IV.14 to 20).

(ii) SCHCYC1-6 in the CYC-TB1 clade

Most analyses on the *CYC-TB1* clade produced trees with a congruent topology. It divided the clade into four major sub-clades (sub-clade 1 to 4) supported by with varying branch support (Table IV.3, 4 and 5, appendix IV. 21-36). The ML analysis on M3 with Paup4b10 produced a poorly resolved strict consensus tree with bootstrapping. Therefore, it will not be discussed further

Sub-clade 1 includes *SCHCYC4* to *6*, *OsTB1* and *MaizeTB1*. This sub-clade is well supported in ML analyses on the protein matrix (BS: 93-97%). When ML analyses were run on the nucleotide matrix, only the Bayesian approach produced a well supported sub-clade (BS: 97%). In other ML analyses carried on the nucleotide matrix, sub-clade 1 is only weakly supported (BS: 52-59%). In distance analyses and parsimony analyses, this sub-clade is either not supported (BS<50%) or weakly

Method	Type of analysis	Phylogenetic program	BS for *SCHCYC1* to *6*, *NICYC1-2* and *PETCYC1* in the *CYC-TB1* group (class II)	BS for *SCHCYC1* to *6*, *NICYC1-2* and *PETCYC1* in the *CYC-TB1* clade
Distance	Neighbour Joining (Appendix IV.14)	PAUP 4.0b10	100%	97%
Distance	UPGMA (Appendix IV.15)	PAUP 4.0b10	100%	98%
Parsimony	Heuristic Search (Appendix IV.16)	PAUP 4.0b10	99%	74%
ML	VT model (Appendix IV.17)	Puzzle 5.2	99%	93%
ML	Dayhoff model (Appendix IV.18)	Puzzle 5.2	97%	82%
ML	JTT model (Appendix IV.19)	Puzzle 5.2	97%	90%
ML	WAG model (Appendix IV.20)	Puzzle 5.2	98%	90%

Table IV.2: Summary of the results obtained with the phylogenetic analyses carried out with the matrix M1 (amino-acids)

This set of analyses was carried out to show the grouping and corresponding internal branch support of the new solanaceous genes within the TCP family using the amino-acid sequence of the TCP domain (M1, appendix IV.37). BS: branch support (see corresponding appendices for detail of settings).

Table IV.3: Summary of the results obtained with the ML analyses carried out with the matrix M2 (amino-acids) and M3 (nucleotides)

Detail of analyses is given in appendix IV.21-30 and in material and methods. BS: branch support (see corresponding appendices for detail of settings).

Method	Type of analysis	Phylogenetic program	BS for *SCHCYC4* to 6 in the *TB1* clade	BS for *SCHCYC1-2-3*, *NICYC1-2* and *PETCYC1* as a separate clade	BS for *CYC*, *DICH* and *LvCYC* as a separate clade	BS for legumes sequences forming a separate clade	BS for solanaceous clade including *SCHCYC1-2-3* to form a sister group to *CYC-TB1* clade
ML (protein)	VT model (Appendix IV.21)	Puzzle 5.2	**94%**	**87%**	56%	**94%**	<50%
ML (protein)	Dayhoff model (Appendix IV.22)	Puzzle 5.2	**93%**	**94%**	52%	**95%**	<50%
ML (protein)	JTT model (Appendix IV.23)	Puzzle 5.2	**93%**	**96%**	54%	**92%**	<50%
ML (protein)	WAG model (Appendix IV.24)	Puzzle 5.2	**94%**	**94%**	56%	**94%**	<50%
ML (nucleotide)	Bayesian approach (Appendix IV.25)	Mr Bayes	**97%**	**100%**	**100%**	70%	**98%**
ML (nucleotide)	HKY model (Appendix IV.26)	Puzzle 5.2	59%	**96%**	**92%**	67%	<50%
ML (nucleotide)	TN model (Appendix IV.27)	Puzzle 5.2	60%	**97%**	**92%**	69%	<50%
ML (nucleotide)	GTR model (Appendix IV.28)	Puzzle 5.2	52%	**96%**	**90%**	63%	<50%
ML (nucleotide)	SH model (Appendix IV.29)	Puzzle 5.2	57%	**95%**	**90%**	67%	<50%
ML (nucleotide)	TrN+I+G model (Appendix IV.30)	PAUP 4.0b10	<50%	62%	63%	<50%	<50%

Table IV.4: Summary of the results obtained with the distance analyses carried out with the matrix M2 (amino-acids) and M3 (nucleotides)
Detail of analyses is given in appendix IV.31-34 and in material and methods. BS: branch support (see corresponding appendices for detail of settings).

Method	Type of analysis	Phylogenetic program	BS for *SCHCYC4* to 6 in the *TB1* clade	BS for *SCHCYC1-2-3*, *NICYC1-2* and *PETCYC1* forming a separate clade	BS for *CYC*, *DICH* and *LvCYC* forming a separate clade	BS for legumes sequences forming a separate clade	BS for solanaceous clade including *SCHCYC1-2-3* to form a sister group to *CYC-TB1* clade
Distance (protein)	Neighbour Joining (Appendix IV.31)	PAUP 4.0b10	69%	58%	57%	**99%**	<50%
Distance (protein)	UPGMA (Appendix IV.32)	PAUP 4.0b10	<50%	<50%	63%	**99%**	<50%
Distance (nucleotide)	Neighbour Joining (Appendix IV.33)	PAUP 4.0b10	<50%	**90%**	70%	70%	60%
Distance (nucleotide)	UPGMA (Appendix IV.34)	PAUP 4.0b10	<50%	**89%**	**95%**	**100%**	**64%**

Table IV.5: Summary of the results obtained with the parsimony analyses carried out with the matrix M2 (amino-acids) and M3 (nucleotides)
Detail of analyses is given in appendix IV.35-36 and in material and methods. BS: branch support (see corresponding appendices for detail of settings).

Method	Type of analysis	Phylogenetic program	BS for *SCHCYC4* to 6 in the *TB1* clade	BS for *SCHCYC1-2-3*, *NICYC1-2* and *PETCYC1* as a separate clade	BS for *CYC*, *DICH* and *LvCYC* forming a separate clade	BS for legumes sequences forming a separate clade	BS for solanaceous clade including *SCHCYC1-2-3* to form a sister group to *CYC/DICH* clade
Parsimony (protein)	Heuristic Search (Appendix IV.35)	PAUP 4.0b10	67%	57%	Polytomy	**99%**	Polytomy
Parsimony (nucleotide)	Heuristic Search (Appendix IV.36)	PAUP 4.0b10	<50%	84%	71%	68%	50%

supported for the NJ analysis and the parsimony analyses carried out on the protein matrix (BS: 69% and 67% respectively).

Sub-clade 2 includes *SCHCYC1* to *3*, *NICYC1-2* and *PETCYC1*. It is strongly supported in all ML analyses (protein and nucleotide matrices, BS: 87-100%). This sub-clade is also strongly supported in the distance and the parsimony analyses carried out on the nucleotide matrix (BS: 84-90%). Finally, it is less supported in the distance and parsimony analysis on the protein matrix (BS: <50% for the UPGMA analysis and BS: 67-69% for parsimony and NJ analyses).

Sub-clade 3 comprises *CYC*, *DICH* and *LvCYC*. It is well supported for ML analyses on the nucleotide matrix (BS: 92-100%) and on the UPGMA analysis with the same matrix (BS: 95%). For all other analyses with the exception of the parsimony analysis on the protein matrix, the branch support for this sub-clade varies between 50-70%.

Finally, sub-clade 4 includes the legumes sequences. It is strongly supported in all analyses carried out on the protein matrix (BS: 92-100%) and more weakly supported when using the nucleotide matrix (BS: 63-70%).

AtTCP1, the putative *Arabidopsis* ortholog of *CYC* is sometimes found grouping with the scrophulariaceous sub-clade (sub-clade 3) and often on its own, sitting on a polytomic node in most analyses (Appendix IV. 14 to 36).

The identification of the solanaceous sub-clade (sub-clade 2) as a sister group to the *CYC-DICH* sub-clade (sub-clade 3) is not supported or weakly supported (BS: 50-64%) on all analyses except for the bayesian approach in which this grouping achieves 98% branch support (Appendix IV.14 to 36).

In summary, in most trees, the phylogenetic analyses carried out on the protein and the nucleotide matrices for the *CYC-TB1* clade suggest that this group can be further sub-divided into four major sub-clades. These are the *TB1* sub-clade including often *SCHCYC4* to *6*, the solanaceous sub-clade (*SCHCYC1* to *3*, *NICYC1-2* and *PETCYC1*), the *CYC/DICH* sub-clade and the legume sub-clade. However, the topology of these sub-clades within the *CYC-TB1* clade could not be confidently resolved.

IV.3 Discussion

IV.3.1 *S. wisotonensis*, hybrid or not?

S. wisotonensis is traditionally considered as a diploid hybrid between *S. pinnatus* and *S. grahamii* (*S.* x *wisotonensis*).

The origin of *S. wisotonensis* has been challenged by Walters (1969). By doing crosses and observing the natural variation of *S. Pinnatus* in the wild compared to that of *S. wisotonensis*, he proposed that *S. wisotonensis* is in fact the result of crosses between variants of *S. Pinnatus*.

In this project, putative alleles of TCP genes were isolated in *S. wisotonensis*. The sequence variation found in the 5' upstream region of *SCHCYC2* is mostly unalignable. This observation supports the hypothesis of the hybrid origin of *S. wisotonensis*. When the sequences obtained by Reeves and Olmstead (2003) in *S. pinnatus* are compared to that obtained in this project for *S. wisotonensis* (table IV.6), the sequence similarity between the sequences in both species indicates that indeed, *S. pinnatus* is a putative parent of *S. wisotonensis* (100% DNA sequence similarity found between *PRSCHCYC3* and *SCHCYC3lib*). Therefore, the isolation of putative

	PRSCHCYC7 (*S. pinnatus*)
SCHCYC3 (*S. wisotonensis*)	100%

	PRSCHCYC1 (*S. pinnatus*)	*PRSCHCYC2* (*S. pinnatus*)
SCHCYC4 (*S. wisotonensis*)	97.5%	97.5%
PRSCHCYC2 (*S. pinnatus*)	100%	-

	PRSCHCYC5 (*S. pinnatus*)	*PRSCHCYC6* (*S. pinnatus*)
SCHCYC5 (*S. wisotonensis*)	98.5%	99.4%
PRSCHCYC6 (*S. pinnatus*)	98.5%	-

	PRSCHCYC3 (*S. pinnatus*)	*PRSCHCYC4* (*S. pinnatus*)
SCHCYC6 (*S. wisotonensis*)	96.3%	98.1%
PRSCHCYC4 (*S. pinnatus*)	94.4%	-

Table IV.6 Nucleotide sequence similarity between the genes isolated in *S. wisotonensis* and *S. pinnatus*

The region situated between the TCP and the R box was aligned to determine the sequence similarity.

alleles in *S. wisotonensis* and *S. pinnatus* provide preliminary data which support the hybrid hypothesis regarding the origin of this species.

IV.3.2 Allelic variation in *S. wisotonensis*: how many copies of *SCHCYC1, 2, 4, 5 & 6* are present in the genomes of *S. wisotonensis*?

S. wisotonensis cultivars are known to produce a reduced seed set and low vigor progeny after a few generations of self-pollination (M. Möller, pers. comm.). This observation suggests that this species is outbreeding and that panmixis pollination is required. Therefore, it is not possible to generate pure inbred lines and a degree of variation is being maintained purposely within the population by the breeders themselves. Consequently, whether *S. wisotonensis* is a hybrid or not, its obscure origin and outbreeding characteristics suggest that allelic variation is expected when comparing the DNA sequence from the same putative locus isolated in separate plants. Alternatively, gene duplication might be at the origin of some of the variation observed.

In this project, for every putative locus, at least two almost identical genes were isolated. To determine if all sequences labelled as the same putative locus are indeed alleles and not duplicated genes, a Southern hybridization approach was undertaken. As mentioned above, the data obtained by Southern hybridization suggested the possibility of *SCHCYC2* being single copy in *S. wisotonensis*. However, for *SCHCYC1, 3* and *4*, despite several attempts, a mixture of single and double bands was found, providing a confusing picture. Although more experiments are needed to clarify this question, this data can be used to draw preliminary conclusions.

Except for *SCHCYC1*, the overall variation in banding patterns for *SCHCYC3* and *4* is similar to that found for *SCHCYC2* on equivalent blots. This similarity suggests that, if the frequency of the double bands is attributed to allelic variation as it could be for *SCHCYC2,* then *SCHCYC3* and *SCHCYC4* could also be present as single copies in the genome of *S. wisotonensis*. For *SCHCYC1,* the detection of 4 bands of similar intensity in a single line (Fig IV.13a, *EcoR*I digest) is clearly not similar to any of the patterns obtained so far. One obvious explanation would be the presence of duplicated loci in addition to allelic variation. Such a phenomenon could be the result of unequal crossing-over during meiosis or to a transposition event, both phenomena being relatively frequent in genes belonging to gene families (Ridley, 1996, Lawton-Rauh, 2002). Alternatively, since the four bands were only observed in only one plant, this particular specimen could be a tetraploid hybrid within the otherwise diploid population.

To determine accurately how many copies of each gene are present in the genome of *S. wisotonensis*, a similar study on a segregating population obtained from selfing plants should be carried out.

IV.3.3 Are any of the solanaceous TCP genes isolated in this study likely orthologs of *CYC*?

The study carried out in the Solanaceae is similar in its purpose and principle to that perfomed by H. Citerne in legumes (Helene Citerne, pers. comm.).

For the high order analyses, the basic structure of all trees is congruent with previously described TCP family trees (Citerne *et al.,* 2003, Cubas, 2002, Fukuda,

Yokoyama and Mura, 2003) suggesting that the sampling strategy was suitable for the analysis.

In Citerne *et al.* (2003), Fukuda, Yokoyama and Maki (2003) and Lukens and Doebley (2001), the detailed study of the *CYC-TB1* clade indicates that the *CYC-TB1* group is sub-divided into two clades: the clade containing *CYC* and *TB1* and another clade including genes for which, apart from *AmCINCINNATA* (Nath *et al.*, 2003; Crawford *et al.*, 2004), the function is still unknown (Citerne *et al.*, 2003). In our study, the same topology is recovered and the *CYC-TB1* clade is also strongly supported. This result suggests that all genes belonging to the *CYC-TB1* clade are likely to be derived from a common ancestor. Interestingly, in the *CYC-TB1* sub-clade, more than one gene has been isolated for *S. wisotonensis*, *Cadia*, *Pueraria lobata* and *A. thaliana* (Citerne *et al.*, 2003) (Fukuda, Yokoyama and Maki, 2003). In each of these species, phylogenetic analyses support a division of these genes in two groups (Citerne *et al.*, 2003; Fukuda, Yokoyama and Maki, 2003). One group corresponds to the genes related to *TB1* such as *SCHCYC4* to *6* in *S. wisotonensis*, *Cadia4* in legumes (Citerne *et al.*, 2003), PITCP3 in *P. lobata* and *AtTB1* in *Arabidopsis* (Fukuda, Yokoyama and Maki, 2003). The other group includes all the non-*TB1*-like sequences. Within this group, family-specific sub-clades are present (Citerne *et al.*, 2003; Fukuda, Yokoyama and Maki, 2003) except for *AtTCP1* which can therefore be considered as the only putative ortholog of *CYC* in *A. thaliana.*

This observation suggests that at least one duplication event might have taken place before the split between the monocots and the eudicots. The most parsimonious hypothesis would be that this duplication generated the ancestor of the *TB1*-like genes and that of the non-*TB1* genes. In the latter group, the genes speciated faster than in

the *TB1*-like group resulting in the split of the group into family-specific sub-clades.

In maize and rice, the absence of a *CYC*-like gene could be explained either by a gene loss or because it has not been found yet.

This hypothesis would explain that neither the work in legumes nor the study on the Solanaceae can determine accurately orthologous relationships to *CYC* and *DICH*. In the present study, the more likely candidates to have conserved role in *S. wisotonensis* with that of *CYC* and *DICH* in *A. majus* are by default the genes which are not putative orthologs of *TB1,* i.e. *SCHCYC1* to *3*. However, it is not possible to determine which one of these genes is the most likely candidate.

Overall, the results obtained in this study agree with what was found by Reeves and Olmstead (2003). Using a predictive functional approach based on amino-acid sequences, they suggested that amongst the gene isolated in their study (i.e. *SCHCYC3* to *6*), only *SCHCYC3* was the most likely TCP gene in the Solanaceae to have a role similar to *CYC* in the establishment of dorso-ventral asymmetry. They also found that their alleles of *SCHCYC4* to *6* belong to the *TB1* clade. However, two major differences in the methology can explain why our analyses produce more strongly supported trees. Firstly, only genes for which the sequence of the entire TCP domain was known were included in our analysis, thereby increasing the number of phylogenetic informative characters available. In addition, a more balanced data set was obtained in this study which included many sequences closer to *CYC* and *DICH* than to *TB1*. On the contrary, in their work, Reeves and Olmstead (2003) isolated mostly members of the *TB1* clade which provided only a partial view of the range of *CYC* and *TB1*-like genes present in *Schizanthus* and in the Solanaceae.

IV.3.4 Is PCR a reliable technique to isolate new member of multi-genes families?

In this project, both the advantages and disadvantages of using PCR as a reliable technique to isolate new members of multi-gene families have been clearly illustrated.

In the TCP gene family, the presence of two conserved domains (TCP and R domains) in many members of class II provides the required data to isolate new genes using PCR based techniques. Degenerate primers can be designed and used in PCR or RT-PCR with low annealing temperatures. This technique contributed to the isolation of partial TCP sequences in many angiosperm species from non-related families (e.g. Gesneriaceae, Leguminoseae, Asteraceae). In a recent paper, Reeves and Olmstead (2003) reported the use of nine pairwise primer combinations in PCR on gDNA to isolate TCP genes from a variety of solanaceous species. This technique enabled them to isolate 12 sequences, 3 in *Solanum* (a genus with regular flowers), 2 in *Nicotiana* and 7 in *Schizanthus pinnatus*. However, in the latter, the 7 sequences are very likely to correspond to only 4 loci. A simple comparison with the sequence isolated here indicates that Reeves and Olmstead (2003) were not able to isolate *NICYC1*, *NICYC2*, *SCHCYC1* and *SCHCYC2*, all genes closely related to *CYCLOIDEA* and *DICHOTOMA*. Therefore their technique proved to be unreliable to address the type of biological and developmental question relevant to their study. Conversely, the primer combinations used in this project did not allow the isolation of other TCP genes in *Nicotiana* than *NICYC1* and *NICYC2,* and did not amplify *SCHCYC6* in *S. wisotonensis*. This suggests that the design of primers and the material used (gDNA and cDNA) may lead to preferential amplification. Therefore, using a PCR approach with arrays of primers cannot guarantee the isolation of all *CYC*-like genes. In

addition, the forward primers being designed against the TCP box itself entails the loss of phylogenetic informative sequence upstream and at the primer's location. Therefore, although a simple PCR approach enables the isolation of new *CYC*-like genes from non-model species, preferential amplification and shortened TCP domains are likely to lead to incomplete data sets. Consequently, without further experiments, the relevance of such data to study the evolution of members of this gene family and to propose evolutionary theories concerning floral symmetry is open to discussion.

In conclusion, the present study shows that in *S. wisotonensis*, *SCHCYC1* to *3* are clearly the most likely candidates to have a role resembling that of *CYC* in the control of floral dorso-ventral asymmetry. It also shows that *SCHCYC4* to *6* are not *CYC*-like genes as such and instead, they should be renamed *SCHTB1*-like genes since they are more related to *TB1* than to *CYC*. The putative origin of the split between the *SCHCYC*-like genes and the *SCHTB1*-like genes possibly predates the split between the monocots and the eudicots. In addition, this study confirmed the existence of related genes to *SCHCYC1* to *3* in *Petunia* and *N. tabaccum*. Their relationship suggests a duplication event near the base of the Solanaceae. Therefore, the phylogenetic analysis of the *CYC*-like genes in this project provides an interesting data set to further study the evolution of *CYC*-like genes in the Solanaceae.

In the next chapter, the expression pattern of *SCHCYC1* to *3* will be studied in detail in the wild-type and in the *rz* mutant flower to further explore their putative role in the control of zygomorphy.

V The molecular genetics of *CYC*-like genes in *Schizanthus wisotonensis*

V.1 Introduction

In *S. wisotonensis*, 6 TCP genes have been isolated so far. The phylogenetic analysis carried out in chapter IV suggests that *SCHCYC1, SCHCYC2* and *SCHCYC3*, are the most likely *CYC*-like genes in this species. This suggestion is further supported by the work of Marc Chadwick who determined that *SCHCYC1* is expressed in the primordia of staminodes. This expression pattern is clearly reminiscent of that of *CYC* and *DICH* which are both expressed in the dorsal staminode of *A. majus*. Therefore, taken together these results suggest that *SCHCYC1, SCHCYC2* and *SCHCYC3* (both as related as *SCHCYC1* to *CYC* and *DICH*) are candidates genes for roles in the establishment of floral dorso-ventral asymmetry in *S. wisotonensis*..

In this final result chapter, tests of this hypothesis are reported. Firstly, the isolation and test of two positive controls for *in situ* hybridization experiments will be described. Secondly, an overview of the pattern of expression found for *SCHCYC1* to *6* in the reproductive and the vegetative tissue will be presented. All pattern of expression reported here have been observed repeatedly over the 9 sets of *in situ* hybridization experiments carried out for this project. Finally, the genetics of the *rz* mutant will be discussed together with the result of the corresponding RNA *in situ* hybridization experiments.

V.2. Experimental approach and results

V.2.1 Isolation and characterization of a B-type cyclin gene and a *LEAFY*-like gene in *S. wisotonensis* to be used as positive controls for RNA *in situ* hybridization experiments

V.2.1.1 Isolation and characterization of the partial cDNA sequence of a cyclin B gene in S. wisotonensis

B-type cyclins are classified as mitotic cyclins (Mironov *et al.*, 1999). They are regulatory sub-units of cyclin-dependent kinases (CDKs) belonging to the B-type class. The activity of B-type CDKs is prominently linked to mitosis (Mironov *et al.*, 1999). In many plant species including *Arabidopsis* (Ferreira *et al.*, 1994), *Catharanthus roseus* (Ito *et al.*, 1998) and *Nicotiana sylvestris* (Tréhin *et al.*, 1999), G2 and M phase-specific peaks of expression of B-type cyclins have been reported. Consequently, if B-type cyclin genes are expressed in dividing tissues such as meristems (Himanen *et al.*, 2003), they are suitable genes to be used as positive controls for *in-situ* hybridization for this project. To my knowledge, no sequences of mitotic cyclins have ever been published from *S. wisotonensis*. Therefore, to obtain a cyclin B clone from this species, a screening of the cDNA library was carried out at low stringency using a tobacco cyclin B cDNA fragment as a probe.

(i) Isolation of a tobacco cyclin B probe

Two primers (F-186; R-1380) designed to amplify a B-type cyclin from cDNA in tobacco were kindly provided by Dr. Peter Doerner. They were used to amplify by PCR a B-type cyclin sequence in the same species using the 5' race cDNA mix as a template (see II.2.2). When the PCR reaction mix was run on an agarose gel, a single band of the expected size (about 1.2 kb) was observed. The PCR

product was then cloned in pGEM®-T Easy vector (KC30-8). The plasmid was used as a template to amplify by PCR the corresponding fragment with F-186 and R-1380. The resulting PCR product was purified, sequenced and used as a template to produce a radio-active probe to screen the cDNA library made for *S. wisotonensis* (see material and methods II.1.12).

(ii) Screening of the cDNA library in S. wisotonensis

As expected for a B-type cyclin gene, many positive plaques were observed and only ten of them were selected to be tested by PCR using vector specific primers. The corresponding agarose gel picture showed a smear and the gel was blotted. A subsequent Southern hybridization of the gel revealed than in 6 of these plaques, a phage containing an insert of between 1.5 and 2kb that hybridized with the tobacco radio-active probe was present. Aliquots of two separate plaques were carried through to the second run of screening. The corresponding phagemids were excised and re-ligated resulting in two pBluescript® SK vectors named CK 11-1 and CK 11-2. For both plasmids, an *EcoR*I and *Xho*I digest revealed two bands, one of about 700 bp and the other of about 1.1 kb. Single digests reactions with *EcoR*I and *Xho*I confirmed later that a recognition site for *EcoRI* was present within the cDNA fragment (Fig V.1). The sequencing of CK11-2 was carried out using vector specific primers to verify the identity of the clone. The resulting sequences did not overlap suggesting that the fragment was too long to be sequenced with vector specific primers (Appendix V.1). However, when submitted to a BLAST query, both DNA sequences showed a highest sequence similarity with the same tobacco cyclin-B gene (D89635.1). Consequently, CK11-2 was renamed *SwCYCLINB1*.

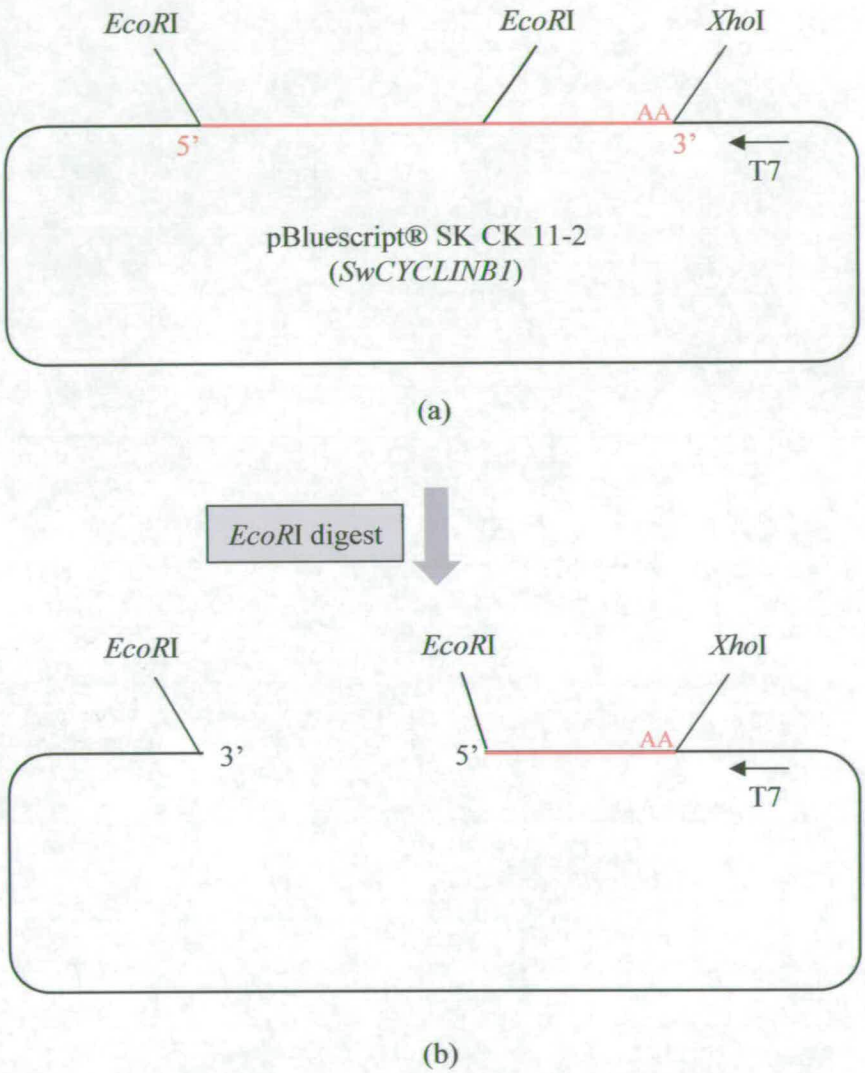

Fig V.1: Synthesis of the template for the *SwCYCLINB1* anti-sense probe
(a) Map of the pBluescript®SK CK 11-2 plasmid containing a ±1.8 kb cDNA corresponding to a *SwCYCLINB* (in red) (b) template for the *SwCYCLINB* probe (in red) obtained by digestion of CK11-2 with *EcoR*I. AA: indicates the presence of a polyA+ tail, T7 indicates binding site for the RNA polymerase T7.

Fig V.2: Characteristic expression pattern of *SwCYCLINB1* in developing tissues
A "spotty" expression pattern likely to correspond to individual cells at the G2 and M phase (prior to cell-division) was observed throughout all developing tissues.

(iii) Testing the experimental conditions for RNA in situ hybridization using a cyclin B probe in S. Wisotonensis

For the probe, the pBluescript® vector was linearised with *EcoR*I so that only about 700 bp of the 3' end of the *SwCYCLINB1* cDNA was available as template for the synthesis the anti-sense probe using T7 RNA polymerase (Fig V.1). The standard conditions were used to synthesize the *SCHCYCLINB1* probe (see II.2.3.2).

Several RNA *in situ* hybridizations were carried at the beginning of the project using fragments of *SCHCYC1* and *SCHCYC2* as probes. The protocol was exactly as described in material and methods (II.2.3) except for the rinses which were done in 0.2X SSC at 55°C instead of 50% formamide in 2X SSC at 50°C. However, the level of the background signal was such that it was not possible to interpret the results. Consequently, a series of *in situ* hybridization reactions were set-up to test experimental conditions using a probe designed to hybridize to *SwCYCLINB1* transcripts. In this experiment, the standard protocol (II.2.3) was followed (post-hybridization rinses in 50% in 2X SSC formamide at 50°C). A range of experimental conditions were tested including the standard conditions and the following modifications: dilution of the probe by 100 and by 1000 fold, doubling of the amount of Proteinase K and hybridization at 65°C. The results showed a "spotty" hybridization pattern in young inflorescences apices and young flower buds (Fig V.2). This pattern of expression was recovered for all conditions except when the probe was diluted by 1000 folds. However, the intensity of the signal varied between the different slides. It was found to be the strongest when using twice the amount of proteinase K compared to standard conditions. However, the corresponding slides had a higher level of background than slides with lower concentration of Proteinase K. Therefore, it was decided to use 1.5X the normal concentration of Proteinase K in

future experiments on the assumption that it could probably enhance the signal strength without resulting in background interference.

V.2.1.2 Isolation and characterization of the partial cDNA sequence of a LEAFY ortholog in S. wisotonensis

Given the complexity of the structure of the inflorescence in *S. wisotonensis,* it was decided to try and isolate a marker to identify the domain in the juvenile IM and the bifurcating structure which has acquired floral fate.

(i) PCR strategy to isolate a LEAFY ortholog in S. wisotonensis

In *Petunia,* tobacco and tomato, *LEAFY*-like genes have been isolated and characterized (Souer *et al.,* 1998, Molinero-Rosales *et al.,* 1999, Kelly *et al.,* 1995). With the help of a published alignment of *LEAFY*-like genes isolated in various species (Souer *et al.,*1998, Fig V.3a), a set of primers corresponding to highly conserved regions was designed (Salf-F and Salf-R)(Fig V.3b). A medium stringency PCR was carried out (annealing temperature: 55°C) on Poly A^+ cDNA (II.2.2) and a unique band of about 800bp was observed on the corresponding gel. The reaction mix was cloned into the pGEM®-T Easy vector (KC 57). Two types of inserts with different length were observed when individual clones were digested with *EcoR*I. The most frequent clones were about 100bp larger than the less frequent ones. The sequencing of one plasmid of each type revealed 100% DNA sequence identity between them except for the presence of an additional 81 bp "in frame" in the larger clones. The visual comparison to other *LEAFY*-like sequences isolated in the Solanaceae confirmed the identity of the cloned products as *LEAFY*-like genes. The longer clone was selected to produce templates for an *in situ* hybridization probe

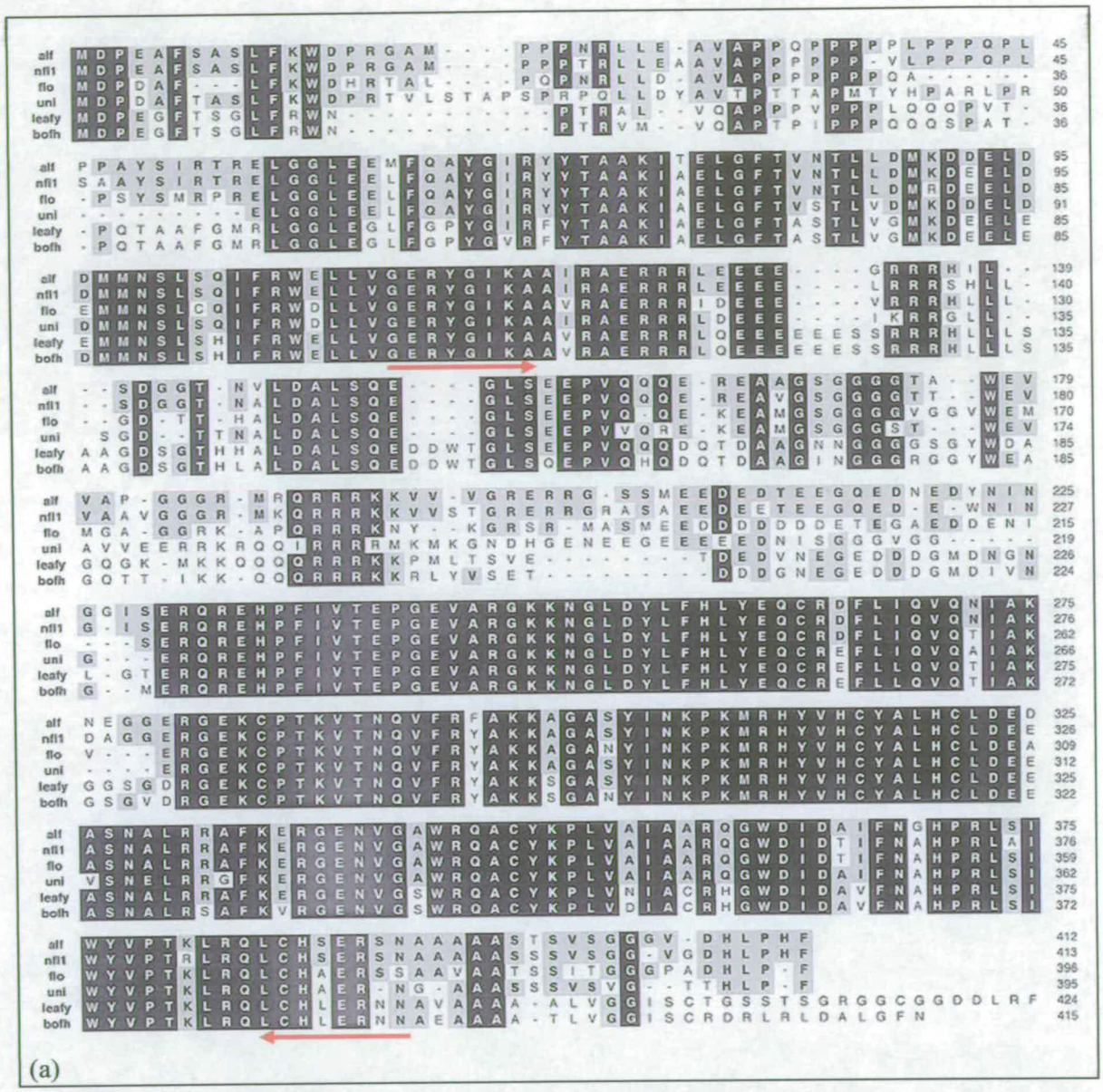

SalfF: 5'-GGA GAA AGG TAT/C GGT ATC AAA GC-3'
SalfR: 5'-TT/C CGT TCA GAG/G TGG CAA AGC-3'
(b)

Fig V.3: Position and sequence of the degenerate primers designed to amplify a *LEAFY*-like gene in *S. wisotonensis*

(a) The red arrow indicates the position of the primers on the alignment of the protein sequences of *LEAFY (*leafy) in *A. thaliana,* and *LEAFY*-like genes in petunia (alf), tobacco (nfl1), *A. majus* (flo), *Brassica oleracea* (Bofh). (b) Primers sequences.

(Appendix V.2). The plasmid (KC57-6) was chosen so that it could be linearized using *Spe*I and allow the use of the T7 RNA polymerase. The 5' end of KC57-6 was sequenced to confirm its identity. It was renamed *SwLFY*1.

(ii) RNA in situ expression pattern obtained with SwLFY1 probe in S. wisotonensis

The probe was synthesized using the standard method (see II.2.3.2) and the T7 RNA polymerase. The pattern of expression showed a very strong signal in developing floral organ with the exception of the central domain of the flower (Fig V.4a). In bifurcating structures, the signal was found to be stronger only in one of meristems (Fig IV.4b). In addition, a strong signal was also observed in meristems growing in axillary positions with respect to flowers (Fig V.4 a&c). In the latter, the signal was found either throughout the meristem (Fig IV.4a) or only to one side (FigV.4b).

When the pattern of expression of *SwLFY1* was compared to that of other *LEAFY*-like genes in the Solanaceae (see discussion, V.3.2), the *SwLFY1* probe was deemed suitable to be used as a marker to identify which domain of a juvenile meristem was destined to become either a bract or a flower. Therefore, by default, when the signal was not detected in a meristematic structure, the corresponding domain was identified as inflorescence.

V.2.2 The pattern of expression of *SCHCYC1, SCHCYC2 and SCHCYC3* in *S. wisotonensis (WT)*

In all the experiments described below, the *SwCYCLINB1* probe was used as a positive control alongside other samples. All the inflorescences used for this

Fig V.4: RNA *in-situ* hybridisation pattern of *SwLFY1* in a young flower and axillary meristems
See overleaf

In the developing flower, the signal is very strong in all floral organs except for the gynoecium. In meristem-like structures borne in axillary positions with respect to the flower, the signal can be either throughout the meristem (a) or only to one side (b&c). This pattern of expression is reminiscent of that of *LEAFY*-like genes in other solanaceous flowers suggesting that in meristematic structures, *SwLFY* transcripts indicates regions destined to become flowers and bracts. The inflorescence moiety of the juvenile inflorescence meristem is shaded in green.

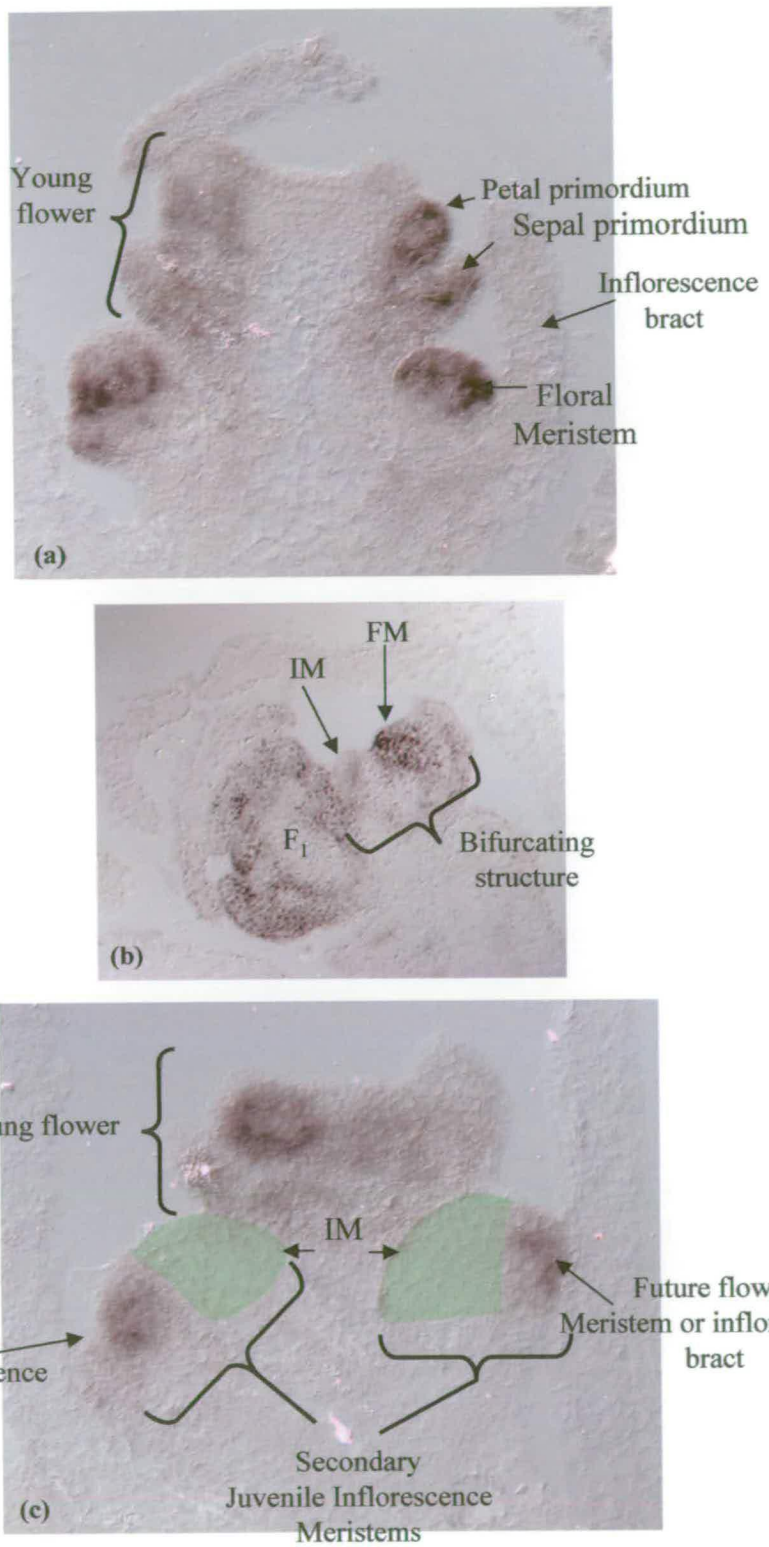
Young flower
Petal primordium
Sepal primordium
Inflorescence bract
Floral Meristem
(a)
FM
IM
F_1
Bifurcating structure
(b)
Young flower
IM
Future flower Meristem or inflorescence bract
Future flower Meristem or inflorescence bract
Secondary Juvenile Inflorescence Meristems
(c)

project were secondary inflorescences, i.e. no vegetative meristems should be present in the sectioned tissue. With each probe, the plant material included a range of developmental stages from the juvenile inflorescence meristem to flower up till stage 6.

V.2.2.1 SCHCYC1

In his PhD, Marc Chadwick found that *SCHCYC1* is expressed in the staminodes of *S. wisotonensis*. However, he did not have the time to obtain information on the dynamics of this expression pattern along the different stages of development.

(i) Anti-sense probe design and synthesis

For this project, CK4, the plasmid containing the longest cDNA fragment corresponding to *SCHCYC1* was used to as a template to produce an RNA *in situ* probe. This plasmid includes the poly-A tail, a feature which may cause background hybridization with other transcripts. To prevent this, a ligation strategy was designed to excise the poly-A tail from CK4 (Fig V.5). A double digest was carried out with *EcoR*I and *Hinc*II. The resulting fragment was smaller than the original cDNA but it did not include the 3' poly-A tail (1320 bp/ 1453bp). A pBluescript® SK vector with intact poly-linker was digested with *EcoR*I and *Hinc*II and both fragments were successfully ligated together (KC54). A clone was isolated which contained a fragment of the expected size (KC 54-1) and its identity was confirmed by sequencing. The plasmid was linearised by a digestion with *EcoR*I, and using this template, the RNA probe was synthesized using the standard techniques (II.2.2) and a T7 RNA polymerase.

Fig V.5: Summary of the strategy followed to obtain the template for the *SCHCYC1* anti-sense probe

(See overleaf)

(a) Map of the pBluescript® SK CK 4 plasmid containing the *SCHCYC1* cDNA (in red). (b) Map of an empty pBluescript® SK vector. (c) Partial fragment of the cDNA of *SCHCYC1* after digestion with *EcoR*I and *Hinc*II of CK4. (d) Map of the empty pBluescript vector after digestion with *EcoR*I and *Hinc*II.(e) Plasmid KC 54-1 corresponding to the template used to produce the *SCHCYC1* anti-sense probe.(f) Linearisation of this template with *EcoR*I.

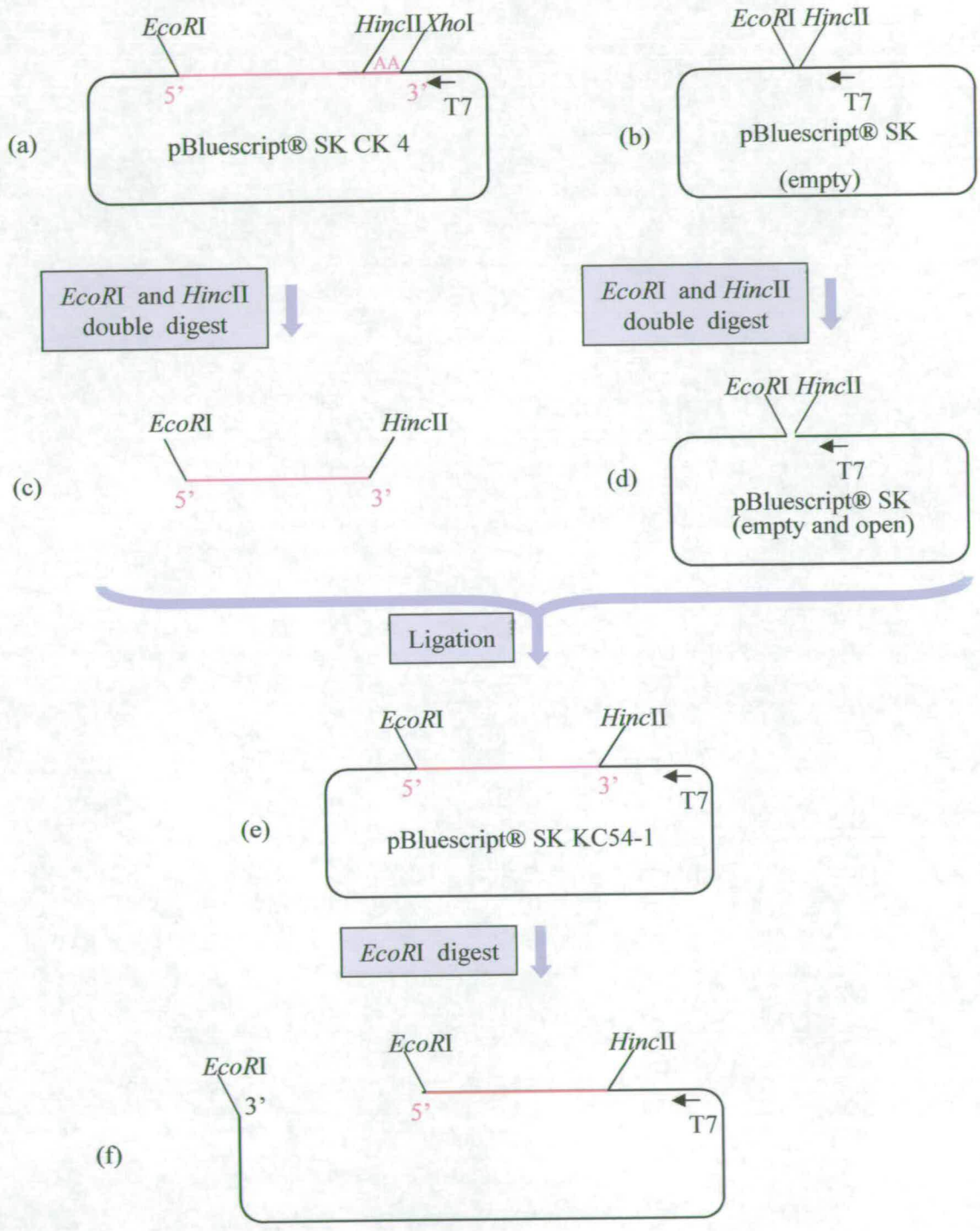
EcoRI
HincII XhoI
AA
5'
3'
T7
(a)
pBluescript® SK CK 4
EcoRI HincII
T7
(b)
pBluescript® SK
(empty)
EcoRI and HincII
double digest
EcoRI and HincII
double digest
EcoRI
HincII
(c)
5'
3'
EcoRI HincII
T7
(d)
pBluescript® SK
(empty and open)
Ligation
EcoRI
HincII
5'
3'
T7
(e)
pBluescript® SK KC54-1
EcoRI digest
EcoRI
HincII
EcoRI
3'
5'
T7
(f)

(ii) RNA in situ hybridization pattern of SCHCYC1 in reproductive tissues

A strong signal was detected throughout the primodia of all three staminodes from stage 3 onwards (Fig V.6). In later stages, the signal appears confined to the inner part of the anther and its filament, possibly in the vascular system (Fig V.7).

(iii) RNA in situ hybridization pattern of SCHCYC1 in vegetative tissue

No signal was detected in apical and axillary vegetative meristem or any vegetative organ.

(iv) Negative control using a SCHCYC1 sense probe

A similar strategy to that followed to produce the anti-sense probe was designed except that the *EcoR*I–*Hinc*II fragment was ligated to an empty pBluescript® KS vector (reverse order of restriction sites in the poly-linker). As a result, the sense probe could also be synthesised using the T7 RNA polymerase. No hybridization was detected when using the *SCHCYC1* sense probe.

V.2.2.2 Expression pattern of SCHCYC2

In his PhD, Marc Chadwick did not find any pattern of expression for *SCHCYC2m*.

(i) Anti-sense probe design and synthesis

It was not possible to use the plasmid CK9 obtained from the cDNA library to make a probe for *SCHCYC2* because a recombination had taken place which resulted in a chimeric cDNA (the 5' end of a *SCHCYC2* cDNA was fused to the 3'

Fig V.6: RNA *in situ* hybridisation of a flower bud at stage 3-4 with the *SCHCYC1* probe (See overleaf)

Fig (a) shows the earliest stage (stage 3) at which the expression of *SCHCYC1* was detected in a staminode primordia. Fig (b) and (d) are two sections obtained from the same flower bud at stage 4. In (c) and (e), the red line indicates the plane of sectioning on a SEM of a flower bud at a similar stage of development. G: gynoecium; LP: lateral petal; VP: ventral petal; DS: dorsal sepal; VS: ventral sepal; Lst: lateral stamen; Dst: dorsal staminode; Vst: ventral staminode.

(a)

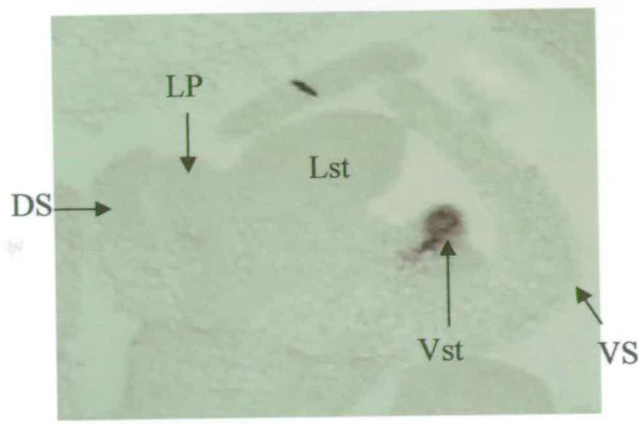

(b)

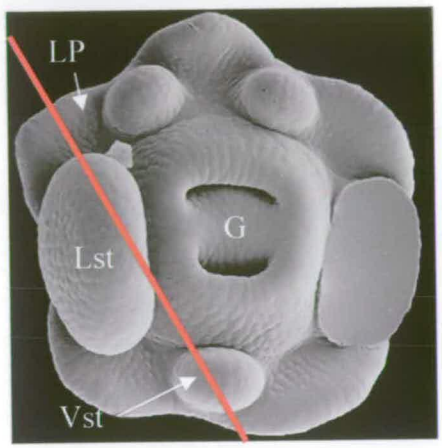

(c)

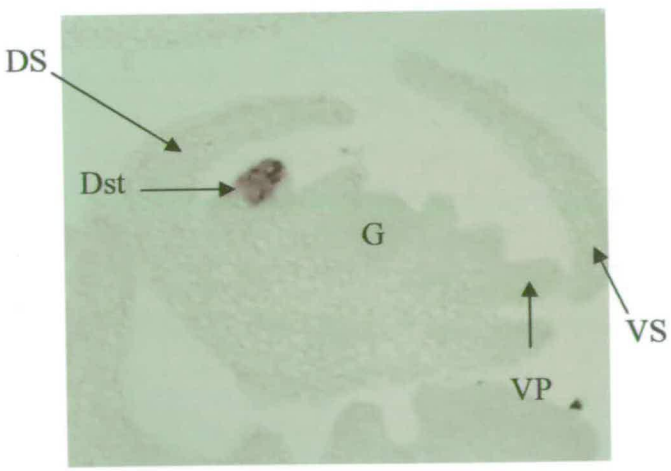

(d)

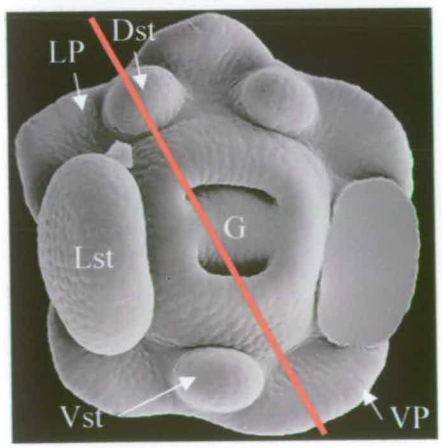

(e)

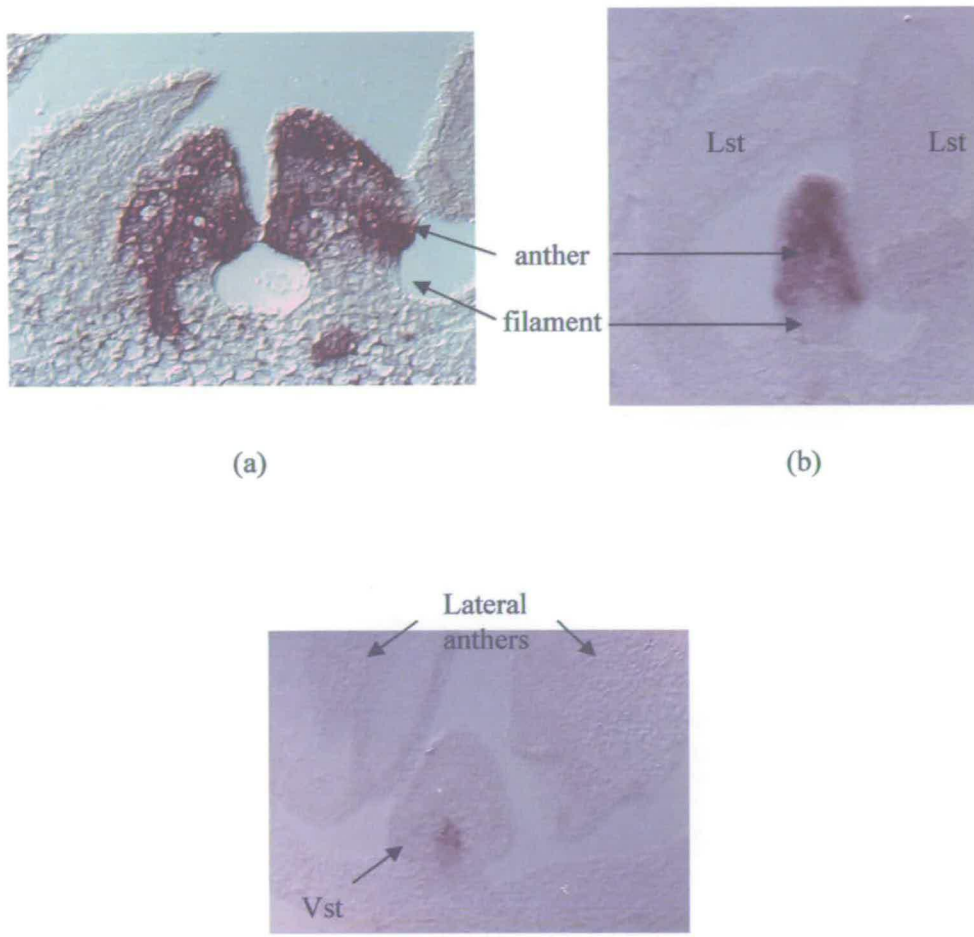

Fig V.7: RNA *in-situ* hybridisation in the staminodes at stage 5-6 with a *SCHCYC1* probe

Fig (a) and (b) shows that in stage 5, when it is possible to distinguish the anther from the filament, *SCHCYC1* transcript is found throughout the anther and in the vascular tissue of the filament. The same pattern of expression is found in the dorsal staminodes (a) and in the ventral staminode (b). In stage 6, the signal is weaker and mostly confined to the vascular tissue in the filament (c). Lst:lateral stamen; Vst: ventral stamen;

end of a *RUBISCO*–like gene cDNA). Plasmids containing the gDNA sequence of *SCHCYC2B* were chosen instead as templates for the production of the RNA *in situ* probe. The plasmid KC40-6 was chosen so that the anti-sense probe could be produced using the T7 RNA polymerase. To linearize it, the restriction enzyme *Mfe*I was chosen. Its restriction site is 58bp downstream of the 5' end of the insert resulting in a slightly shorter probe with respect to the original DNA fragment (Fig V.8).

(ii) RNA in situ hybridization pattern of SCHCYC2 in reproductive tissues

The hybridization pattern obtained for *SCHCYC2* was not as easy to interpret as for *SCHCYC1*. The signal was also weaker than for *SCHCYC1*. As explained above, the region of the gDNA used to produce the probe features a 3' intron. Therefore, to ensure that the best conditions to obtain a strong signal were met, a hydrolysed anti-sense probe was used alongside the non-hydrolysed one. The signal strength obtained with both probes was similar.

The signal was only observed in meristematic structures and never on organ primordia (Fig V.9-12). In meristems, it was usually visible only in a sub-set of successive sections, and sometimes totally absent, even when the *SwCYCLINB* controls indicated that the experiment had been successful.

To determine if the signal was found in the inflorescence meristem or the floral one, successive sections of a bifurcating structure were alternately probed with *SwLFY1* and *SCHCYC2* (Fig V.9-10). The *SCHCYC2* transcript was detected where *SwLFY1* was not expressed. This finding is a good indication that *SCHCYC2* is not likely to be expressed in FM and flower buds.

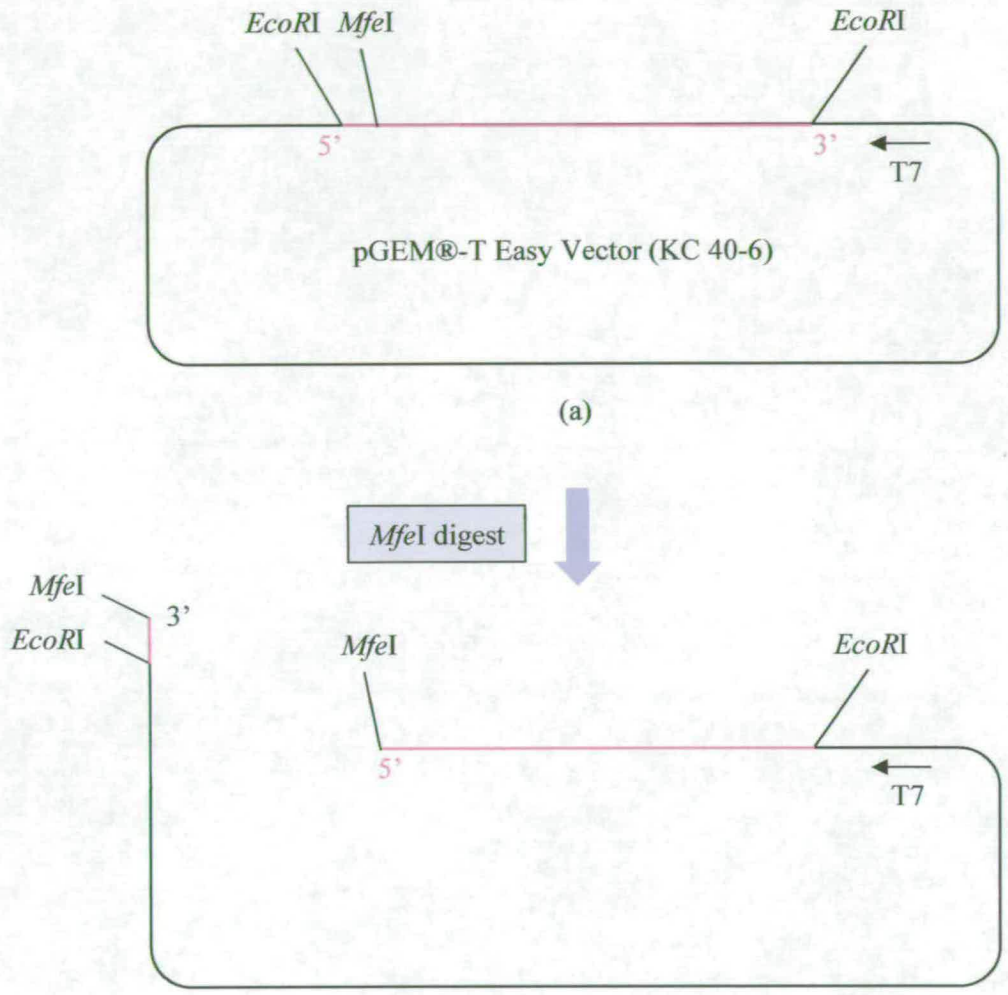

Fig V.8: Synthesis of the template for the *SCHCYC2* anti-sense probe

(a)Map of the pGEM®-T Easy Vector (KC 40-6) (b) Linearised probe. The insert (*SCHCYC2B*) is indicated as a red line.

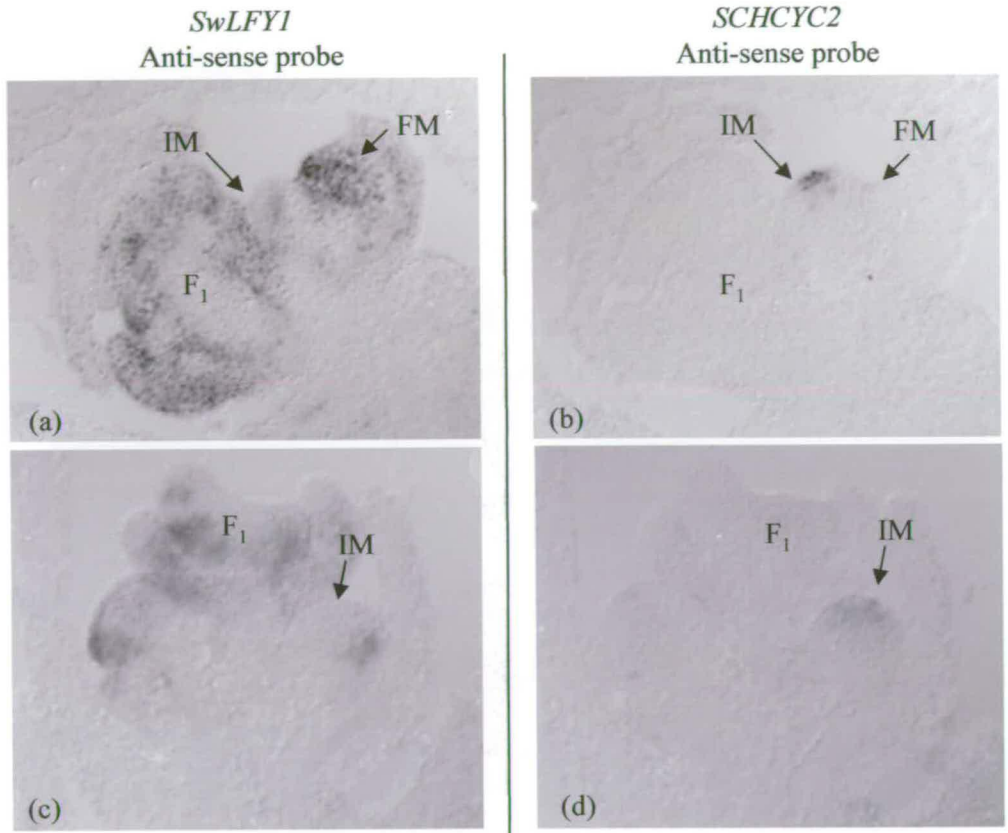

Fig V.9: Comparison of the expression pattern of *SwLFY1* and *SCHCYC2* in juvenile and bifurcating structures

(a&b) are two are successive sections hybridised with *SwLFY1* (a) and *SCHCYC2* (b) anti-sense probes. (a) The presence of the *SwLFY1* transcript indicates which meristem has acquired floral identity and by default, which meristem retains inflorescence identity. (b) The *SCHCYC2* transcript is only found in the inflorescence meristem. (c&d) show another example of the pattern of expression of *SwLFY* and *SCHCYC2* in successive sections. IM: Inflorescence Meristem, FM: Floral Meristem, F: flower.

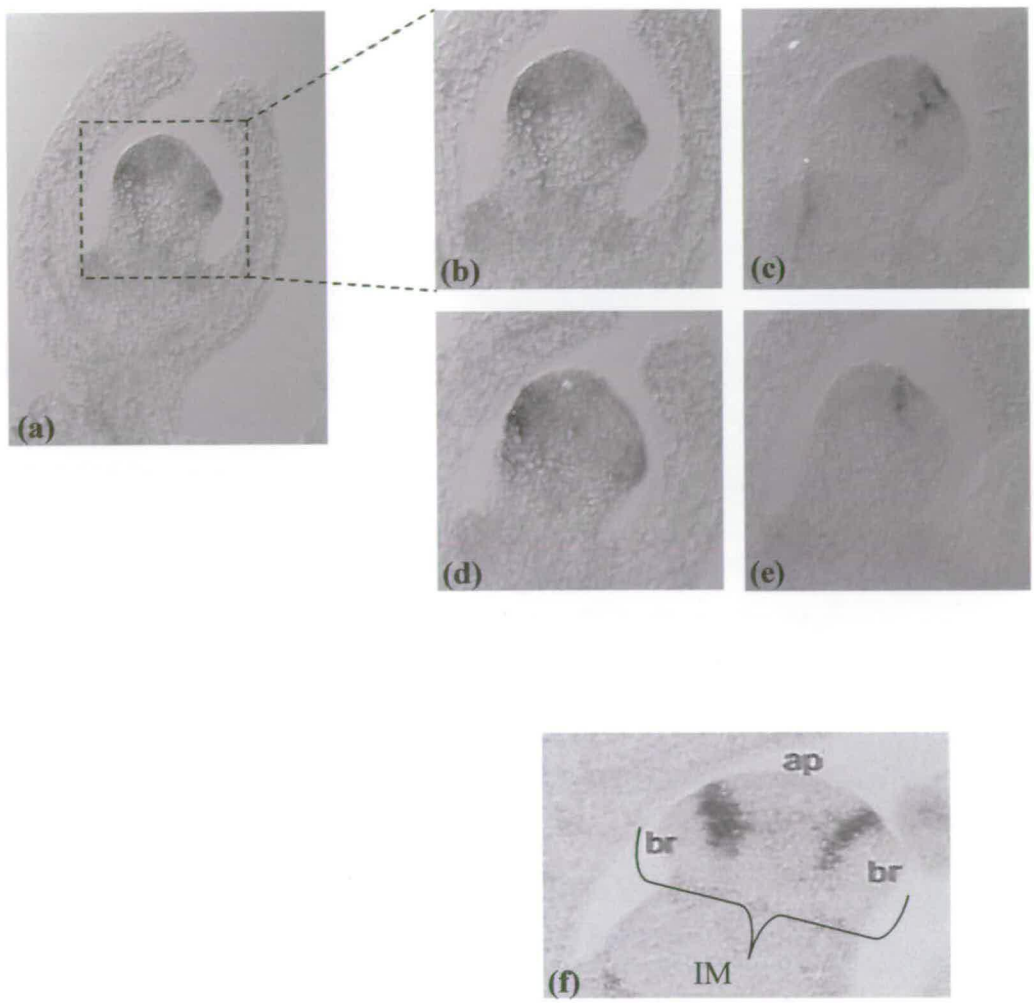

Fig V.10: Comparison of the expression of *SCHCYC2* and *SwLFY1* in the **apical** inflorescence meristem

(b-e) are consecutive slides corresponding to an IM which has not yet bifurcated. (a) shows a larger view of this apical IM (b&d) show the signal obtained with the *SwLFY1* anti-sense probe. (c&e) show the signal obtained with the *SCHCYC2* probe. (f) In *Petunia,* this picture corresponds to an RNA *in situ* hybridisation with the *NAM* anti-sense probe on an apical IM in a similar stage of development. The signal was interpreted as the boundary between the apical IM (ap) and the region where bracts primordia will develop (br). The comparison between the pictures obtained in *S. wisotonensis* and in *Petunia* suggests that the *SwLFY1* signal is present indicates where the bract primordia will form and that*SCHCYC2* is expressed in the middle in the IM.

Fig V.11: Expression pattern of *SCHCYC2* in the inflorescence meristem (longitudinal sections)
(See overleaf)

(a) & (b) are sections in different inflorescence meristems (IMs). (c-h) These pictures represent successive sections of the same reproductive unit. *SCHCYC2* transcript is detected in both inflorescence meristems (IMa and IMb). In IMa, it is expressed in the central region of the meristem, in IMb, it appears as a line in the middle of the meristem. F0 indicates a young floral bud.

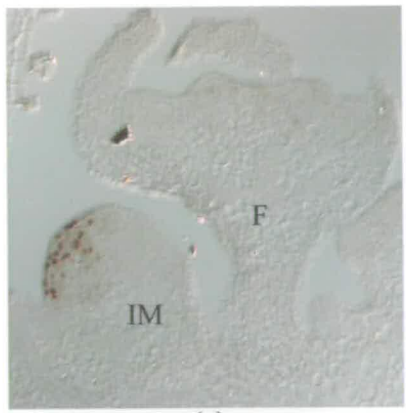

(a)

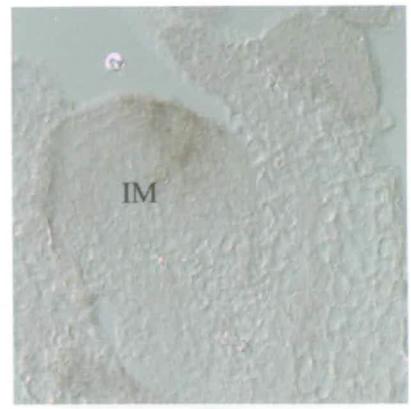

(b)

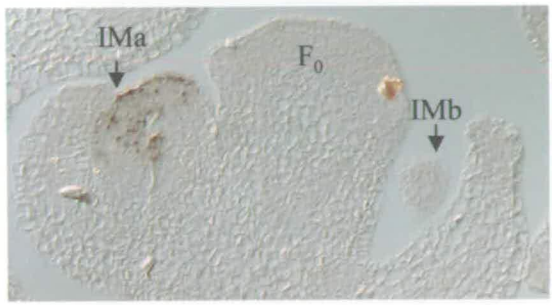

(c)

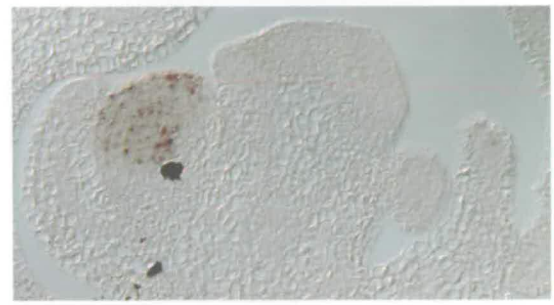

(d)

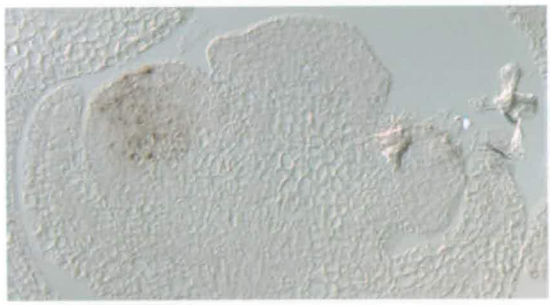

(e)

(f)

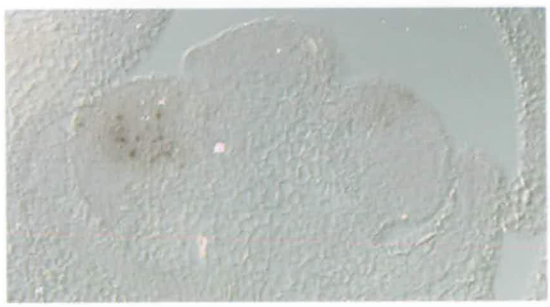

(g)

(h)

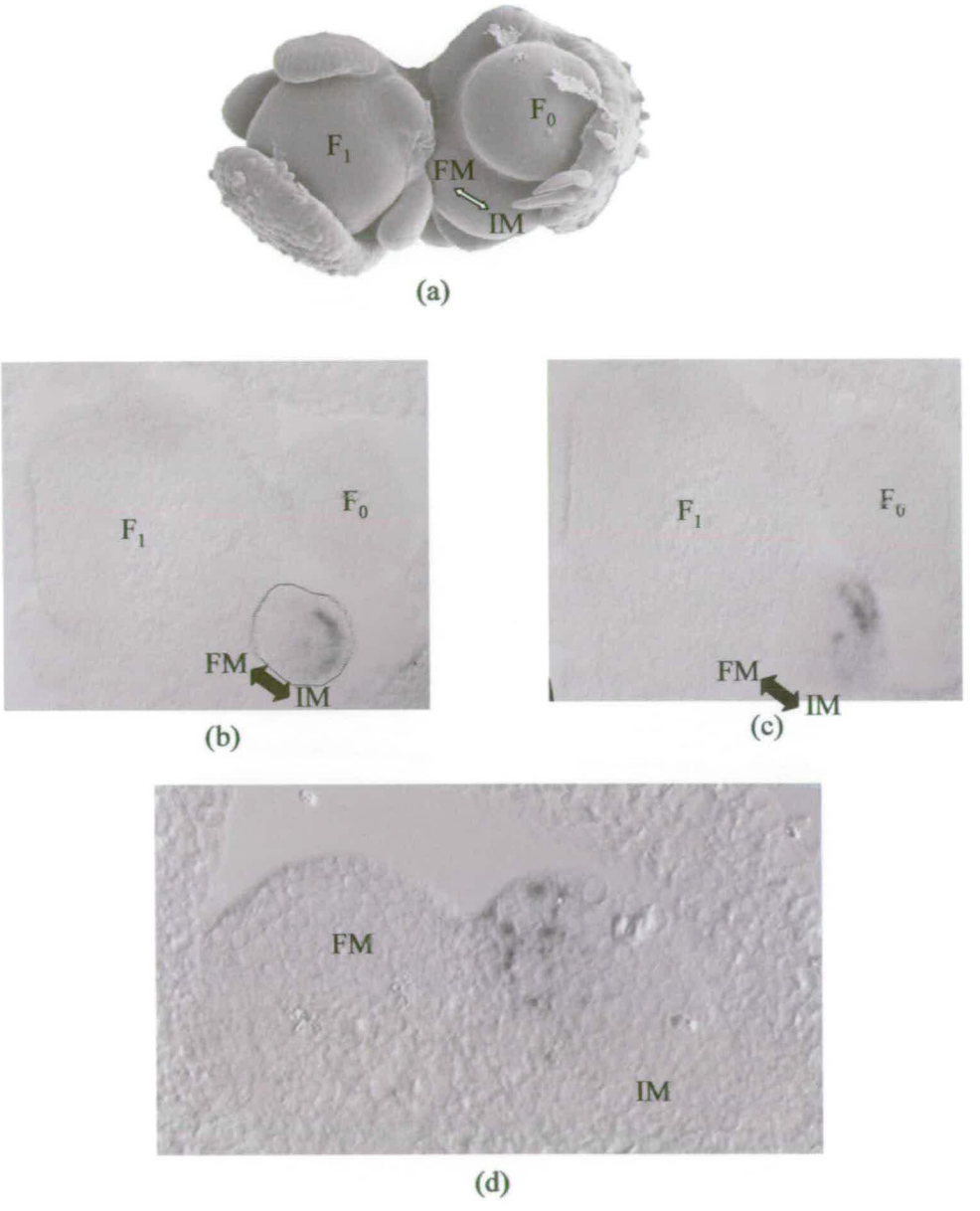

Fig V.12: Expression pattern of *SCHCYC2* in the inflorescence meristem (transversal sections) and in the bifurcating structure (longitudinal section)

(a) SEM of bifurcating structure and corresponding older flower bud. (b&c) These pictures show successive sections of the same reproductive unit probed with *SCHCYC2*. *SCHCYC2* transcript is not detected throughout the whole juvenile meristem but only in its region destined to retain inflorescence identity (IM). (d) bifurcating structure. F: flower, FM: flower meristem, IM inflorescence meristem.

A detailed analysis of the expression pattern of *SCHCYC2* shows that in longitudinal sections of juvenile IM, *SCHCYC2* transcript is found in the central zone of the meristem, both in peripheral and internal cell layers (Fig V.9-12). The signal was often only detected in a few consecutive sections covering the innermost region of the meristem, sometimes along its entire length (Fig.11, complete set of sections not shown). Generally, the pattern of expression spanned over a group of neighboring cells (Fig V.9, 10 and 11). However, cells where the signal was detected could also be interspaced with cells without signal (Fig V.12). Finally, in the juvenile meristem, the signal sometimes resembled a line "cutting" through the meristem, from the outside cell layer to the inner zone domain (Fig.V.11h).

In the bifurcating structure, *SCHCYC2* is expressed either in the central region of the IM or next to the splitting site. The transcript of *SCHCYC2* was never detected across the region where the split is taking place, i.e. it was always found confined to what was identified as the IM (Fig V.9, 12).

In summary, this set of results show that *SCHCYC2* is only expressed in the inflorescence meristem. Its domain of expression varies from one inflorescence bud to another suggesting that the expression of *SCHCYC2* is dynamic in the inflorescence meristem.

(iii) RNA in situ hybridization pattern of SCHCYC2 in vegetative tissue

No signal was detected in apical and axillary vegetative meristems or in any vegetative or floral organ tested.

(iv) Negative control with a SCHCYC2 sense probe

The template for the sense probe corresponded to the whole gDNA insert (1387bp) present in KC 40-10 linearised with *Sal*I. The probe was also produced using the T7 RNA polymerase.

Interestingly, a signal was also detected in meristems using this sense probe (Fig V. 13-14). The signal produced by the sense probe was apparently overlapping with the region hybridized by the anti-sense probe (Fig V.13). However, in Fig V.14, the sense probe was detected where the anti-sense probe is not found. The experiment was reconducted once with the same probe and a third time with *de-novo* synthesis of the sense probe. A similar "inconsistent" expression pattern was observed at all times. These experiments were conducted towards the end of the project and there was no time to further characterize the expression pattern of a putative anti-sense transcript of *SCHCYC2*.

(v) Comparing the expression patterns of SCHCYC1-2 and SwCYCLINB

Successive sections from the same reproductive unit were alternately hybridized with *SCHCYC1, SCHCYC2* and *SwCYCLINB1* anti-sense probes (Fig V.15). The pattern of expression of *SCHCYC1* is not shown in Fig V.15 but it corresponds to what has been described previously. Interestingly, the domain of expression of *SCHCYC2* and that of *SwCYCLINB1* overlap for both inflorescence meristems. However, further attempts to confirm this result were unsuccessful in showing overlapping domains of expression for both genes and there was no time to further investigate this point.

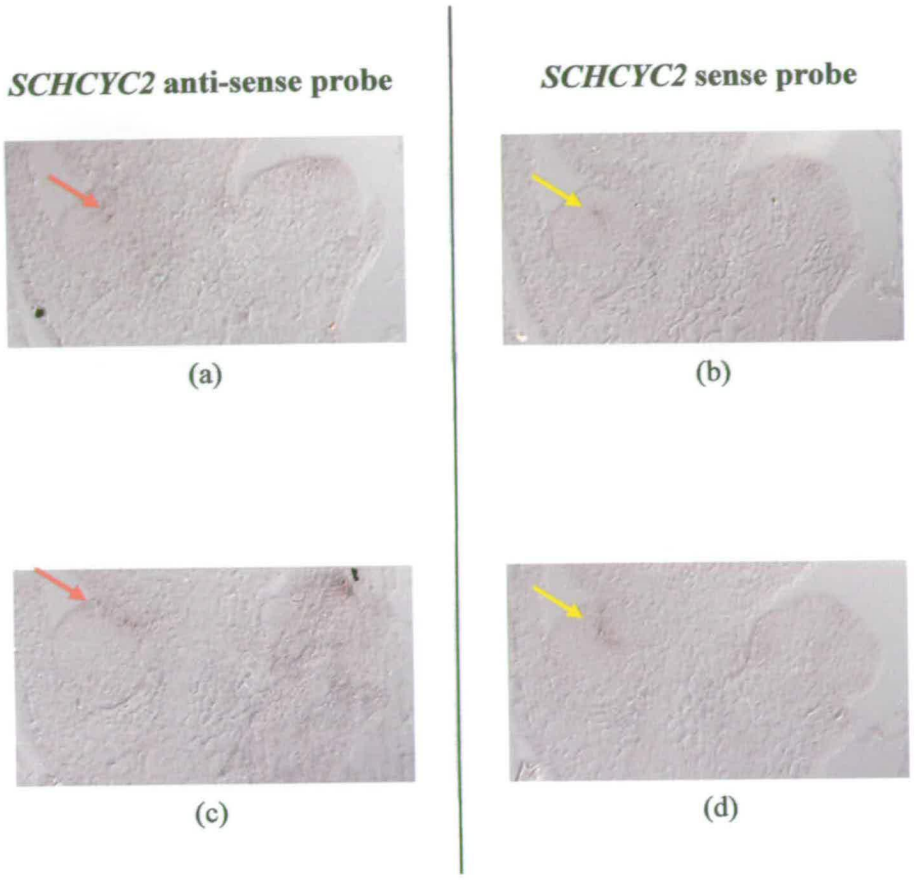

Fig V.13: Expression pattern obtained on successive sections hybridized with the anti-sense and the sense probes corresponding to *SCHCYC2*
The red arrow indicates the position of the signal obtained with the anti-sense probe (a&c) and the yellow arrow indicates that of the sense probe (b&d).

Fig V.14: Expression pattern obtained on successive sections hybridized with the sense probe for *SCHCYC2*.
A signal was observed in a meristematic structure.

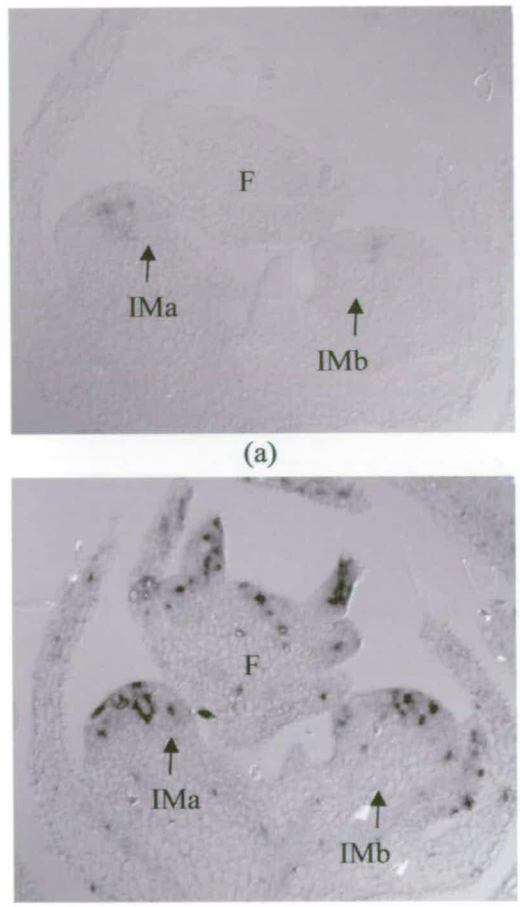

Fig V.15: Expression of *SCHCYC2* and *SwCYCLINB* on successive sections
Sections in the same reproductive unit were successively probed with a *SCHCYC2* anti-sense probe (a) and the *SwCYCLINB1* probe (b).

V.2.2.3 Expression pattern of SCHCYC3

(i) Anti-sense probe design and synthesis

The pBluescript® SK CK1 vector containing the cDNA sequence for *SCHCYC3* was used to produce a suitable template. This vector includes the poly-A tail which needed to be removed to produce a specific RNA probe. A restriction site for *BamH*I 820 bp downstream of the 5' end of the cDNA was identified. The insert was excised from the plasmid with a double digest (*EcoR*I and *BamH*I) and religated into a pBluescript® KS vector previously digested with *EcoR*I and *BamH*I (Fig V.16). A plasmid was isolated (KC56-1) and its sequencing confirmed its identity. It was then linearized with *EcoR*I to be used as a template to synthesis a *SCHCYC3* RNA probe with the T7 RNA polymerase.

(ii) RNA in situ hybridization pattern of SCHCYC3 in reproductive tissues

The signal observed with the *SCHCYC3* probe was very similar to that of *SCHCYC2* (Fig V.17) and confined to meristem-like structures. It was not possible to detect *SCHCYC3* transcript in a bifurcating structure. The signal was generally weaker and less frequently observed than that obtained with the anti-sense probe of *SCHCYC2*. The synthesis of the probe was carried out three times (once with carbonate hydrolysis). All probes gave the same signal strength.

To determine if the pattern of expression of *SCHCYC2* and *SCHCYC3* overlap, successive sections were hybridized alternately with a *SCHCYC2* and a *SCHCYC3* anti-sense probe. The results shown in Fig V.17 (e&f) demonstrate convincingly that transcripts of *SCHCYC2* and *SCHCYC3* are found in overlapping

Fig V.16: Summary of the strategy followed to obtain the template for the *SCHCYC3* anti-sense probe
(See overleaf)

(a) Map of the pBluescript® SK CK 1 plasmid containing the *SCHCYC3* cDNA (in red). (b) Map of an empty pBluescript® KS vector. (c) Partial fragment of the cDNA of *SCHCYC3* after digestion of CK1 with *EcoR*I and *Bam*HI. (d) Map of the empty pBluescript® vector after digestion with *EcoR*I and *Bam*HI .(e) Plasmid KC 56-1 corresponding to the template used to produce the *SCHCYC1* anti-sense probe. (f) Linearisation of this template with *EcoR*I.

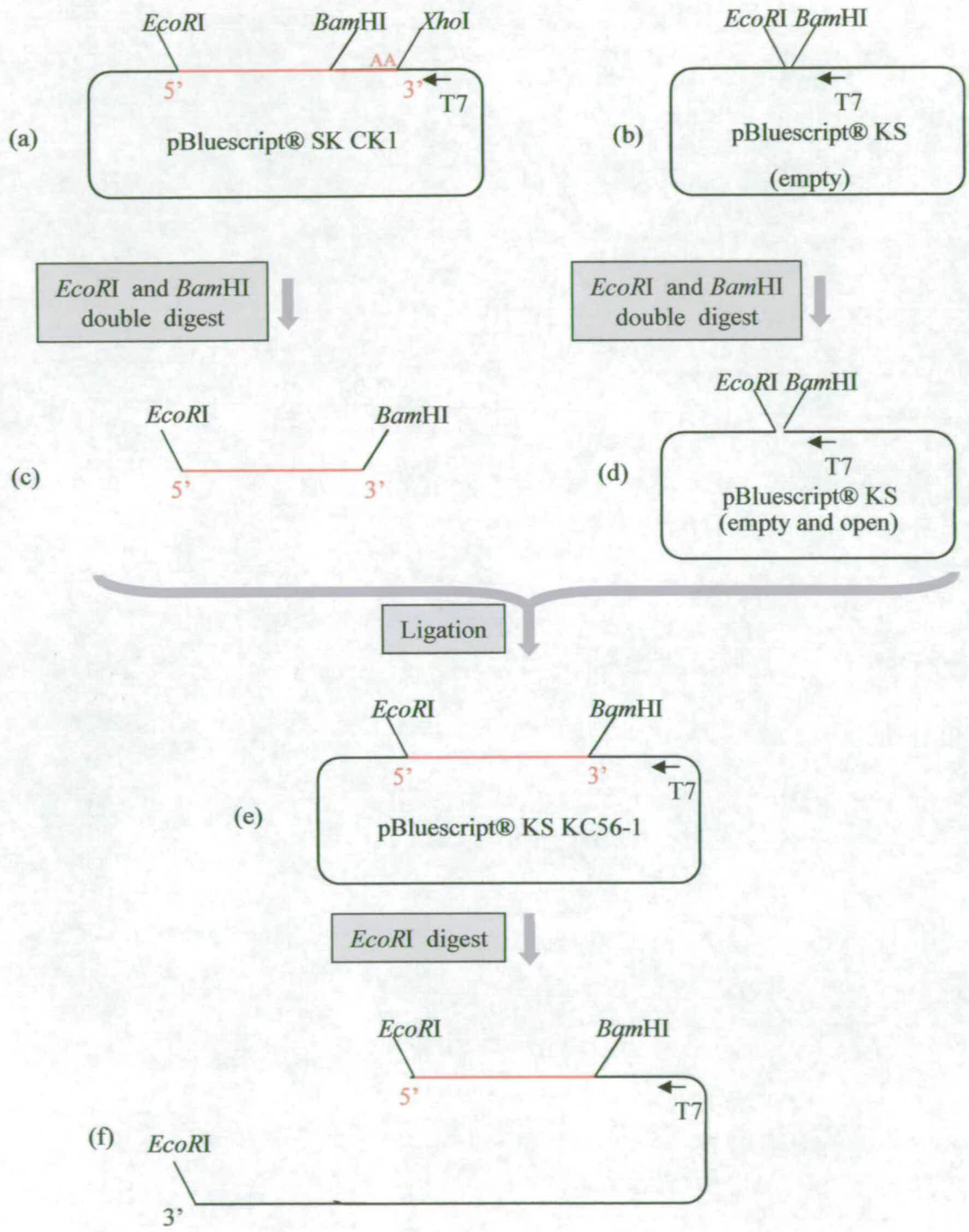
(a)
EcoRI
BamHI
XhoI
AA
5'
3'
T7
pBluescript® SK CK1
(b)
EcoRI BamHI
T7
pBluescript® KS
(empty)
EcoRI and BamHI
double digest
EcoRI and BamHI
double digest
(c)
EcoRI
BamHI
5'
3'
(d)
EcoRI BamHI
T7
pBluescript® KS
(empty and open)
Ligation
(e)
EcoRI
BamHI
5'
3'
T7
pBluescript® KS KC56-1
EcoRI digest
EcoRI
BamHI
5'
T7
(f)
EcoRI
3'

Fig V.17: Expression pattern of *SCHCYC3* in inflorescence meristems and its comparison to that of *SCHCYC2*
(See overleaf)

(a&b) are two are successive sections through an inflorescence meristem (IM) hybridised with the *SCHCYC3* anti-sense probe. (c&d) are two separate example of the typical pattern of expression obtained with the *SCHCYC3* anti-sense probe in IMs. (e&f) are two are successive sections through a meristem hybridised with *SCHCYC2* (e) and *SCHCYC3* (f) anti-sense probes.

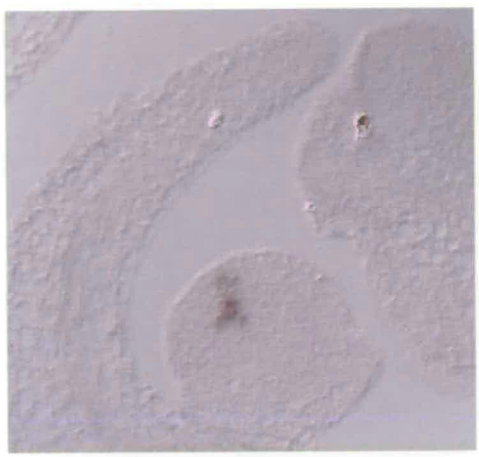

(a)

(b)

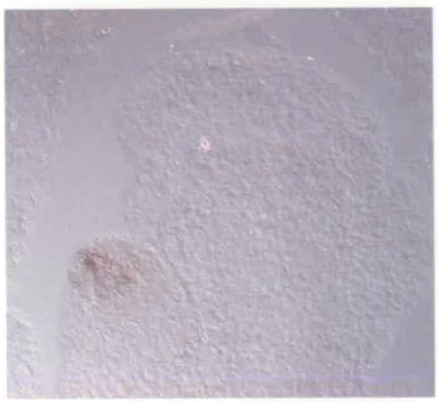

(c)

(d)

(e)

(f)

domains. Consequently, as for *SCHCYC2, SCHCYC3* is likely to be expressed only in inflorescence meristems.

(iii) RNA in situ hybridization pattern in vegetative tissue

No signal was detected in apical and axillary vegetative meristem or any vegetative or floral organs investigated.

(iv) Negative control with a SCHCYC3 sense probe

To produce a *SCHCYC3* sense template, the pBluescript® CK1 KS plasmid was cut with *BamH*I and *Xho*I. The resulting fragment corresponds to the entire cDNA for *SCHCYC3*. This was then ligated in an empty pBluescript® SK vector previously digested with *BamH*I and *Xho*I. Finally, after a successful cloning, a plasmid (KC56-1) was sequenced which confirmed its identity. KC56-1 was then used as a template for the synthesis of a sense probe for *SCHCYC3* using the T7 RNA polymerase.

No signal was detected when this probe was used.

(v) Comparative expression pattern between SCHCYC3 and SwCYCLINB1

Successive sections probed with the *SCHCYC3* and the *SwCYCLINB* did not show overlapping expression pattern of both genes (Fig V.18).

V.2.2.4 Expression pattern of SCHCYC4, SCHCYC5 and SCHCYC6

To check if *SCHCYC4, 5* and *6* were expressed in developing inflorescences, a RT-PCR was carried out on cDNA obtained for the 5' race PCR (see II.2.2). This

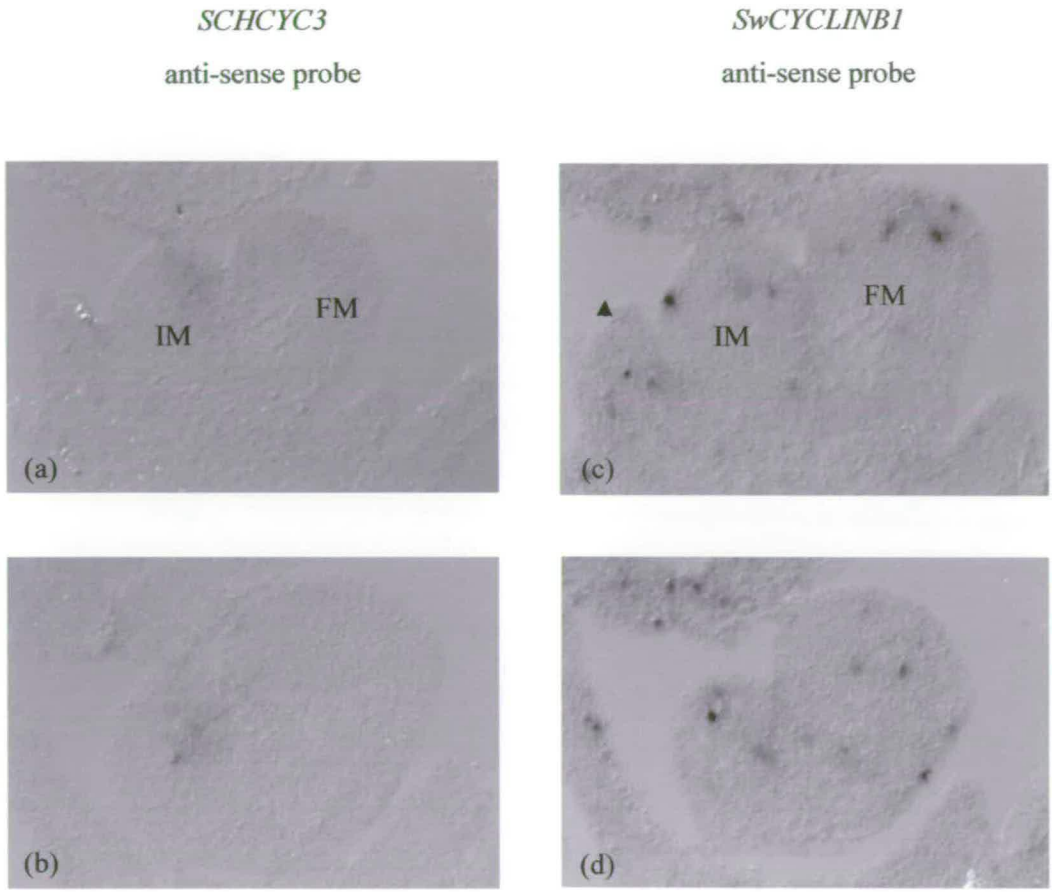

Fig V.18: Expression of *SCHCYC3* and *SwCYCLINB* on consecutive sections
Consecutive sections in the same reproductive unit were successively probed with a *SCHCYC3* anti-sense probe (a&b) and the *SwCYCLINB1* probe (c&d).

test was carried out on gDNA too (positive control) and it included *SCHCYC1, 2* and *3* as positive controls alongside (Fig V.19). The results show convincingly that there is no gDNA contamination in the cDNA otherwise double bands would have been observed for *SCHCYC2* and *SCHCYC3*. In addition, the gel picture shows that *SCHCYC4, 5* and 6 are expressed in the developing inflorescence.

To obtain a pattern of expression for *SCHCYC4, SCHCYC5* and *SCHCYC6*, a complete set of probes (anti-sense and sense) was synthesized. The templates were PCR fragments amplified with vector specific primers on plasmids isolated from KC 65, 66 and 67. The resulting purified fragments included the T7 RNA polymerase binding site, except for *SCHCYC4* which was synthesized with the Sp6 RNA polymerase.

Both reproductive (inflorescence meritems and floral bud) and vegetative tissues (apical and axillary vegetative meristems) were hybridized with each probe. No signal was detected on any of the tissue probed. The experiment was reproduced once. The probes were synthesized *de novo*. This time, the templates were linearized plasmids for *SCHCYC4* and *SCHCYC6*, and PCR fragments as described above for *SCHCYC5*. The tissue probed included the same as for the previous experiment and a range of sections through older flowers, from stage 2 to 6. No signal was detected in any of the sections.

V.2.3 A comparative study of the *rz* mutant with a reduced dorso-ventral asymmetry

V.2.3.1 Genetics of the rz mutant

A cross was carried out between a mutant (pollen) from the seed stock provided by Anne-Marie Houtbraken and a wild-type plant (female) from which

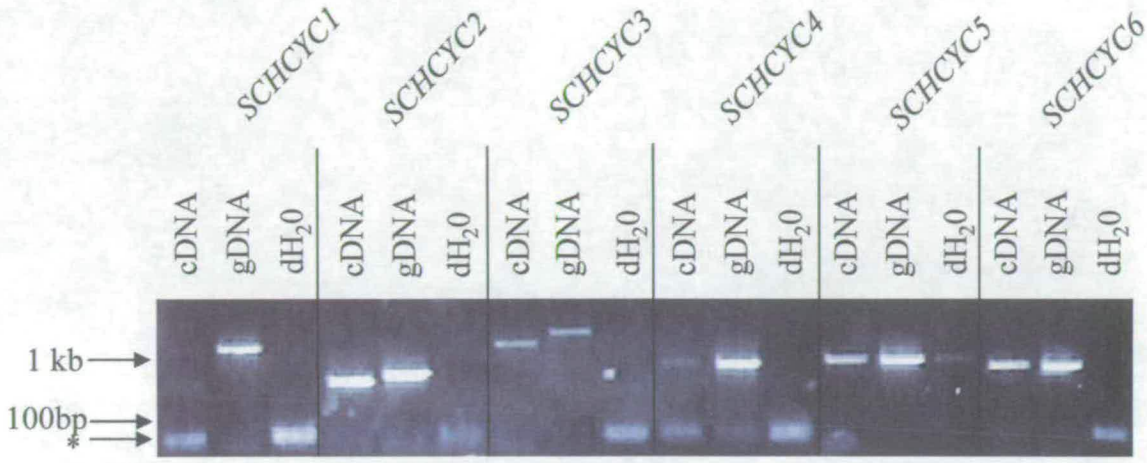

Fig V.19: RT-PCR on inflorescence buds in *S. wisotonensis* (WT)
Primers designed to amplify the region of the gDNA which includes introns were chosen for *SCHCYC1, 2* and 3. The absence of signal in the *SCHCYC1* cDNA lane was later proved to be arte-factual. The RT-PCR on *SCHCYC2* and *3* shows that there is no gDNA contamination in the cDNA. cDNA: complementary DNA, gDNA: genomic DNA, *primer dimers.

anthers had been removed. The phenotype of the progeny was scored after floral transition. The cross produced about _ wild-type progeny and _ mutant plants (Table V.1). This result, later confirmed for all crosses performed during this project, indicates that the mutation is dominant and will therefore from now on be denoted as the *Rz* mutant.

Wild-type looking plants	*rz* mutant plants
13	15

Table V.1: Phenotype of the progeny from a cross between a male-sterilized female wild-type and mutant pollen which produced a progeny of 28 plants

Interestingly, a few crosses produced plants with unstable phenotype (Fig V.20). Such plants always started their reproductive phase with the *rz* mutant phenotype. Then, they started to produce wild-type looking flowers on a branch (Fig V.20a). Such wild-type branches would often revert back to produce mutant flowers (Fig V.20b).

Taken together, these observations suggest that the mutation is dominant and likely to be epigenetic in nature.

V.2.3.2 RNA in situ on the mutant plants

A series of RNA *in situ* hybridizations were carried out on reproductive meristems of the mutant plant. The results of these experiments can be summarized as follows: the same pattern of expression as for the wild-type was observed for *SCHCYC1*, *2* and *3* anti-sense and sense probes except for the *SCHCYC2* sense probe (Fig V. 21, 22 and 23). For the latter, the detection of the anti-sense and the sense probe in consecutive sections through a bifurcating structure show a mutual

Fig V.20: Example of the unstable nature of some *Rz* alleles
(See overleaf)

These pictures show two branches from the same *Rz* mutant which grew initially as a mutant plant. (a) shows a reversion which produces a wild-type branch, (b) shows that reverted branches which exhibit a WT phenotype can revert back to the mutant form.


(a)


(b)

Fig V.21: Expression pattern obtained with the anti-sense probe for *SCHCYC1* in the *Rz* mutant
(See overleaf)

As for the wild-type, the signal was detected in the staminodes primordia. (a&b) shows two consecutive sections where expression of *SCHCYC1* is found in a dorsal and a ventral staminode (st) on each side of developing lateral stamen. These sections correspond to a longitudinal section of a flower bud at late stage 3. (c) shows a transversal section of a flower at stage 4. (d) shows a transversal section of a slightly older flower, probably at late stage 5. Finally, (e) shows only the two dorsal staminodes (the signal was also detected in the ventral staminode) of an older flower (stage 8). DP: dorsal petal, LP: lateral petal, VP: ventral petal, G: gynoecium, Dst: dorsal staminode, Lst: lateral stamen, Vst: ventral staminode.

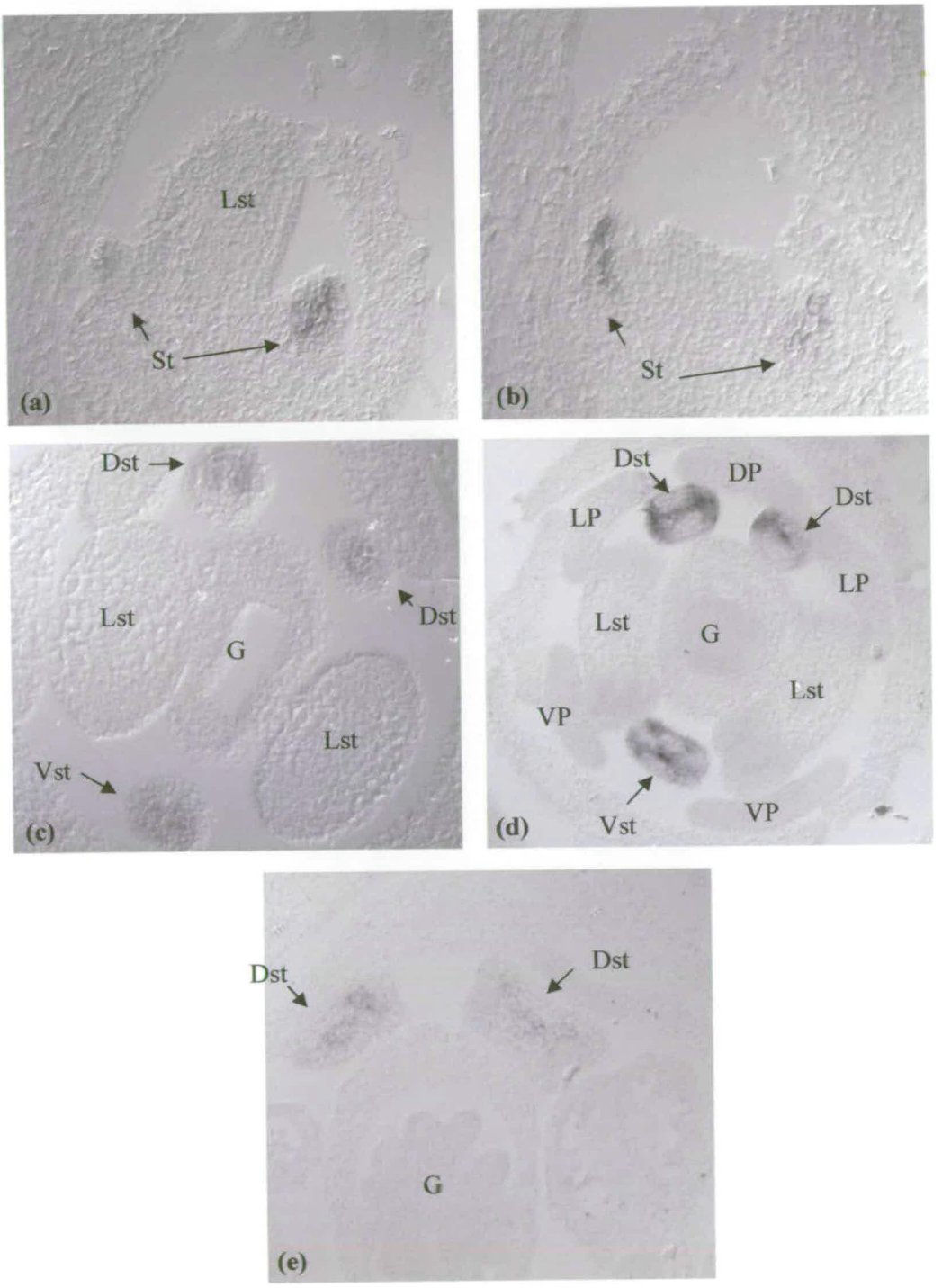
Lst
St
(a)
St
(b)
Dst
Lst
G
Dst
Lst
Vst
(c)
Dst
DP
Dst
LP
LP
Lst
G
Lst
VP
Vst
VP
(d)
Dst
Dst
G
(e)

Fig V.22: Expression pattern detected with *SCHCYC2* anti-sense and sense probe in the *Rz* mutant
(See overleaf)

(a&b) and (c&d) show consecutive longitudinal sections across a bifurcating structure hybridized with the anti-sense (a&c) and sense (b&d) probes for *SCHCYC2*. (e&f) show two consecutive longitudinal sections across a juvenile IM hybridized with the anti-sense probe.

SCHCYC2
anti-sense probe
(Rz Mutant)

(a)

(c)

(e)

(f)

SCHCYC2
sense probe
(Rz Mutant)

(b)

(d)

Fig V.23: Expression pattern of *SCHCYC3* in the inflorescence meristem of the *Rz* mutant
See overleaf

(a-d) correspond to sections through inflorescence meristems (IMs) hybridized with the *SCHCYC3* anti-sense probe. The signal is indicated by the black arrows. F: flower bud.

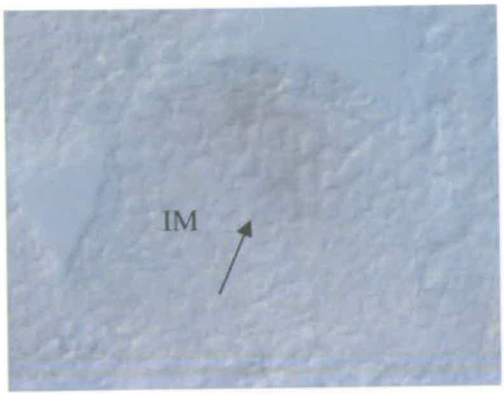

(a)

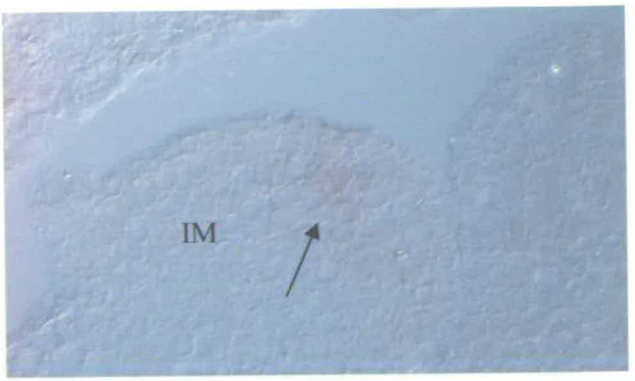

(b)

(c)

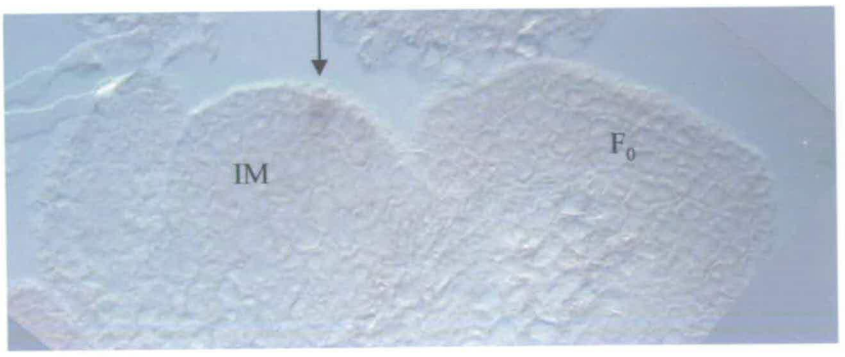

(d)

exclusion of the signal (Fig V.22 a-d). However, this pattern will not be discussed further as a mutant phenotype because the corresponding experiments on wild-type bifurcating structure did not provide informative data.

SCHCYC4 to *6* anti-sense and sense probes were also tested on reproductive meristems in the mutant, but no signal was detected.

V.3. Discussion

V.3.1 *SwCYCLINB1*, a helpful positive control

The isolation of the *SwCYCLINB1* cDNA and the synthesis of the corresponding probe proved to be a valuable tool in this project. For all slides, including sections through vegetative meristems, the same expression pattern was detected with the *SwCYCLINB1* probe, albeit with signals of variable strength. Therefore, the strength of the *SwCYCLINB1* signal was a good indicator to determine how successful a hybridization experiment had been and to assess the quality of the sectioned tissue.

SwCYCLINB1 pattern of expression was found to be characteristic of B-type mitotic cyclins, i.e. a stochastic pattern of labeling. In other species where similar experiments have been conducted, this pattern of expression corresponds to isolated cells on the transition from G2 to M phase (Fobert *et al.*, 1994, Mironov *et al.*, 1999, Himanen *et al.*, 2003).

V.3.2 *SwLFY*, more than a helpful marker gene?

V.3.2.1 SwLFY1: a good marker of floral identity?

(i) The expression of SwLFY1 in reproductive meristems

With SEMs, it is easy to determine which domain of an IM corresponds to the future FM and flower bract and which corresponds to the IM and its bract. However, once the tissue is embedded in wax and sectioned in 7μm thick slices, it is more difficult determine accurately which is which. RNA *in situ* hybridization experiments with the *SwLFY1* anti-sense probe revealed that the transcript was either found expressed very strongly throughout a meristem or confined to only one domain of the sectioned meristem. In the latter, the domain hybrized by the *SwLFY1* anti-sense probe was not larger than half of the meristem.

Petunia is the most related species to *S. wisotonensis* for which similar experiments have been carried out. In *Petunia* the *LEAFY*-like gene (*ALF*) is expressed in the IM before the bifurcation becomes anatomically visible (Souer *et al.*, 1998). At this developmental stage, *ALF* transcript is detected over more than half of the IM. In addition, *ALF* was found to be also expressed in floral and inflorescence bracts. Therefore, in the inflorescence of *Petunia*, the meristematic cells where the *ALF* signal is NOT detected are by default very likely to correspond to the reservoir of undifferentiated stem cells within the inflorescence meristem.

The expression pattern of *SwLFY1* in *S. wisotonensis* is clearly very similar to that described for *ALF* in *Petunia*. This observation suggests that in *S. wisotonensis*, the presence of the *SwLFY1* transcript is likely to indicate regions of the meristems which have acquired an identity, whether these cells are committed to become bracts (inflorescence and flower) or flower buds.

(ii) The expression of SwLFY1 in the flower meristem and flower bud

In the flower meristem and the flower bud, the *SwLFY1* signal was present in all floral organs but excluded from the central domain during early stages. The presence of *SwLFY1* in the gynoecium in older flower was not tested. In young flowers, the pattern of expression of *SwLFY1* resembles closely that of *Petunia*. In this species, *ALF* is expressed in the organ primordia from whorl 1-3 and not expressed in the central zone of the young flower (Souer *et al.*, 1998). A similar pattern is also found in tobacco where the *LEAFY*-like genes are expressed in a ring-like pattern at the periphery of floral meristems. As for *Petunia* and *S. wisotonensis*, their transcripts are not detected in the central domain of these meristems (Kelly, Bonnlander and Meeks-Wagner, 1995). In tomato, the signal of the *LEAFY*-like gene appears to be detected in the central zone of the floral meristem too (Molinero-Rosales *et al.*, 1999).

In *Petunia*, tomato and tobacco, *LEAFY*-like genes are strongly expressed in vegetative meristems (Souer *et al.*, 1998, Molinero-Rosales *et al.*, 1999, Kelly, Bonnlander and Meeks-Wagner, 1995). Unfortunately, in this project, there was no time to test the presence of *SwLFY1* transcript in vegetative tissue.

In summary, the pattern of expression obtained for *SwLFY1* is very similar but not identical to that obtained in other solanaceous species. More specifically, its close resemblance to the well characterized pattern of expression of *ALF* in *Petunia* strongly supports the use of *SwLFY1* as a marker. Its expression is very likely to mark the formation of bracts and flowers. Therefore, in meristems, cells where *SwLFY1* is not expressed are very likely to correspond to the indeterminate and

undifferentiated inflorescence. However, in the absence of functional studies, it is not possible to further extrapolate on the role of *SwLFY1* in the development of flowers and inflorescences *S. wisotonensis*

V.3.2.2 SwLFY1: more than a marker?

In biology, molecular studies have provided a new source of data for phylogenetic analyses aiming to reconstruct of the tree of life. Different sets of coding sequences can be used according to the taxonomic level targeted. For example, in plants, studies of higher taxonomic level can be carried out with the conserved plastid gene *rbcL* (Chase *et al.*, 1993). Alternatively, chloroplasts genes are used for intra and inter-specific studies (Doyle and Doyle, 1999). So far, except for ribosomal DNA sequences, nuclear genes have not been often used because of the difficulties created by allelic variation, gene duplication and rapid sequence evolution (Doyle and Doyle, 1999). *LEAFY*-like genes have been shown to be single copy in many angiosperm species, therefore, they are good candidates-genes to help the resolution of lower taxonomic levels (Doyle and Doyle, 1999).

Can *SwLFY1* be used to solve the origin of *S. wisotonensis* (i.e. hybrid or not?) and provide a tool to resolve the phylogenetic relationships in the genus *Schizanthus* and in the Schizanthoideae?

To use *SwLFY1* for such a purpose, it is necessary to determine if the smaller cDNA isolated corresponds to another allele, a PCR artefact or second locus. The first two hypotheses are more likely since *LEAFY*-like genes are single copy genes in many of the diploid species where they have been isolated so far (Souer *et al.*, 1998; Molinero-Rosales *et al.*, 1999, Wang, Möller and Cronk, 2004, Hofer *et* al.,

1997). However, a study of an F1 segregrating population should be carried out to test this hypothesis.

If *SwLFY1* is present as a single copy in the genome of *S. wisotonensis*, the isolation of its partial cDNA provides the sequence data required to designed new degenerate primers targeting specifically the amplification of less conserved regions such as putative introns (see Appendix V.2). This type of study could potentially help to resolve the origin of *S. wisotonensis*.

V.3.3 What does the expression of *SCHCYC1, 2* and *3* in wild-type plants tell us about their potential role in development?

V.3.3.1 SCHCYC1

The pattern of expression obtained with *SCHCYC1* confirms the preliminary results obtained by Marc Chadwick. However, a more thorough study was carried out in this project. It revealed that during reproductive development in *S. wisotonensis, SCHCYC1* is only expressed in the staminode. The strongest expression is detected in the emerging staminode primordia with decreasing signal strength thereafter.

Are these results indicative of a role for *SCHCYC1* in the abortion of the dorsal and the ventral stamens? *SCHCYC1* is only expressed in the staminodes, and therefore, it is very likely to have a function in their development which is not required in the fertile stamens. Therefore, by default, the most likely function of *SCHCYC1* is in the repression of stamen growth. This suggestion is strongly supported by the fact that closely related *CYC*-like genes such as *CYC*, *DICH* and *LvCYC* are also expressed in the staminodes of their respective species (Luo *et al.*,

1999; Cubas, Vincent and Coen, 1999). Their expression has been shown to be correlated with their role for the repression of normal growth in these organs (Luo *et al.,* 1999, Cubas, Vincent and Coen, 1999). However, *CYC, DICH* and *LvCYC* are expressed in the dorsal domain before and after organ primordium emergence from the floral meristem (Luo *et al.,* 1996, Cubas, Vincent and Coen, 1999). In *S. wisotonensis,* the morphological study (chapter III) suggests that growth repression of the staminodes is likely to be initiated before the emergence of their primordia. However, the expression of *SCHCYC1* was not detected until the emergence of the staminodes primordia. This result suggests that, although *SCHCYC1* is likely to be involved in the inhibition of growth in the staminodes where it is specifically and strongly expressed, other genes are probably involved in the control of early growth inhibition along the dorso-ventral axis.

V.3.3.2 SCHCYC2

(i) Expression pattern observed with the anti-sense probe for SCHCYC2

The expression of *SCHCYC2* was detected in the IM but not in the floral meristem and in developing floral organs (from stage 1 to 6). This result does not support a putative role for this gene in the control of floral dorso-ventral asymmetry. In the IM, *SCHCYC2* signal was detected in the central domain of the IM. The expression pattern was either detected on 2-3 consecutive sections, or along its entire length. This region broadly corresponds to the site of the future bifurcation (central domain) and to the plane of the bifurcation which will take place in the next round of meristem division (expression in the central region along the entire length) (Fig V.24). However, the signal was not detected in all IM meristems, even when

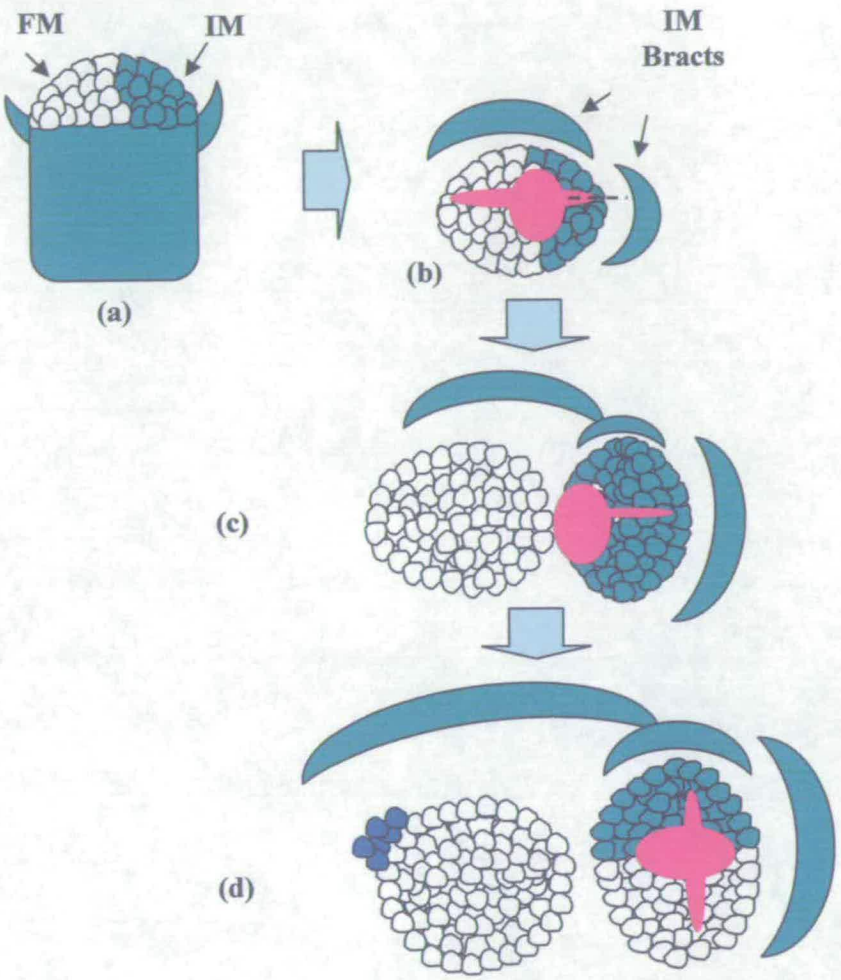

Fig V.24: Summary and synthesis of the expression pattern observed for *SCHCYC2*
(a) Simplified transversal view on the bifurcating inflorescence meristem.(b) Views from above corresponding to the same structure. (c&d) successive stages of development following the initial bifurcation. The red colour indicates the region of putative expression of *SCHCYC2* sense transcript as inferred by the RNA *in situ* hybridisation experiments. The blue colour corresponds to the site where the ventral sepal develops.

sections were carried through the same tissue and in the same hybridization reaction. Therefore, it was not possible to demonstrate that the different phases in the expression pattern shown in Fig V.24 correspond to a continuum.

This project shows the first example of a pattern of expression for a *CYC*-like gene which, at the site of the split between the inflorescence and the flower meristem, is confined to the IM rather than the FM. This expression pattern of *SCHCYC2* is reminiscent of the early expression of *CYC, DICH , LvCYC, AtTCP1* and *LotusCYC* genes. Their transcript was also detected at or next to the split site between the flower and inflorescence meristem (Luo *et al.,* 1999, Cubas, Coen and Zapater, 2001, Luo, D., pers.comm). This result reinforces the hypothesis proposed by Cubas, Coen and Zapater (2001) that the ancestor of *CYC*-like genes might have had a role in the bifurcation between the floral and the inflorescence meristem. This role possibly pre-dated the split between the asterids and the rosids since this pattern of expression is found in both groups. The resulting asymmetrical expression in emerging meristems could have been recruited for different purposes depending on species. In *A. majus* and *L. vulgaris,* this expression pattern is confined to the FM where it sets up a dorso-ventral asymmetry. In *S. wisotonensis,* it is confined to the IM where it has an unknown function.

The expression pattern of *SCHCYC2* in the region of the IM and not the FM next to the site of the bifurcation is very interesting from an evolutionary view point. One way to reconcile the expression of *SCHCYC2* with that of other members of the *CYC-TB1* clade is to view the IM in *S. wisotonensis* as an axillary meristem. Following this scenario *SCHCYC2* would be partially expressed as other members of the *CYC-TB1* clade mentioned previously, i.e. in the domain of the axillary meristem

which is closer to the main axis (Luo *et al.*, 1999, Takeda *et al.*, 2003, Hubbard *et al.*, 2002). This axis is the growing inflorescence in *A. majus*, *L. vulgaris* and *A. thaliana* or the main shoot in maize and rice (Luo *et al.*, 1999, Cubas *et al.*, 1999, Cubas, Coen and Zapater, 2001, Takeda *et al.*, 2003, Hubbard *et al.*, 2002). In *S. wisotonensis*, for this theory to hold true, the main axis would have to be the terminal flower. However, as mentioned in chapter III, the sympodial nature of solanaceous inflorescence is not supported by the data obtained in tomato, *petunia* and *S. wisotonensis*. In these species, even though the inflorescence stem appears contorted, its growth is continuous and therefore the IM is the main axis. Interestingly, the sister family to the Solanaceae, the Convolvulaceae (Olmstead *et al.*, 2000), comprises species with scorpoid cymes (i.e. with sympodial growth). This character is also found the Boraginaceae, a sister family to the Solanaceae and the Convolvulaceae. This observation suggests that the ancestor of the clade which includes all three families could have been a species with a scorpoid cyme. Following this hypothesis, it would be possible to propose that the bifurcating structure is a modified scorpoid cyme, i.e. an evolutionary step towards (or back to) a racemose-like inflorescence structure. In this evolutionary context, the expression of *SCHCYC2* in a "terminal" IM would be in fact a consequence of the repositioning of the sympodial meristem with IM identity to an apical position in the Solanaceae (Fig V.25).

(ii) Putative function of SCHCYC2 in the inflorescence meristem

What is the function of *SCHCYC2* in the IM? In the absence of functional studies, it is only possible to propose "educated suggestions" based on functional studies of other TCP genes.

Fig V.25: Simplified diagram of three different types of inflorescences
(See overleaf)

(a-c) correspond to a racemose inflorescence where the terminal structure is the inflorescence meristem (IM) (a) and the flower develops in an axillary position (b). In (c), the red colour indicate the region of the axillary meristem where *CYC*-like genes are found expressed in *A. majus* and *L. vulgaris*.(d-f) correspond to a scorpoid cymose inflorescence where the terminal structure is the flower (d) and the IM develops in an axillary position (e). In (f), the red colour indicate the region of the axillary meristem where *CYC*-like genes could be expected to be expressed based on what has been found so far about the expression of these genes in the dorsal domain of axillary structures. (g-i) correspond to a bifurcating inflorescence where the terminal structure is the inflorescence (g) and the flower meristem is formed by bifurcation (h). In (i), the red colour indicates the region of the IM where *CYC*-like genes are expressed.

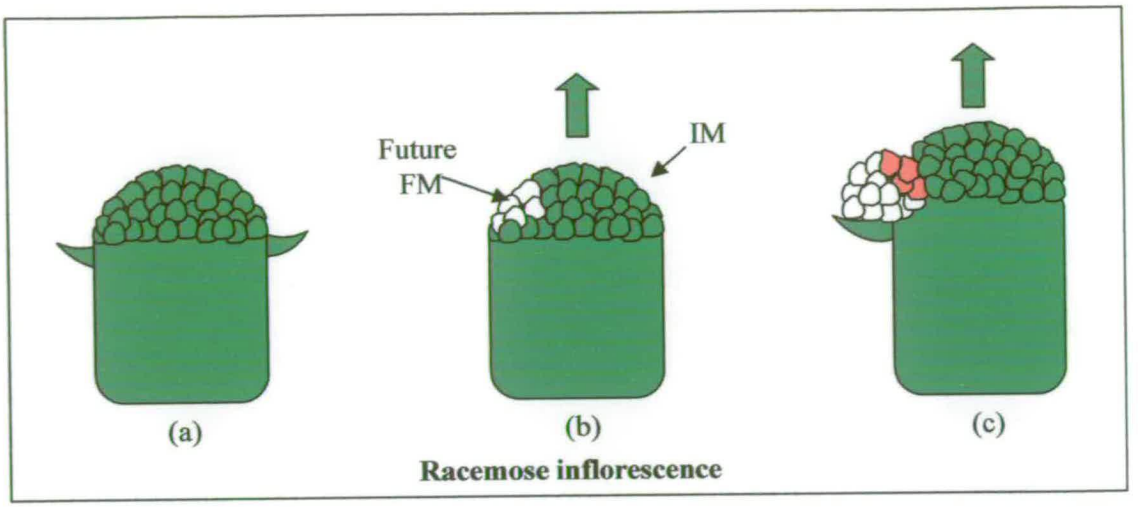

Racemose inflorescence

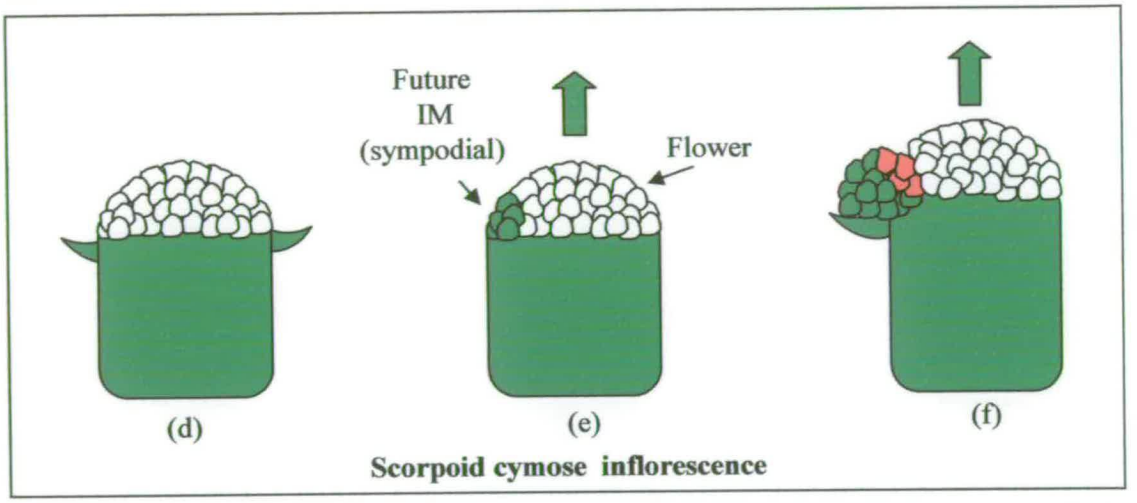

Scorpoid cymose inflorescence

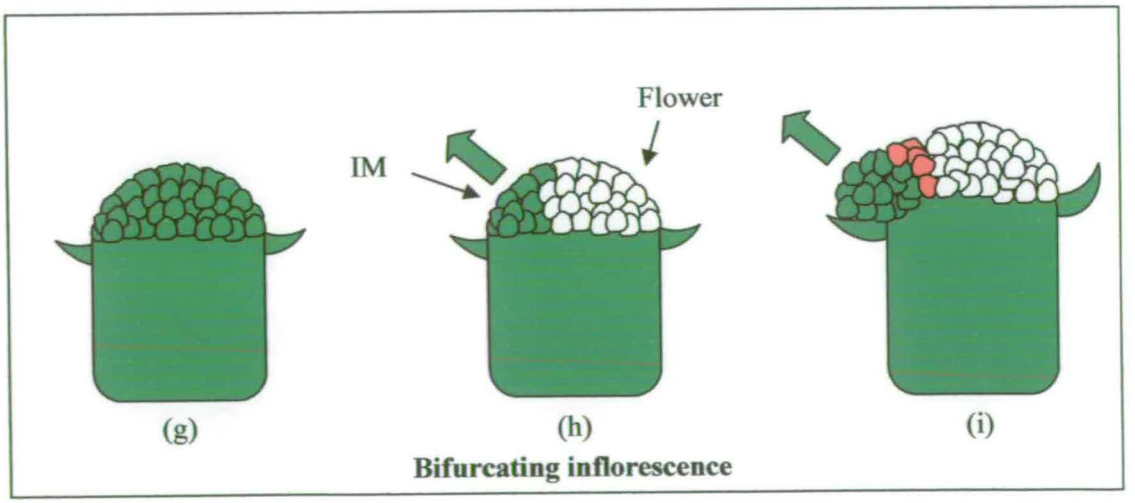

Bifurcating inflorescence

The role of TCP genes as transcription factors was firmly established in rice and *A. thaliana.* PCF1 and 2 were initially isolated for their ability to bind to cis-elements (site I and II) of a gene promoter in rice (Kosugi and Ohashi., 1997). Complementary studies have shown that at least in rice, all TCP proteins (TCP1-8 from class I and II) have the ability to bind to either or both consensus sequences, site II being further characterized as a positive regulatory cis-element (Kosugi and Ohashi., 1997, 2002). A similar study in *Arabidopsis* has shown that TCP20 (putative ortholog of PCF1&2) is also able to bind a similar consensus sequence in *A. thaliana*, resulting in the up-regulation of target genes (Trémousaygue *et al,.* 2002).

So far, all target genes with a TCP binding sequence are either directly or indirectly involved in the control of cell proliferation, and therefore growth (Trémousaygue *et al,.* 2002., Kosugi and Ohashi., 2002). For example, in rice, PCF 1&2 bind the promotor of the *PROLIFERATING CELL NUCLEAR ANTIGEN* (PCNA) gene which is transcriptionaly regulated and believed to be involved in various processes such as DNA replication and cell cycle control (Kosugi and Ohashi.,1997, Warbrick, 2000). In *Arabidopsis,* TCP 20 similarly targets a variety of proteins, including the *At*PCNA genes and ribosomal proteins (RP). Both are involved in the translational machinery, and interestingly, the enhanced expression of RP has been shown to promote cell division and growth (Trémousaygue *et al,.* .2002). In *A. majus,* the comparative study of expression patterns of *D3-cyclin* genes between the wild-type and a *cyc* mutant has shown that *CYC* downregulates locally the *D3b-cyclin* gene during floral development in *Antirrhinum* (Gaudin *et al* , 2000).

Therefore, the most likely function of *SCHCYC2* in actively dividing tissue is to be involved in the regulation of cell proliferation. The finding that in juvenile IM, *SCHCYC2* is expressed in the central region further supports a potential role for *SCHCYC2* in the regulation of cell division. In the inflorescence meristem, both types of regulators (i.e. growth enhancer and repressor) are needed. Obviously, cells need to actively divide to sustain organ formation (Carles and Fletcher, 2003). However, a developmental switch takes place on a sub set of cells at the future site of the split between the IM and the FM. These cells define the boundary between the two meristems. To do so, they are believed to divide more slowly than cells on either sides of this plane (Breuil *et al.,* 2004, Weir *et al.,* 2003). Consequently, the slower rate and even the arrest of cell division in the middle of the meristem results in a divide between both groups of actively dividing cells.

My data suggest that *SCHCYC2* may have a role in the setting up boundaries within the IM. *SCHCYC2* expression may participate either directly or indirectly in the successive bifurcation (Fig V.24). This hypothesis is supported by a recent study of the *cupuliformis* mutant in *A. majus* (Weir *et al.*, 2003). They discovered that *CUP,* which has a role in the establishment of above-ground meristems boundaries, interacts directly with a TCP gene from class I (i.e. PCF group).

(ii) Expression pattern observed with the sense probe for SCHCYC2

Interestingly, a signal in inflorescence-like meristems was detected when using the sense probe. This experiment was repeated twice with *de novo* synthesis of the probe. Therefore, unless a structural feature of the linearized vector results in

anti-sense transcription as well as sense transcription, the anti-sense transcript is not expected to be detected with the sense probe.

If this finding is not an artifactual, two possible scenarios can be proposed.

Firstly, although it has not been shown before in the TCP gene family, some plant genes are transcribed in both directions (Terryn and Rouze, 2002). The most common function of anti-sense transcripts is to regulate their corresponding sense RNA. The presence of anti-sense transcript could be tested by RT-PCR.

Alternatively, it could indicate that this gene is post-transcritionally regulated by micro RNAs (miRNA) or short interfering RNAs (siRNAs) (Baulcombe, 2004). Micro RNAs can be detected by RNA *in situ* hybridisation as demonstrated in maize (Juarez *et al.*, 2004). Interestingly, non-coding RNAs have been shown to regulate the function of several plant genes including TCP4, the *A. thaliana* homologue of *CINCINNATA* in *A. majus* (Palatnik *et al.*, 2003).

If the signal detected by the *SCHCYC2* sense probe corresponds to the detection of miRNAs, a Northen blot should be carried out to confirm this hypothesis. MiRNAs and SiRNAs are characterized by their small size (21-26 nucleotides), therefore on a Northen blot, the presence of a band corresponding to RNAs of that size would support this hypothesis. In addition, a thorough study of the expression of the sense RNAs should be carried out.

V.3.3.3 SCHCYC3

The pattern of expression found with *SCHCYC3* was similar to that of *SCHCYC2*. In the IM, the signal detected for *SCHCYC3* was often but not always weaker than that obtain with the *SCHCYC2* anti-sense probe. However, the intrinsic

variability of their respective signals in developing IM renders the interpretation of these observations difficult.

Although *SCHCYC3* was not detected in bifurcating structures, the probing of bifurcating structures with the anti-sense probe for *SCHCYC3* was not repeated enough to support the statement that *SCHCYC3* is not expressed there.

In summary, the overlapping pattern of expression of *SCHCYC2* and *SCHCYC3* suggests that the discussion of expression pattern and function for *SCHCYC2* can also be applied to *SCHCYC3* (see *V.3.3.2i&ii*).

V.3.3.4 SCHCYC2 and SCHCYC3 and their overlapping domains of expression

What could be the significance of the overlapping domains of expression of *SCHCYC2* and *SCHCYC3*?

In gene families, gene duplication is believed to often result in either functional redundancy, or functional diversification of duplicated genes (Hofer and Ellis, 2002, Pickett and Meeks-Wagner, 1995).

In *S. wisotonensis*, *SCHCYC1, 2* and *3* belong to a monophyletic group suggesting that they are derived from a common ancestor through gene duplication.

Are the overlapping domains of expression of *SCHCYC2* and *SCHCYC3* likely to reflect functional redundancy between two duplicated genes? In *S. wisotonensis,* the data available for the determination of duplication events is generating conflicts. On one hand, in most phylogenetic analyses carried on the *CYC-TB1* group, *SCHCYC1* and *SCHCYC2* are grouped together on the same terminal node. This result, although weakly supported in most analyses, suggests that they are closer to each other than to *SCHCYC3*. However, when compared

visually, the predicted nucleotide and protein sequences of *SCHCYC1, 2* and *3*, are overall equally dissimilar to each other except for the TCP and the R box.

Therefore, functional redundancy due to recent duplication is not supported by the sequence data.

This argument is interesting in itself. It suggests that despite the evolution of the coding sequence, the pattern of expression of *SCHCYC2* and *SCHCYC3* have remained similar. This is likely to be caused by a conservation in cis and trans-regulatory elements. Alternatively, their overlapping expression patterns may be the result of convergent evolution between distant paralogs. In both scenarios, the relative similarity of expression pattern compared to that of their coding sequence probably suggests that both genes could be functional and their overlapping expression pattern meaningful. An obvious possibility is that *SCHCYC2* and *SCHCYC3* could form heterodimers. Heterodimerisation of TCP protein has been reported previously for TCP genes. In rice and *A. thaliana*, the work of Kosugi and Ohashi (2002) and Trémousaygue *et al.* (2002) suggest that the binding of TCP genes to DNA is dependent on the formation of protein-protein complexes. These may involve homo and heterodimerisation of TCP proteins, heterodimerisation being restricted to genes belonging to the same class (Kosugi and Ohashi, 2002). The function of homologous or heterologous multimeric protein complexes may provide a way to competitively or co-ordinately regulate the transcription of target genes (Kosugi and Ohashi (1997, 2002), Trémousaygue *et al.,* (2002)). Although dimerisation has never been shown (and possibly never been tested) for *CYC*-like genes, in *S. wisotonensis,* the putative dimerisation of *SCHCYC2* and *SCHCYC3* could be tested by a yeast-two hybrid experiment.

Another interesting aspect of the domain of expression of *SCHCYC2* and *SCHCYC3* is that it is completely different from that of *SCHCYC1*. This difference can be explained by a "gain" theory whereby duplicated genes undergo sub-functionalisation and functional divergence. Alternatively, it can be explained by a "loss" theory. In the latter, both patterns of expression were present in the ancestor gene to the solanaceous sub-clade and one or the other pattern was lost. The evolutionary argument would favor the loss theory since both patterns of expression are reminiscent to what has been described previously for this gene family (Cubas, 2002). Therefore, in *S. wisotonensis*, the ancestor of *SCHCYC1, 2* and *3* is likely to have been expressed both in the IM and in the FM, with the two patterns of expression later separated by loss in duplicated copies.

V.3.4 Interpretation of the *Rz* mutant

The pleiotropic nature of the *Rz* mutant suggests that one developmental pathway which affects organs along the dorso-ventral is not switched on. This indicates that either the function of a gene in this pathway has been abolished (loss of function) or that a negative regulator for one gene or more is up-regulated or de-repressed (gain of function). The unstable heritable alleles in *Rz* mutant plants revealed that the mutation was very likely to be epigenetic in nature, since double revertants were commonly found in the population. Such epigenetic mutations can be caused by transcriptional gene silencing (TGS) or post-transcriptional gene silencing (PGTS). These phenomena are now believed to play an important role in gene regulation during plant development (Steimer, Schöb and Grossniklaus, 2004). In this project, the unstable nature of some *Rz* mutant is reminiscent to what was found in *L.*

vulgaris. In the latter, the peloric mutant was caused by the heavy methylation of *LvCYC* at the DNA level, with revertions of some branches to wild-type (Cubas, Vincent and Coen, 1999). The similarity between the peloric mutant in *L. vulgaris* and the *Rz* mutant suggests that the *Rz* mutant is also likely to be caused by a change in the degree of methylation at the *Rz* locus. This change could be the methylation and therefore silencing of gene, which adequates to a loss of function mutation. Alternatively, a gain of function could be caused by the loss of function of a negative regulator. In the latter, the *rz* mutant flower could be interpreted as a gain of lateral identity due to ectopic expression of a lateral identity gene in the dorsal and the ventral domain where it is downregulated in the wild-type.

V.3.5 What is the expression of *SCHCYC1, 2* and *3* in the *Rz* mutant telling us about their putative role in the control of dorso-ventral asymmetry?

In chapter III, the *Rz* mutant was described as a mutant unable to interpret a pre-pattern affecting organ growth along the dorso-ventral axis and required to produce wild-type dorso-ventral asymmetry in *S. wisotonensis*. In this chapter, I reported that the *Rz* mutation was dominant and very likely to be epigenetic.

Is the pre-pattern absent in the *Rz* mutant controlled by one of the *CYC*-like genes isolated in this study? Are any of these *CYC*-like genes targets of the pre-pattern?

Overall, the pattern of expression of *SCHCYC1, 2* and *3* were found to be similar in the wild-type and the *Rz* mutant.

V.3.5.1 SCHCYC1

In the *Rz* mutant, as in the wild-type, the dorsal and the ventral stamens are aborted, albeit not to such a great extent. The phenotypic analysis of the mutant does not affect the initial growth retardation of the staminodes. However, in the *Rz* mutant, the staminodes are less aborted than in the wild-type suggesting that in the mutant, the genetic control of growth repression is not completely functional. Therefore, if *SCHCYC1* is responsible for the growth inhibition of the staminode after primordium emergence, its expression pattern would be expected to be reduced in the *Rz* mutant where the staminodes are less inhibited than in the wild-type. This was not observed, possibly due to technical limitations. If confirmed by additional experiments, this could show that *SCHCYC1* function is independent of the developmental pathway affected in the *Rz* mutant, a pathway required to produce a fully aborted stamen. An alternative explanation could be that downstream target genes of *SCHCYC1* required for stamen abortion might not be responsive in the *Rz* mutant.

V.3.5.2 SCHCYC2 and SCHCYC3

There were no obvious changes in the expression pattern of *SCHCYC2* and *SCHCYC3* in the wild-type and in the mutant. This finding was expected given that both are expressed in the IM whereas the phenotype of the *Rz* mutation affects the dorso-ventral axis in the flower.

V.3.5.3 SCHCYC4, 5 and 6, an experimental failure?

The phylogenetic analysis presented in chapter IV did not support *SCHCYC4, 5* and *6* as putative *CYC* orthologs. Their transcript was detected by RT-PCR on cDNA obtained from inflorescences suggesting that they are expressed in reproductive tissues. However, successful RNA *in situ* hybridization experiments failed to produce expression patterns for these genes. This result suggests that the transcripts detected by RT-PCR are background levels of expression throughout the reproductive tissue. Alternatively, a problem may have taken place during the synthesis of the RNA probes.

In summary, the study of the expression pattern of *SCHCYC1* to *3* in *S. wisotonensis* was very successful. It has shown that zygomorphy is not likely to be genetically "governed" by *SCHCYC1* to *3* in *S. wisotonensis*. Nevertheless, the expression pattern of *SCHCYC1* indicates that it is likely to be involved in the control of growth repression in the staminode. Finally, the expression pattern of *SCHCYC2* and *SCHCYC3* suggest a role for these genes in the setting up of boundaries between the IM and the emerging FM.

VI Discussion

This project is based on the work of Marc Chadwick in *S. wisotonensis* and on the role of TCP genes in the control of dorso-ventral asymmetry in the Scrophulariaceae, a related family to the Solanaceae (Luo *et al.*, 1999, Cubas, Vincent and Coen, 1999). The starting hypothesis was that the genetic of floral dorso-ventral zygomorphy in *S. wisotonensis* could be controlled by *CYC*-like gene in this species too.

How did the results of this research improve the understanding of the developmental mechanisms linked to zygomorphy and its genetic control in *S. wisotonensis*?

VI.1 The developmental dynamics of floral zygomorphy in *S. wisotonensis*, a surprise or a predictable story?

The comparative study between the wild-type and the *Rz* mutant showed that in the corolla and the androecium, dorso-ventral asymmetry is established via what appears to be two independent pathways. One pathway (unaffected in the *Rz* mutant) corresponds to what is called the Robyns' rule, i.e. the ventral organ is often the only or the most affected organ (Knapp, 2002). This pathway can be viewed as a unidirectional polarization of the corolla resulting in a difference in size between the ventral petals and their lateral and dorsal counterparts. This size gradient can be interpreted as a dorsalisation or a ventralisation. Following the Robyns' rule applicable to many other solanaceous species, the polarization is very likely to be a ventralisation. This type of unidirectional polarization resembles in principle that of

A. majus or *L. vulgaris*, even though in these species, a dorsalisation rather than a ventralisation is observed (Luo *et al.*, 1996, Cubas, Vincent and Coen, 1999). The second set of developmental cues (missing in the mutant) corresponds to what appears to be a genetic mechanism which is required to modulate organs growth along the dorso-ventral axis. The pleiotropic nature of the *Rz* mutant indicates that this secondary development cue/pathway is normally interpreted differently in the dorsal or in the ventral domain, and during the different stages of floral development.

Therefore, this study has shown that two sets of developmental cues (i.e. trans-regulators) are required for the normal establishment of the floral symmetry in *S. wisotonensis*. The first set controls dorso-ventral asymmetry as in the Robyns' rule. The second set controls organ development along the DV axis.

The major difference between the model proposed in *S. wisotonensis* and that of *A. majus* lies in the polarization of morphological changes along the Dv axis in whorls 2 & 3 which is not observed in *A. majus*. This finding illustrates nicely the view held by many developmental biologists that the morphology of the flower depends upon the developmental cues and constraints created by the inflorescence on which it is borne (Coen, 1991, Coen *et al.*, 1995, Coen and Nugent, 1994, Endress, 1999).

The model proposed in this study fits well with the morphology of species related to *S. wisotonensis* where zygomorphy is more moderate. For example, in the flower of *Salpiglossis*, the larger stamens are dorsal and the petals size decreases towards the ventral domain (Fig VI.1). Therefore, this flower resembles a stronger *Rz* mutant in principle (loss of staminode abortion in the dorsal domain) which has retained the pre-pattern corresponding to Robyns' rule. In more advanced species

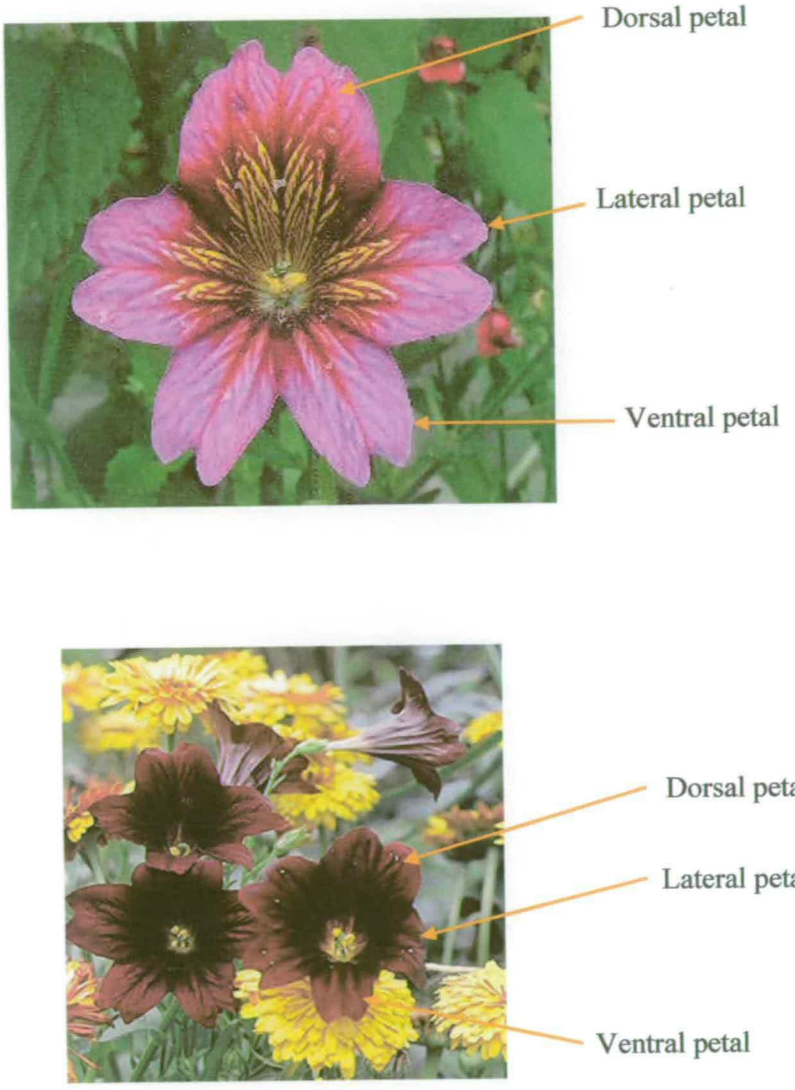

Fig VI.1: Two members of the genus *Salpiglossis* (Solanaceae)

such as *Petunia,* the manifestations of a possibly *RZ* –like controlled dorso-ventral asymmetry is confined to heterandry amongst stamens. In this species, although all stamens are fertile, the two dorsal stamen are shorter than the lateral ones, and the shortest stamen is in the ventral position. This finding agrees with Tucker (1999) who suggests that early manifestation of zygomorphy in ontogeny (here staminode abortion) are more likely to be conserved through evolution than later manifestation.

VI.2 TCP genes in *S. wisotonensis*, usual suspects or innocent protagonists in the control of floral dorso-ventral asymmetry ?

Three *CYC*-like genes have been found in *S. wisotonensis* (*SCHCYC1, 2* and *3*) and only one of them appears to have a potential role in floral development. Indeed, the expression pattern of *SCHCYC1* clearly suggests a role for this gene in the abortion of the ventral and dorsal staminodes. This function was already described for *CYC, DICH* and *LvCYC* where it contributes to the dorso-ventral asymmetry of the androecium (Luo *et al.*, 1996, Cubas, Vincent and Coen, 1999). In *S. wisotonensis*, even if the function of *SCHCYC1* was proven to control stamen abortion, can it regarded as a gene which participates in the elaboration of dorso-ventral asymmetry? The expression data does not support this hypothesis because *SCHCYC1* is expressed in the dorsal AND the ventral staminodes in the WT and the *Rz* mutant. However, in the absence of more data, it is not possible to draw any conclusions regarding the role of *SCHCYC1* in the establishment of DV asymmetry in the androecium.

The other two potential candidates, *SCHCYC2* and *SCHCYC3,* were not found to be expressed in the young flower bud but in the IM instead, where their

pattern of expression suggests a role in the bifurcation process. Therefore, the data does not suggest any function for these genes in the control of dorso-ventral asymmetry, unless they are expressed in the FM at very low levels undetected in my experiments.

VI.3 Does this project suggests that these *CYC*-like genes are not involved in the control of dorso-ventral asymmetry in *S. wisotonensis*? Or has the *CYC*-like gene implicated not yet been identified?

The most "parsimonious" answer would be that, yes, another *CYC*-like gene might be present in the genome of *S. wisotonensis* which has not been isolated yet. Unfortunately, the difficulties encountered with a Southern blot approach in chapter III suggest that it would not be easy to investigate this by carrying out a low stringency Southern hybridization using a *CYC* probe. Therefore, instead, a thorough screening of the cDNA library should be carried out.

Although the above hypothesis would be the easiest explanation behind the lack of evidence for involvement of *SCHCYC1* to *3* in the control of dorso-ventral asymmetry, it is not really supported by the data. The expression pattern and putative function of *SCHCYC1, 2* and *3* are clearly reminiscent to that of other *CYC*-like genes (see discussion in chapter V). Therefore, there are no reasons to think that these genes do not represent the putative descendants of a *CYC*-like ancestor for which functional divergences has been driven by the evolution of the solanaceous inflorescence structure.

A striking feature of *SCHCYC1*, *2* and *3* is that they are all expressed across the central region of their respective meristems. Therefore, in the juvenile bifurcating structure, if the plane corresponding to the next split in the IM was

visible, it would form a line which, if continued in the emerging FM (from the on-going bifurcation) would correspond approximately to the dorso-ventral axis of this flower (Fig VI.2). In this extrapolated vision of the IM and FM during the bifurcation, *SCHCYC1, 2* and *3*, would be in principle expressed in the same plane, albeit at opposite ends of the same dividing structure and during different developmental stages. Therefore, a developmental cue for the next bifurcation might be set up by *SCHCYC2* and *SCHCYC3* before the split of the former bifurcation. Following this hypothesis, the expression of *SCHCYC2* and *SCHCYC3* could provide a developmental cue for the dorso-ventral axis of the flower (Fig VI.2).

This model reconciles the pattern of expression of *CYC*-like genes in *S. wisotonensis* with a putative role for *SCHCYC2* and *SCHCYC3* in the establishment of dorso-ventral asymmetry in the flower of *S. wisotonensis.* It would entail that the original expression pattern (i.e. along the bifurcation) of a *CYC*-like gene would have been co-opted for a novel function. This function would not be to provide a dorso-ventral asymmetry by "dorsalising" the adaxial region of the FM like in *A. majus*. Instead, this function could be in part to set-up a developmental cue which will become the dorso-ventral axis of flowers (Fig VI.2). This putative function would be directly linked to the fact that the inflorescence of *S. wisotonensis* produces flowers by bifurcation at right angle to each other (Fig VI.2).

VI.4 How did this project contribute to the nascent field of evo-devo?

VI.4.1 Evo-devo, a new discipline with hopes and limitations

Over the past decade, our ever-increasing understanding of developmental genetics in model species has enabled the long awaited birth of a new discipline

Fig VI.2: Model integrating the expression pattern of *SCHCYC2* and *3* in the inflorescence meristem with a potential role in the establishment of a developmental cue corresponding to the DV axis of the future flower

(See overleaf)

(a) Simplified transversal view on the bifurcating inflorescence meristem. (b) View from above corresponding to the same structure. (c-f) successive stages of development following the initial bifurcation. The red colour indicates the region of putative expression of *SCHCYC2* as inferred by the RNA *in situ* hybridisation experiments. The blue colour indicates the site where the ventral sepal develops. The region highlighted with red and white stripes shows the location of a possible developmental cue for the DV axis of the flower which could linked to the expression of *SCHCYC2* and *3* just prior the bifurcation..

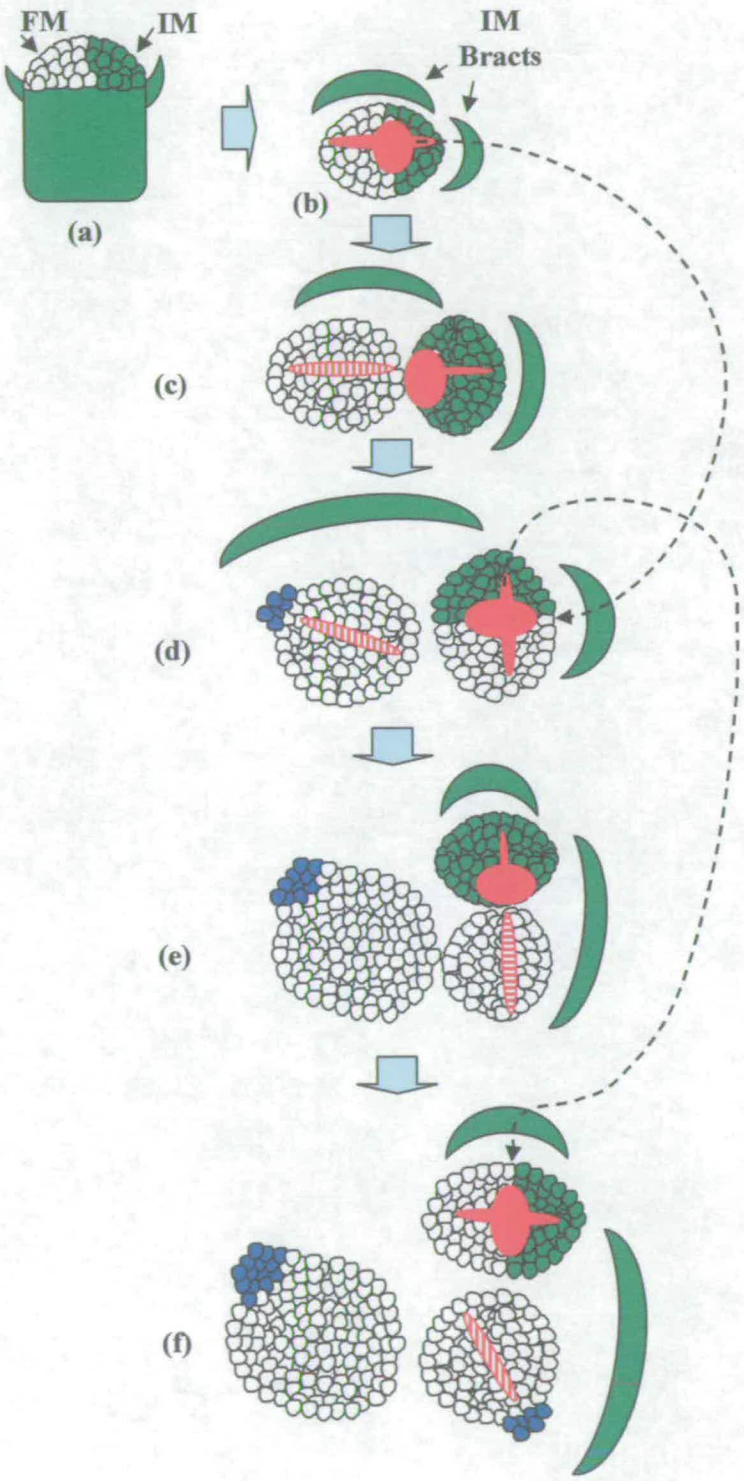
FM
IM
(a)
IM
Bracts
(b)
(c)
(d)
(e)
(f)

called evo-devo (evolution and development) (Raff, 2000). This discipline aims at unraveling the genetic mechanisms underlying the evolution of developmental processes. So far, developmental studies have focused on a few model-species. In plant science, the range of model species span different taxonomic groups (i.e. maize, tobacco), a welcomed bi-product of a scientific attention originally biased towards species of agronomical importance! Only a few species are exceptions to this rule. The best studied species of the plant kingdom is the famous *A. thaliana*. The prospect of an *Arabidopsis* salad could probably only appeal to a plant scientist lost at sea. Therefore, this species was rather selected for its convenient size, weedy attributes, compact (and now fully sequenced) genome, and also because it belongs to the Brassicaceae, a family including many crop plants. Another non-agronomically important model-species in plant developmental studies is *A. majus*. The latter belongs to a genus which has attracted the attention of biologists since Darwin and Mendel for its huge variety of morphological traits and its convenience for inheritance studies. Therefore, overall, a few well studied model species are found in a few unrelated families scattered within the angiosperms.

Can the comparison between these model species provide the ultimate tool for evo-devo studies? Many breakthroughs in the past 20 years of plant developmental biology (e.g. the ABC model in flowers) were discovered in either *A. majus* or *A. thaliana* and tested afterwards in other model species. In the angiosperms, the Solanaceae is probably the family comprising the greatest number of model species in which genetic studies are possible. Therefore, in this family, an impressive body of knowledge has been accumulated regarding inflorescence and floral development. However, most of this research seems to have been carried out as routine comparative

tests to what has been found in *A. majus* and in *A. thaliana*, and since all model species in this family are completely or almost completely actinomorphic, the genetic control of zygomorphy has remained so far mostly unexplored.

Therefore, the study of the role of *CYC*-like genes in floral zygomorphy in *S. wisotonensis* is the first of this kind, in the Solanaceae (Knapp, 2002). It arguably uses the best species for this purpose (rather than a model species) and tools that were not available before. These include the knowledge and data accumulated concerning the TCP gene family in a range of species in the Solanaceae (Chadwick, 1996) and across the angiosperms (Cubas, 2002, 2004), and a mutant with simple genetics and decreased dorso-ventral asymmetry (the *Rz* mutant). In the larger picture, the goal of this project was therefore to provide a primer and a stepping stone for evo-devo studies of zygomorphy in the Solanaceae.

Part of the challenges of evo-devo lies in the use of non-model species. A few example of such studies carried out in the field of floral symmetry include research in the legumes (H. Citerne, pers. comm.) and in the Scrophulariaceae (Hileman, Kramer and Baum, 2003). However, in the use of non-model species, lie the limits of evo-devo. In the absence of a technique which would guarantee the feasibility of transgenic experiments in all species, evo-devo studies on non-model species are prone to the proposition of models which are almost impossible to test. For example, my project revealed interesting observations related to *CYC*-like genes such as their potential role in bifurcating inflorescences and the potential regulation of *SCHCYC2* by RNA-related mechanisms. But testing these biological questions in a species which cannot be genetically modified is extremely difficult. Therefore, beside a wealth of enthusiasm lies a wall of technical difficulties. However, whether gene

function can be demonstrated or not, it can be expected that evo-devo studies will produce unexpected results, thereby feeding back inspiration to developmental biologists working on model species.

VI.4.2 Evo-devo, the many promises of over simplified models

For every complex problem, there is a solution that is simple, neat, and wrong (Henry Louis Mencken (1880-1956)). In this project, we learned that this quotation, previously used in a paper about the ABC model (Gutierrez-Corines and Davies, 2000) applies also to the control of floral symmetry by *CYC*-like genes. In other words, the promised land (i.e. a simple model involving *CYC*-like genes in the control of zygomorphy in *S. wisotonensis*) was not found. However, far from being disappointing, this project has shed a new light on what had started to be an almost too predictable developmental quest. Floral symmetry has attracted a great deal of attention from the scientists interested in evo-devo studies. This is due to the fact that associated morphological changes are easy to analyze and rarely affect viability in mutants. In addition, *CYC*-like genes have two conserved regions which permit the easy designs of PCR primers and therefore the promise of some molecular data to start a project. The results found in the Scrophulariaceae, in *A. thaliana*, in *Senecio* and even in legumes support very strongly the suggestion that *CYC*-like genes have been recruited to establish dorso-ventral asymmetry in a wide range of species across the angiosperms (Cubas, 2002, 2004). However, most of the species studied so far have a racemose inflorescence. By targeting this type of study in a family related to the Scrophulariaceae which has a different inflorescence architecture, this project has opened a new chapter in the "traditional" story of the *CYC*-like genes.

Such unexpected results suggesting sub-functionalisation of orthologous genes have been show in many other studies (Shepard and Purugganan, 2002). For example, in pea, the *LEAFY*-like gene is required for compound leaf development (Gourlay, Hofer and Ellis, 2000). Interestingly, this function was not demonstrated in other species even when *LEAFY*-like genes are expressed in vegetative meristems (Kelly, Bonnlander and Meeks-Wagner, 1995, Molinero-Rosales *et al.*, 1999, Souer *et al.*, 1998). The MADS-box gene family has also been very thoroughly studied in non-model species. In many studies across both related and un-related species, a degree of conservation was found together with evidences for sub-functionalisation of putative orthologs (Becker and Theissen, 2003). Such examples are likely to be only the beginning of a myriad of unexpected developmental and evolutionary pathways that will be uncovered by evo-devo studies.

VI.4.3 Evo-devo, the reconciliation of molecules, organisms and evolution

One of the first and the most elegant piece of research showing how the evolution of morphological traits can take place at the DNA level is that of Doebley and co-workers in maize (Wang *et al.*, 1999, Clark *et al.*, 2004, *Baum*, 1998). From their study, they concluded that changes in the *cis*-regulatory region of the transcription factor *TB1* are responsible for the major change in branching pattern observed between maize and its ancestor and wild relative, teosinte (*Z. mays* subsp. *mexicana* and subsp. *parviglumis*).

The study of the pleiotropic effects of the *Rz* mutant is also a wonderful example of the impact of a mutation at a single locus on floral morphology. In this mutant, the morphological changes result in protruding anthers open to generalist

pollinators (Cronk and Möller, 1997). This is a drastic change from the wild-type flower where the ventral petals hold the stamens in a protected position, so that only specialized pollinators can trigger pollen release (Cocucci, 1989). It shows how *S. wisotonensis* could escape its pronounced zygomorphy within one generation. Obviously, if the specialist pollinator is no longer available, the *Rz* mutation may provide a selective advantage and may be fixed in the population, a process eventually leading to speciation (Ridley, 1996).

Therefore, from the general view point of the evolution of plant form, this project contributes to the ever increasing knowledge and understanding on how simple molecular changes can provide the template for important evolutionary shifts.

References

Allen, K. D. and Sussex, I. M. 1996. *Falsiflora* and *anantha* control early stages of floral meristem development in tomato (*Lycopersicon esculentum* Mill.) *Planta.* **200,** 254-264.

Almeida, J., Rocheta, M., Galego, L. 1997. Genetic control of flower shape in *Antirrhinum majus. Development.* **124,** 1387-1392.

Ampornan, L and Armstrong, J. E. 1988. The floral ontogeny of *Schizanthus,* a zygomorphic member of the Solanaceae. *American Journal of Botany.* **75,** suppl., 54.

Ampornan, L and Armstrong, J. E. 1989. The floral ontogeny of *Salpiglossis,* a zygomorphic member of the Solanaceae. *American Journal of Botany.* **76,** suppl., 64.

Ampornan, L and Armstrong, J. E. 1990. The floral ontogeny of *Schwenkia* (Solanaceae). *American Journal of Botany.* **77,** suppl., 168.

Angenent, G. C., Franken, J., Busscher, M., Colombo, L. and van Tunen, A. J. 1993. Petal and stamen formation in petunia is regulated by the homeotic gene fbp1. *Plant J.* **4(1),** 101-112.

Baulcombe, D. 2004. RNA silencing in plants. *Nature.* **431,** 356-363.

Baum, D. A. 1998. The evolution of plant development. *Current Opinion* in *Plant Biology.* **1,** 79-86.

Becker, A. and Theissen, G. 2003. The major clades of MADS-box genes and their role in the development and evolution of flowering plants. *Mol Phylogenet Evol.* **29(3),** 464-489.

Breuil-Broyer, S., Morel, P., de Almeida-Engler, J., Coustham, V., Negrutiu, I. and Trehin, C. 2004. High-resolution boundary analysis during Arabidopsis thaliana flower development. *Plant J.* **38(1),** 182-192

Carles, C. C. and Fletcher, J. C. 2003. Shoot apical meristem maintenance: the art of a dynamic balance. *Trends in Plant Science.* **8 (8),** 394-401.

Carpenter, R., Copsey, L., Vincent, C., Doyle, S., Magrath, R. and Coen, R. 1995. Control of flower development and phyllotaxy by meristem identity genes in *Antirrhinum. The Plant Cell.* **7,** 2001-2011.

Carpenter, R. Coen, E.S. 1990. Floral homeotic mutations produced by transposon-mutagenesis in *Antirrhinum majus. Genes Dev.* **4,** 1483-1493.

Chadwick, M. 1996. *A molecular genetic analysis of floral symmetry.* PhD Thesis. University of East Anglia.
Chase, M. W., Soltis, D. E., Olmstead, R. G., Morgan, D., Les, D. H., Mishler, B. D., *et al.* 1993. Phylogenetics of seeds plants: an analysis of nucleotide sequences from the plastid gene *rbcL*. *Annals of the Missouri Botanical Garden.* **80,** 528-580.

Child, A. 1979. A review of branching patterns in the Solanaceae. *In:* J. G. Hawkes, R. N. Lester & A. D. Skelding (editors). The biology and taxonomy of the Solanaceae, pp. 345-356. Linnean society of London, Academic press.

Citerne, H. L., Luo, D., Pennington, T. R., Coen, E. S. and Cronk, Q. C. B. 2003. A phylogenomic investigation of *CYCLOIDEA*-like TCP genes in Leguminosae. *Plant physiology,* **131,** 1042-1053.

Citerne, H. L., Möller, M. and Cronk, Q. C. 2000. Diversity of *cycloidea*-like genes in Gesneriaceae in relation to floral symmetry. *Annals of Botany.* **86,** 167-176.

Clark J. I., and Coen E. S. 2002. The cycloidea gene can respond to a common dorsoventral prepattern in Antirrhinum. *Plant J.* **30(6),** 639-48.

Clark, R. M., Linton, E., Messing, J., Doebley, J. F. 2004. Pattern of diversity in the genomic region near the maize domestication gene tb1. *Proc Natl Acad Sci U S A.* **101(3),** 700-7

Cocucci, A.1989. El mechanismo floral en *Schizanthus* (Solanaceae). *Kurtziana,* **20,** 113-132.

Coen, E. S. 1991. The role of homeotic genes in flower development and evolution. *Ann. Rev. Plant. Physiol. Plant. Mol. Biol.* **42,** 241-279.

Coen, E.S., Doyle, S., Romero, J. M., Elliott, R., Magrath, R. and Carpenter, R. 1991. Homeotic genes controlling flower development in *Antirrhinum. Development.* suppl.1, 149-155

Coen, E.S., and Meyerowitz, E.M. 1991. The war of the whorls: Genetic interactions controlling flower development. *Nature.* **353,** 31–36.

Coen, E.S. and Nugent, J. M. 1994. Evolution of flowers and inflorescences. *Development.* sup. 107-116.

Coen, E. S., Nugent, J., Luo, D., Bradley, D., Cubas, P., Chadwick, M., Copsey, L., Carpenter, R. 1995. Evolution of floral symmetry. *Phil. Trans. R. Soc. Lond. B.* **350,** 35-38.

Coen, E. S., Romero, J. M., Doyle, S., Elliott, R., Murphy, G., Carpenter, R. 1990. *floricaula,* A homeotic gene required for flower development in *Antirrhinum majus*. *Cell,* **63,** 1311-22.

Crawford, B. C., Nath, U., Carpenter, R. and Coen, E. S. 2004. *CINCINNATA* controls both cell differentiation and growth in petal lobes and leaves of *Antirrhinum*. *Plant Physiol.* **135(1),** 244-53.

Cronk, Q. and Moller, M. 1997.Genetics of floral symmetry revealed. *Trends in Evol. Ecol.***12,** 85-86.

Cubas, P. 2002. Role of the TCP genes in the evolution of morphological characters in angiosperms. *In* QCB Cronk, RM Bateman, JA Hawkins, eds, Developmental Genetics and Plant Evolution. Taylor and Francis, London, pp 247-266.

Cubas, P. 2004. Floral zygomorphy, the recurring evolution of a successful trait. *Bioessays*. **26(11),** 1175-84.

Cubas, P., Coen, E. S., Zapater, J. M.M. 2001. Ancient asymmetries in the evolution of flowers. *Current Biology.* **11,** 1050-1052.

Cubas, P., Lauter, N., Doebley, J., Coen, E.S. 1999. The TCP domain: a motif found in proteins regulating plant growth and development. *The Plant Journal.* **18,** 215-222.

Cubas, P., Vincent, C., Coen, E. 1999. An epigenetic mutation responsible for natural variation in floral symmetry. *Nature.* **401,** 157-161.

Davies, B., Di Rosa, A., Eneva, T., Saedler, H. and Sommer H. 1996. Alteration of tobacco floral organ identity by expression of combinations of Antirrhinum MADS-box genes. *Plant J.* **10(4),** 663-77.

Dayhoff, M. O., Schwartz, R. M. and Orcutt, B. C. 1978. A model of evolutionary change in proteins. In Dayhoff, M. O. (ed.) *Atlas of protein Sequence Structure*, volume 5, pp. 345-352, National Biochemical Research Foundation, Washington DC.

Doebley, J. and Lukens, L. 1998. Transcriptional regulators and the evolution of plant form. *Plant cell.* **10,**1075-82.

Doebley, J., Stec, A. and Hubbard, L. 1997. The evolution of apical dominance in Maize. *Nature.* **386,** 485-488.

Donoghue, M.J., Ree, R. H., Baum, D. A. 1998. Phylogeny and the evolution of flower symmetry in the Asteridae. *Trends in Plant Science*, **3,** 311-317.

Doyle and Doyle, 1999. Nuclear protein-coding genes in phylogeny reconstruction and homology assessment: some examples from Leguminosae. *In* P. M. Hollingworth, R.M. Bateman, R. J. Gornall, eds, Molecular systematics and plant evolution. Taylor and Francis, London, pp 229-254.

Endress, P. K. 1999. Symmetry in flowers: diversity and evolution. *International Journal of Plant Science.* **160,** S3-S23.

Endress, P. K. 2001. Evolution of floral symmetry. *Current Opinion in Plant Biology.* **4,** 86-91.

Ferreira, P., Hemerly, A., de Almeida Engler, J., Bergounioux, C., Burssens, S., Van Montagu, M., Engler, G., Inzé, D. 1994. Three discrete classes of *Arabidopsis* cyclins are expressed during different intervals of the cell cycle. *Proc. Natl. Acad. Sci. USA..* **91,** 11313-11317.

Fischer, J. A.2000. Molecular motors and developmental asymmetry. *Current Opinion in Genetics and Devlopment.* **10,** 489-496.

Fisher, J. B. 1974. Axillary and dichotomous branching in the Palm *Chameadorea. Can. J. Bot.* **61(10),** 1046-1056.

Fisher, J. B. 1975. Development of dichotomous branching and axillary buds in *Strelitzia* (Monocotyledoneae). *Can. J. Bot.* **54,** 578-592.

Fobert, P. R., Coen, E. S., Murphy, G. J. and Doonan, J. H. 1994. Patterns of cell division revealed by transcriptional regulation of genes during the cell cycle in plants. *EMBO J.* **13,** 616– 624.

Fukuda, T., Yokoyama, J. and Maki, M. 2003. Molecular evolution of *cycloidea*-like genes in Fabaceae. *J. Mol. Evol.* **57,** 588-597.

Galego, L. and Almeida, J. 2002. Role of *DIVARICATA* in the control of dorsoventral asymmetry in *Antirrhinum* flowers. *Genes Dev.* **16(7),** 880-91.

Gaudin, V., Lunness, P. A., Fobert, P. R., Towers, M., Riou-Khamlichi, C., Murray, J. A. H., Coen, E., Doonan, J. H. 2000. The expression of *D-Cyclin* genes defines distinct devlopmental zones in Snapdragon apical meristem and is locally regulated by the *Cycloidea* gene. *Plant Physiology.* **122,** 1137-1148.

Gomez, P., Jamilena, M., Capel, J., Zurita, S., Angosto, T., Lozano, R. 1999. *Stamenless,* a tomato mutant with homeotic conversions in petals and stamens. *Planta.* **209,** 172-179.

Gourlay, C. W. Hofer, J. M. I. and Ellis, T. H. N. 2000. Pea compound leaf architecture is regulated by interactions among the genes *UNIFOLIATA, COCHLEATA, AFILA,* and *TENDRIL-LESS. Plant Cell.* **12,** 1279-1294.

Gübitz, T., Caldwell, A. and Hudson, A. 2003. Rapid molecular evolution of *CYCLOIDEA*-like genes in *Antirrhinum* and its relative. *Molecular Biology and Evolution.* **20(9),** 1537-1544.

Gutierrez-Cortinez and Davies, B. 2000. Beyond the ABCs: ternary complex formation in the control of floral organ identity. *Trends in Plant Science.* **5,** 471-476.

Hall, B. G. 2001. Using MrBayes to create Bayesian DNA trees, in *Phylogenetic trees made easy*, Sinauer Associates, pp 98-111.

Hasegawa, M., Kishino, H. and Yano, T.-A. 1985. Dating of the human-ape splitting by a molecular clock of mitochondrial DNA. *J. Mol. Evol.* **22,** 160-174.

Hawkes, J. G. (1999). The economic importance of the family Solanaceae. In: M. Nee, D. E. Symon, R. N. Lester & J. P. Jessop (editors). Solanaceae IV, pp. 1-8. Royal Botanic Gardens, Kew.

Henikoff, S. and Henikoff, J. G. 1992. Amino acid substitution matrices from protein blocks. *Proc. Nat. Acad. Sci. USA.* **89,** 10915-10919.

Hilamen, L. C., Kramer, E. M. and Baum, D. A. 2003. Differential regulation of symmetry genes and the evolution of floral morphologies. *PNAS.* **100(22),** 12814-12819.

Himanen, K., Reuzeau, C., Beeckman, T., Melzer, S. and Grandjean, O. 2003. The Arabidopsis Locus *RCB* Mediates Upstream Regulation of Mitotic Gene Expression. *Plant Physiology.* **133,** 1862-1872.

Hofer, J., Turner, L., Hellens, R., Ambrose, M., Matthews, P.,Michael, A., and Ellis, N. 1997. *Unifoliata* regulates leaf and flower morphogenesis in pea. *Curr. Biol.* **7,** 581–587.

Hofer, J. and Ellis, N. 2002. Conservation and diversification of gene function in plant development. *Current Opinion in Plant Biology.* **5,** 56-61.

Honma, T. and Goto, K. 2001. Complexes of MADS-box proteins are sufficient to convert leaves into floral organs. *Nature.* **409(6819),** 525-9.

Hubbard, L., Mc Steen, P., Doebley J, Hake S 2002. Expression Patterns and Mutant Phenotype of *teosinte branched1* Correlate With Growth Suppression in Maize and Teosinte. *Genetic.* **162,** 1927-1935.

Inoue H, Nojima H, Okayama H. 1990. High efficiency transformation of Escherichia coli with plasmids. *Gene.* **96(1),** 23-28.

Ito, M., Iwase, M., Kodama, H., Lavisse, P., Komamine, A., Nishihama, R., Machida, Y., Doonan, J. H., Watanabe, A. 1998. A novel *cis*-acting element in

promoters of plant B-type cyclin genes activates M phase-specific transcription. *Plant Cell.* **10,** 331-341.

John, D.T., Taylor, W. R. and Thornton, J. M. 1992. The rapid generation of mutation data matrices from protein sequences. *Comput. Appl. Biosci.,* **8,** 275-282.

Juarez, M.T., Kui, J. S., Thomas, J., Heller, B. A., Timmermans, M. C. 2004. MicroRNA-mediated repression of rolled leaf1 specifies maize leaf polarity. Nature. **428(6978),** 84-8.

Kelly, A. J., Bohnlander, M. B.and Meeks-Wagner, D. R. 1995. *NFL,* the tobacco homolog of *FLORICAULA* and *LEAFY* , is transcritionally expressed in both vegetative and floral meristem. *The Plant Cell.* **7,** 225-234.

Knapp, S. 2002. Floral morphology in Solanaceae. *In* QCB Cronk, RM Bateman, JA Hawkins, eds, Developmental Genetics and Plant Evolution. Taylor and Francis, London, pp 268-293.

Kosugi, S. and Ohashi, Y. 1997. PCF1 and PCF2 specifically bind to cis elements in the rice proliferating cell nuclear antigen gene. *Plant Cell.* **9(9),** 1607-1619.

Kosugi, S. and Ohashi, Y. 2002. DNA binding and dimerization specificity and potential targets for the TCP protein family. *Plant J.* **30(3),** 337-348

Krizek, B. A. and Meyerowitz, E. M. 1996. The Arabidopsishomeotic genes APETALA3 and PISTILLATA are sufficient to provide the B class organ identity function. *Development.***122,** 11-22.

Lanave, C., Preparata, G., Saccone, C. and Serio, G. 1984. A new method for calculating evolutionary substitution rates. *J. Mol. Evol,* **20,** 86-93.

Lawton-Rauh, A. 2002. Evolutionnary dynamics of duplicated genes in plants. *Molecular phylogenetics and evolution.* **29,** 396-409.

Lukens, L. and Doebley, J. 2001. Molecular evolution of the *Teosinte branched* gene among maize and related grasses. *Mol. Biol. Evol.* **18(4),** 627-638.

Luo, D., Carpenter, R., Copsey, L., Vincent, C., Clark, J. and Coen, E. 1999. Control of organ asymmetry in flowers of Antirrhinum. *Cell.* **99(4),** 367-76.

Luo, D., Carpenter, R., Vincent, C., Copsey, L. and Coen, E. 1996. Origin of floral asymmetry in Antirrhinum. *Nature.* **383(6603),** 794-9.

Maberley, D. J. 1997.The Plant Book. A portable dictionary of the vascular plants. 2nd edition, 858p, Cambridge University Press.

Mandel, M. A., Bowman, J. L., Kempin, S. A., Ma, H., Meyerowitz, E. M., Yanofsky, M. F. 1992. Manipulation of flower structure in transgenic tobacco.*Cell,* 133-143.

Mauseth, J. D. 1998. Development and morphogenesis. In: Botany, an introduction to plant biology. pp. 376-391. Jones and Bartlett Publishers.

Mironov, V., De Veylder, L., Van Montagu, M. and Inzé, D. 1999. Cyclin-Dependent Kinases and cell division in plants-The Nexus. *The Plant Cell.* **11,** 509-521.

Molinero-Rosales N., Jamilena M., Zurita S., Gomez P., Capel J. and Lozano R. 1999. FALSIFLORA, the tomato orthologue of FLORICAULA and LEAFY, controls flowering time and floral meristem identity. *Plant J.* **20(6),** 685-93.

Morgenstern, B. and Atchley, W. 1999. Evolution of bHLH transcription factors: Modular evolution by domain shuffling? *Mol. Bio. Evol.* **16,** 1654-1663.

Müeller, T. and Vingron, M. 2000. Modelling amino-acid replacement. *J. Comput. Biol.* **7,** 761-776.

Napoli, C. A. and Ruehle, J. 1996. New mutations affecting meristem growth and potential in *Petunia hybrida* Vilm . *The Journal of Heredity* . **87(5),** 371-377.

Nath, U., Crawford, B. C., Carpenter, R. and Coen E. 2003. Genetic control of surface curvature. Science. *Science.* **299(5611),** 1404-1407.

Neal, P. R., Dafni, A. and Giurfa, M. 1998. Floral symmetry and its role in plant - pollinator systems: Terminology, Distribution, and Hypotheses. *Annu. Rev. Ecol. Syst.* **29,** 345-373.

Nolan, J; R. 1969. Bifurcation of the stem apex in *Asclepias Syriaca. Amer. J. Botany.* **56(6),** 603-609.

Olmstead, R.G., Kim, K. J., Jansen, R. K. and Wagstaff, S. J. 2000. The phylogeny of the Asteridae sensu lato based on chloroplast *ndhF* gene sequences. *Mol. Phylog. Evo.* **16,** 96-112.

Olmstead, R. G. and Palmer, J. D. 1992. A chloroplast DNA phylogeny of the Solanaceae: subfamilial relationships and character evolution. *Ann. Missouri. Bot. Gard.* **79,** 346-360.

Page, R. D. M. 1996. TREEVIEW: An application to display phylogenetic trees on personal computers. *Computer Applications in the Biosciences.* **12,** 357-358.

Palatnik, J. F., Allen, E., Wu, X., Schommer, C., Schwab, R., Carrington, J. C. and Weigel, D. 2004. Control of leaf morphogenesis by microRNAs. *Nature.* **425(6955),** 257-263

Pelaz, S., Ditta, G. S., Baumann, E., Wisman, E. and Yanofsky M. F. 2000. B and C floral organ identity functions require SEPALLATA MADS-box genes. *Nature.* **405(6783),** 200-203.

Pickett, F. B. and Meeks-Wagner, D. R. 1995. Seeing double: Appreciating genetic redundancy. *The Plant Cell.* **7,** 1347-1356.

Pnueli, L., Abu-Abeid, M., Zamir, D., Nacken, W., Schwarz-Sommer, Z. and Lifschitz, E. 1991. The MADS box gene family in tomato: temporal expression during floral development, conserved secondary structures and homology with homeotic genes from *Antirrhinum* and *Arabidopsis*. *Plant J.* **1(2),** 255-66.

Raff, R. A. 2000. Evo-devo, the evolution of a new discipline. *Nature reviews genetics*. **1,** 74-79.

Reeves, P. A. and Olmstead, R. G. 2003. Evolution of the TCP gene family in Asteridae: cladistic and network approaches to understanding regulatory gene family diversification and its impact on morphological evolution. *Mol. Biol. Evol.* **20(12),** 1997-2009;

Reinhardt, D. and Kuhlemeier, C. 2002. Plant architecture. *EMBO reports.* **3(9),** 846-851.

Ridley, 1996. Genome evolution *in* Evolution. Chapter 10, pp 255-278. Blackwell science.

Robyns, W. 1931. Líorganisation florale des Solanacees zygomorphes. *Mem. Acad. Roy. Belgique, Class des Sciences* 11 (8): 1-84

Ronquist, F., and J. P. Huelsenbeck. 2003. MrBayes 3: Bayesian phylogenetic inference under mixed models. *Bioinformatics.* **19,** 1572–1574

Rudall, P. J. and Bateman, R. M. 2003. Evolutionary change in flowers and inflorescences: evidence from naturally occurring terata. *Trends Plant Sci.* **8(2),** 76-82

Sambrook, J. Fristch, E.F. and Maniatis, T. 1989. Transfer of DNA from agarose gels to solid supports. *in MolecularCloning: A laboratory Manual,* Cold Spring Harbor Laboratory Press. pp 9.34.

Schmidt, H. A., Strimmer, K., Vingron, M. and von Haeseler, A. 2002. TREE-PUZZLE: maximum likelihood phylogenetic analysis using quartets and parallel computing. *Bioinformatics*. **18,** 502-504.

Schmitz G and Theres K. 1999. Genetic control of branching in Arabidopsis and tomato. *Curr Opin Plant Biol.* **2(1),** 51-55.

Schöniger, M. and von Haeseler, A. 1994. A stochastic model for the evolution of autocorrelated DNA sequences. *Mol. Phylogenet. Evol.* **3,** 240-247.

Schwarz-Sommer, Z., Huijser, P., Nacken, W., Saedler, H. & Sommer, H. 1990. Genetic control of flower development: homeotic genes in Antirrhinum majus. *Science.* **250,** 931-936.

Siebert , P. D., Chenchick, A., Kellog, D. E., Lukyanov, K. A. and Lukyanov, S. A. 1995. An improved PCR method for walking in uncloned genomic DNA. *Nucleic Acids Research.* **23,** 1087-1088.

Sheppard, K. A. and Purugganan, M. D. 2002. The genetics of plant morphological evolution. *Current Opinion in Plant Biology.* **5,** 49-55.

Soltis, P. S., Soltis, D. E. & Chase, M. W. 1999. Angiosperm phylogeny inferred from multiple genes as a tool for comparative biology. *Nature.* **402,** 402-404.

Sommer, H., Beltran, J. P., Huijser, P., Pape, H., Lonnig, W. E., Saedler, H. and Schwarz-Sommer, Z. 1990. Deficiens, a homeotic gene involved in the control of flower morphogenesis in Antirrhinum majus: the protein shows homology to transcription factors. *EMBO J*. **9(3),** 605-13.

Souer, E., Van Houwelingen, A., Kloos, D., Mol, J., Koes, R. 1996.The *No Apical Meristem* gene of Petunia is required for pattern formation in embryos and flowers and is expressed at meristem and primordia boundaries. *Cell.* **85,** 159-170.

Souer, E., Van der Krol, A., Kloos, D., Spelt, C., Bliek, M., Mol, B. and Koes, R. 1998. Genetic control of branching pattern and floral identity during *Petunia* inflorescence development. *Development.* **125,** 733-742.

Stebbins, G. L. 1974. Trends in evolution in the flower. *in* Flowering plants, evolution above the species level. M.A. Harvard University Press. Chapter 12, pp 284-311.

Steimer, A., Schöb, H and Grossniklaus, U. 2004. Epigenetic control of plant development: new layers of complexity. *Current Opinion in Plant Biology.* **7,** 11-19.

Spichiger, R. E., Savolainen, V. V., Figeat, M and Jeanmonod D. 2002.Botanique systemtatique des plantes a fleur. Presses polytechniques et universitaires romandes. 406p

Swofford, D.L. 2002. PAUP*. Phylogenetic Analysis Using Parsimony (*and other methods). Version 4. Sinauer Associates, Sunderland, Massachusetts.

Takeda, T., Suwa, Y., Suzuki, M., Kitano, H., Ueguchi-Tanaka, M., Ashikari, M., Matsuoka, M., and Ueguchi, C. 2003. The OsTB1 gene negatively regulates lateral branching in rice. *The Plant Journal.* **33,** 513-520.

Tamura, K. and Nei, M. 1993. Estimation of the number of nucleotide substitutions in the control region of mitochondrial DNA in humans and

Terryn, N. and Rouze, P. 2000. The sense of naturally transcribed anti-sense RNAs in plants. *Trends in Plant Science.* **5,** 394-396.

Theißen, G., Becker, A., Di Rosa, A., Kanno, A., Kim, J.T., Munster, T., Winter, K.-U., Saedler, H., 2000. A short history of MADS-box genes in plants. *Plant Mol. Biol.* **42,** 15–149.

Tomlinson, P. B. and Posluszny, U. 1977. Apical dichotomy demonstrated in the angiosperm *Flagellaria. Science.* **196,** 1111-1112.
Tréhin, C., Glab, N., Perennes, C., Planchais, S. and Bergounioux, C. 1999. M phase-specific activation of the *Nicotiana sylvestris Cyclin B1* promoter involves multiple regulatory elements. *Plant J.* **17,** 263-273.

Tremousaygue, D., Garnier, L., Bardet, C., Dabos, P., Herve, C. and Lescure B. 2003. Internal telomeric repeats and 'TCP domain' protein-binding sites co-operate to regulate gene expression in Arabidopsis thaliana cycling cells. *Plant J.* **33(6),** 957-66.

Tucker, S.C. 1989. Overlapping organ initiation and common primordia in flowers of *Pisum sativum* (Leguminosae: Papilionoideae). *Am J Bot* . **76,** 714-729.

Tucker, S. C. 1999. Evolutionary Lability of Symmetry in Early Floral Development. Int *J Plant Sci.* **160(S6),** S25-S39.

Vandenbussche M, Zethof J, Souer E, Koes R, Tornielli GB, Pezzotti M, Ferrario S, Angenent GC, Gerats T. 2003. Toward the analysis of the petunia MADS box gene family by reverse and forward transposon insertion mutagenesis approaches: B, C, and D floral organ identity functions require SEPALLATA-like MADS box genes in petunia. *Plant Cell.* **15(11),** 2680-93

Vandenbussche, M., Zethof, J., Royaert, S., Weterings, K. and Gerats, T.2004. The duplicated B-class heterodimer model: whorl-specific effects and complex genetic interactions in Petunia hybrida flower development. *Plant Cell.* **16(3),**741-54

Walters, D. R. 1969. A revision of the genus *Schizanthus* (Solanaceae). PhD. Indiana University.

Walters, D. and D. Keil. 1996. Vascular Plant Taxonomy. Fourth edition. Kendall Hunt Publishing Company, Dubuque. 608 pp

Wang, C.N., Möller, M. and Cronk, Q. C. 2004. Altered expression of *GFLO*, the Gesneriaceae homologue of *FLORICAULA/LEAFY*, is associated with the

transition to bulbil formation in *Titanotrichum oldhamii*. *Dev Genes Evol.* **214(3),** 122-127

Warbrick, E. 2000. The puzzle of PCNA's many partners. *Bioessays.* **22(11),** 997-1006.

Weberling, F. 1989. Morphology of flowers and inflorescences. Cambridge, Cambridge University Press.

Weigel, D., Alvarez, J., Smyth, D. R., Yanofsky, M. F. and Meyerowitz, E. M. 1992. LEAFY controls floral meristem identity in Arabidopsis. *Cell.* **69(5),** 843-59.

Weir, I., Lu, J., Cook, H., Causier, B., Schwarz-Sommer, Z. and Davies, B. 2004 *CUPULIFORMIS* establishes lateral organ boundaries in *Antirrhinum*. *Development.* **131(4),** 915-22

Whelan, S. and Goldman, N. 2001. A general empirical model of protein evolution derived from multiple protein families using a maximum likelihood approach. *Mol. Biol. Evol.,* **18,** 691-699.

Yanofsky, M.F., Ma, H., Bowman, J. L., Drews, G. N., Feldmann, K. A. and Meyerowitz, E . M.1990. The protein encoded by the Arabidopsis homeotic gene agamous resembles transcription factors. *Nature*. **346(6279),** 35-9.

Yoon, H. S. and Baum, A. D. 2004. Transgenic study of parallelism in plant morphological evolution. *PNAS.* **101(17),** 6524-6529.

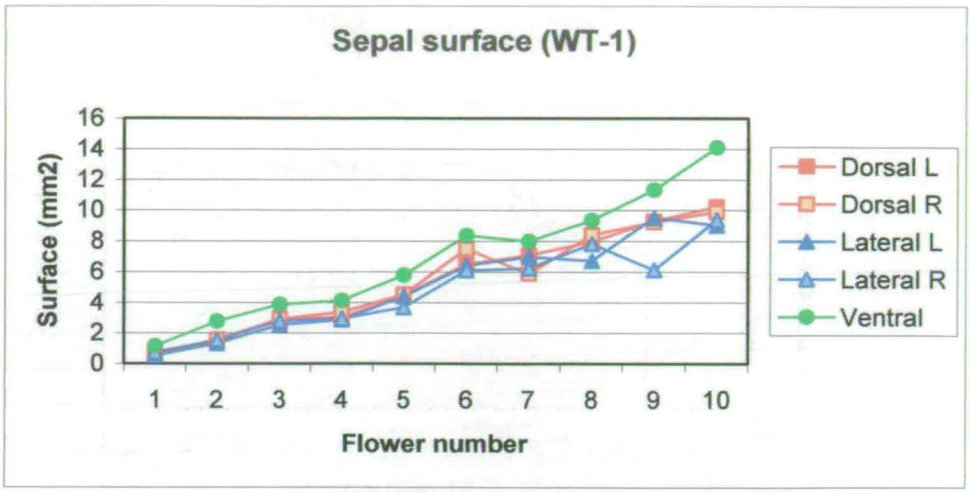

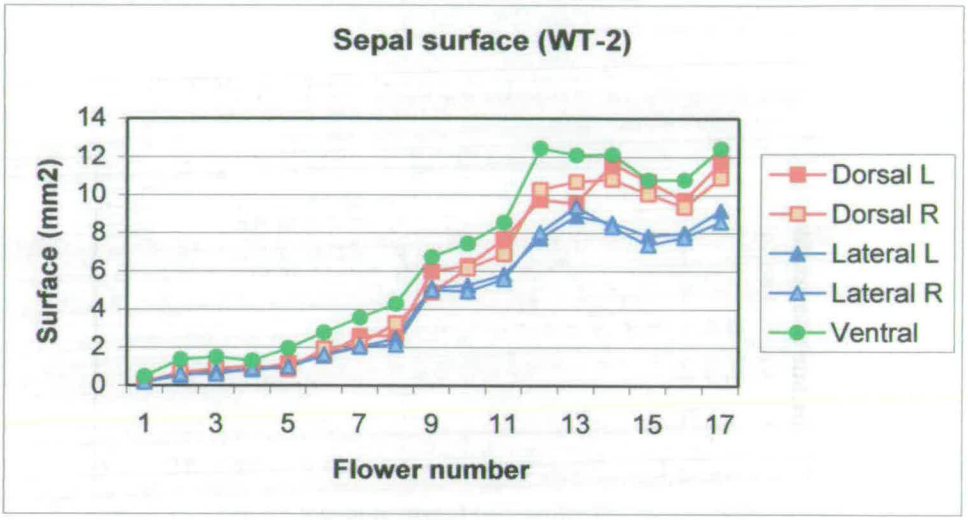

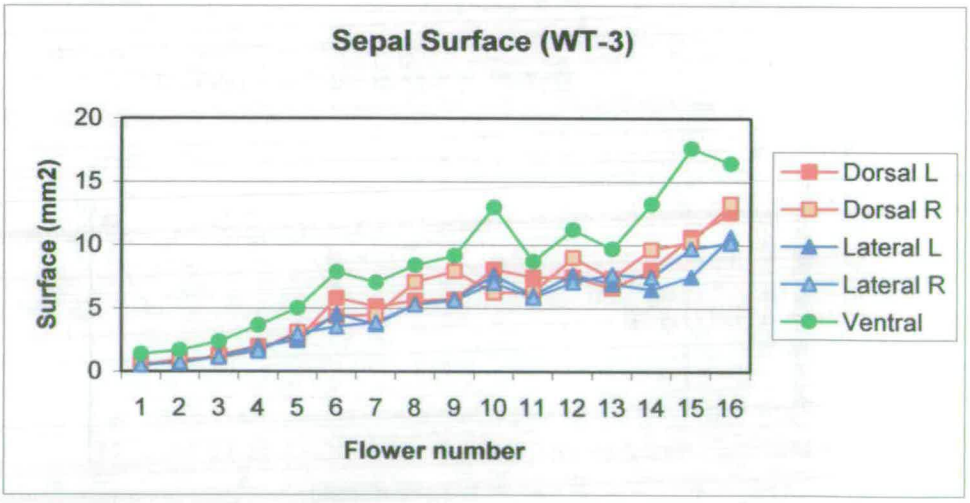

Appendix III.2: Sepal surface during flower development in *S. wisotonensis* (WT)
These graphs represent the growth dynamic of individual sepals during development as measured for organ surface. L is for left sepal and R for right sepal. On the x axis, flower number is labelled so that flower 1 is the youngest (stage 6) and flower 10 (WT-1), flower 17 (WT-2) and flower 16 (WT-3) represent mature flowers (average of the values obtained in 3 mature flowers except for WT2 for which measurements where taken from only one adult flower).

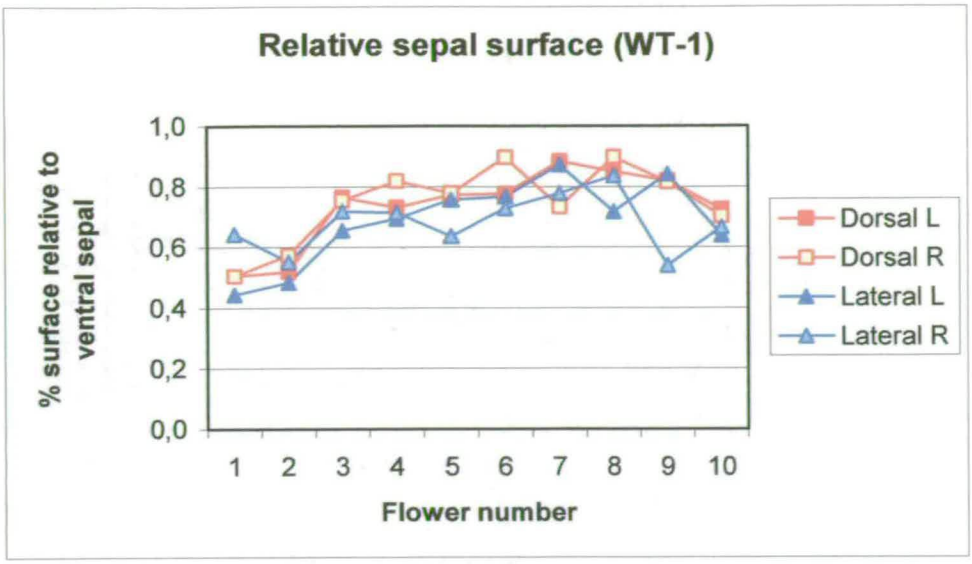

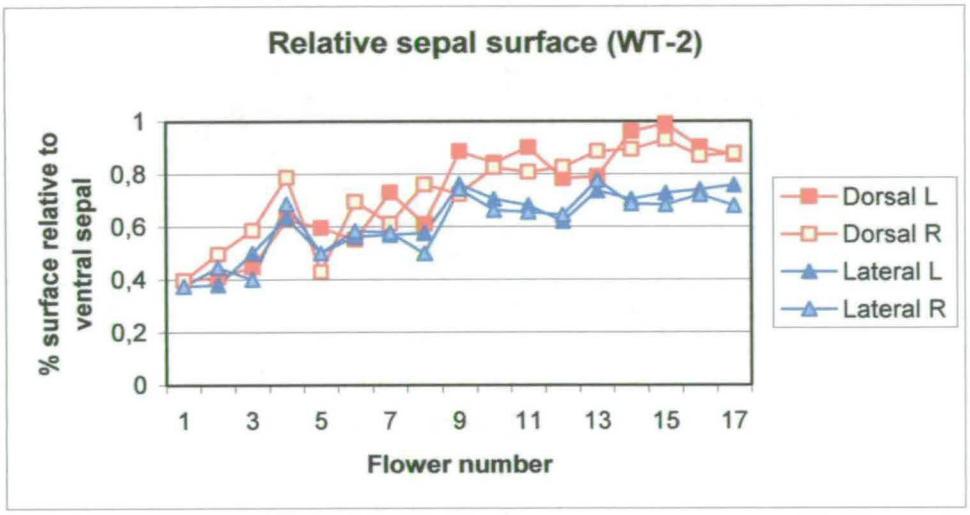

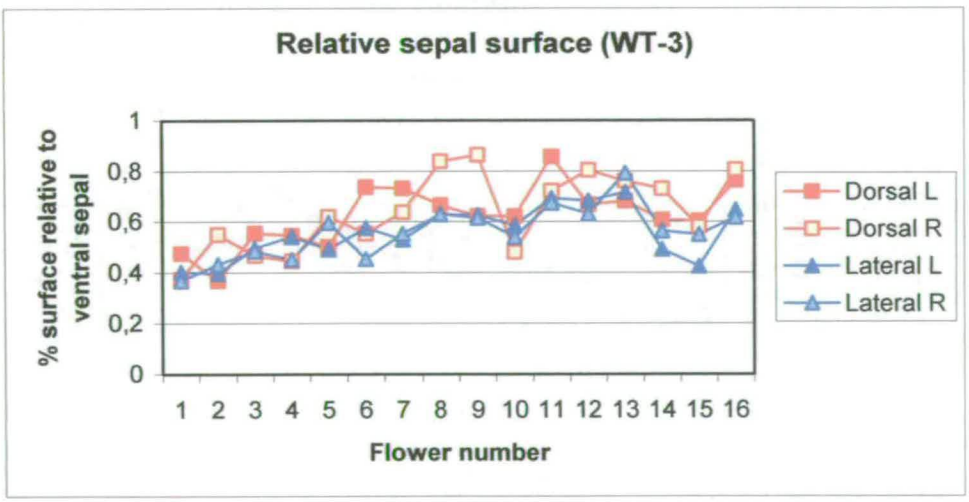

Appendix III.1: Relative sepal surface compared to that of the ventral sepal in *S. wisotonensis*(WT)

The ventral sepal is always bigger than the other sepals (ratio <1). The other four sepals show size variation without any particular trend. On the x axis, flower number is labelled so that flower 1 is the youngest (stage 6) and flower 10 (WT-1), flower 17 (WT-2) and flower 16 (WT-3) represent mature flowers (average of the values obtained in 3 mature flowers except for WT2 for which measurements where taken from only one adult flower).

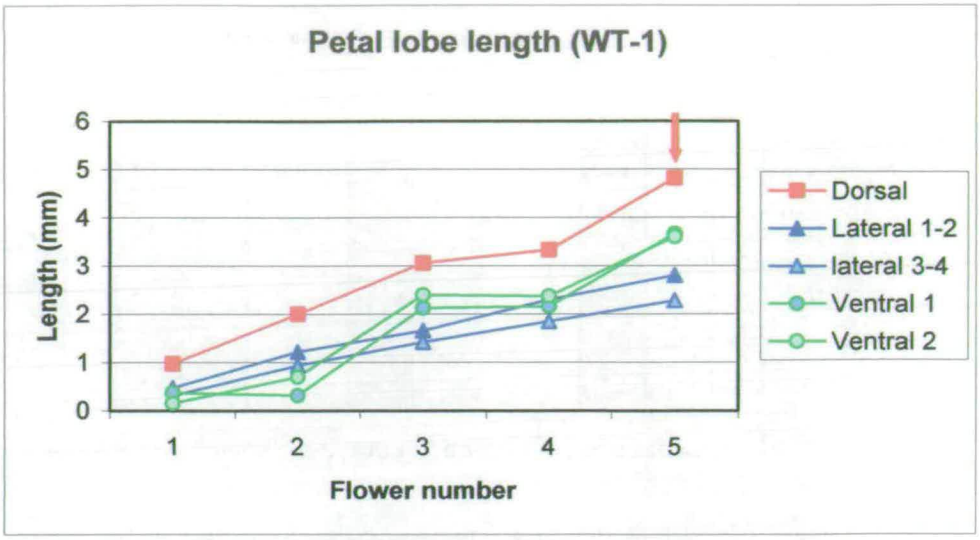

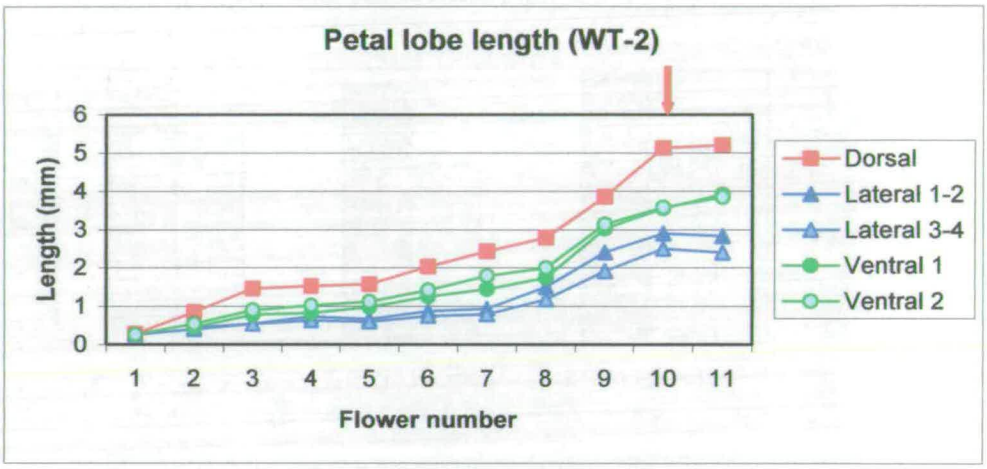

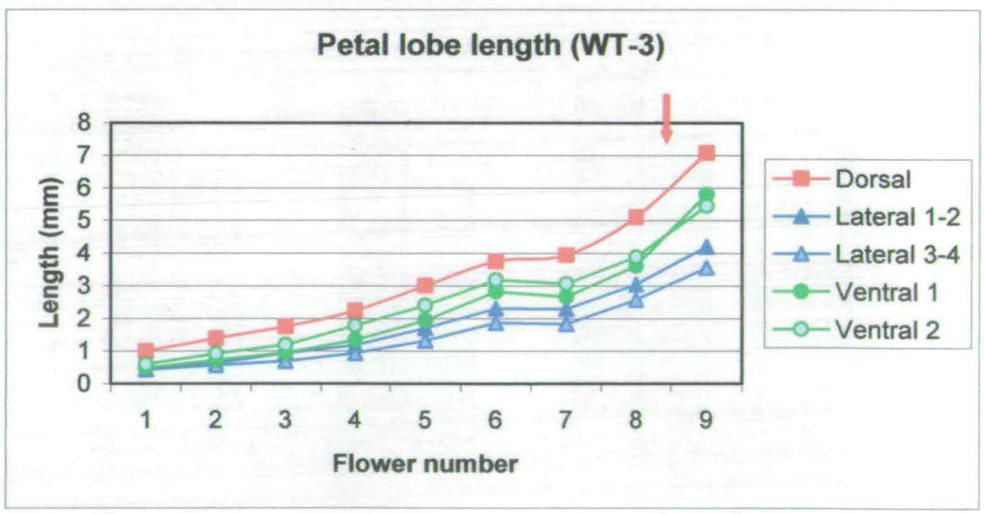

Appendix III.4a: Growth profile of petal lobes in the wild-type flower of *S. wisotonensis* from stage 6 up till stage 7

The red arrow indicates stage 7 when both lobes of the ventral petal have a similar length and anthesis takes place for the staminodes (See appendix III.4b). Flower 1 correspond to stage 6, flowers 5 (WT-1); flower 11 (WT-2) and flower 9 (WT-3) correspond to flower at stage 7 or slightly older.

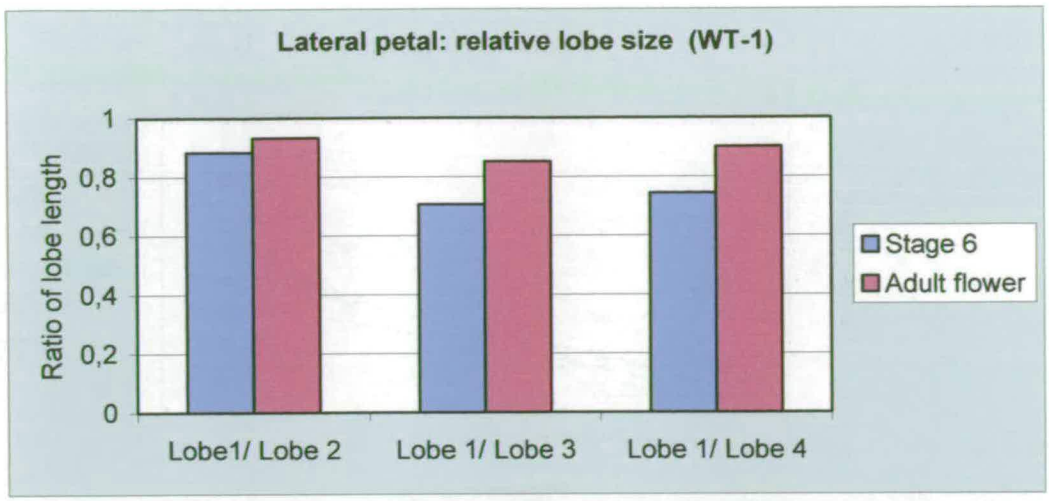

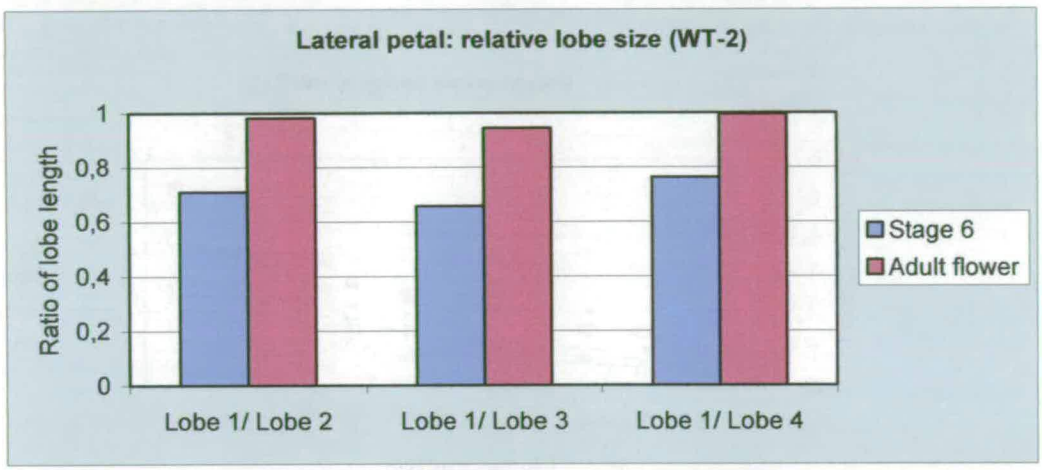

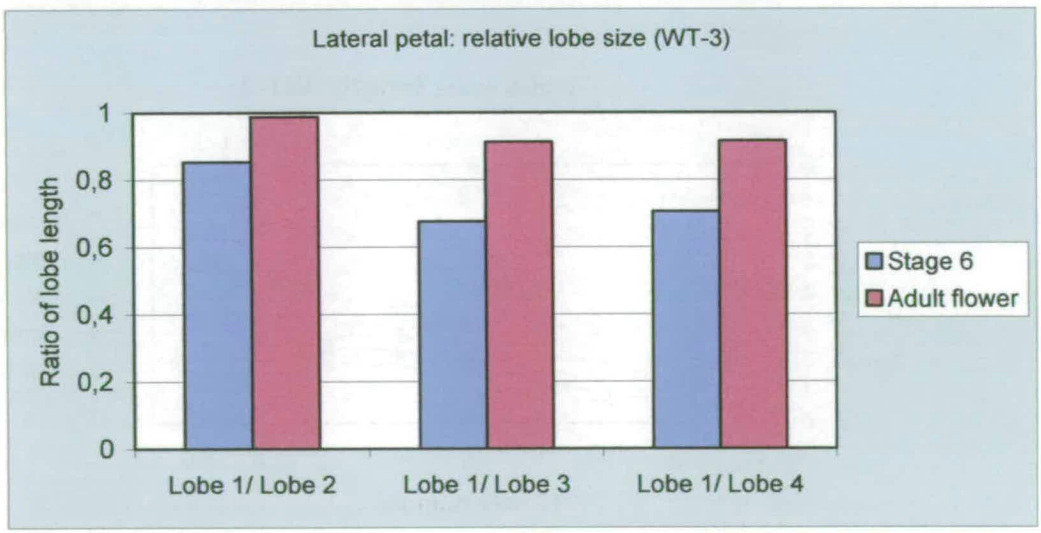

Appendix III.3: Growth dynamics of lateral petal lobes 2-3-4 relative to lobe 1 from stage 6 to the adult flower in *S. wisotonensis* (WT)

During stage 6, lobes 2, 3 and 4 are smaller than lobe 1 (ratio<1). In the mature flower, this difference in size is less marked as shown by the ration of lobe length closer to 1 than at stage 6.

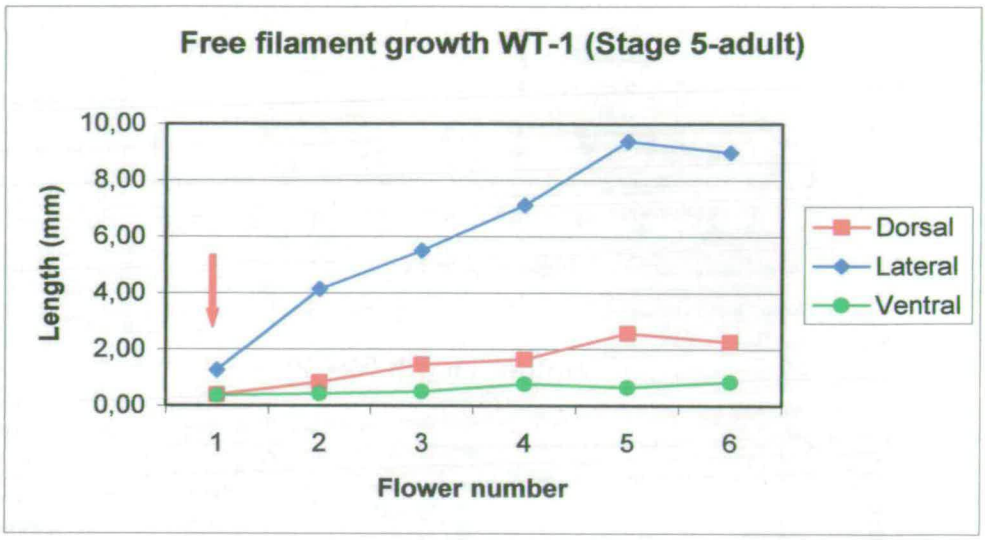

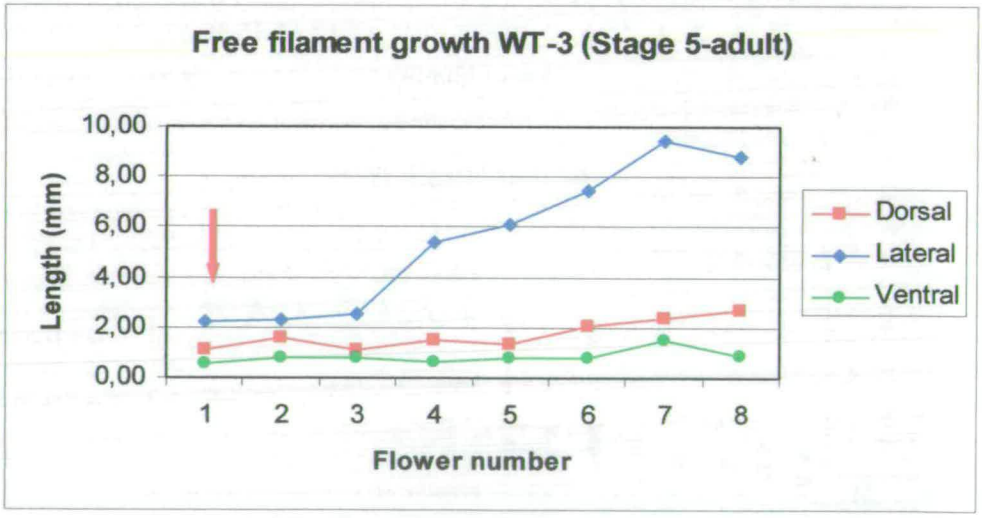

Appendix III.5: Elongation of the free filament from stage 7 onwards in *S. wisotonensis* (WT)
The data is not available for WT-2. The red arrow indicates stage 7. On the x axis, flower number is labelled so that flower 1 is the youngest (stage 6). The last point of the graph corresponds to an average of the values obtained in 3 mature flowers. This does not apply to WT2 for which measurements where taken from only one adult flower.

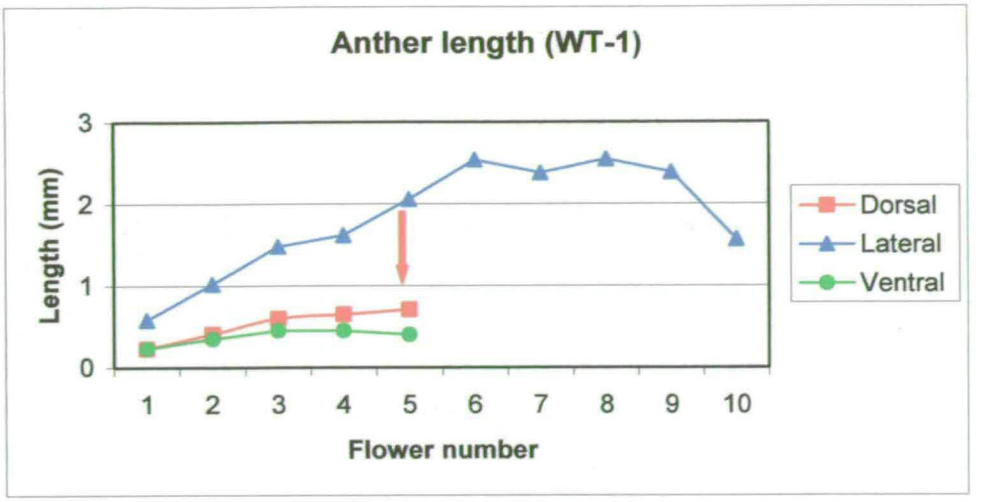

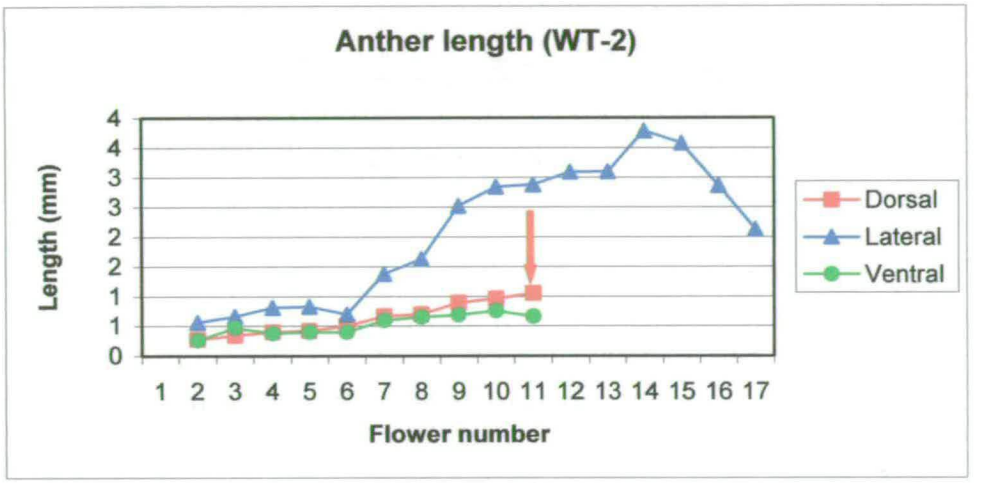

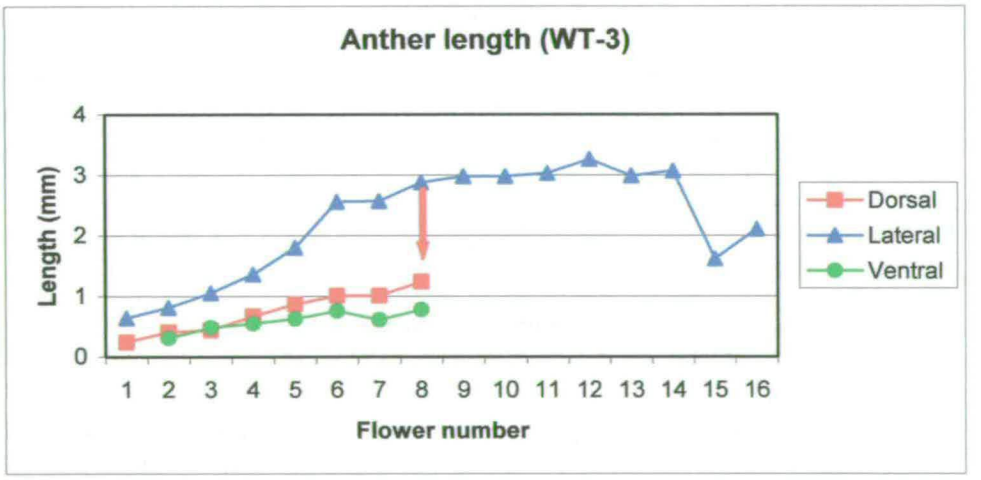

Appendix III.4b: Anther length during development in the wild-type flower of *S. wisotonensis*

The red arrow indicates stage 7. The measurement of anther length for the staminodes is not possible after anthesis, when the anther breaks down. On the x axis, flower number is labelled so that flower 1 is the youngest (stage 6) and flower 10 (WT-1), flower 17 (WT-2) and flower 16 (WT-3) represent mature flowers (average of the values obtained in 3 mature flowers except for WT2 for which measurements where taken from only one adult flower).

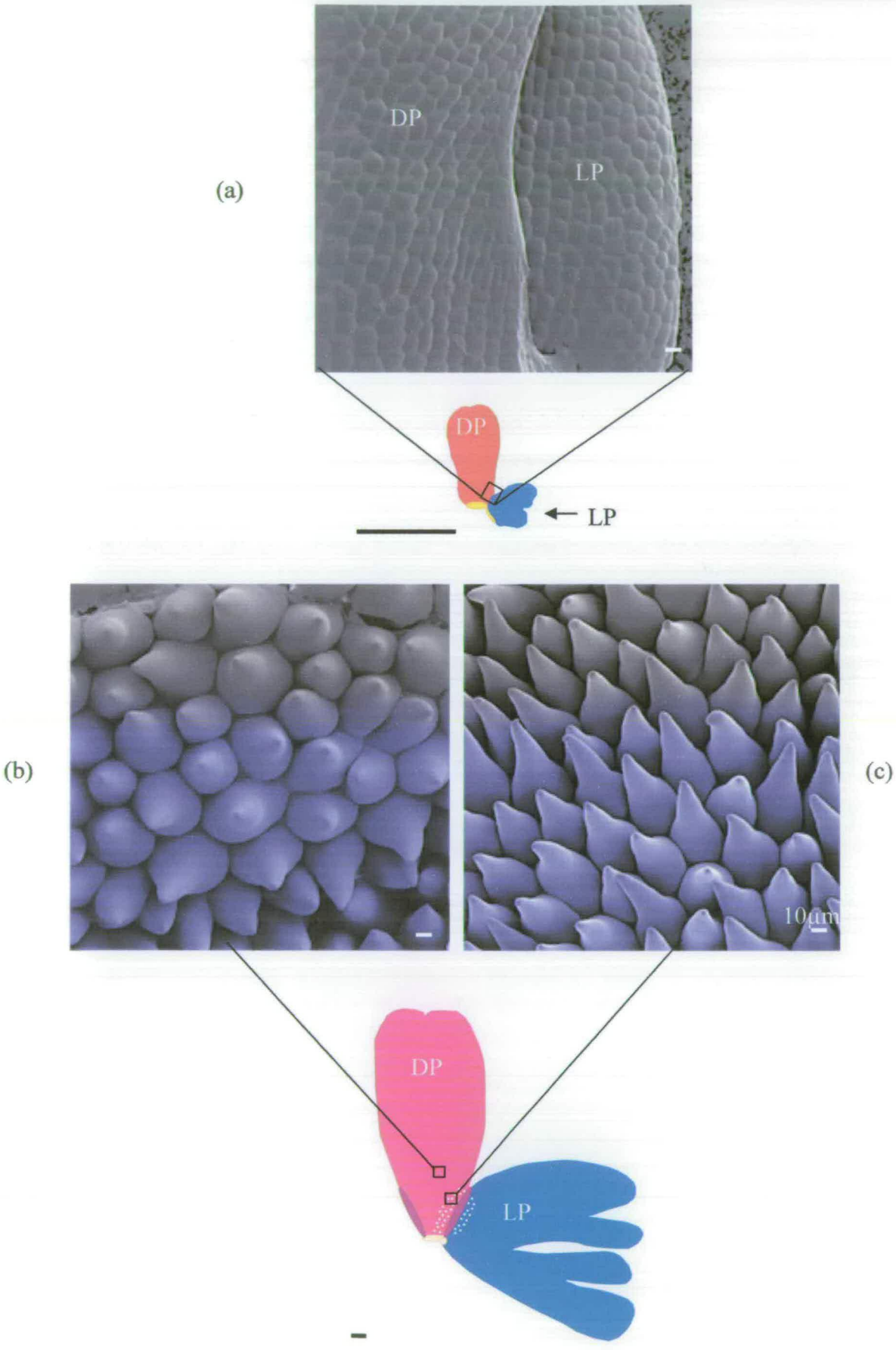
(a)
DP
LP
DP
LP
(b)
(c)
10μm
DP
LP

Appendix III.6: Cells morphology and size within and around the furrow formed at the junction of the dorsal and lateral petals in *S. wisotonensis* (WT)

(a) There is no difference in cell size between cells from the dorsal petal (DP) and the dorsal part of the lateral petal (LP) at stage 6. (b&c) Cells from the same dorsal petal in a mature flower: (b) within the furrow (white spots on diagram corresponding to (b&c)), (c) out with the furrow. In the furrow, cells appear slightly smaller.

These SEMs indicate that it is cell division rather than cell elongation which is likely to be responsible for the development of a furrow in the region of the corolla situated at the junction between the dorsal and lateral petal. White scale bar: 10 µm; black scale bar: 1 cm.

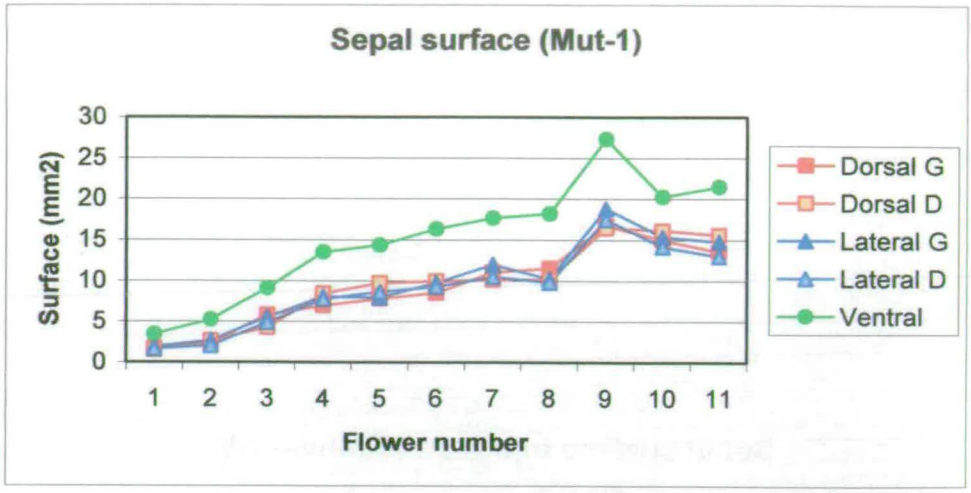

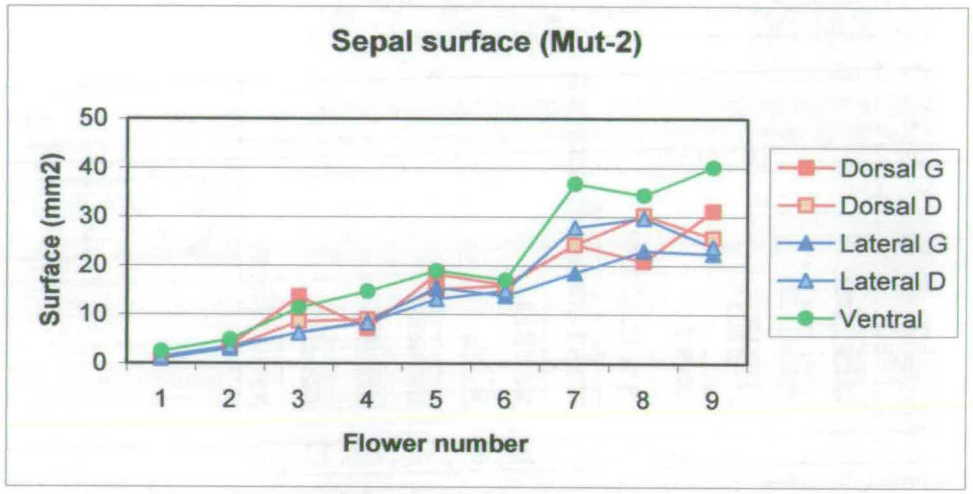

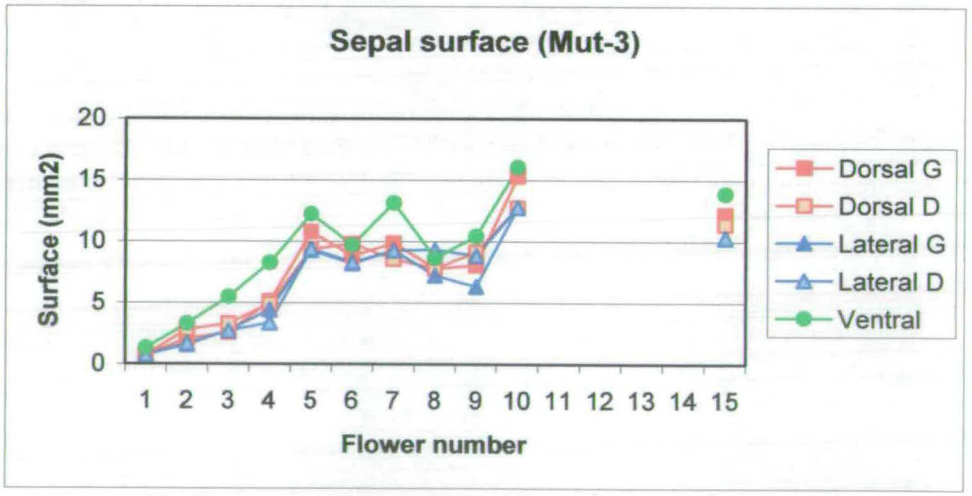

Appendix III.8: Variation in sepal surface in three *rz* mutant plants (Mut 1, 2&3) (*S. wisotonensis*)

Flower number 1 corresponds to stage 5-6 and flowers n.11-9-15 to mature flowers. Some measurements are missing for Mut-3 because the inflorescence was partially fasciated and sepals were difficult to identify.

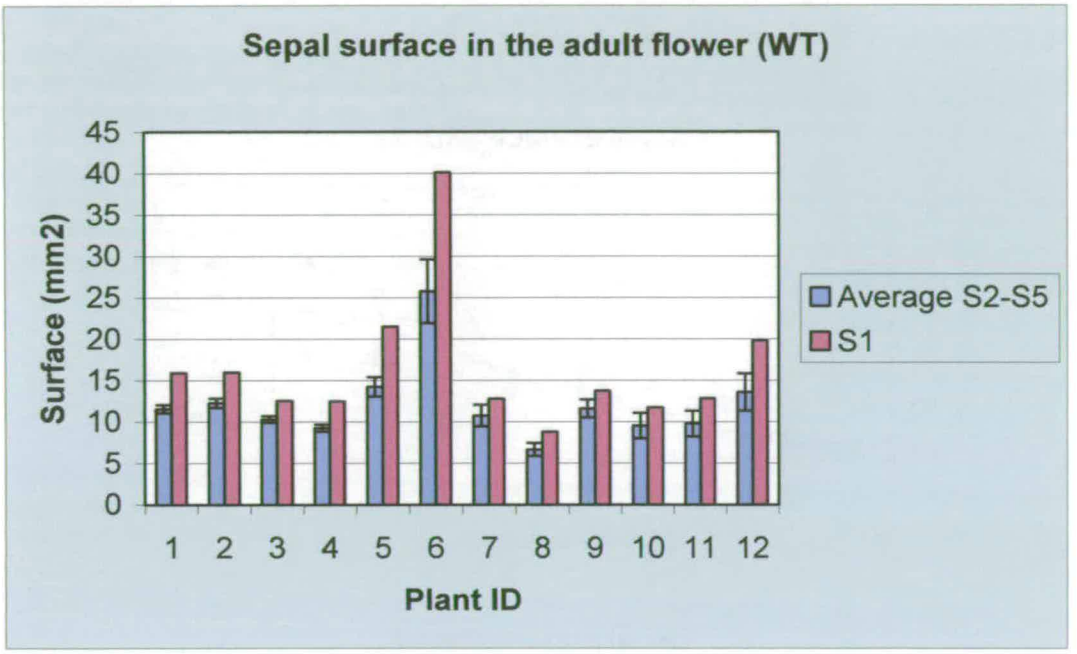

Appendix III.7: Sepal surface in mature flowers of *S. wisotonensis* (WT)
The measurements of sepal surface were done on single flowers from twelve plants grown under the same conditions.

Appendix III.10: Quantitative morphological comparison between of the flower of *S. wisotonensis* (WT) and the *rz* mutant

Measurements of organ surfaces and length were taken from flowers of 12 individual plants of *S. wisotonensis* (WT) (same as Fig III.14) and 7 plants for the *rz* mutant. The bars correspond to the average of the values obtained in each plant separately. The error bar is the standard deviation of all the averages.

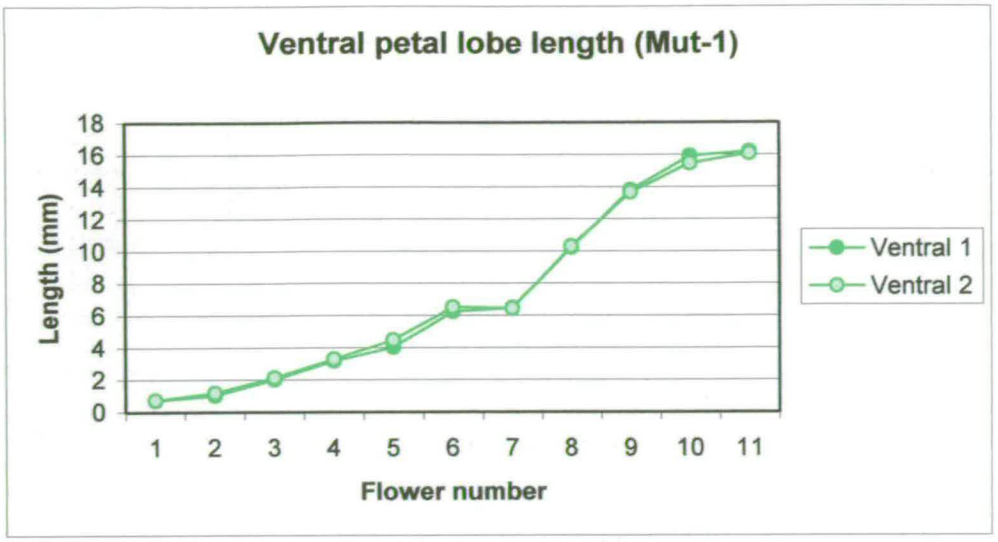

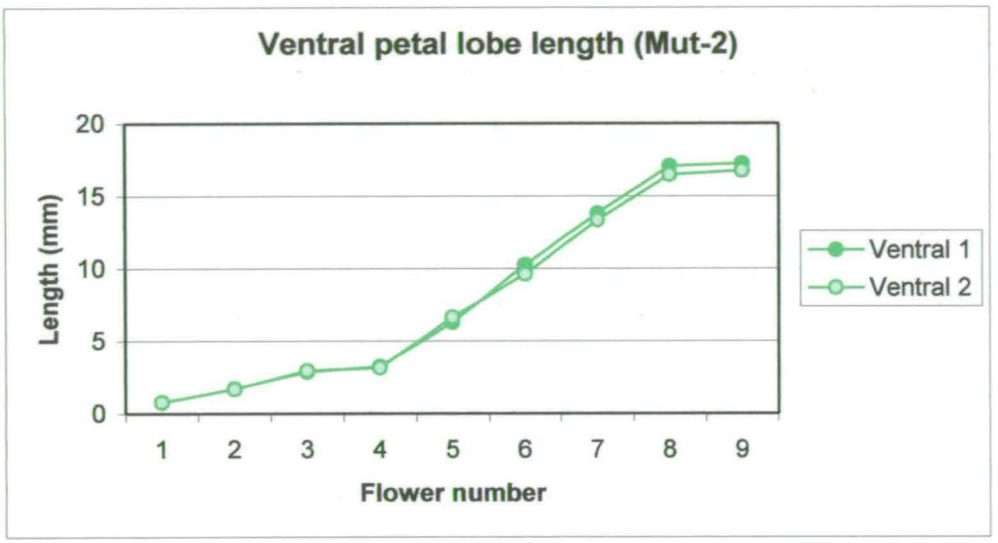

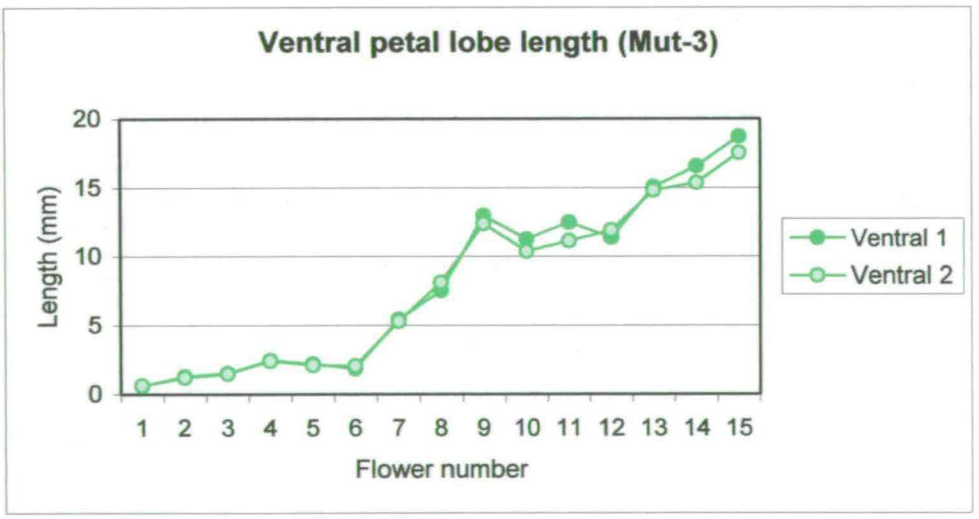

Appendix III.9: Individual ventral lobes size in *rz* mutants of *S. wisotonensis*

In the *rz* mutant flower, both lobes in the ventral petal have a similar size from early on in development (Flower number 1 corresponds to stage 5-6 and flowers n.11-9-15 to mature flowers in Mut-1, Mut-2 and Mut-3 respectively). Ventral 1 is the upper ventral lobe, V2 is the lower ventral lobe.

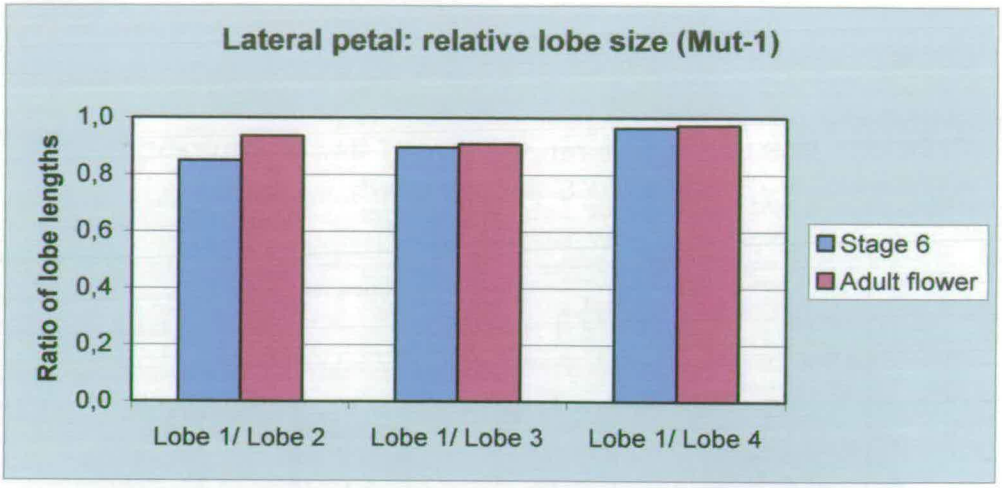

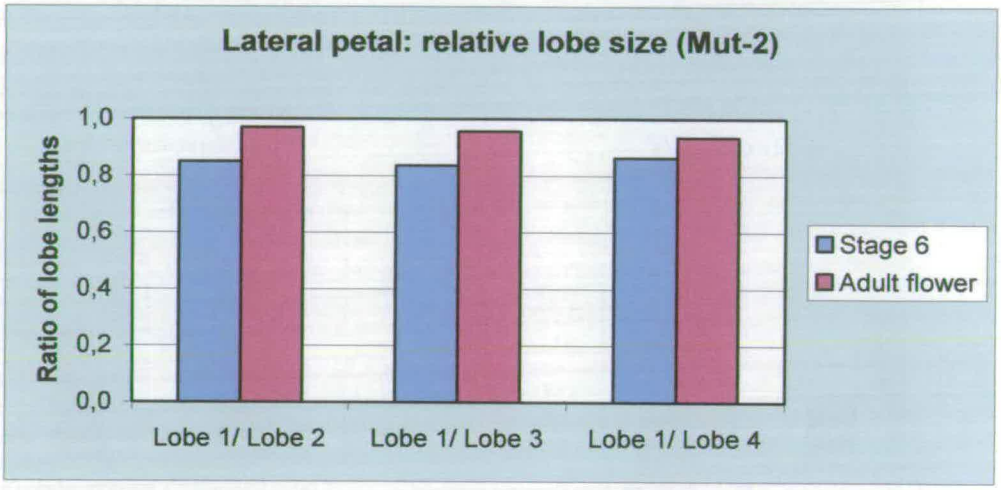

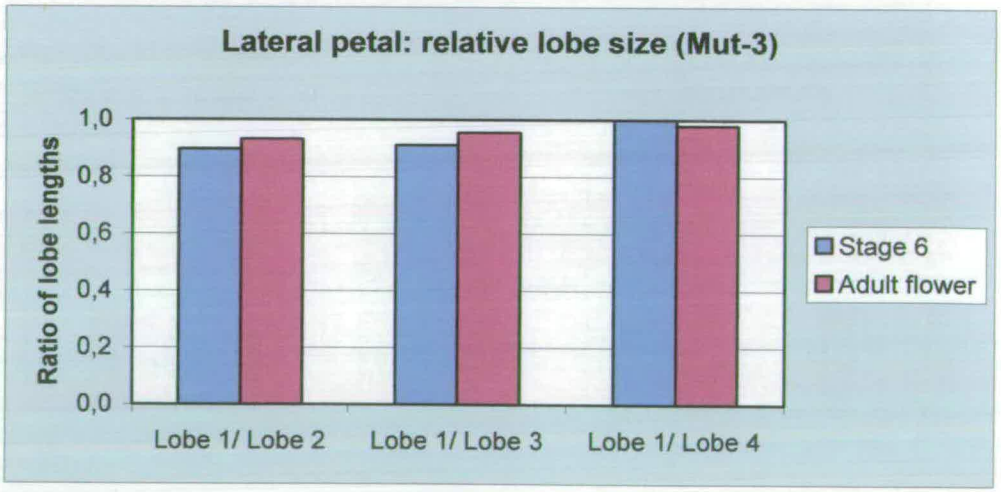

Appendix III.11: Growth dynamics of lateral petal lobes 2-3-4 relative to lobe 1 from stage 6 to the adult flower in *S. wisotonensis* (WT)

As for the wild-type flower, during stage 6, lobes 2, 3 and 4 are smaller than lobe 1 (ratio<1). In the mature flower, this difference in size is less marked as shown by the ration of lateral L1 length/lateral lobe length being closer to 1.

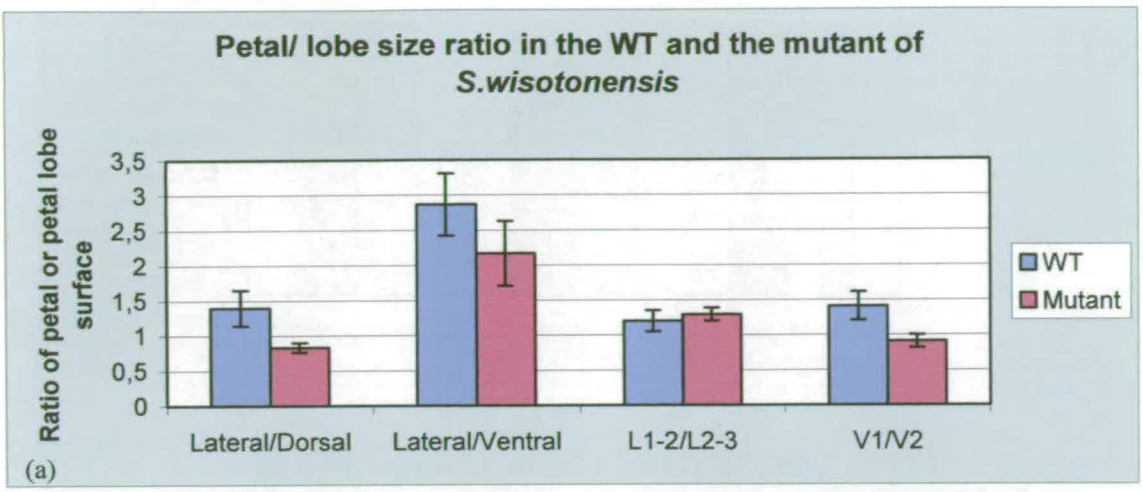
Petal/ lobe size ratio in the WT and the mutant of S.wisotonensis
Ratio of petal or petal lobe surface
3,5
3
2,5
2
1,5
1
0,5
0
Lateral/Dorsal
Lateral/Ventral
L1-2/L2-3
V1/V2
WT
Mutant
(a)

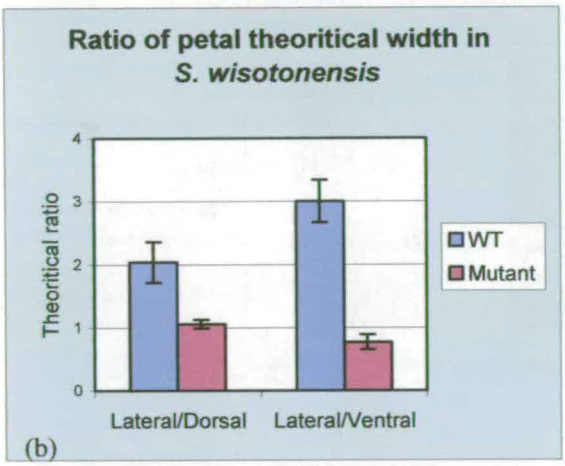
Ratio of petal theoritical width in S. wisotonensis
Theoritical ratio
4
3
2
1
0
Lateral/Dorsal
Lateral/Ventral
WT
Mutant
(b)

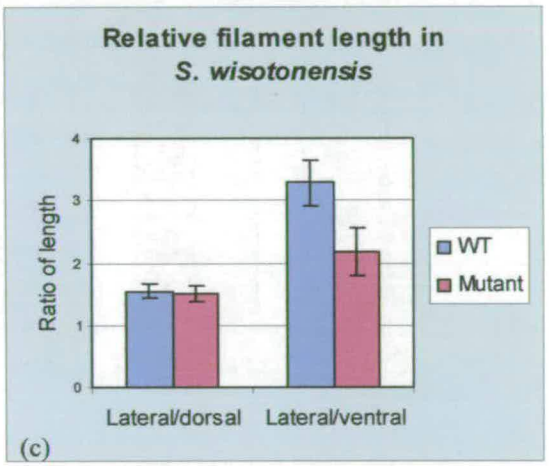
Relative filament length in S. wisotonensis
Ratio of length
4
3
2
1
0
Lateral/dorsal
Lateral/ventral
WT
Mutant
(c)

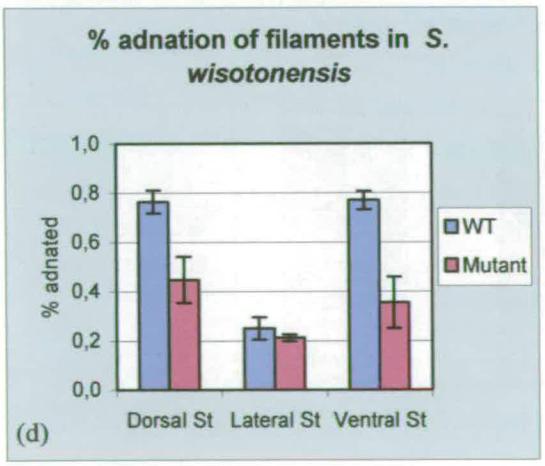
% adnation of filaments in S. wisotonensis
% adnated
1,0
0,8
0,6
0,4
0,2
0,0
Dorsal St
Lateral St
Ventral St
WT
Mutant
(d)

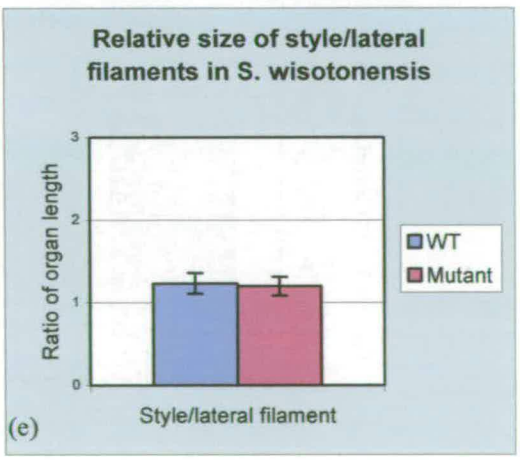
Relative size of style/lateral filaments in S. wisotonensis
Ratio of organ length
3
2
1
0
Style/lateral filament
WT
Mutant
(e)

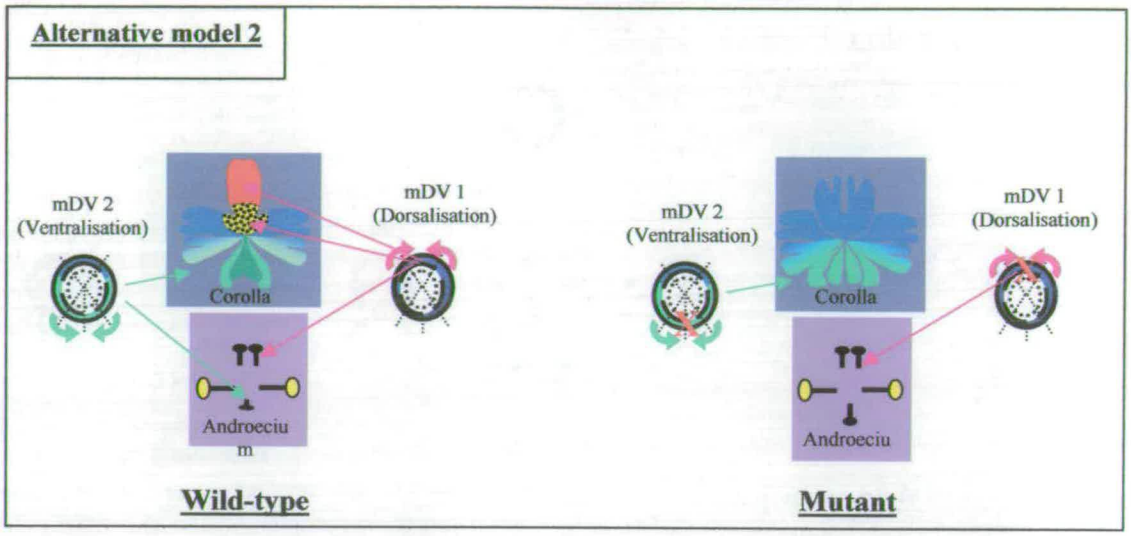

Appendix III.13: Alternative model 2 for the control of dorso-ventral asymmetry in *S. wisotonensis*.

For clarity, the corolla (purple background) and the androecium (pink background) are represented separately. In the androecium, black stamens correspond to staminodes. The manifestations of dorso-ventral asymmetry are indicated as mDV. In this model, two opposite gradients exist along the dorso-ventral axis of the wild-type flower. mDV1 corresponds to a developmental gradient polarized towards the dorsal half of the flower (i.e. dorsalisation). It includes early effects such as the growth inhibition of the dorsal stamens and that of the central zone of the dorsal petal. Late effects of mDV1 are the formation of a furrow at the junction between the dorsal and the lateral petal and the production of nectar guides and changes in cell types (pink arrows). mDV2 corresponds to a developmental gradient polarized towards the ventral half of the flower (i.e. ventralization). mDV2 include the decrease in size of petals lobes along the dorso-ventral axis the growth inhibition of the ventral-most lobes of the ventral petal and that of the ventral staminode (green arrows). In the mutant, both ends of these gradients are lost resulting in morphological changes confined to the ventral-most and the dorsal-most region of the flower (red crosses).

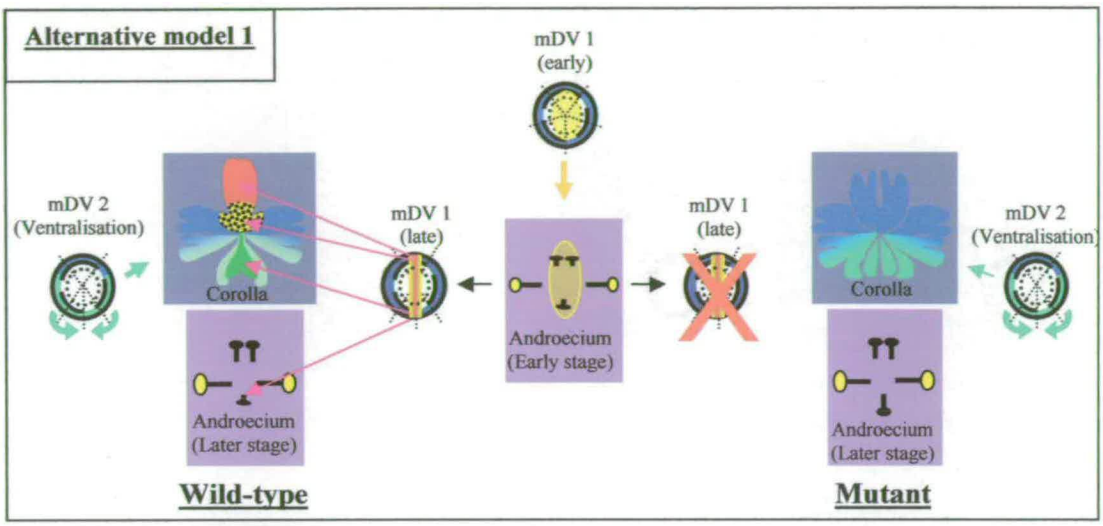

Appendix III.12: Alternative model 1 of the establishment of dorso-ventral asymmetry in a wild-type and the *rz* mutant of S. wisotonensis

For clarity, the corolla (purple background) and the androecium (pink background) are represented separately. In the androecium, black stamens correspond to staminodes. The model proposed here corresponds to the simplest developmental pathways (i.e. most parsimonious) extrapolated from the comparison between wild-type and mutant flowers. The manifestations of dorso-ventral asymmetry are indicated as mDV. Early mDV1 correspond to growth inhibition of the dorsal and the ventral stamens during the enlargement of the lateral stamens which results in the division of the floral meristem into two unequal halves (yellow arrows). Late mDV1 corresponds to the manifestations of dorso-ventral asymmetry localised along or close to the dorso-ventral (DV) axis which are affected in mutant. They are indicated with a pink arrow. They comprise the growth inhibition of the central zone of the dorsal petal and the ventral-most lobes of the ventral petal and that of the ventral staminode, the formation of a furrow at the junction between the dorsal and the lateral petal, the production of nectar guides and changes in cell types. mDV2 is the ventralisation of the corolla indicated with green arrows (i.e. reduction in petal lobe size towards the ventral domain) which is not affected in the *rz* mutant. The red cross indicates that in the mutant, the floral meristem cannot interpret the "late" component of the pre-pattern (i.e. trans-acting factors) controlling the downstream genetic machinery required to set up late mDV1.

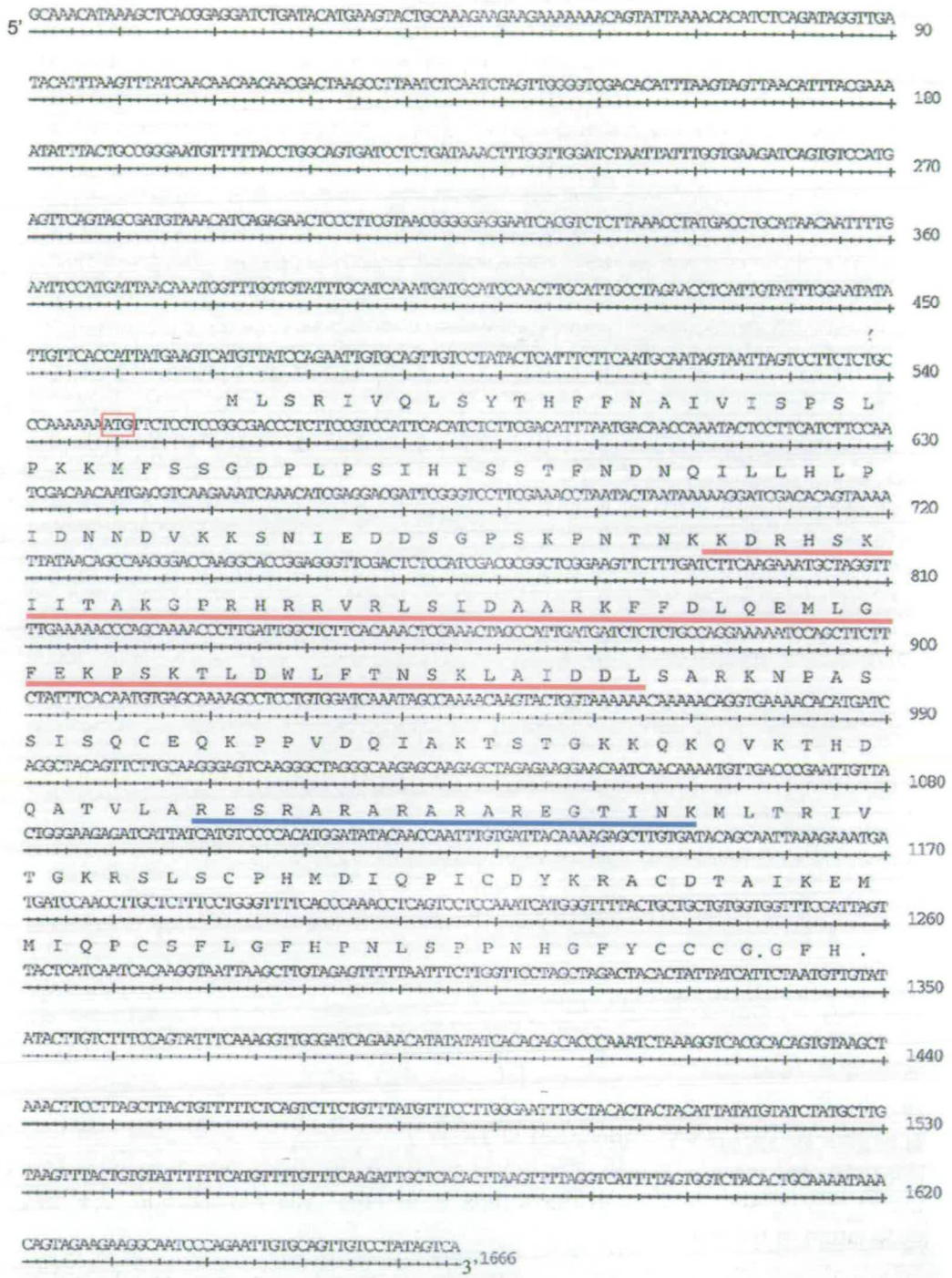

Appendix IV.2: gDNA sequence of *SCHCYC2A*

The predicted protein sequence is indicated under the nucleotide sequence. The TCP box is highlighted in red and the R box is in blue. The first "in frame" methionine may not be the start codon as indicated by the comparison with *SCHCYC2B* (Appendix IV.3). The red box indicates the corrected putative start codon. The sequence corresponding to the intron in the 3' end could not be localised accurately. Therefore, the position of the stop codon is provisional.

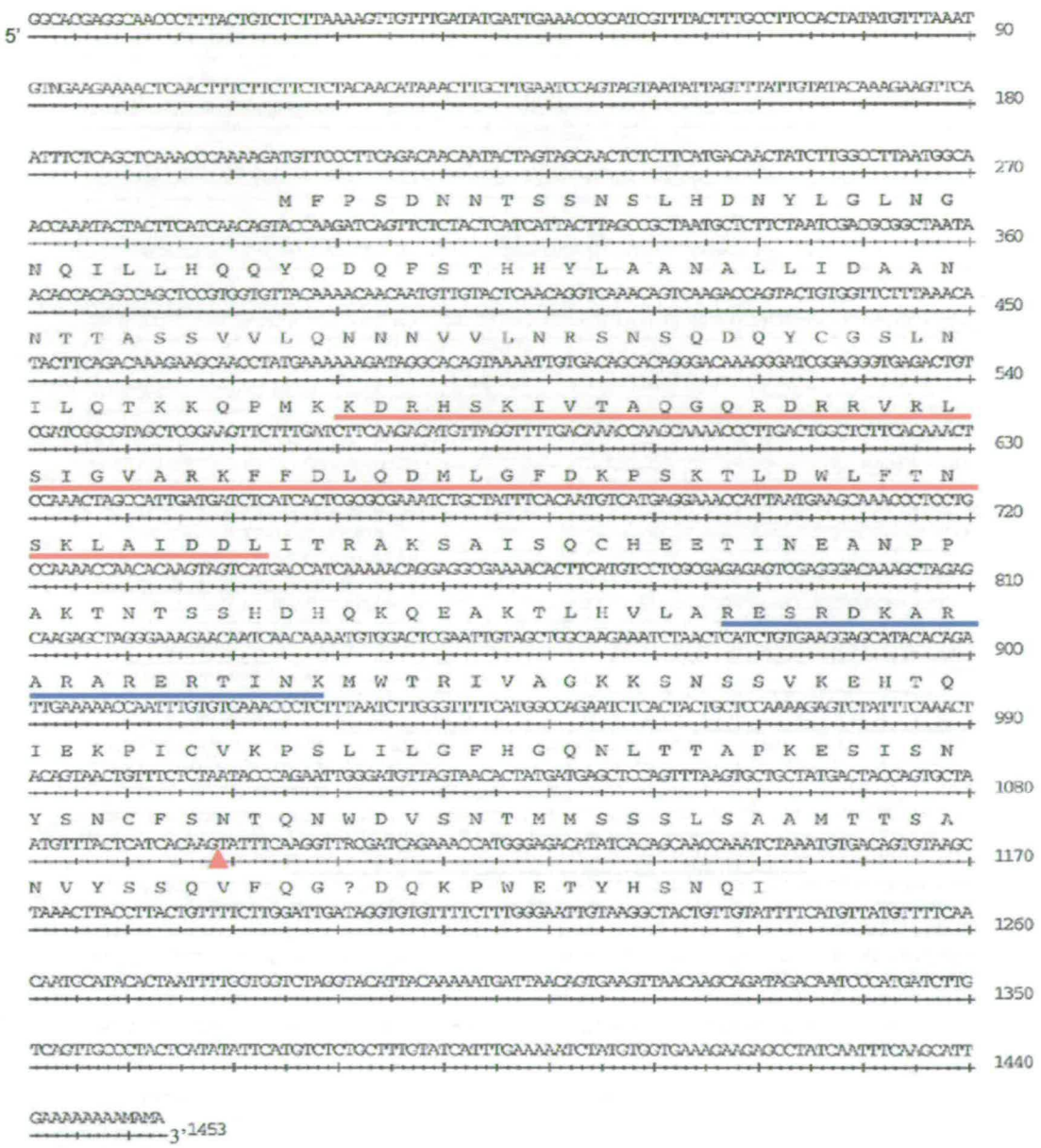

Appendix IV.1a: cDNA sequence of *SCHCYC1*

The predicted protein sequence is indicated under the nucleotide sequence. The TCP box is highlighted in red and the R box is in blue. The red triangle represents the localisation of the intron.

Appendix IV.1b: Nucleotide sequence of the intron in *SCHCYC1*

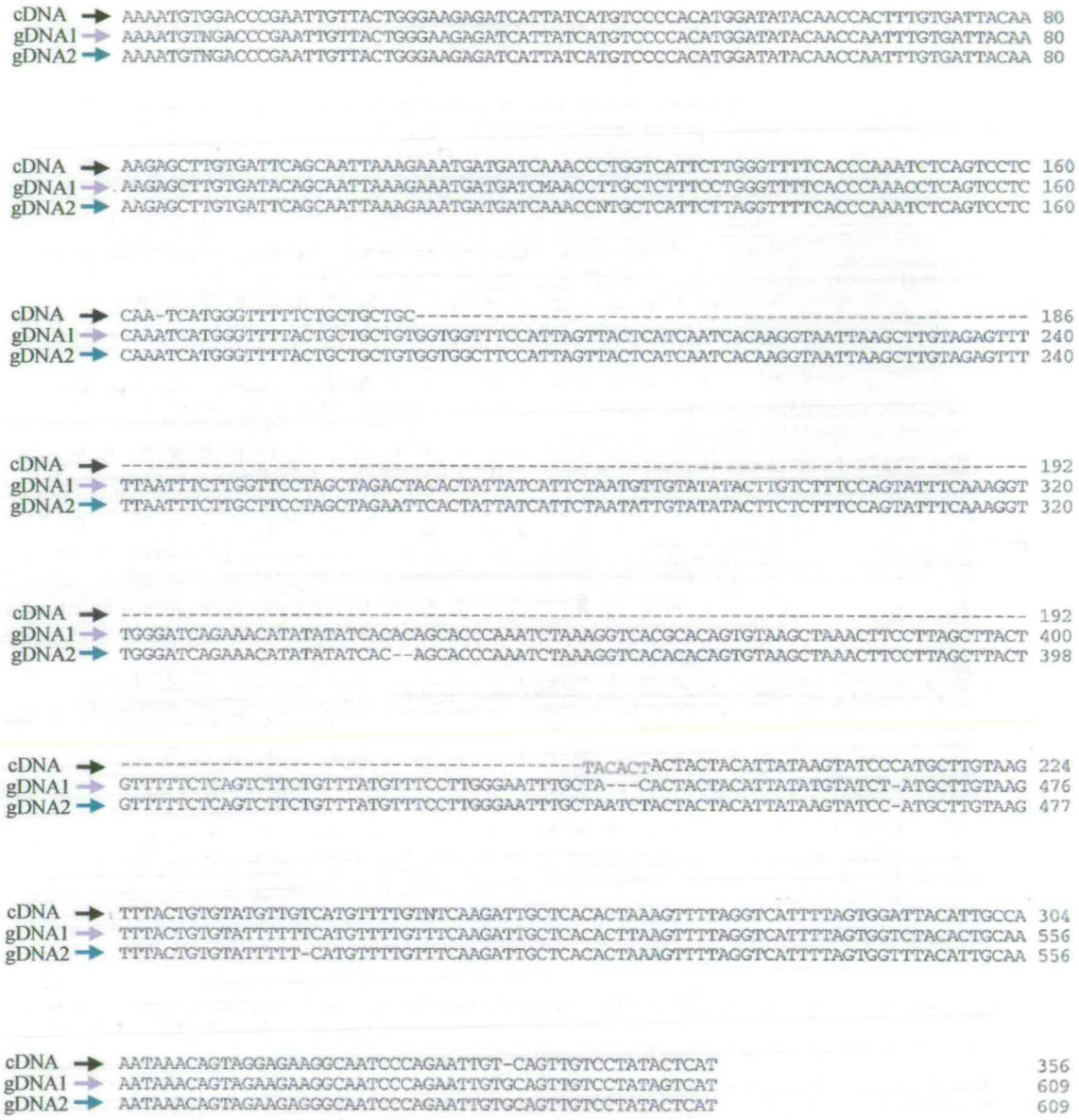

Appendix IV.4: Alignment of the 3' end of *SCHCYC2m*, *SCHCYC2A* and *SCHCYC2B*
The alignment of the 3' end of *SCHCYC2m* (cDNA), *SCHCYC2A* (gDNA1) and *SCHCYC2B* (gDNA2) suggests the presence of a 255bp intron for *SCHCYC2A* and 253bp for *SCHCYC2B*.

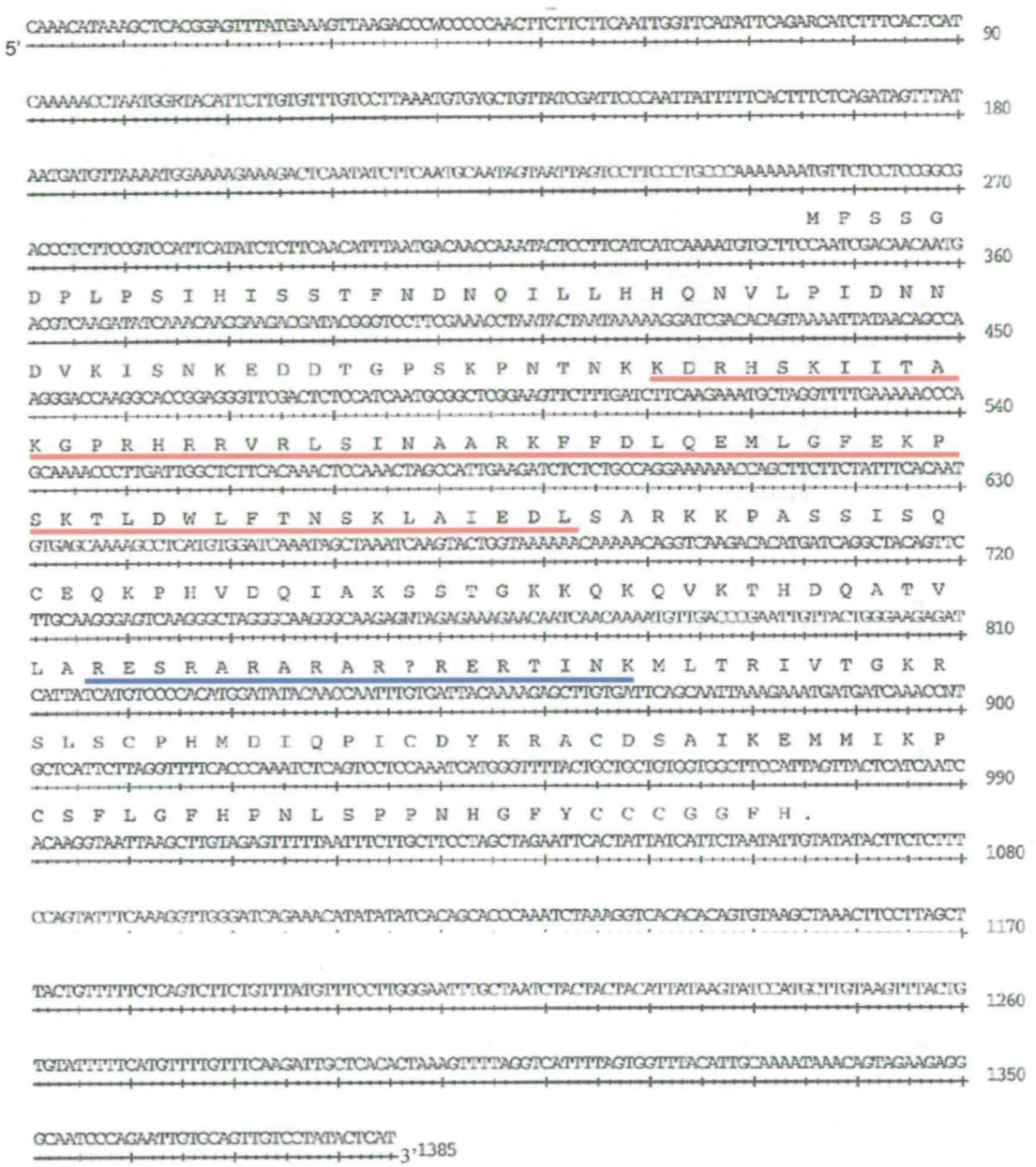

Appendix IV.3: gDNA sequence of *SCHCYC2B*

The predicted protein sequence is indicated under the nucleotide sequence. The TCP box is highlighted in red and the R box is in blue. The sequence corresponding to the intron in the 3' end could not be localised accurately. Therefore, the position of the stop codon is provisional.

Appendix IV.6: Partial DNA sequence of *SCHCYC4*

The predicted protein sequence is indicated under the nucleotide sequence. The TCP box is highlighted in red. The sequence the R box and the 3' end of the gene are not known.

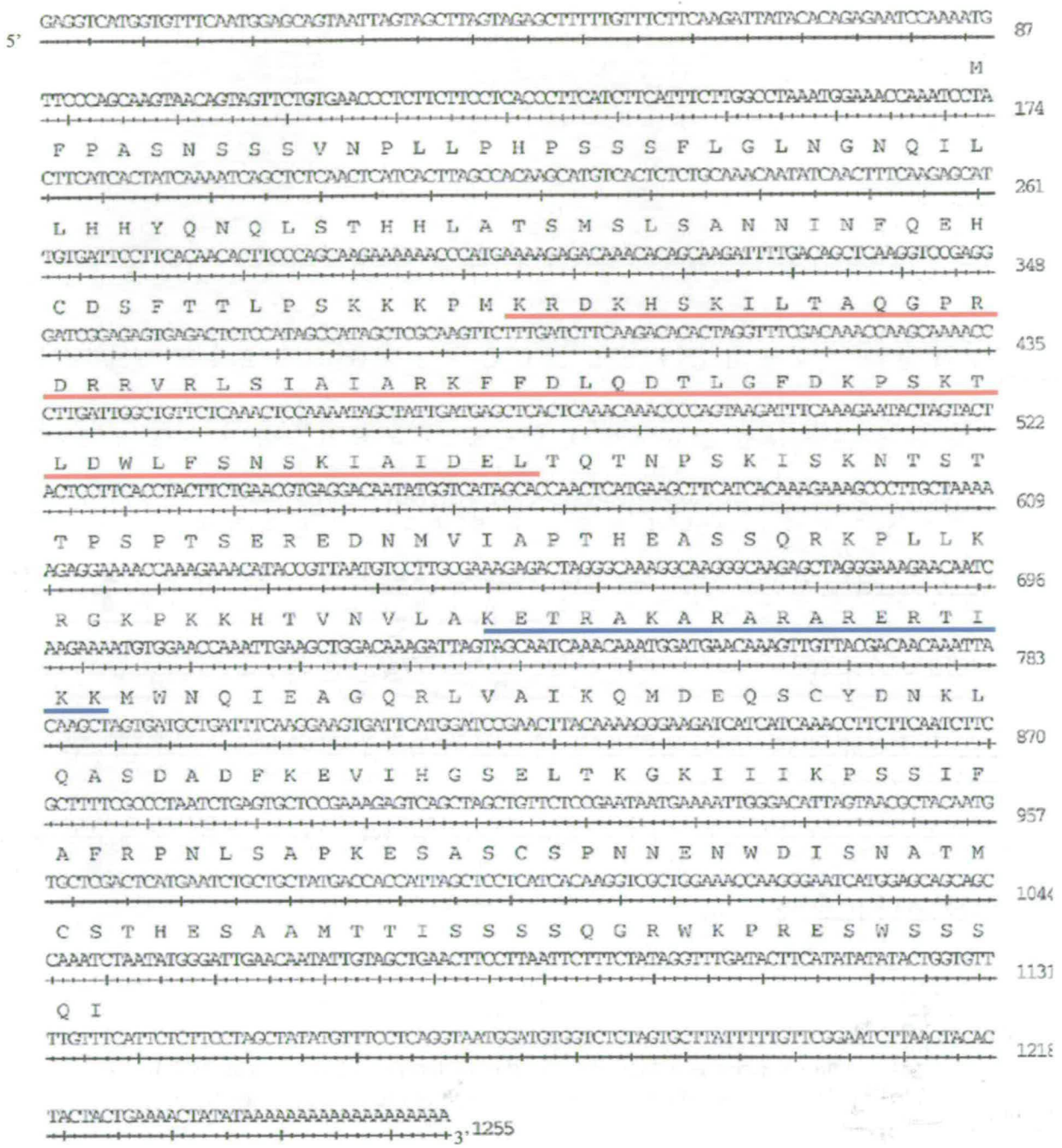

Appendix IV.5: cDNA sequence of *SCHCYC3*

The predicted protein sequence is indicated under the nucleotide sequence. The TCP box is highlighted in red and the R box in blue.

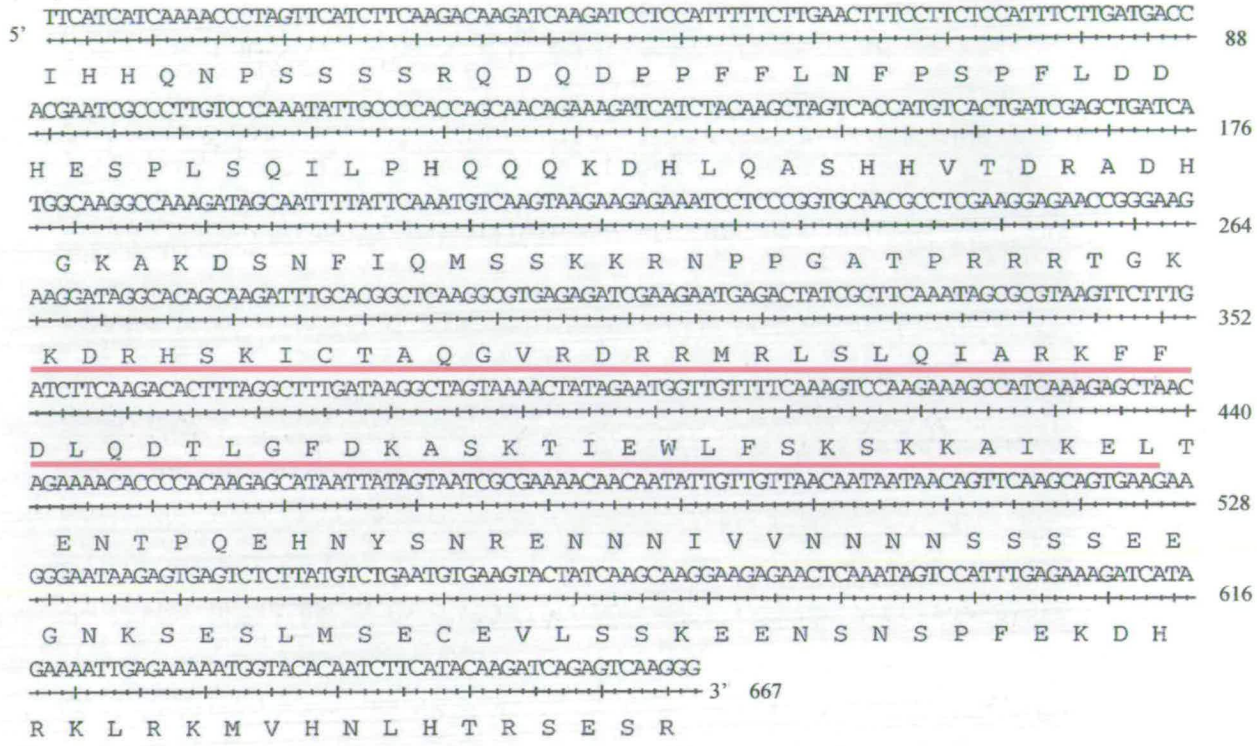

Appendix IV.8: Partial cDNA sequence of *SCHCYC6*

The predicted protein sequence is indicated under the nucleotide sequence. The TCP box is highlighted in red. The sequence of the 5' end (including the start codon), the R box and the 3' end of the gene are not known.

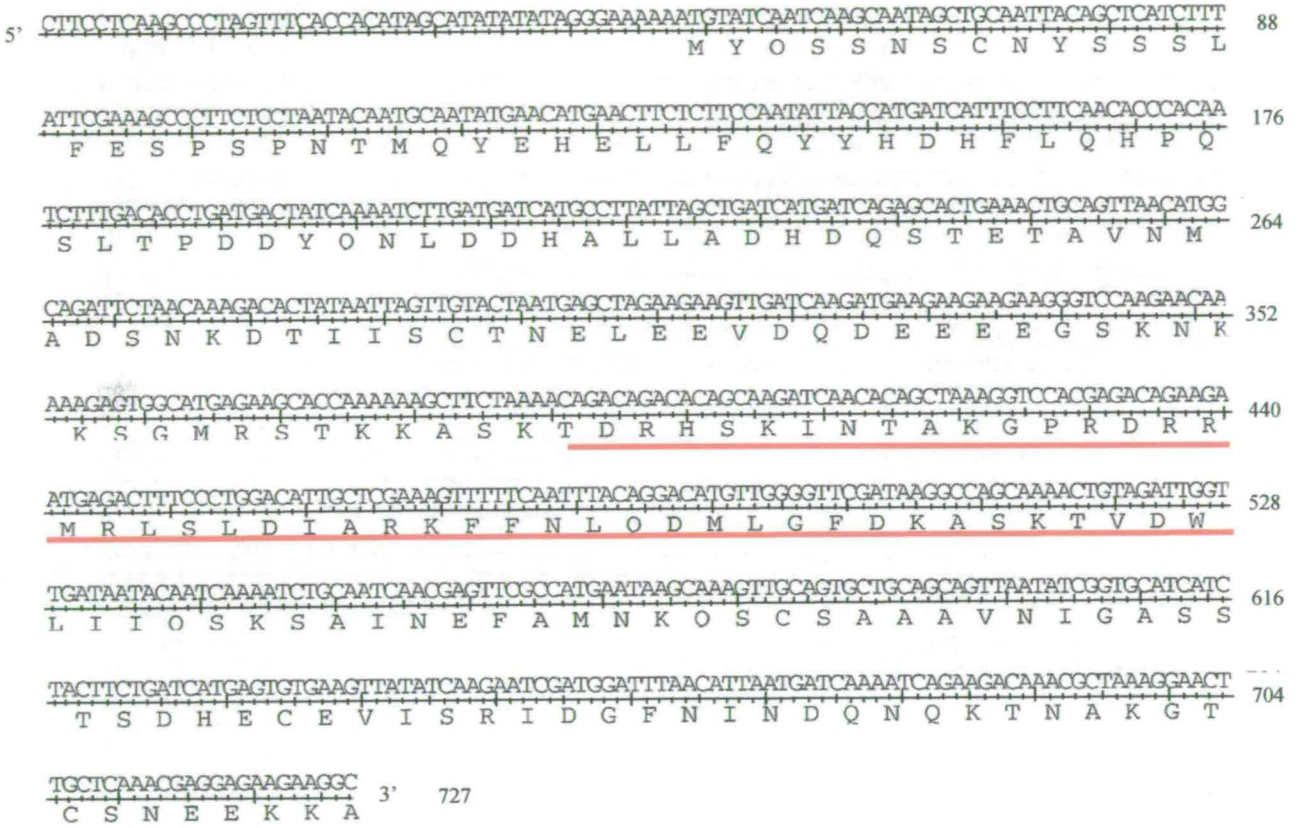

Appendix IV.7: Partial cDNA sequence of *SCHCYC5*

The predicted protein sequence is indicated under the nucleotide sequence. The TCP box is highlighted in red. The sequence the R box and the 3' end of the gene are not known.

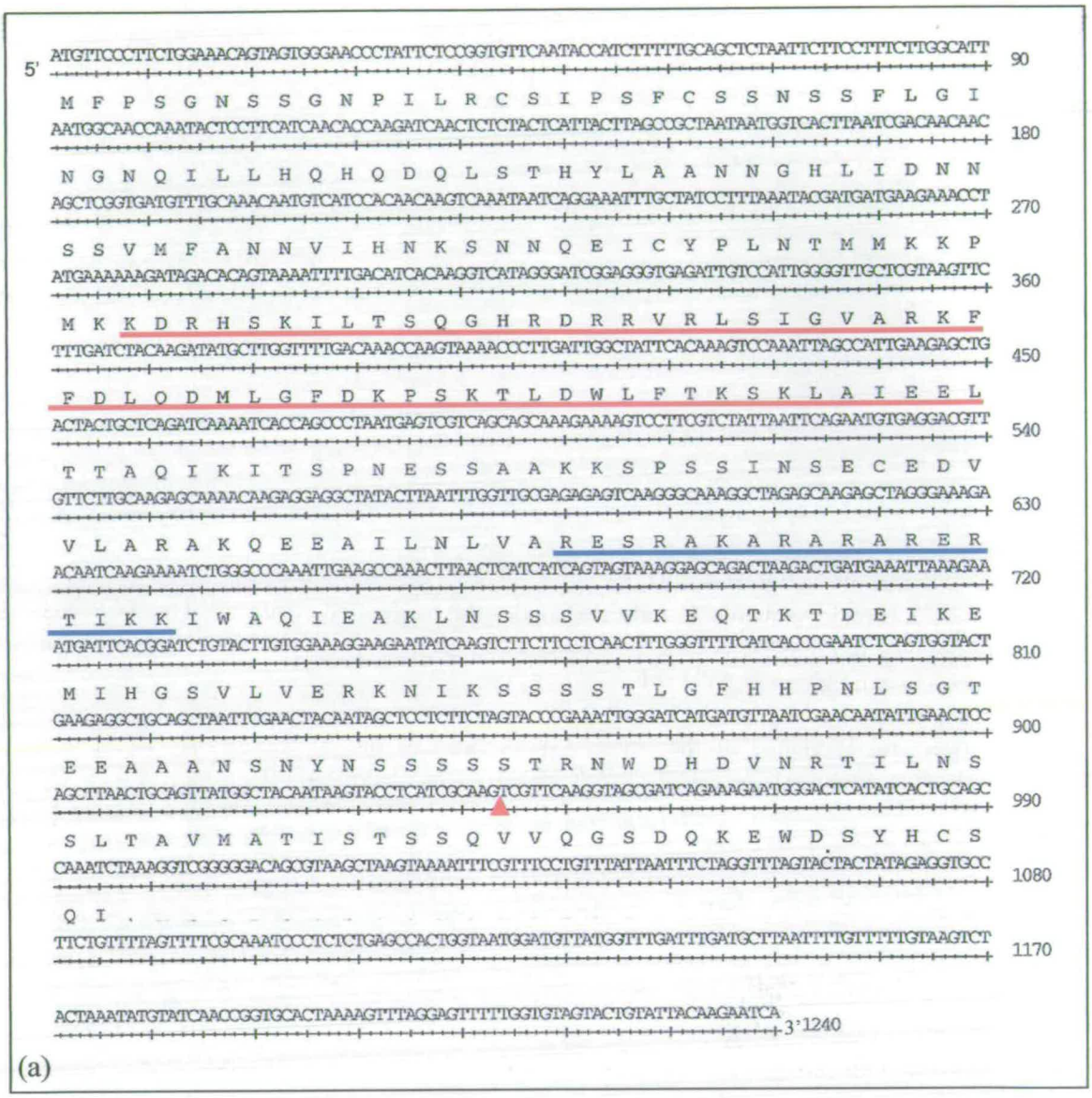
5'
ATGTTCCCTTCTGGAAACAGTAGTGGGAACCCTATTCTCCGGTGTTCAATACCATCTTTTTGCAGCTCTAATTCTTCCTTTCTTGGCATT
90
M F P S G N S S G N P I L R C S I P S F C S S N S S F L G I
AATGGCAACCAAATACTCCTTCATCAACACCAAGATCAACTCTCTACTCATTACTTAGCCGCTAATAATGGTCACTTAATCGACAACAAC
180
N G N Q I L L H Q H Q D Q L S T H Y L A A N N G H L I D N N
AGCTCGGTGATGTTTGCAAACAATGTCATCCACAACAAGTCAAATAATCAGGAAATTTGCTATCCTTTAAATACGATGATGAAGAAACCT
270
S S V M F A N N V I H N K S N N Q E I C Y P L N T M M K K P
ATGAAAAAAGATAGACACAGTAAAATTTTGACATCACAAGGTCATAGGGATCGGAGGGTGAGATTGTCCATTGGGGTTGCTCGTAAGTTC
360
M K K D R H S K I L T S Q G H R D R R V R L S I G V A R K F
TTTGATCTACAAGATATGCTTGGTTTTGACAAACCAAGTAAAACCCTTGATTGGCTATTCACAAAGTCCAAATTAGCCATTGAAGAGCTG
450
F D L Q D M L G F D K P S K T L D W L F T K S K L A I E E L
ACTACTGCTCAGATCAAAATCACCAGCCCTAATGAGTCGTCAGCAGCAAAGAAAAGTCCTTCGTCTATTAATTCAGAATGTGAGGACGTT
540
T T A Q I K I T S P N E S S A A K K S P S S I N S E C E D V
GTTCTTGCAAGAGCAAAACAAGAGGAGGCTATACTTAATTTGGTTGCGAGAGAGTCAAGGGCAAAGGCTAGAGCAAGAGCTAGGGAAAGA
630
V L A R A K Q E E A I L N L V A R E S R A K A R A R A R E R
ACAATCAAGAAAATCTGGGCCCAAATTGAAGCCAAACTTAACTCATCATCAGTAGTAAAGGAGCAGACTAAGACTGATGAAATTAAAGAA
720
T I K K I W A Q I E A K L N S S S V V K E Q T K T D E I K E
ATGATTCACGGATCTGTACTTGTGGAAAGGAAGAATATCAAGTCTTCTTCCTCAACTTTGGGTTTTCATCACCCGAATCTCAGTGGTACT
810
M I H G S V L V E R K N I K S S S S S T L G F H H P N L S G T
GAAGAGGCTGCAGCTAATTCGAACTACAATAGCTCCTCTTCTAGTACCCGAAATTGGGATCATGATGTTAATCGAACAATATTGAACTCC
900
E E A A A N S N Y N S S S S S T R N W D H D V N R T I L N S
AGCTTAACTGCAGTTATGGCTACAATAAGTACCTCATCGCAAGTCGTTCAAGGTAGCGATCAGAAAGAATGGGACTCATATCACTGCAGC
990
S L T A V M A T I S T S S Q V V Q G S D Q K E W D S Y H C S
CAAATCTAAAGGTCGGGGGACAGCGTAAGCTAAGTAAAATTTCGTTTCCTGTTTATTAATTTCTAGGTTTAGTACTACTATAGAGGTGCC
1080
Q I . . . . . .
TTCTGTTTAGTTTTCGCAAATCCCTCTCTGAGCCACTGGTAATGGATGTTATGGTTTGATTTGATGCTTAATTTTGTTTTTGTAAGTCT
1170
ACTAAATATGTATCAACCGGTGCACTAAAAGTTTAGGAGTTTTTGGTGTAGTACTGTATTACAAGAATCA
3'1240
(a)

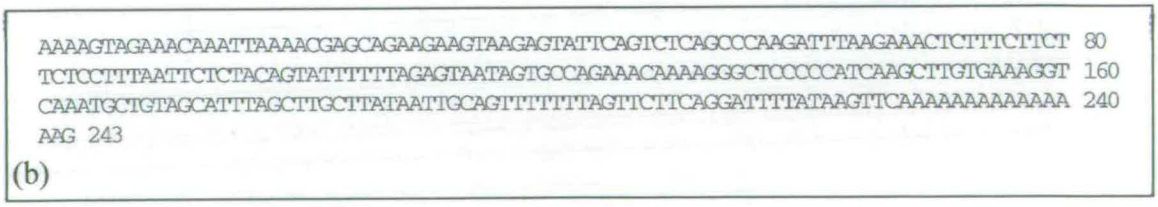
AAAAGTAGAAACAAATTAAAACGAGCAGAAGAAGTAAGAGTATTCAGTCTCAGCCCAAGATTTAAGAAACTCTTTCTTCT 80
TCTCCTTTAATTCTCTACAGTATTTTTTAGAGTAATAGTGCCAGAAACAAAAGGGCTCCCCCATCAAGCTTGTGAAAGGT 160
CAAATGCTGTAGCATTTAGCTTGCTTATAATTGCAGTTTTTTTAGTTCTTCAGGATTTTATAAGTTCAAAAAAAAAAAAA 240
AAG 243
(b)

Appendix IV.9: Sequence information for *NICYC1*

(a) ORF and partial 3'NTR of *NICYC1A*

The predicted protein sequence is indicated under the nucleotide sequence. The TCP box is highlighted in red and the R box is in blue. The red arrow indicates the position of the intron (sequence in appendix IV.11c).

(b) 5' NTR isolated with 5' race PCR

(c) Position and sequence of the intron (pink box) in the 3' end of *NICYC1A* and *NICYC1B.* cDNA: *NICYC2m,* gDNA1: *NICYC1A*, gDNA2: *NICYC1B.*

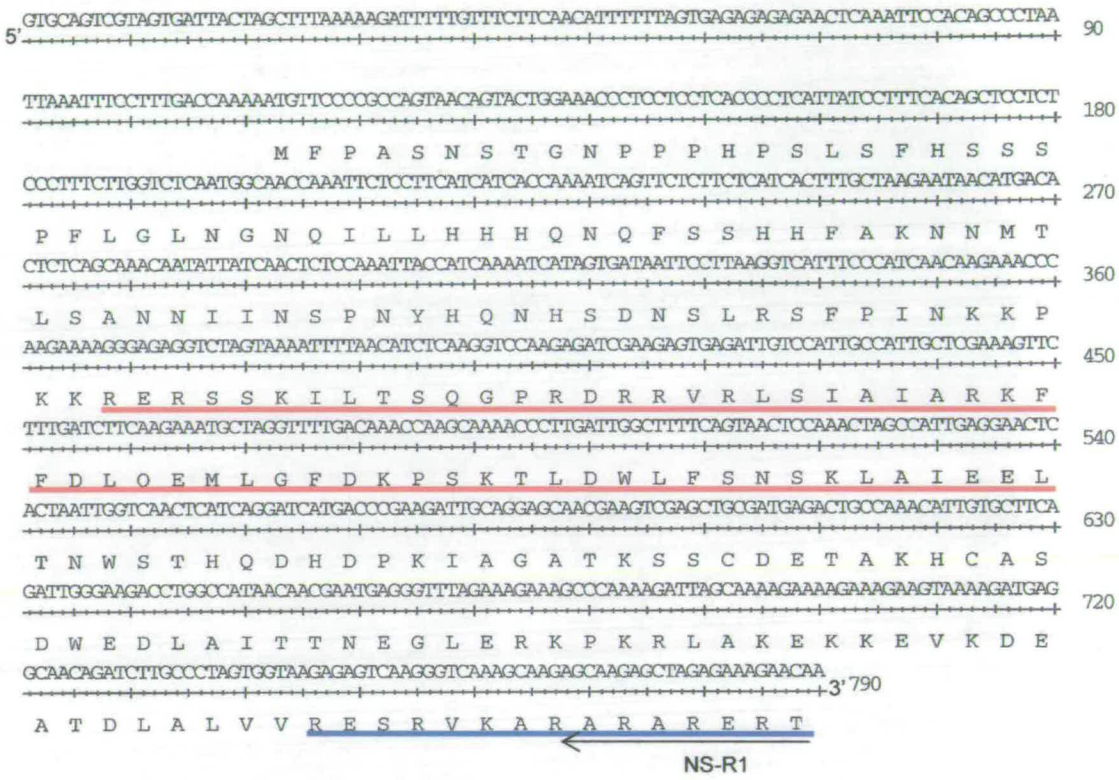

Appendix IV.10: Partial cDNA of *NICYC2B*

The predicted protein sequence is indicated under the nucleotide sequence. The TCP box is highlighted in red and the R box is in blue. The black arrow indicates the nucleotide sequence corresponding to the primer NS-R1.


cDNA ATCACCCGAATCTCAGTGGTACTGAAGAGGCTACAGCTAATTCGAACTACAATAGCTCCTCTTCTA---CCCGAAATTGG 77
gDNA1 ATCACCCGAATCTCAGTGGTCCGGAACAGGNTGCAGCTAATTCTCACTACAAAAGCTCCTCTTCTAGTACCCGAAATTGG 80
gDNA2 ATCACCCGAATCTCAGTGGTACTGAAGAGNCTGCAGCTAATTCGAACTACAATAGCTCCTCTTCTAGTACCCGAAATTGG 80
cDNA GATCATGATGTTAATCGAACAATATTGAACTCCAGCTTAACTGCAGTTATGGCTACAATAAGTACCTCATCGCAAG---- 154
gDNA1 GATCATGACGTTAATCGAACAATAATGAACTCCAGCTTAAGTGCAGTTATGGCTACAATAAGTACCTCATCGCAAGGTAA 160
gDNA2 GATCATGATGTTAATCGAACAATATTGAACTCCAGCTTAACTGCAGTTATGGCTACAATAAGTACCTCATCGCAAGGTAA 160
cDNA ---------- 154
gDNA1 ACTTCTAATTACAAAAGTGGAGTC---CAATTTAGTCATTTAATTACTTCCACAATTCTCATTCTATATATATATATATC 237
gDNA2 ACTTCTAATTCCAAAAGTGGAGTAGTATAATTTAGTCATTTAATTACTTCCACAATTCTCAATCCA-----ATATATATT 235
cDNA ---------- 154
gDNA1 TTCGCTTTGCGAGGGTCTATCGGAAACAACCTCTCTATCCCTCGGGGCAGGGGTAAGGTGTGCATACACACTATCCTCCC 317
gDNA2 T---------- 237
cDNA ----------TCG 156
gDNA1 CAGATCCCACTAGTAGAATTTCACTGGGTCGTTGTTGGTGTTGTTGATATATATATATCTTCTCTTAAAATTTCCAGTTG 397
gDNA2 ----------ATGTCTTCTCTTCAA-TTTCCAGTCG 261
(c)

Appendix IV.12a: Partial cDNA sequence of *PETCYC1*

The predicted protein sequence is indicated under the nucleotide sequence. The TCP box is highlighted in red and the R box (incomplete) is in blue. The 3' end of this gene is missing. The red triangle represents the localisation of the intron.

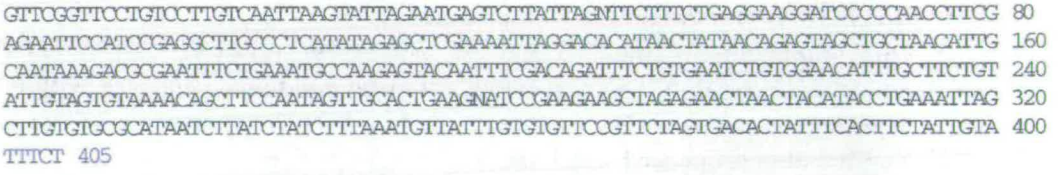

Appendix IV.12b: Nucleotide sequence of the intron *PETCYC1*

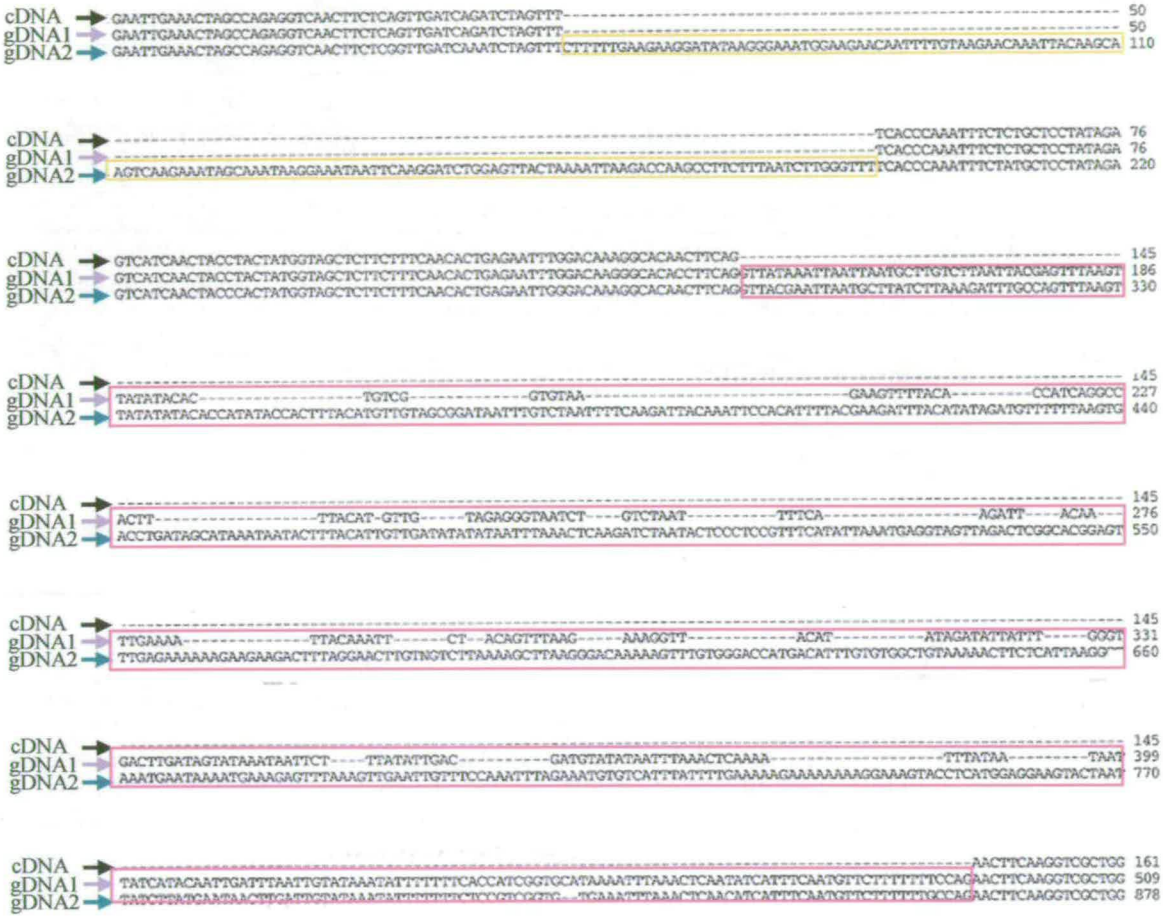

Appendix IV.11: Alignment of the 3' end of *NICYC2m*, *NICYC2(3'x)* and *NICYC2(3'y)*

The alignment of the 3' end of *NICYC2m* (cDNA), *NICYC2(3'x)* (gDNA1) and *NICYC2(3'y)*(gDNA2) indicates that a 144 bp additional sequence within the coding region is present in *NICYC2(3'y)* (yellow box). In *NICYC2(3'x)* and *NICYC2(3'y)*, introns differ in length and in sequence (pink boxes).

NJ

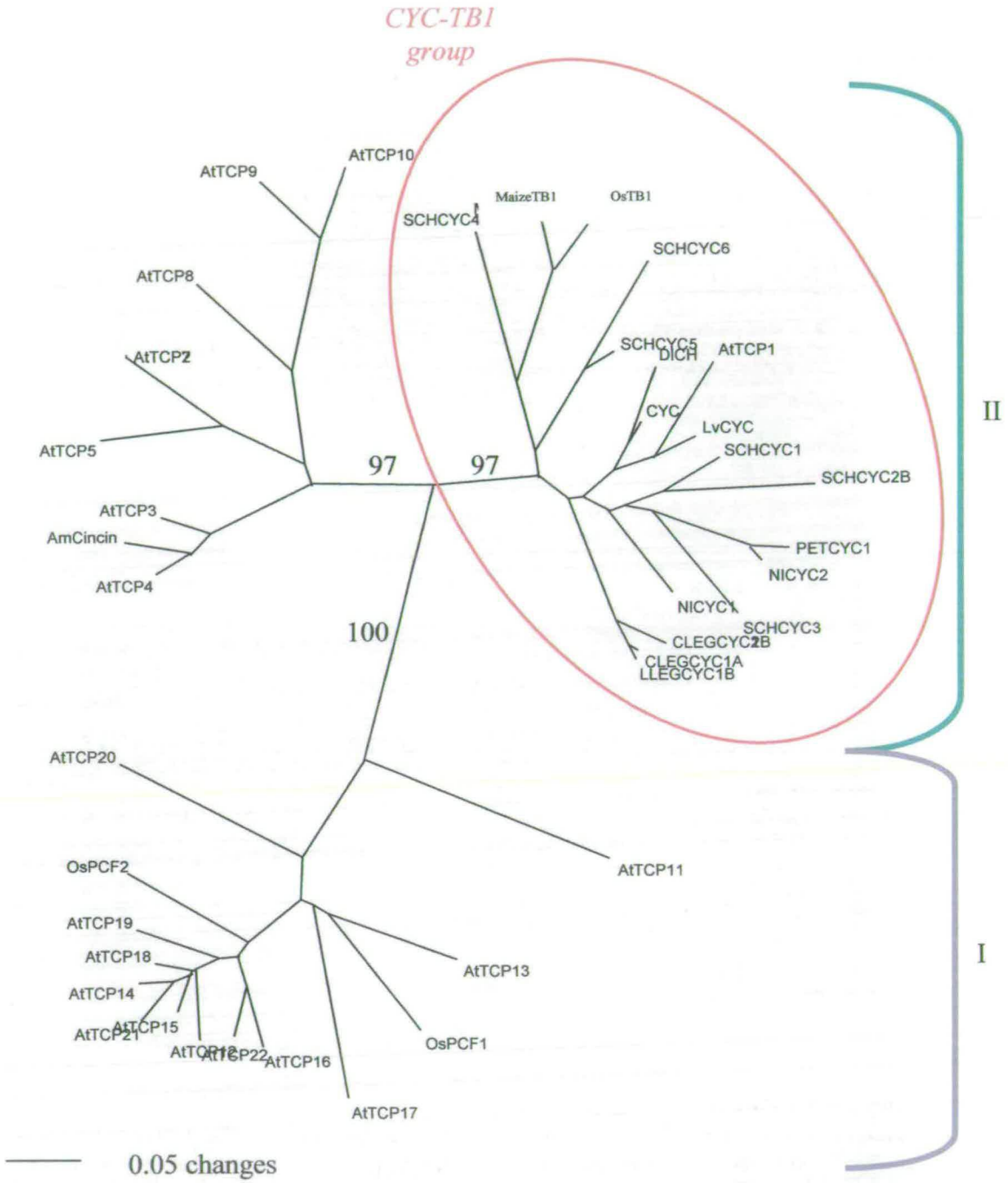

Appendix IV.14: Unrooted phylogram of protein distance NJ analysis on the TCP domain data set with representative genes of the TCP gene family

This tree was obtained with a NJ (Neighbor-Joining) analysis in PAUP 4.0b10 on the protein matrix (M1). For clarity, only the relevant support values obtained with 10 000 bootstrap replicates are included. The grey bracket indicates the PCF group (class I), the green bracket indicates the *CYC-TB1* group (class II), the red circle indicates the clade including *CYC* and *TB1*. At: *Arabidopsis thaliana*; Os: rice; CLEGCYC: *Cadia CYC*-like gene (legume); LLEGCYC: *Lupinus CYC*-like gene (legume); NICYC: tobacco *CYC*-like gene; *PETCYC*: petunia *CYC*-like gene; *SCHCYC*: *Schizanthus wisotonensis CYC*-like gene; Lv: *Linaria vulgaris*; *CYC*: *CYCLOIDEA* (*A. majus*); *DICH*: *DICHOTOMA* (*A. majus*).

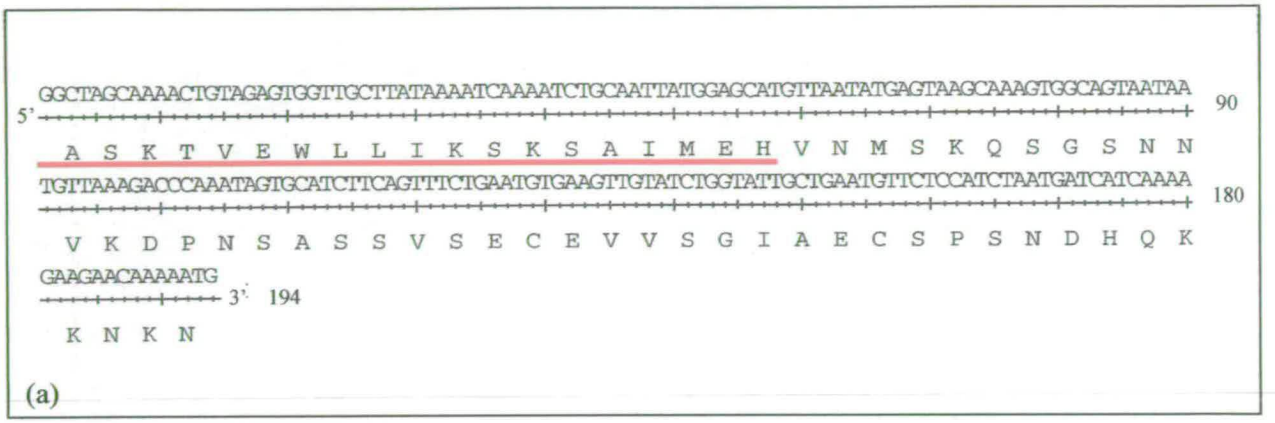

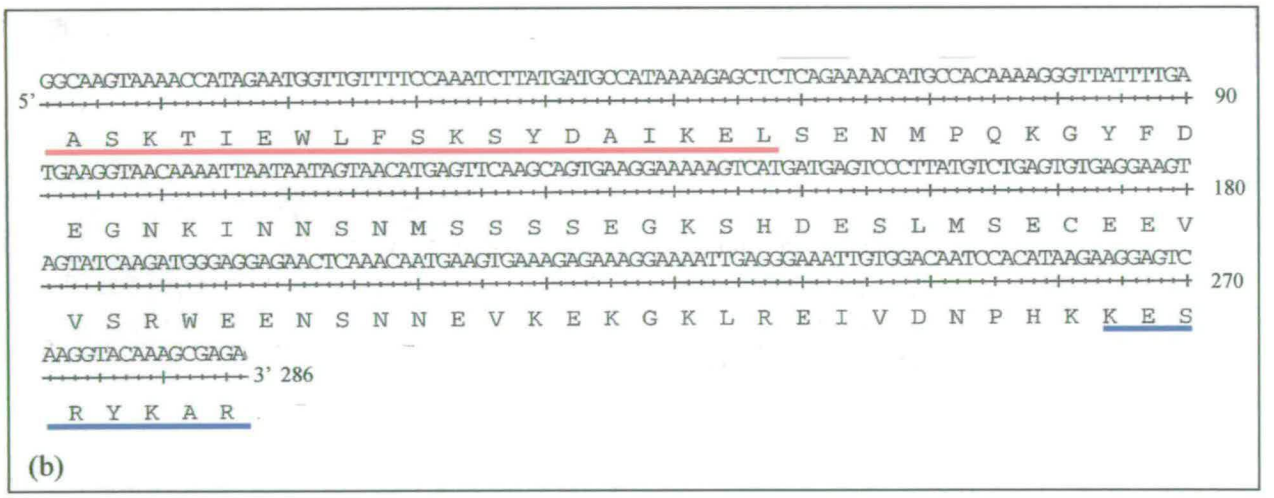

Appendix IV.13: Partial gDNA sequence of *PETCYC2 and 3*

(a) Partial cDNA of *PETCYC2,* some ambiguity remains concerning the 3'of this fragment which may have been lost during the cloning as the sequence of the reverse primer cannot be recognized (b) Partial cDNA of *PETCYC3.* The predicted protein sequence is indicated under the nucleotide sequence. The end of the TCP box is highlighted in red and the beginning of the R box in blue.

Appendix IV.16: Strict consensus parsimony cladogram obtained with a heuristic search on the protein matrix of the TCP domain data set from representative genes of the TCP gene family

The parsimony analysis was carried out in PAUP 4.0b10 on the protein matrix (M1). It produced 86 equally parsimonious trees of 267 steps. The consistency index was: 0.67 and the retention index: 0.86. The branch support values correspond to bootstrap % obtained with 100 000 replicates (no swapping and a random addition sequence with #rep : 1). The grey bracket indicates the PCF group (class I), the green bracket indicates the *CYC-TB1* group (class II), the red bracket indicates the clade including *CYC* and *TB1*. At: *Arabidopsis thaliana*; Os: rice; CLEGCYC: *Cadia CYC*-like gene (legume); LLEGCYC: *Lupinus CYC*-like gene (legume); NICYC: tobacco *CYC*-like gene; *PETCYC*: petunia *CYC*-like gene; *SCHCYC*: *Schizanthus wisotonensis CYC*-like gene; Lv: *Linaria vulgaris*; *CYC*: *CYCLOIDEA* (*A. majus*); *DICH*: *DICHOTOMA* (*A. majus*).

UPGMA

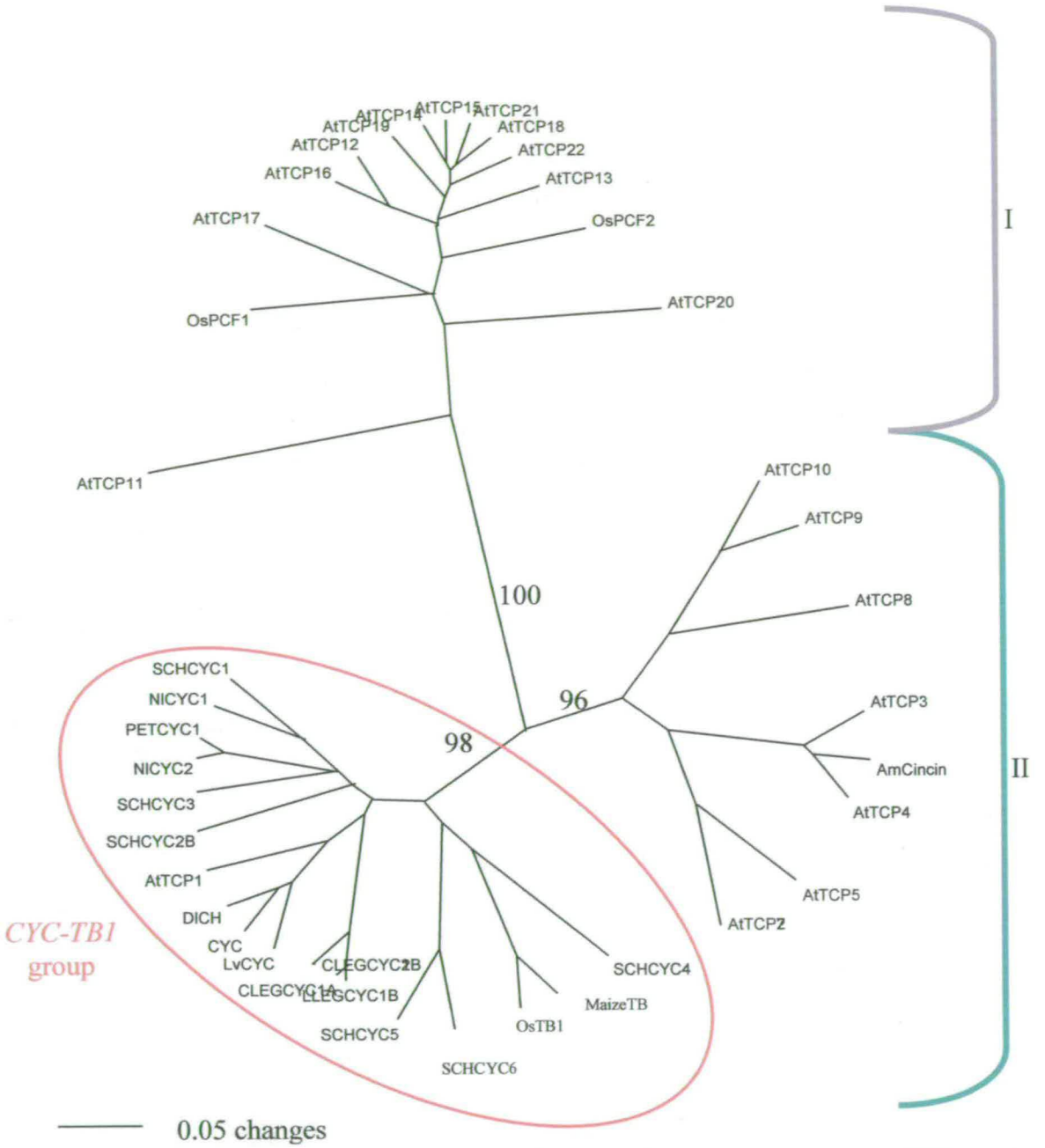

Appendix IV.15: Unrooted phylogram of protein distance UPGMA analysis on the TCP domain data set with representative genes of the TCP gene family

This tree was obtained with a UPGMA analysis in PAUP 4.0b10 on the protein matrix (M1). For clarity, only the relevant support values obtained with 10 000 bootstrap replicates are included. The grey bracket indicates the PCF group (class I), the green bracket indicates the *CYC-TB1* group (class II), the red circle indicates the clade including *CYC* and *TB1*. At: *Arabidopsis thaliana*; Os: rice; CLEGCYC: *Cadia CYC*-like gene (legume); LLEGCYC: *Lupinus CYC*-like gene (legume); NICYC: tobacco *CYC*-like gene; *PETCYC*: petunia *CYC*-like gene; *SCHCYC*: *Schizanthus wisotonensis CYC*-like gene; Lv: *Linaria vulgaris*; *CYC*: *CYCLOIDEA* (*A. majus*); *DICH*: *DICHOTOMA* (*A. majus*).

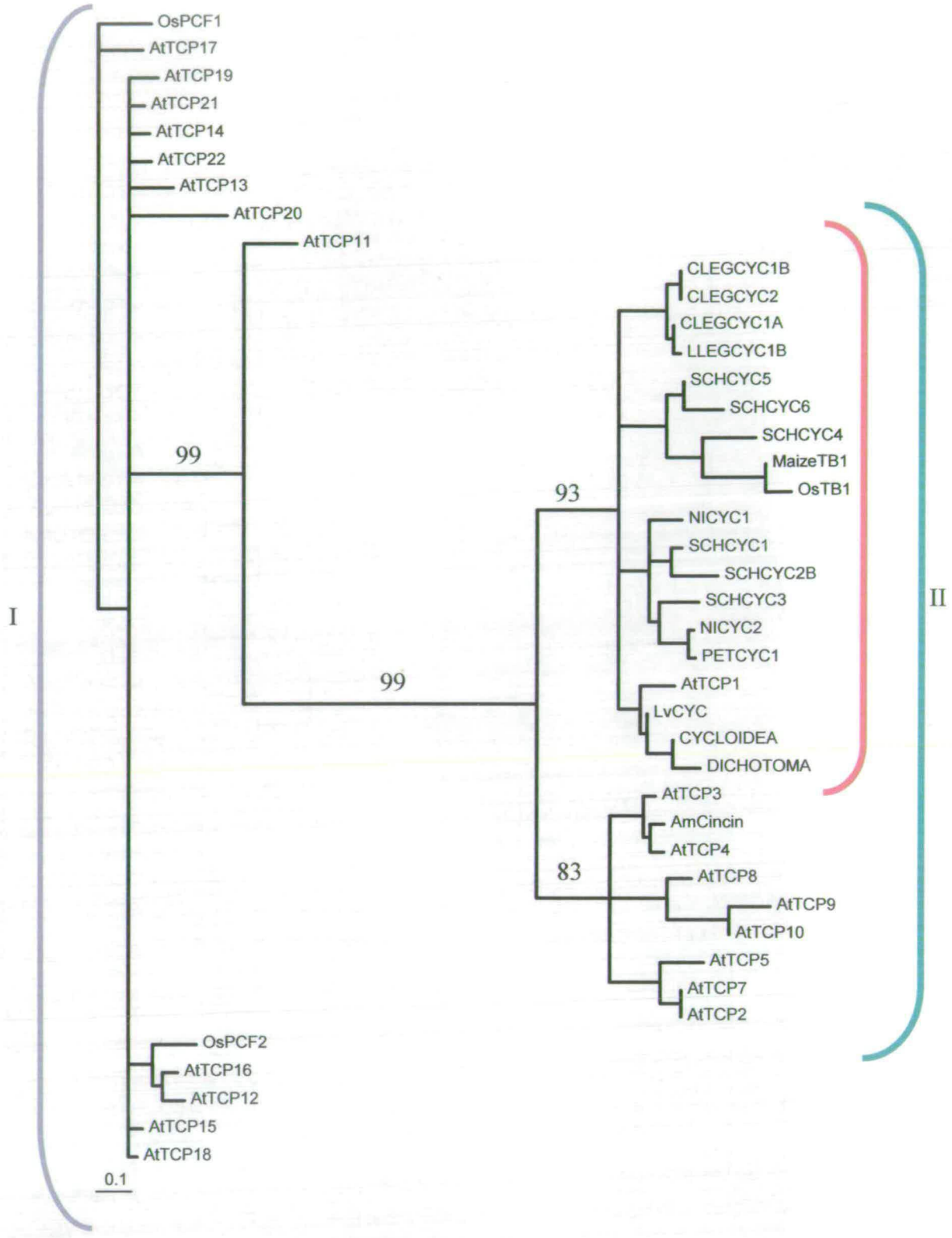

Appendix IV.17: Maximum likelihood phylogram (VT model) on the protein matrix with the TCP domain data set from representative genes of the TCP gene family

This tree was obtained using the VT model of sequence evolution (Mueller – Vingron, 2000) on the amino-acid matrix (M1) in Puzzle 5.2. OsPCF1 was chosen as an outgroup. The figures indicate the relevant branch support. The grey bracket indicates the PCF group (class I), the green bracket indicates the *CYC-TB1* group (class II), the red bracket indicates the clade including *CYC* and *TB1*. At: *Arabidopsis thaliana*; Os: rice; CLEGCYC: *Cadia CYC*-like gene (legume); LLEGCYC: *Lupinus CYC*-like gene (legume); NICYC: tobacco *CYC*-like gene; *PETCYC*: petunia *CYC*-like gene; *SCHCYC*: *Schizanthus wisotonensis CYC*-like gene; Lv: *Linaria vulgaris*; *CYC*: *CYCLOIDEA* (*A. majus*); *DICH*: *DICHOTOMA* (*A. majus*).

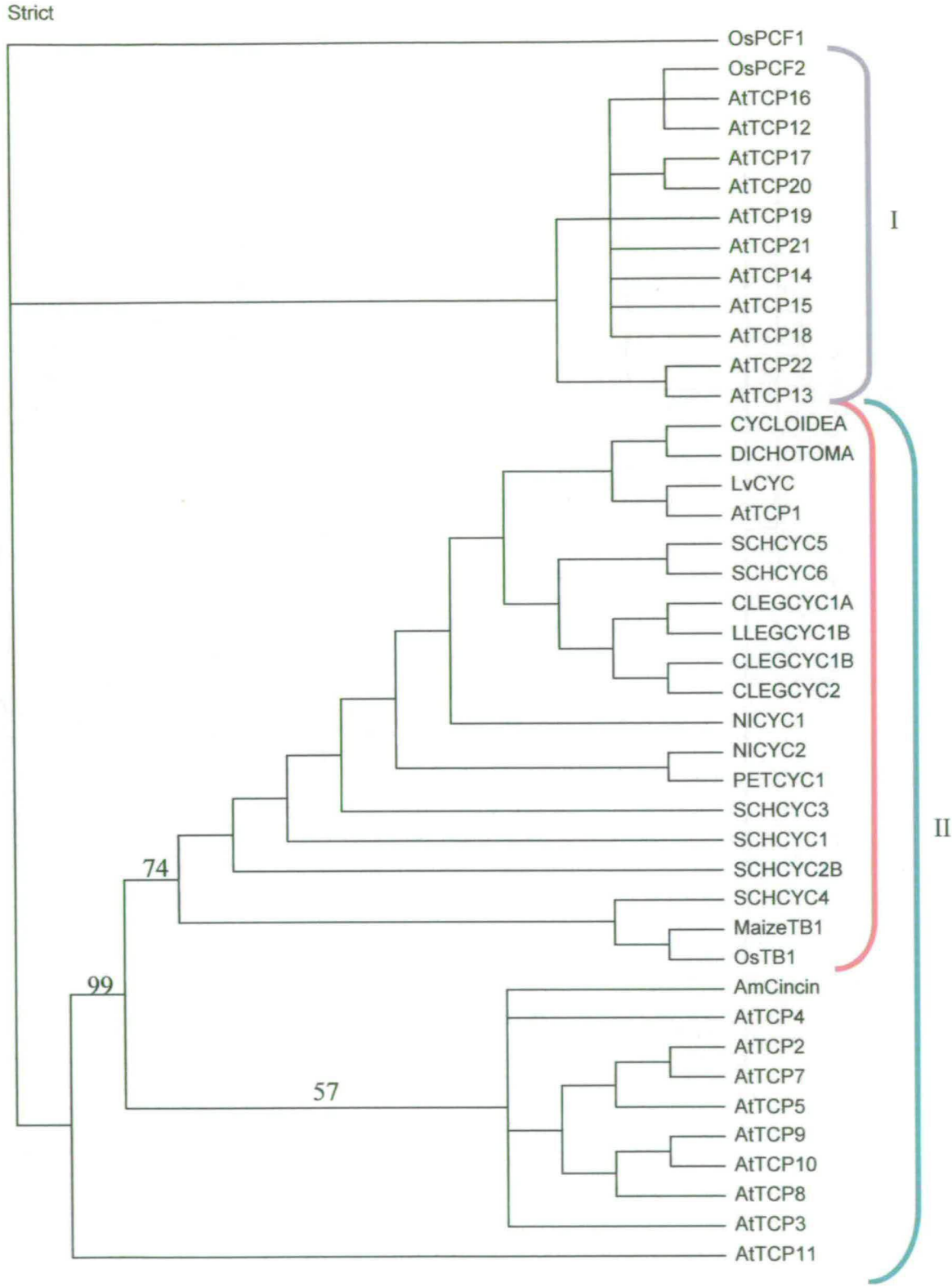
Strict
OsPCF1
OsPCF2
AtTCP16
AtTCP12
AtTCP17
AtTCP20
AtTCP19
AtTCP21
AtTCP14
AtTCP15
AtTCP18
AtTCP22
AtTCP13
CYCLOIDEA
DICHOTOMA
LvCYC
AtTCP1
SCHCYC5
SCHCYC6
CLEGCYC1A
LLEGCYC1B
CLEGCYC1B
CLEGCYC2
NICYC1
NICYC2
PETCYC1
SCHCYC3
SCHCYC1
SCHCYC2B
SCHCYC4
MaizeTB1
OsTB1
AmCincin
AtTCP4
AtTCP2
AtTCP7
AtTCP5
AtTCP9
AtTCP10
AtTCP8
AtTCP3
AtTCP11
74
99
57
I
II

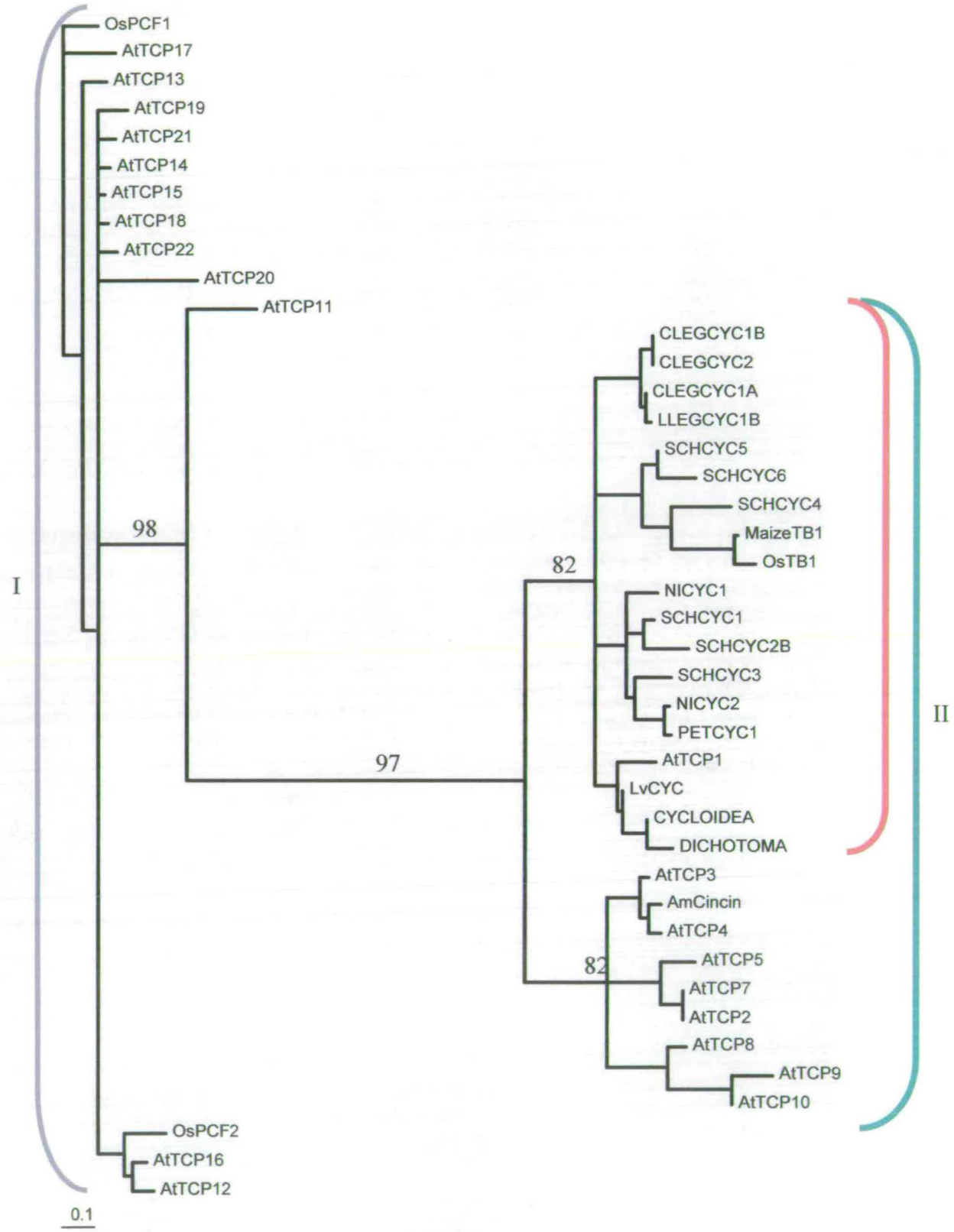
OsPCF1
AtTCP17
AtTCP13
AtTCP19
AtTCP21
AtTCP14
AtTCP15
AtTCP18
AtTCP22
AtTCP20
AtTCP11
98
97
82
82
CLEGCYC1B
CLEGCYC2
CLEGCYC1A
LLEGCYC1B
SCHCYC5
SCHCYC6
SCHCYC4
MaizeTB1
OsTB1
NICYC1
SCHCYC1
SCHCYC2B
SCHCYC3
NICYC2
PETCYC1
AtTCP1
LvCYC
CYCLOIDEA
DICHOTOMA
AtTCP3
AmCincin
AtTCP4
AtTCP5
AtTCP7
AtTCP2
AtTCP8
AtTCP9
AtTCP10
OsPCF2
AtTCP16
AtTCP12
0.1
I
II

Appendix IV.18: Maximum likelihood phylogram (Dayhoff model) on the protein matrix of the TCP domain data set from representative genes of the TCP gene family

This tree was obtained using the Dayhoff model of sequence evolution (Dayhoff *et al*, 1978) on the amino-acid matrix (M1) in Puzzle 5.2. OsPCF1 was chosen as an outgroup. The figures indicate the relevant branch support. The grey bracket indicates the PCF group (class I), the green bracket indicates the *CYC-TB1* group (class II), the red bracket indicates the clade including *CYC* and *TB1*. At: *Arabidopsis thaliana*; Os: rice; CLEGCYC: *Cadia CYC*-like gene (legume); LLEGCYC: *Lupinus CYC*-like gene (legume); NICYC: tobacco *CYC*-like gene; *PETCYC*: petunia *CYC*-like gene; *SCHCYC*: *Schizanthus wisotonensis CYC*-like gene; Lv: *Linaria vulgaris*; *CYC*: *CYCLOIDEA* (*A. majus*); *DICH*: *DICHOTOMA* (*A. majus*).

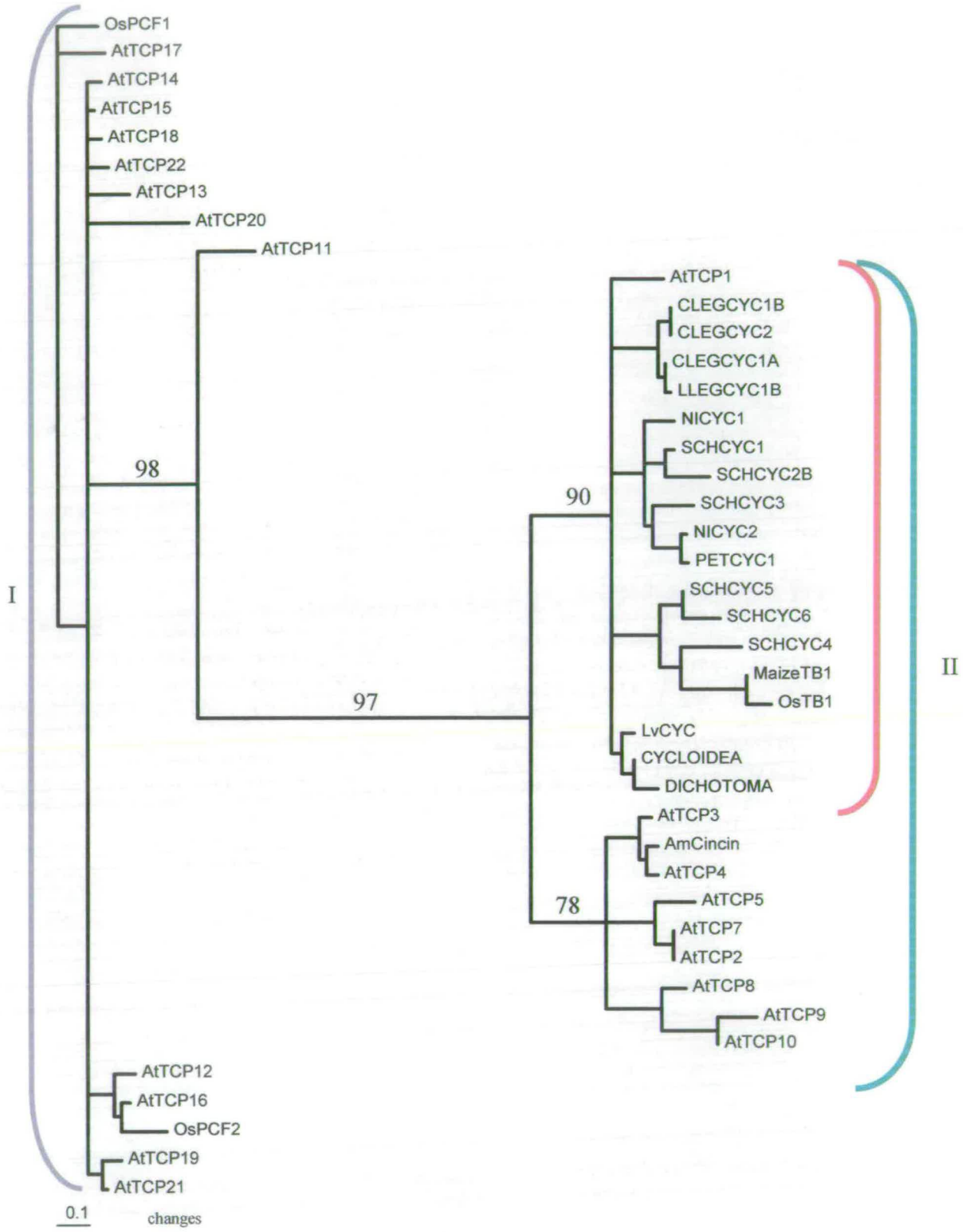
OsPCF1
AtTCP17
AtTCP14
AtTCP15
AtTCP18
AtTCP22
AtTCP13
AtTCP20
AtTCP11
AtTCP1
CLEGCYC1B
CLEGCYC2
CLEGCYC1A
LLEGCYC1B
NICYC1
SCHCYC1
SCHCYC2B
SCHCYC3
NICYC2
PETCYC1
SCHCYC5
SCHCYC6
SCHCYC4
MaizeTB1
OsTB1
LvCYC
CYCLOIDEA
DICHOTOMA
AtTCP3
AmCincin
AtTCP4
AtTCP5
AtTCP7
AtTCP2
AtTCP8
AtTCP9
AtTCP10
AtTCP12
AtTCP16
OsPCF2
AtTCP19
AtTCP21
98
97
90
78
I
II
0.1
changes

Appendix IV.19: Maximum likelihood phylogram (JTT model) on the protein matrix of the TCP domain data set from representative genes of the TCP gene family

This tree was obtained using the JTT model of sequence evolution (Jones *et al*, 1992) on the amino-acid matrix (M1) in Puzzle 5.2. OsPCF1 was chosen as an outgroup. The figures indicate the relevant branch support. The grey bracket indicates the PCF group (class I), the green bracket indicates the *CYC-TB1* group (class II), the red bracket indicates the clade including *CYC* and *TB1*. At: *Arabidopsis thaliana*; Os: rice; CLEGCYC: *Cadia CYC*-like gene (legume); LLEGCYC: *Lupinus CYC*-like gene (legume); NICYC: tobacco *CYC*-like gene; *PETCYC*: petunia *CYC*-like gene; *SCHCYC*: *Schizanthus wisotonensis CYC*-like gene; Lv: *Linaria vulgaris*; *CYC*: *CYCLOIDEA* (*A. majus*); *DICH*: *DICHOTOMA* (*A. majus*).

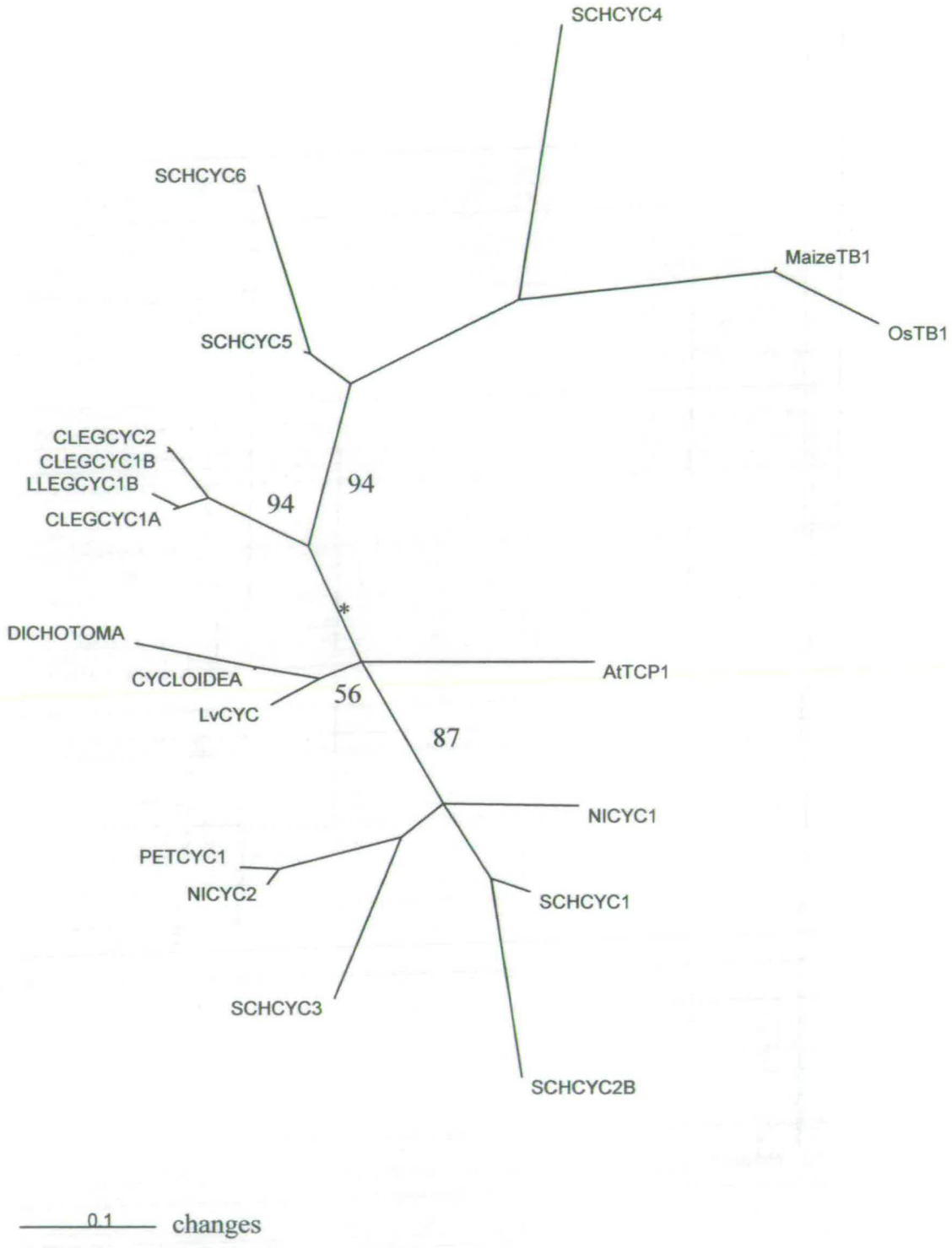

Appendix IV.21: Unrooted Maximum likelihood phylogram (VT model) on the protein matrix of the TCP domain data set from representative genes from the clade including *CYC* and *TB1*
This tree was obtained using the VT model of sequence evolution (Mueller – Vingron, 2000) on the amino-acid matrix (M2) in Puzzle 5.2. *OsTB1* was chosen as an outgroup. The figures indicate the relevant branch support. The asterix indicates BS< 50%. At: *Arabidopsis thaliana*; Os: rice; CLEGCYC: *Cadia CYC*-like gene (legume); LLEGCYC: *Lupinus CYC*-like gene (legume); NICYC: tobacco *CYC*-like gene; *PETCYC*: petunia *CYC*-like gene; *SCHCYC*: *Schizanthus wisotonensis CYC*-like gene; Lv: *Linaria vulgaris*; *CYCLOIDEA* (*A. majus*); *DICHOTOMA* (*A. majus*).

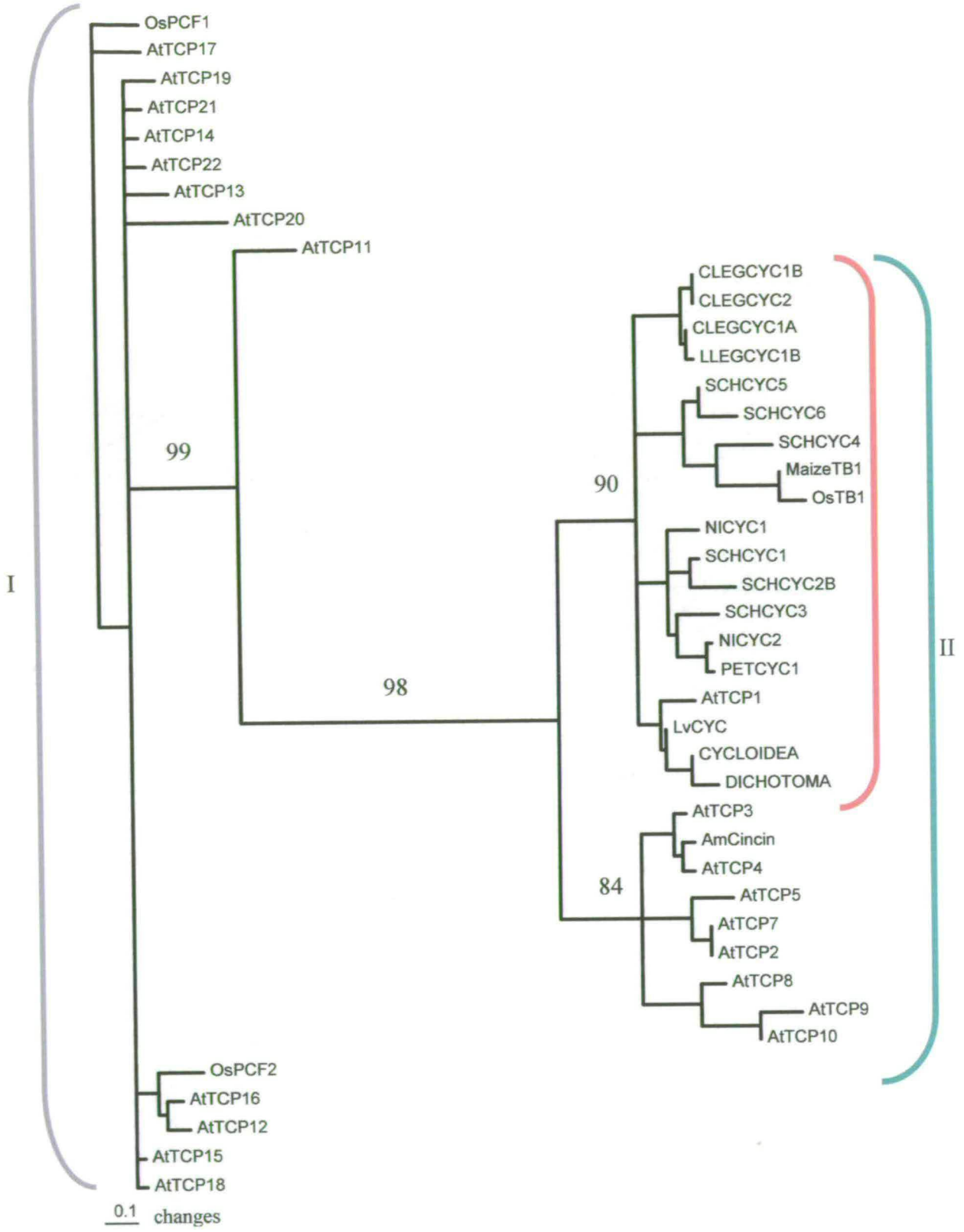

Appendix IV.20: Unrooted Maximum likelihood phylogram (WAG model) on the protein matrix with the TCP domain data set and representative genes of the TCP gene family

This tree was obtained using the WAG model of sequence evolution (Wehlan and Goldman, 2000) on the amino-acid matrix (M1) in Puzzle 5.2. OsPCF1 was chosen as an outgroup. The figures indicate the relevant branch support. The grey bracket indicates the PCF group (class I), the green bracket indicates the *CYC-TB1* group (class II), the red bracket indicates the clade including *CYC* and *TB1*. At: *Arabidopsis thaliana*; Os: rice; CLEGCYC: *Cadia CYC*-like gene (legume); LLEGCYC: *Lupinus CYC*-like gene (legume); NICYC: tobacco *CYC*-like gene; *PETCYC*: petunia *CYC*-like gene; *SCHCYC*: *Schizanthus wisotonensis CYC*-like gene; Lv: *Linaria vulgaris*; *CYC*: *CYCLOIDEA* (*A. majus*); *DICH*: *DICHOTOMA* (*A. majus*).

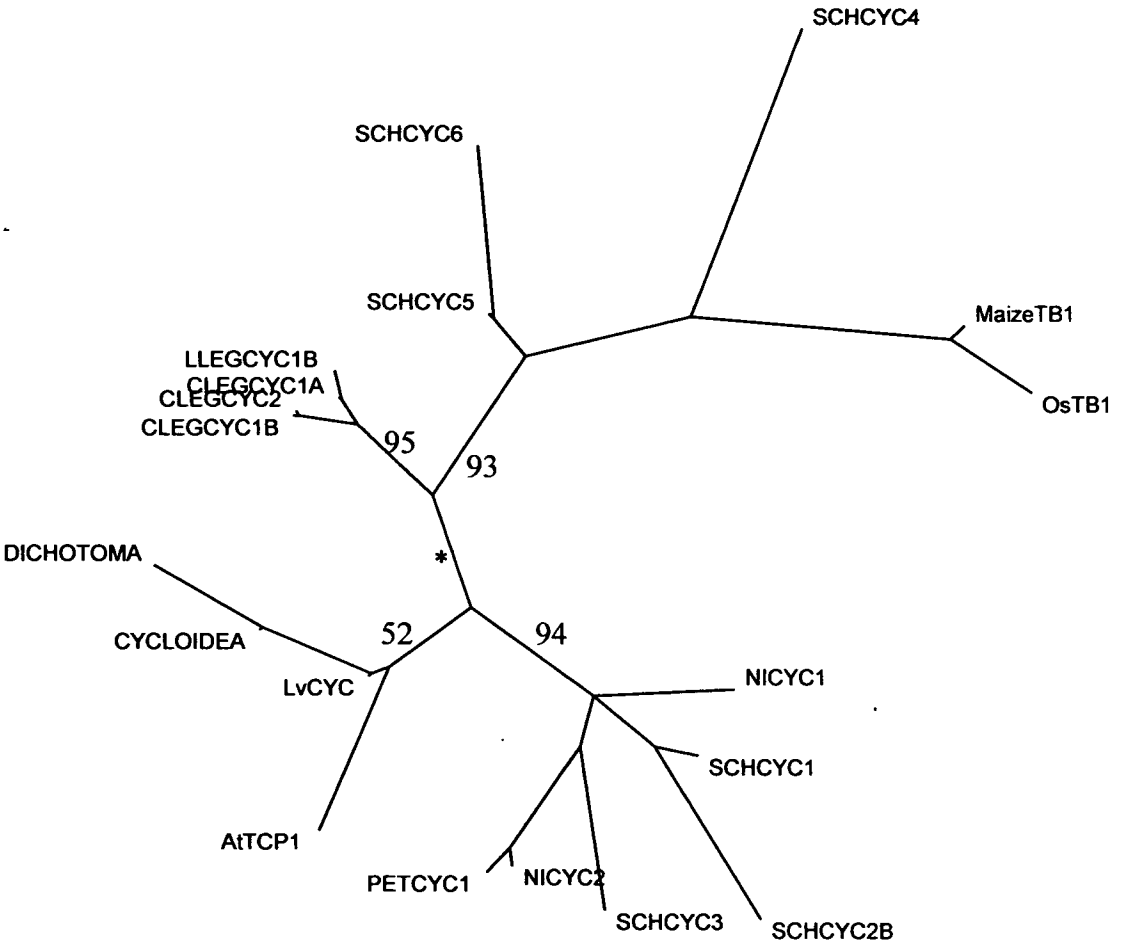

Appendix IV.22: Unrooted Maximum likelihood phylogram (Dayhoff model) on the protein matrix of the TCP domain data set from representative genes of the clade including *CYC* and *TB1*

This tree was obtained using the Dayhoff model of sequence evolution (Dayhoff *et al*, 1978) on the amino-acid matrix (M2) in Puzzle 5.2. *OsTB1* was chosen as an outgroup. The figures indicate the relevant branch support. The asterix indicates BS< 50%. At: *Arabidopsis thaliana*; Os: rice; CLEGCYC: *Cadia CYC*-like gene (legume); LLEGCYC: *Lupinus CYC*-like gene (legume); NICYC: tobacco *CYC*-like gene; *PETCYC*: petunia *CYC*-like gene; *SCHCYC*: *Schizanthus wisotonensis CYC*-like gene; Lv: *Linaria vulgaris*; *CYCLOIDEA* (*A. majus*); *DICHOTOMA* (*A. majus*).

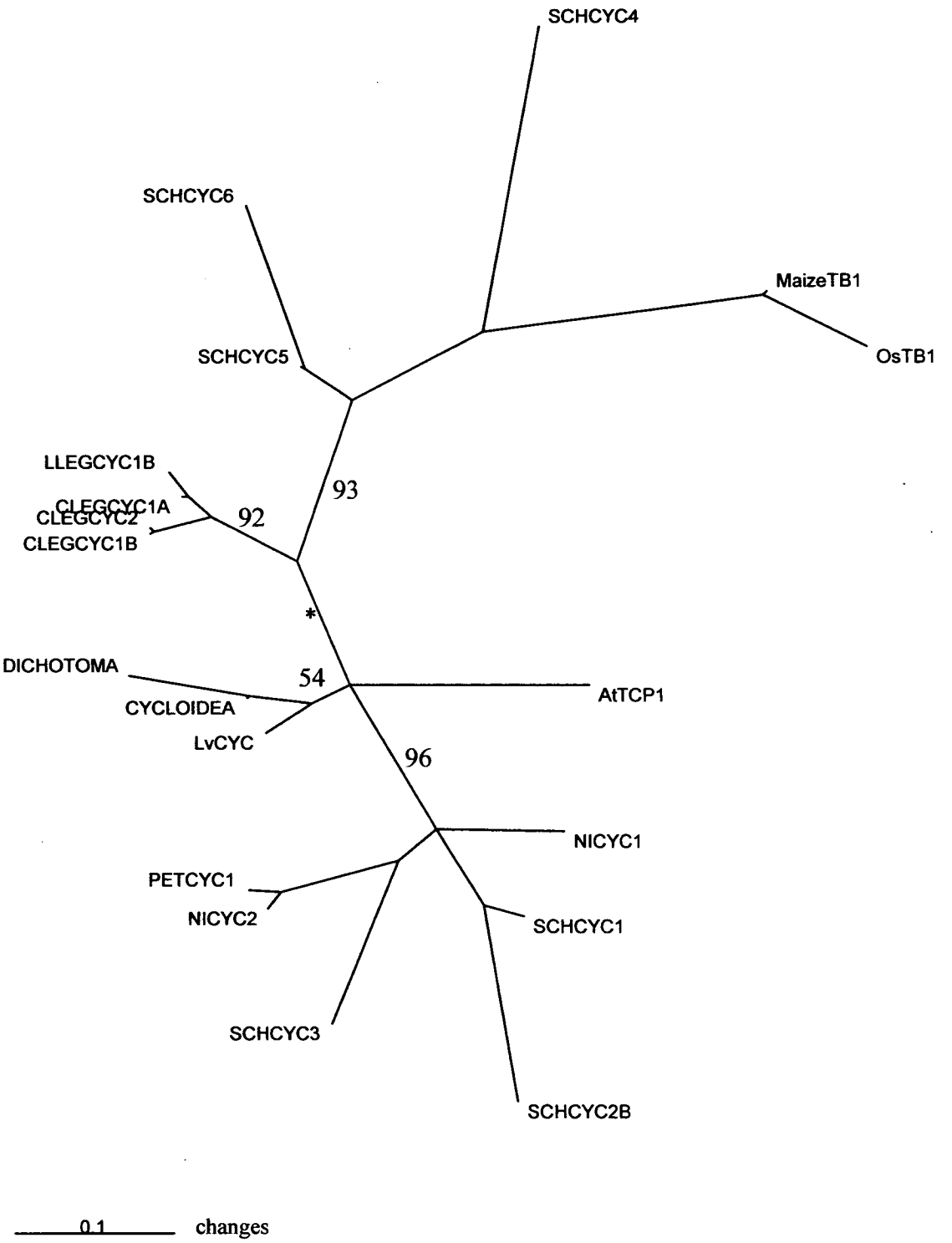

Appendix IV.23: Unrooted Maximum likelihood phylogram (JTT model) on the protein matrix of the TCP domain data set from representative genes of the clade including *CYC* and *TB1*

This tree was obtained using the JTT model of sequence evolution (Jones *et al*, 1992) on the amino-acid matrix (M2) in Puzzle 5.2. *OsTB1* was chosen as an outgroup. The figures indicate the relevant branch support. The asterix indicates BS< 50%. At: *Arabidopsis thaliana*; Os: rice; CLEGCYC: *Cadia CYC*-like gene (legume); LLEGCYC: *Lupinus CYC*-like gene (legume); NICYC: tobacco *CYC*-like gene; *PETCYC*: petunia *CYC*-like gene; *SCHCYC*: *Schizanthus wisotonensis CYC*-like gene; Lv: *Linaria vulgaris*; *CYCLOIDEA* (*A. majus*); *DICHOTOMA* (*A. majus*).

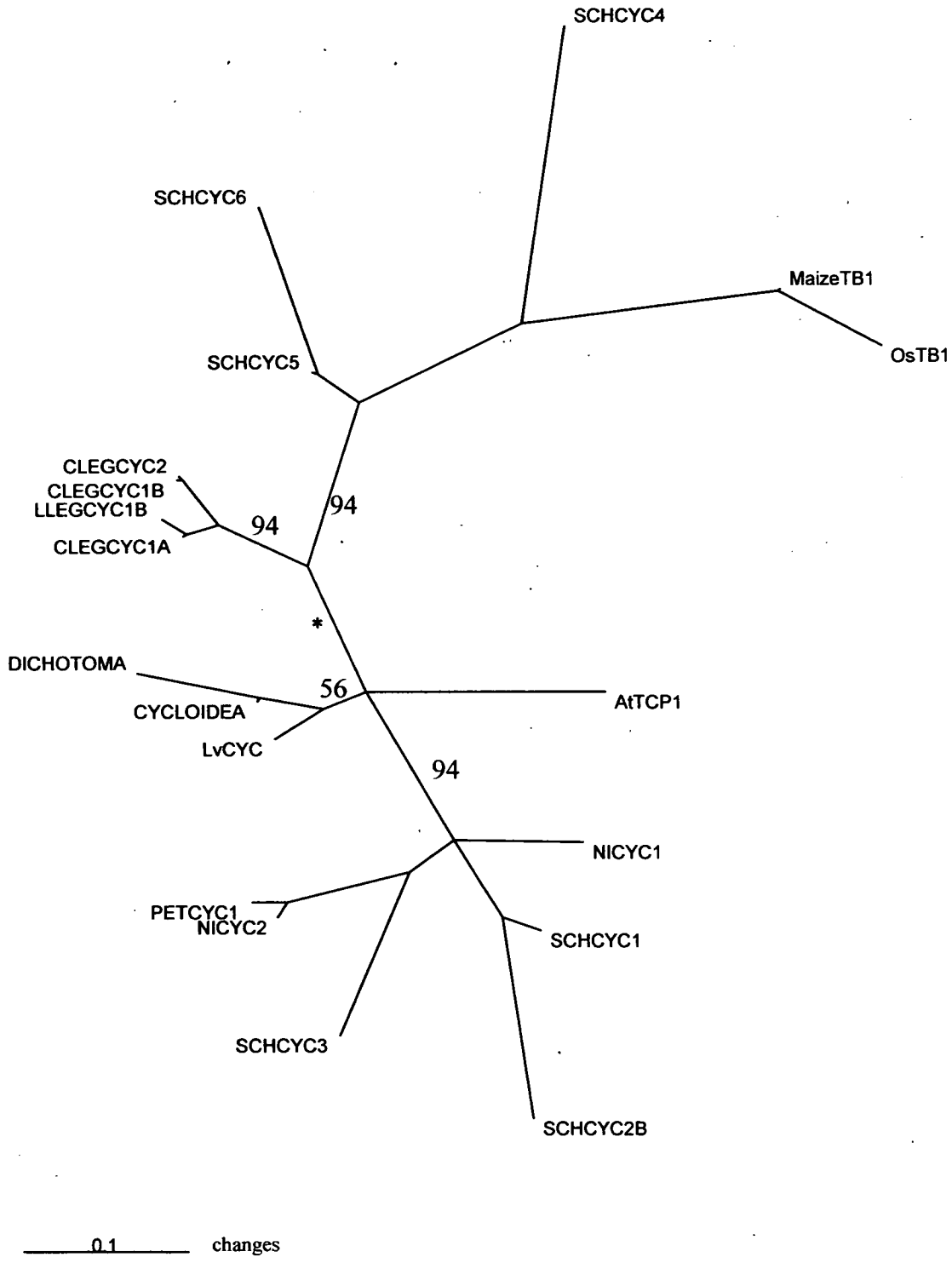

Appendix IV.24: Unrooted Maximum likelihood phylogram (WAG model) on the protein matrix of the TCP domain data set from representative genes of the clade including *CYC* and *TB1*

This tree was obtained using the WAG model of sequence evolution (Wehlan and Goldman, 2000) on the amino-acid matrix (M2) in Puzzle 5.2. *OsTB1* was chosen as an outgroup. The figures indicate the relevant branch support. The asterix indicates BS< 50%. At: *Arabidopsis thaliana*; Os: rice; CLEGCYC: *Cadia CYC*-like gene (legume); LLEGCYC: *Lupinus CYC*-like gene (legume); NICYC: tobacco *CYC*-like gene; *PETCYC*: petunia *CYC*-like gene; *SCHCYC*: *Schizanthus wisotonensis CYC*-like gene; Lv: *Linaria vulgaris*; *CYCLOIDEA* (*A. majus*); *DICHOTOMA* (*A. majus*).

Appendix IV.25: Unrooted strict consensus ML cladogram obtained with a Bayesian approach on the nucleotide matrix of the TCP domain data set from representative genes of the clade including *CYC* and *TB1*.

The analysis was carried out using MrBayes v3.Ob4 and 1 500 000 generations. At: *Arabidopsis thaliana*; Os: rice; CLEGCYC: *Cadia CYC*-like gene (legume); LLEGCYC: *Lupinus CYC*-like gene (legume); NICYC: tobacco *CYC*-like gene; *PETCYC*: petunia *CYC*-like gene; *SCHCYC*: *Schizanthus wisotonensis CYC*-like gene; Lv: *Linaria vulgaris*; *CYCLOIDEA* (*A. majus*); *DICHOTOMA* (*A. majus*).

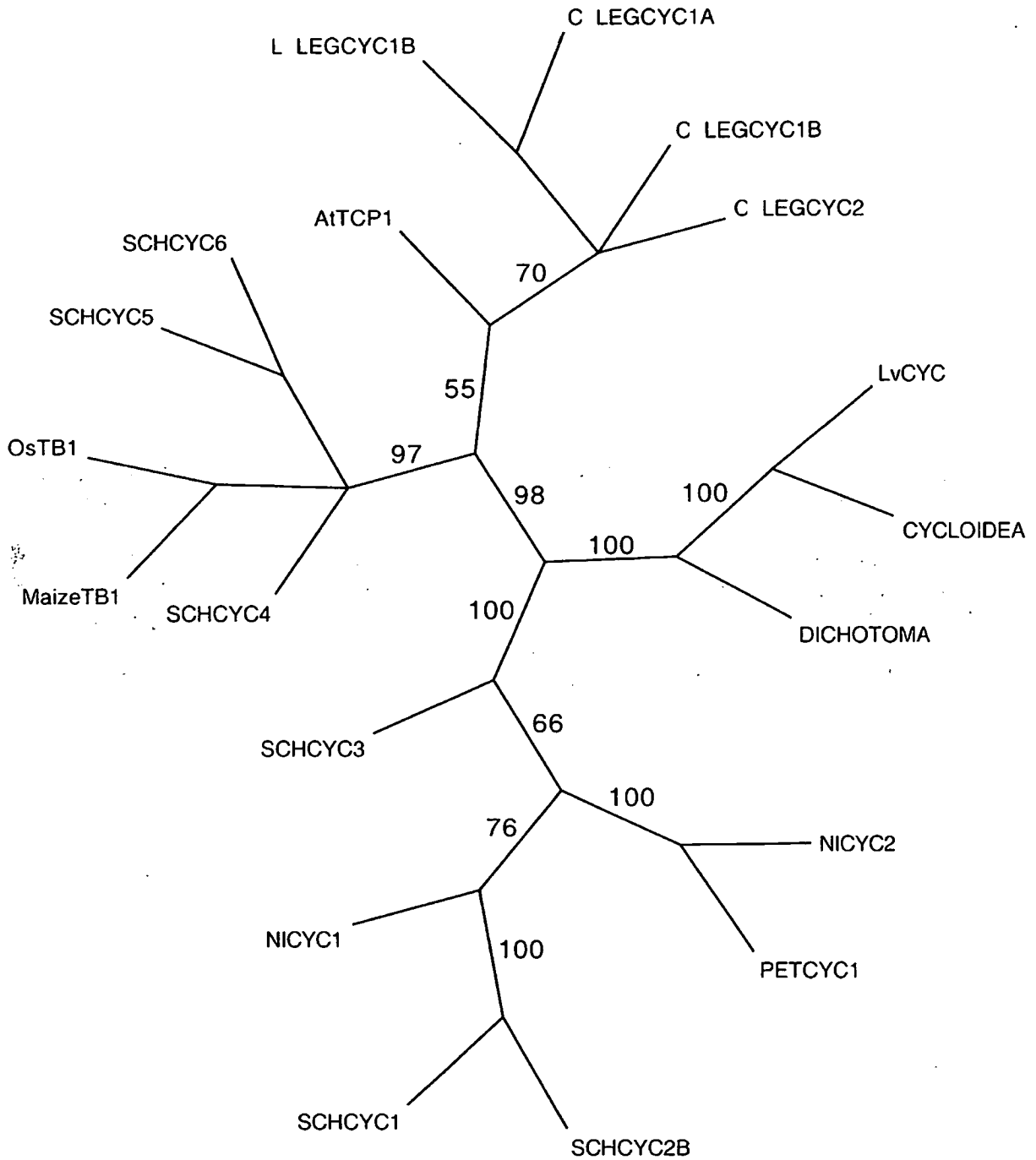
C LEGCYC1A
L LEGCYC1B
C LEGCYC1B
C LEGCYC2
AtTCP1
SCHCYC6
70
SCHCYC5
55
LvCYC
OsTB1
97
98
100
CYCLOIDEA
100
MaizeTB1
SCHCYC4
100
DICHOTOMA
66
SCHCYC3
100
76
NICYC2
NICYC1
100
PETCYC1
SCHCYC1
SCHCYC2B

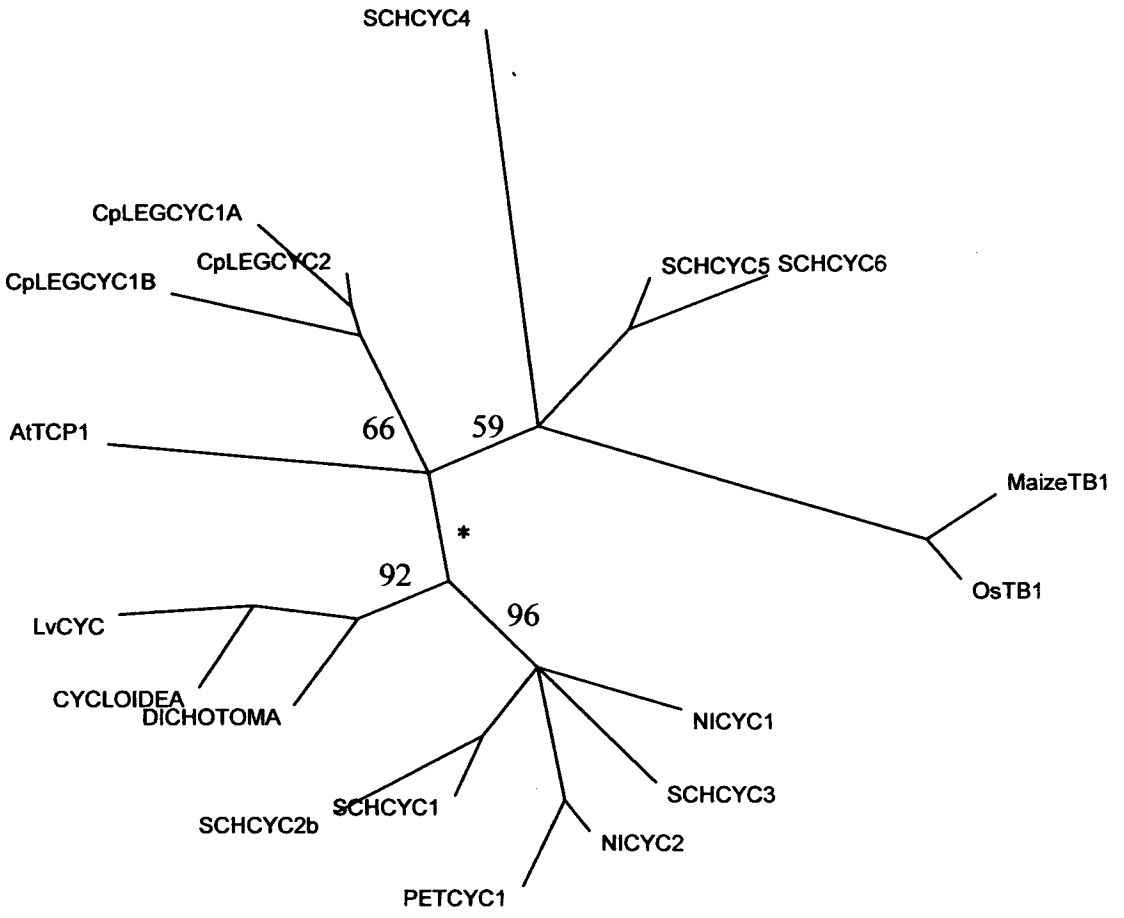

Appendix IV.26: Unrooted Maximum Likelihood phylogram (HKY model) on the nucleotide matrix of the TCP domain data set from representative genes of the clade including *CYC* and *TB1*

This tree was obtained using the HKY model of sequence evolution (Hasegawa *et al.*, 1985) on the nucleotide matrix (M3) in Puzzle 5.2. *OsTB1* was chosen as an outgroup. The asterix indicates BS< 50%. At: *Arabidopsis thaliana*; Os: rice; CLEGCYC: *Cadia CYC*-like gene (legume); LLEGCYC: *Lupinus CYC*-like gene (legume); NICYC: tobacco *CYC*-like gene; *PETCYC*: petunia *CYC*-like gene; *SCHCYC*: *Schizanthus wisotonensis CYC*-like gene; Lv: *Linaria vulgaris*; *CYCLOIDEA* (*A. majus*); *DICHOTOMA* (*A. majus*).

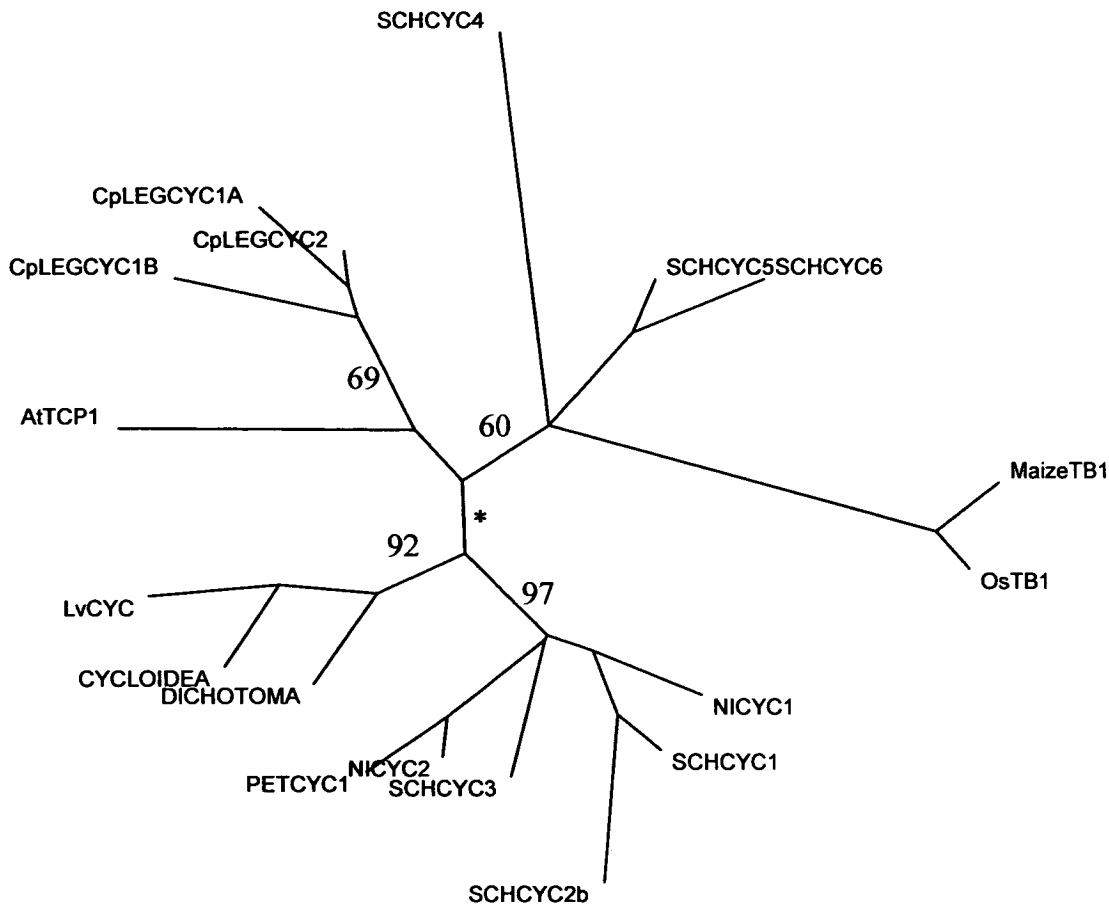

Appendix IV.27: Unrooted Maximum Likelihood phylogram (TN model) on the nucleotide matrix of the TCP domain data set from representative genes of the clade including *CYC* and *TB1*
This tree was obtained using the TN model of sequence evolution (Tumara and Nei, 1993) on the nucleotide matrix (M3) in Puzzle 5.2. *OsTB1* was chosen as an outgroup. The asterix indicates BS< 50%. At: *Arabidopsis thaliana*; Os: rice; CLEGCYC: *Cadia CYC*-like gene (legume); LLEGCYC: *Lupinus CYC*-like gene (legume); NICYC: tobacco *CYC*-like gene; *PETCYC*: petunia *CYC*-like gene; *SCHCYC*: *Schizanthus wisotonensis CYC*-like gene; Lv: *Linaria vulgaris*; *CYCLOIDEA* (*A. majus*); *DICHOTOMA* (*A. majus*).

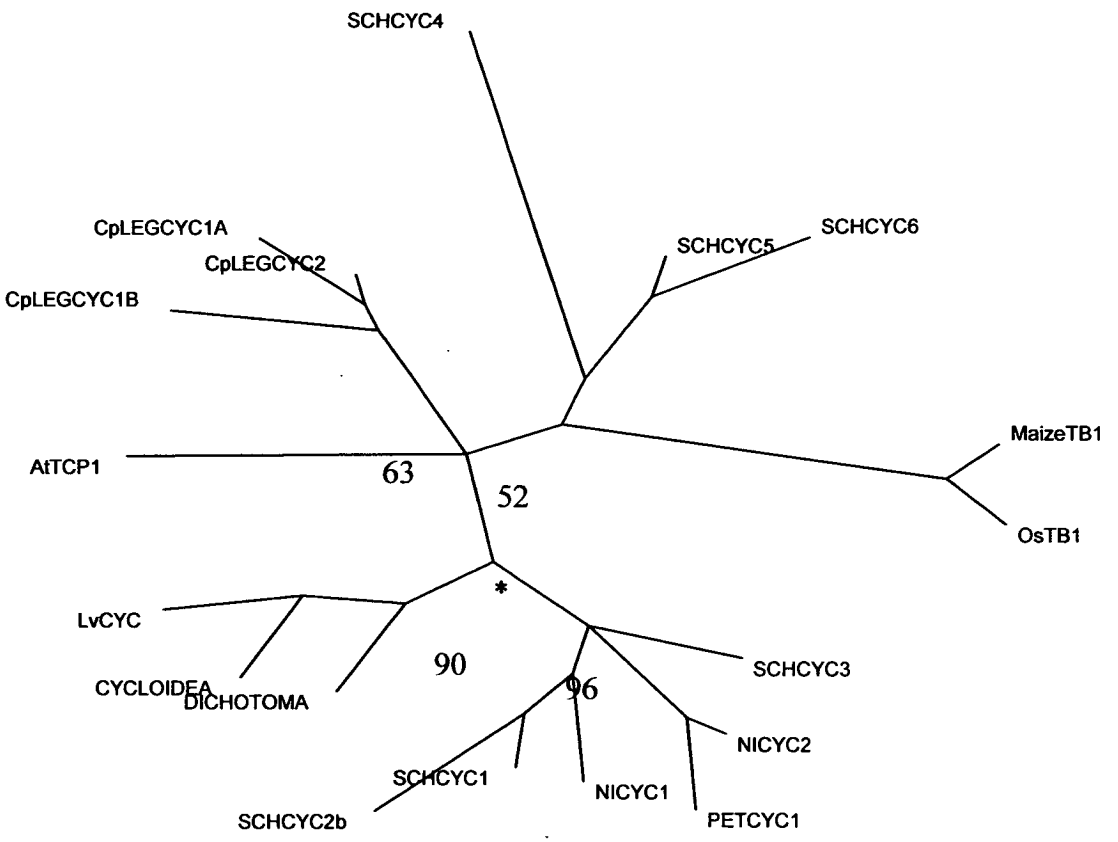

Appendix IV.28: Unrooted Maximum Likelihood phylogram (GTR model) on the nucleotide matrix of the TCP dc changes t from representative genes of the clade including *CYC* and *TB1*

This tree was obtained using the GTR model of sequence evolution (Lanave *et al.*, 1980) on the nucleotide matrix (M3) in Puzzle 5.2. *OsTB1* was chosen as an outgroup. The asterix indicates BS< 50%. At: *Arabidopsis thaliana*; Os: rice; CLEGCYC: *Cadia CYC*-like gene (legume); LLEGCYC: *Lupinus CYC*-like gene (legume); NICYC: tobacco *CYC*-like gene; *PETCYC*: petunia *CYC*-like gene; *SCHCYC*: *Schizanthus wisotonensis CYC*-like gene; Lv: *Linaria vulgaris*; *CYCLOIDEA* (*A. majus*); *DICHOTOMA* (*A. majus*).

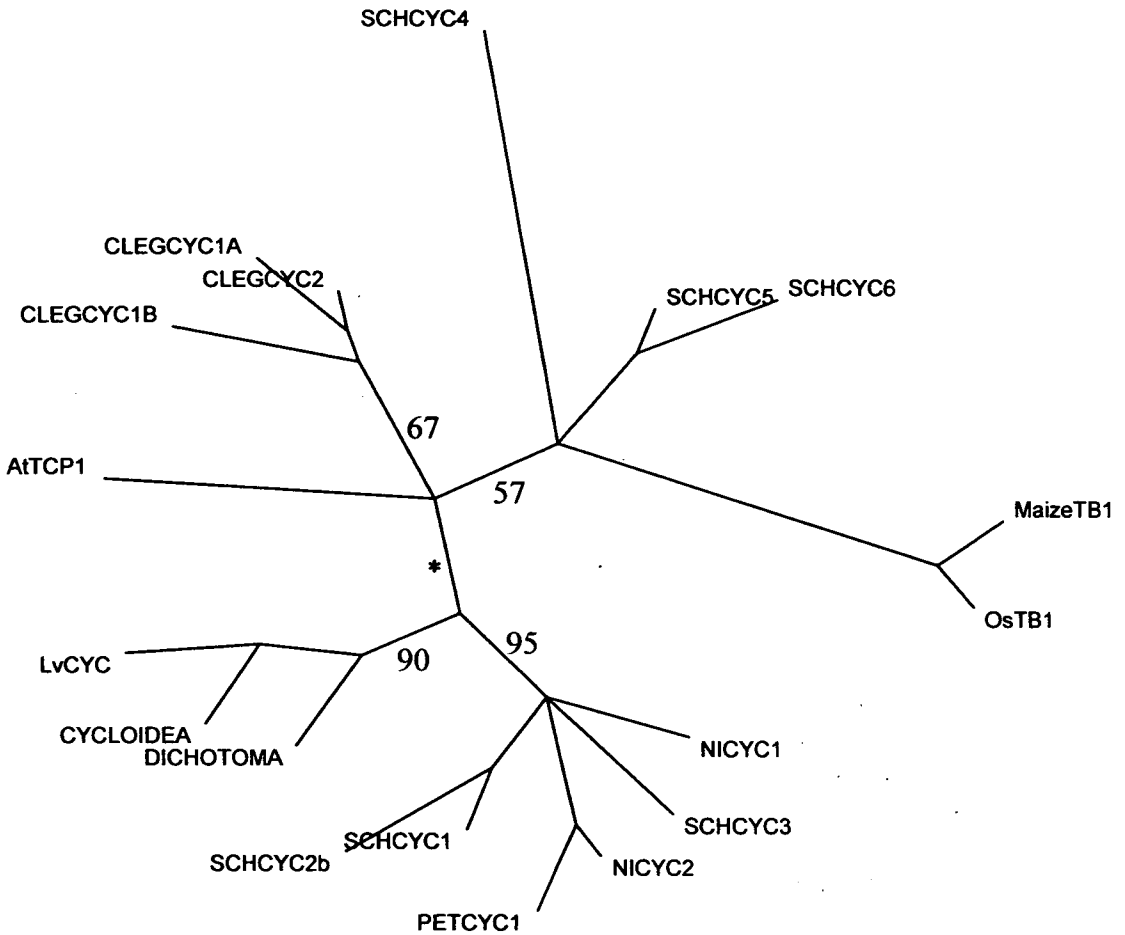

Appendix IV.29: Unrooted Maximum Likelihood phylogram (SH model) on the nucleotide matrix of the TCP domain data set from representative genes of the clade including *CYC* and *TB1*
This tree was obtained using the SH model of sequence evolution (Schöniger, M. and Von Haeseler, 1994) on the nucleotide matrix (M3) in Puzzle 5.2. *OsTB1* was chosen as an outgroup. The asterix indicates BS< 50%. At: *Arabidopsis thaliana*; Os: rice; CLEGCYC: *Cadia CYC*-like gene (legume); LLEGCYC: *Lupinus CYC*-like gene (legume); NICYC: tobacco *CYC*-like gene; *PETCYC*: petunia *CYC*-like gene; *SCHCYC*: *Schizanthus wisotonensis CYC*-like gene; Lv: *Linaria vulgaris*; *CYCLOIDEA* (*A. majus*); *DICHOTOMA* (*A. majus*).

Appendix IV.30: Maximum likelihood strict consensus tree based on the nucleotide matrix of representative genes of the clade including *CYC* and *TB1*

A heuristic search was carried on the nucleotide matrix (M3) in Paup 4.0b10 with the likelihood model (TrN+I+G). This model was selected by AIC in Modeltest 3.5. The heuristic search was carried out using the factory settings except for the addition sequence which was as-is. 3120 rearrangements were tried and the best likelihood score was found to be 1858.9. Bootstrap analysis was done with 100 replicates, no swapping, the addition sequence on random: rep#:1and the option mull tree off. The resulting strict consensus tree was mostly unresolved. At: *Arabidopsis thaliana*; Os: rice; CLEGCYC: *Cadia CYC*-like gene (legume); LLEGCYC: *Lupinus CYC*-like gene (legume); NICYC: tobacco *CYC*-like gene; *PETCYC*: petunia *CYC*-like gene; *SCHCYC*: *Schizanthus wisotonensis CYC*-like gene; Lv: *Linaria vulgaris*; *CYCLOIDEA* (*A. majus*); *DICHOTOMA* (*A. majus*).

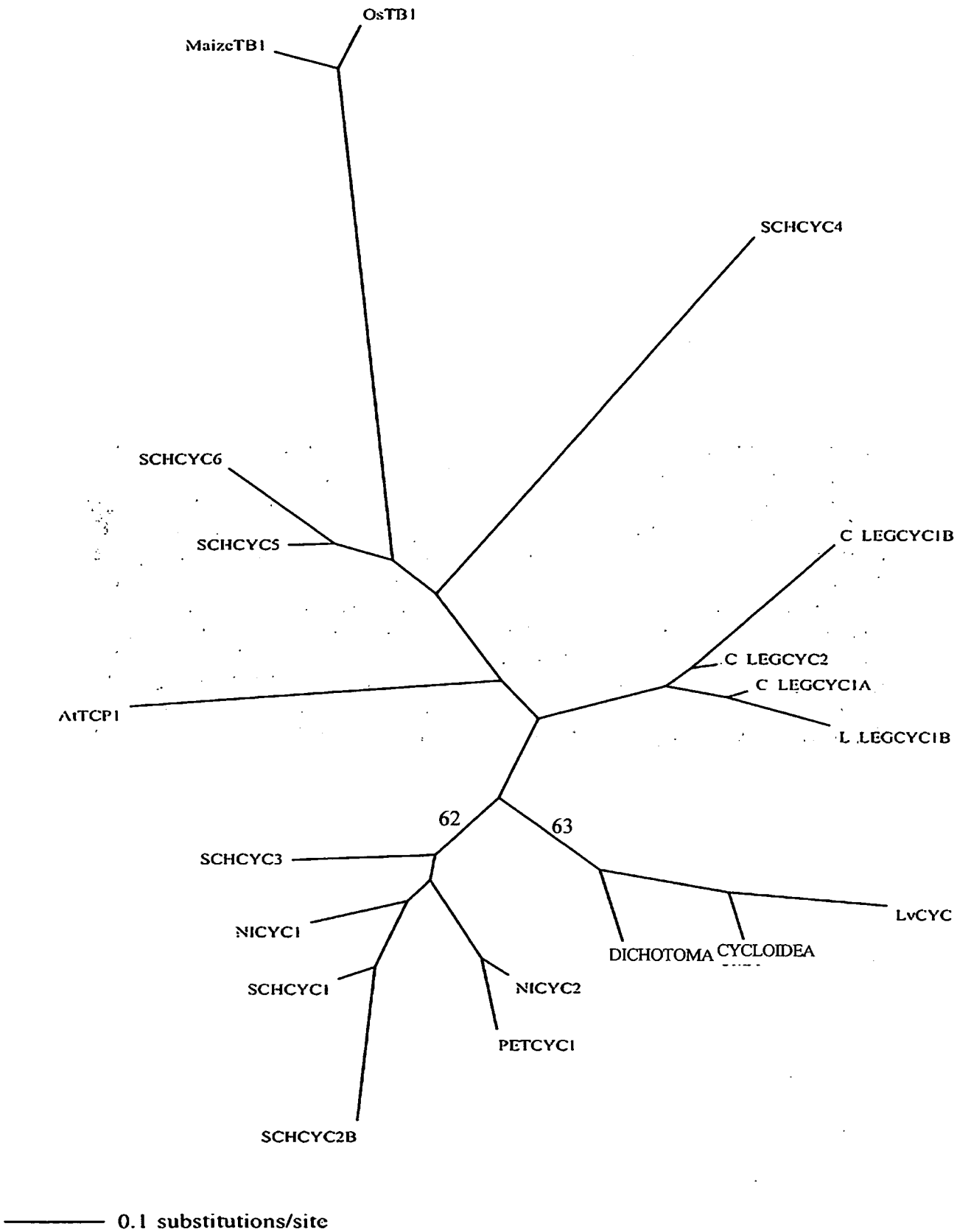
OsTB1
MaizeTB1
SCHCYC4
SCHCYC6
SCHCYC5
C LEGCYC1B
C LEGCYC2
C LEGCYC1A
AtTCP1
L LEGCYC1B
62
63
SCHCYC3
LvCYC
NICYC1
DICHOTOMA
CYCLOIDEA
SCHCYC1
NICYC2
PETCYC1
SCHCYC2B
0.1 substitutions/site

NJ

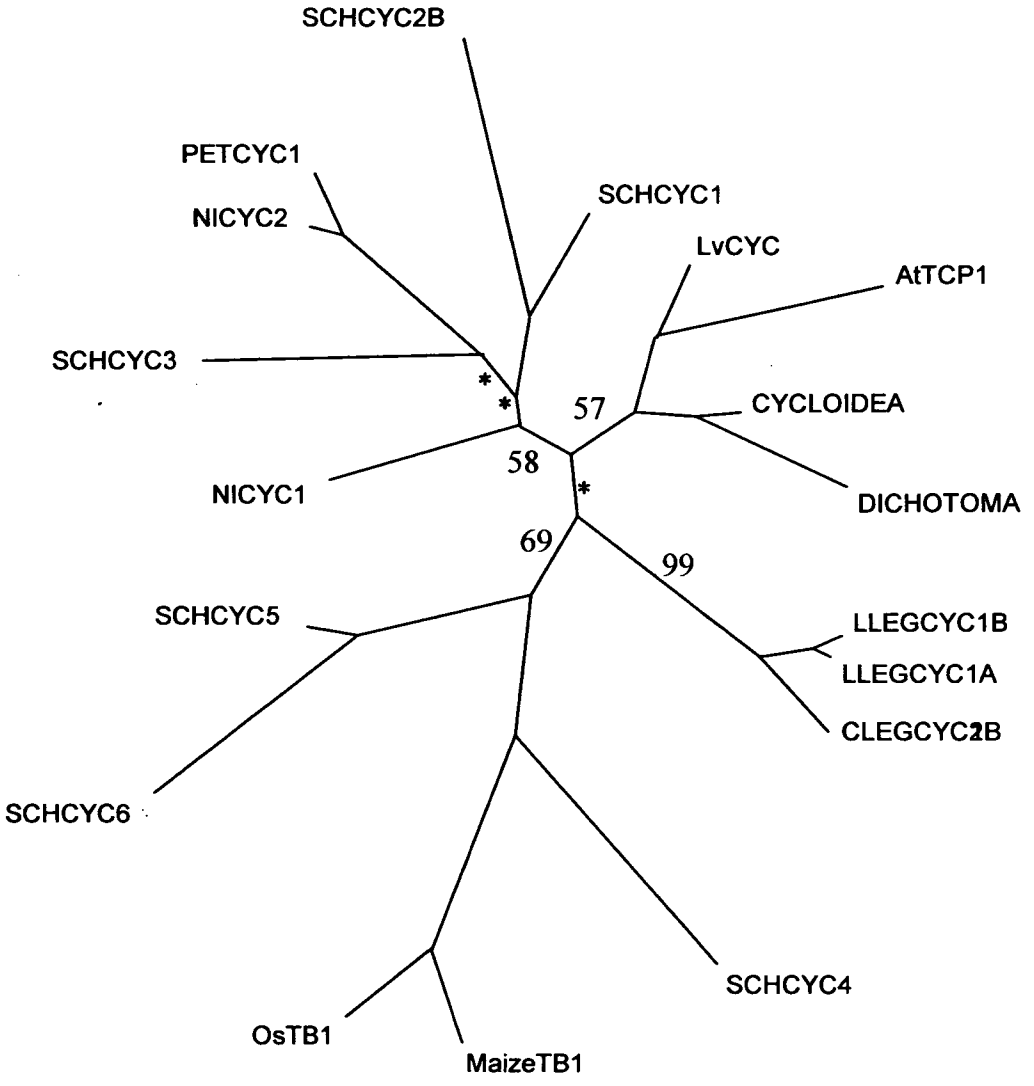

Appendix IV.31: Unrooted phylogram of protein distance NJ analysis of the TCP domain data set from representative genes of the clade including *CYC* and *TB1*

This tree was obtained with a NJ (Neighbor-Joining) analysis in PAUP 4.0b10 on the protein matrix (M2). For clarity, only the relevant support values obtained with 100 000 bootstrap replicates are included. The asterix indicates BS< 50%. At: *Arabidopsis thaliana*; Os: rice; CLEGCYC: *Cadia CYC*-like gene (legume); LLEGCYC: *Lupinus CYC*-like gene (legume); NICYC: tobacco *CYC*-like gene; *PETCYC*: petunia *CYC*-like gene; *SCHCYC*: *Schizanthus wisotonensis CYC*-like gene; Lv: *Linaria vulgaris*; *CYCLOIDEA* (*A. majus*); *DICHOTOMA* (*A. majus*).

UPGMA

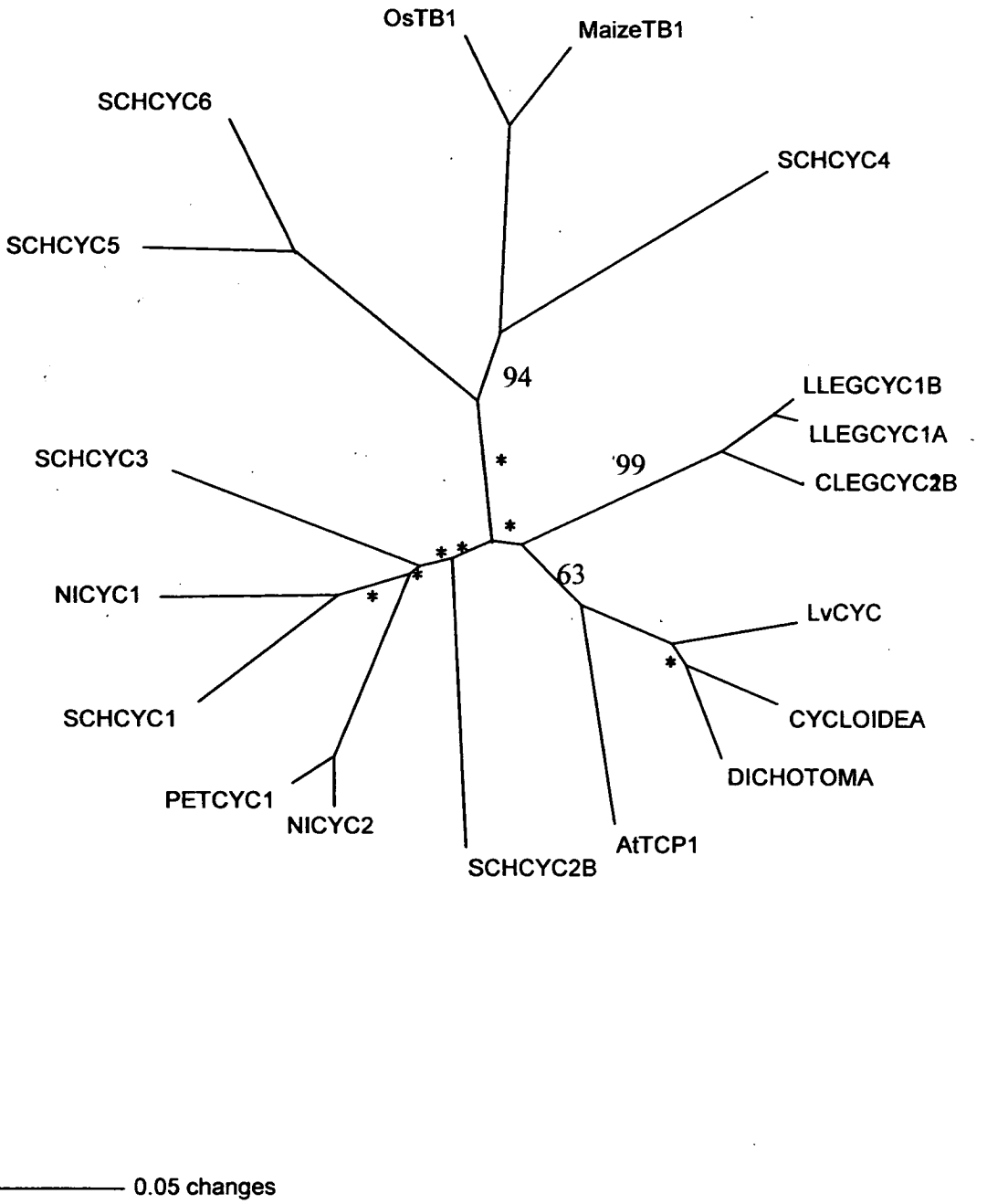

Appendix IV.32: Unrooted phylogram of protein distance UPGMA analysis of the TCP domain data set with representative genes of the clade including *CYC* and *TB1*

This tree was obtained with a UPGMA analysis in PAUP 4.0b10 on the protein matrix (M2). For clarity, only the relevant support values obtained with 100 000 bootstrap replicates are included. The asterix indicates BS< 50%. At: *Arabidopsis thaliana*; Os: rice; CLEGCYC: *Cadia CYC*-like gene (legume); LLEGCYC: *Lupinus CYC*-like gene (legume); NICYC: tobacco *CYC*-like gene; *PETCYC*: petunia *CYC*-like gene; *SCHCYC*: *Schizanthus wisotonensis CYC*-like gene; Lv: *Linaria vulgaris*; *CYCLOIDEA* (*A. majus*); *DICHOTOMA* (*A. majus*).

Appendix IV.33: Unrooted phylogram of nucleotide distance NJ analysis of the TCP domain data set from representative genes of the clade including *CYC* and *TB1*

This tree was obtained with a NJ (Neighbor-Joining) analysis in PAUP 4.0b10 and the maximum likelihood settings obtained in Modeltest 3.5 on the nucleotide matrix (M3). For clarity, only the relevant support values obtained with 10 000 bootstrap replicates are included. The asterix indicates BS< 50%. At: *Arabidopsis thaliana*; Os: rice; CLEGCYC: *Cadia CYC*-like gene (legume); LLEGCYC: *Lupinus CYC*-like gene (legume); NICYC: tobacco *CYC*-like gene; *PETCYC*: petunia *CYC*-like gene; *SCHCYC*: *Schizanthus wisotonensis CYC*-like gene; Lv: *Linaria vulgaris*; *CYCLOIDEA* (*A. majus*); *DICHOTOMA* (*A. majus*).

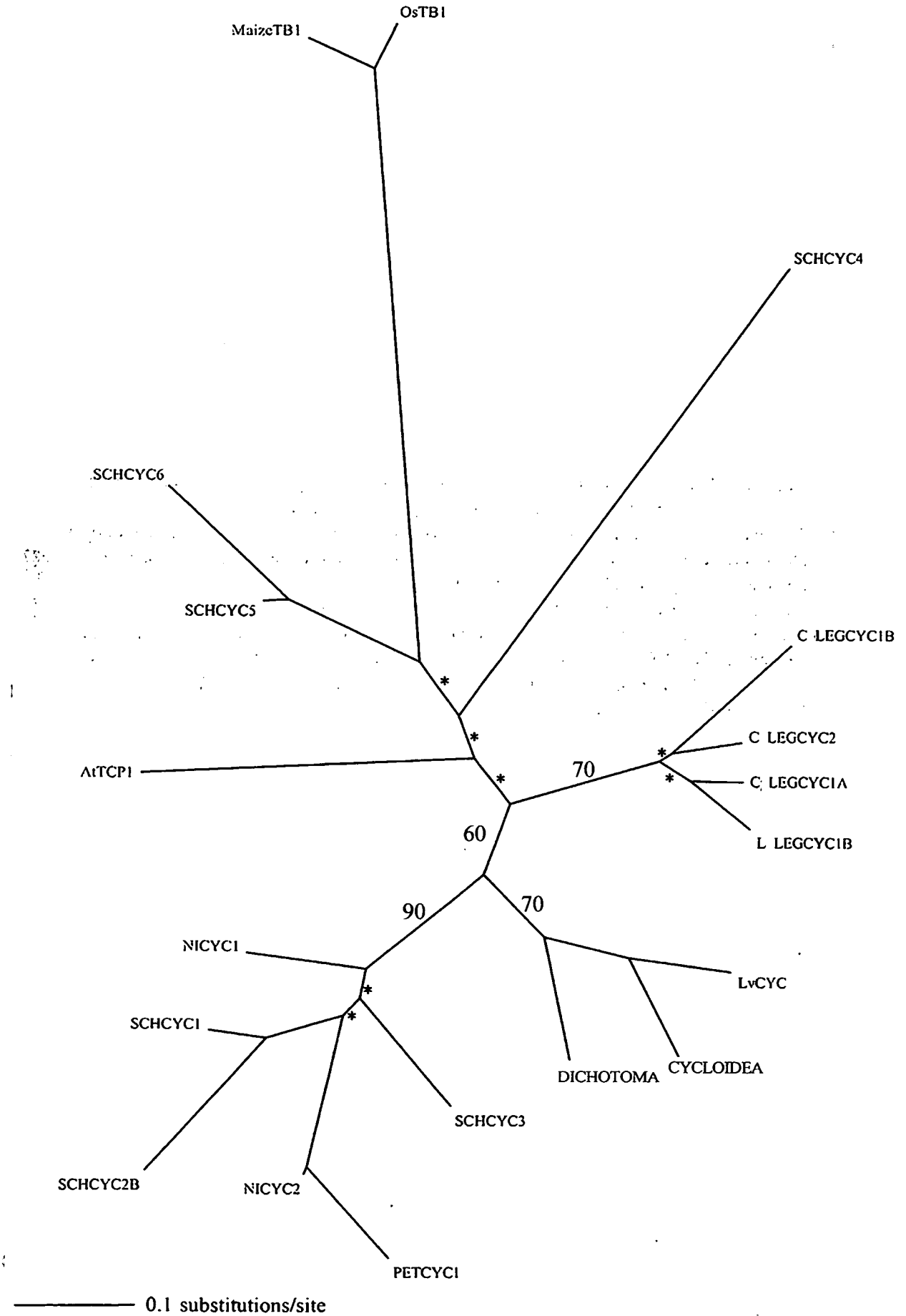
OsTB1
MaizeTB1
SCHCYC4
SCHCYC6
SCHCYC5
C LEGCYC1B
C LEGCYC2
AtTCP1
70
C LEGCYC1A
L LEGCYC1B
60
90
70
NICYC1
LvCYC
SCHCYC1
DICHOTOMA
CYCLOIDEA
SCHCYC3
SCHCYC2B
NICYC2
PETCYC1
0.1 substitutions/site

Appendix IV.34: Unrooted phylogram of nucleotide distance UPGMA analysis of the TCP domain data set from representative genes of the clade including *CYC* and *TB1*

This tree was obtained with a UPGMA analysis in PAUP 4.0b10 and the maximum likelihood settings obtained in Modeltest 3.5 on the nucleotide matrix (M3). For clarity, only the relevant support values obtained with 10 000 bootstrap replicates are included. The asterix indicates BS< 50%. At: *Arabidopsis thaliana*; Os: rice; CLEGCYC: *Cadia CYC*-like gene (legume); LLEGCYC: *Lupinus CYC*-like gene (legume); NICYC: tobacco *CYC*-like gene; *PETCYC*: petunia *CYC*-like gene; *SCHCYC*: *Schizanthus wisotonensis CYC*-like gene; Lv: *Linaria vulgaris*; *CYCLOIDEA* (*A. majus*); *DICHOTOMA* (*A. majus*).

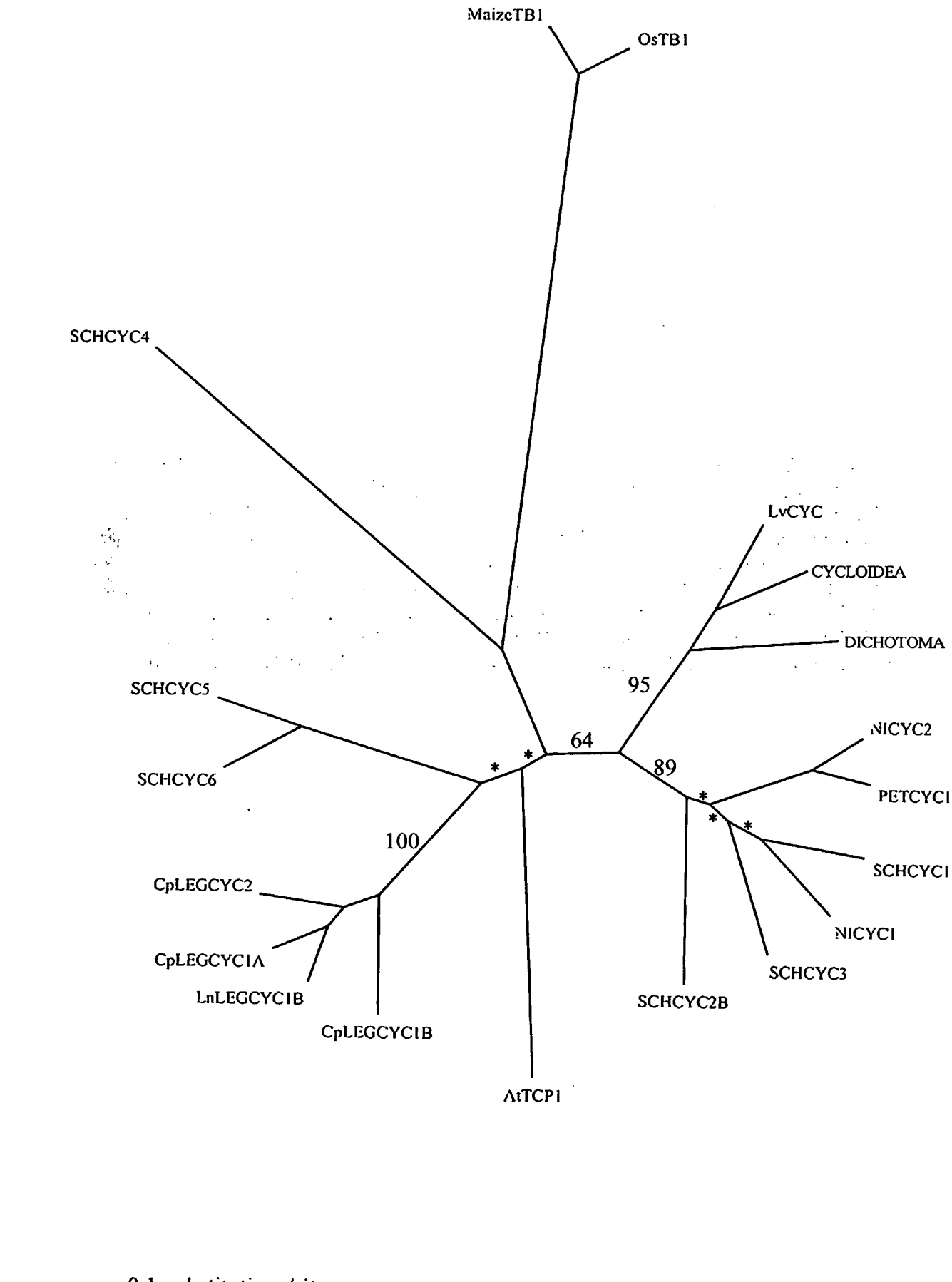
MaizeTB1
OsTB1
SCHCYC4
LvCYC
CYCLOIDEA
DICHOTOMA
SCHCYC5
SCHCYC6
95
64
89
NICYC2
PETCYC1
100
CpLEGCYC2
CpLEGCYC1A
LnLEGCYC1B
CpLEGCYC1B
SCHCYC1
NICYC1
SCHCYC3
SCHCYC2B
AtTCP1
0.1 substitutions/site

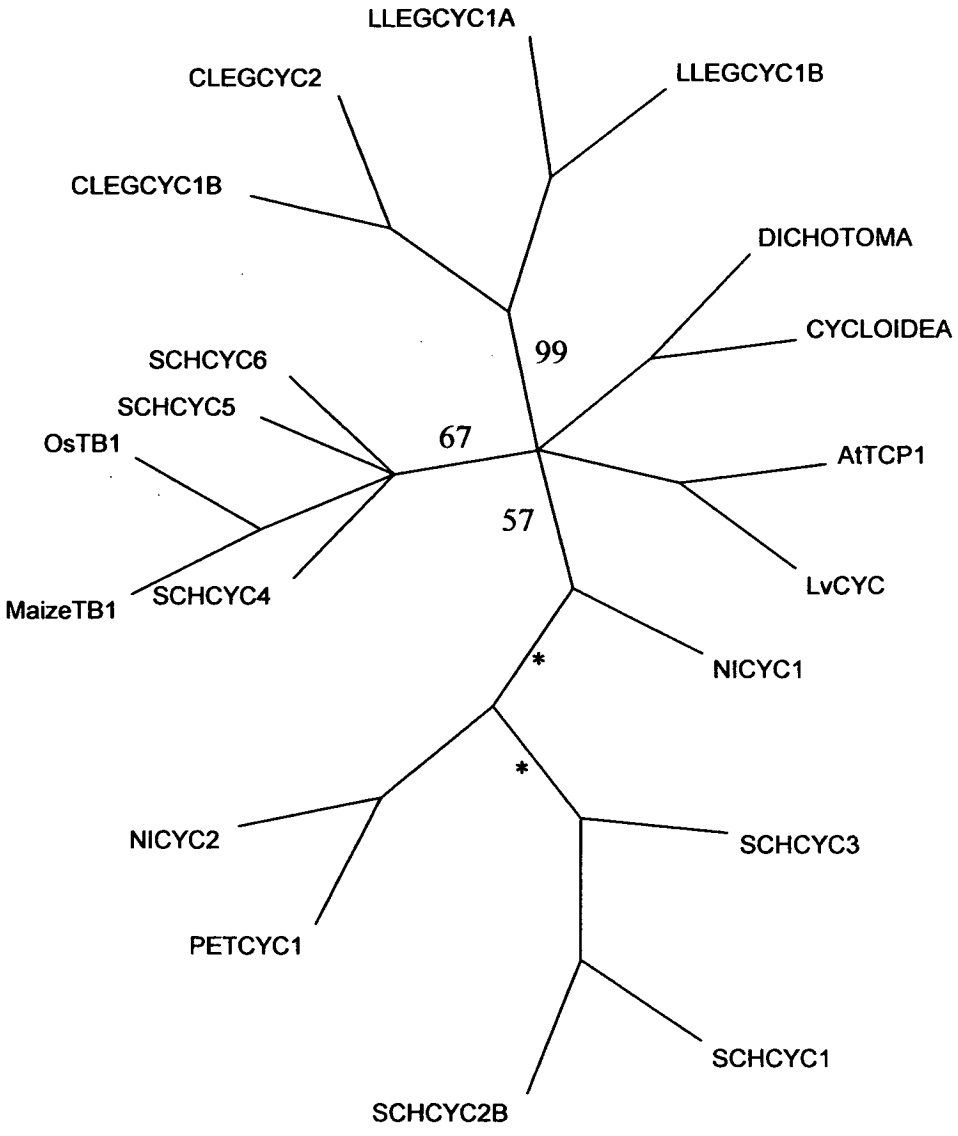

Appendix IV.35: Unrooted strict consensus parsimony cladogram obtained with a heuristic search on the protein matrix of the TCP domain data set from representative genes of the clade including *CYC* and *TB1*

The parsimony analysis was carried out in PAUP 4.0b10 on the protein matrix (M2). It produced 11 equally parsimonious trees of 99 steps. The consistency index was: 0.79 and the retention index: 0.80. The branch support values correspond to bootstrap % obtained with 100 000 replicates (factory settings except for no swapping and addition sequence : asis). The asterix indicates BS< 50%. At: *Arabidopsis thaliana*; Os: rice; CLEGCYC: *Cadia CYC*-like gene (Legume); LLEGCYC: *Lupinus CYC*-like gene (Legume); NICYC: tobacco *CYC*-like gene; *PETCYC*: petunia *CYC*-like gene; *SCHCYC*: *Schizanthus wisotonensis CYC*-like gene; Lv: *Linaria vulgaris*; *CYCLOIDEA* (*A. majus*); *DICHOTOMA* (*A. majus*).

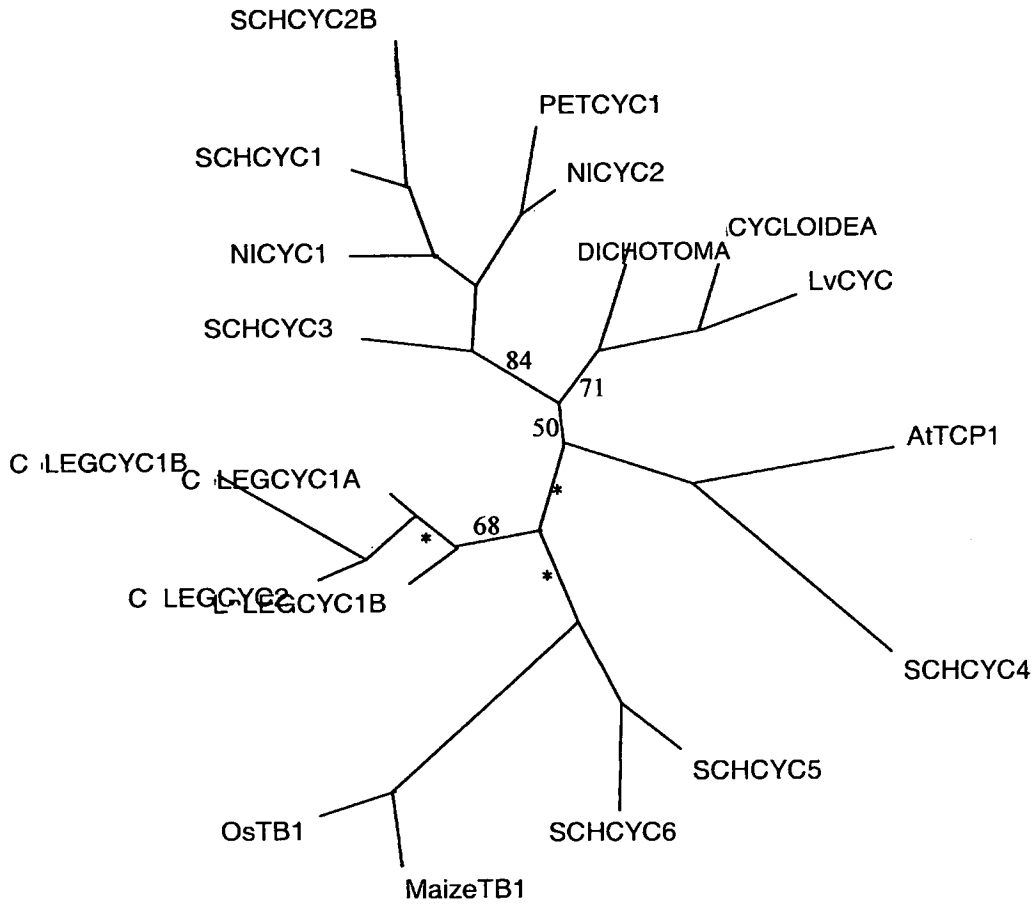

Appendix IV.36: Unrooted strict consensus parsimony phylogram obtained with a heuristic search on the nucleotide matrix of the TCP domain data set from representative genes of the clade including *CYC* and *DICH*

The parsimony analysis was carried out in PAUP 4.0b10 on the nucleotide matrix (M3). It produced 1 tree of 405 steps. The consistency index was: 0.48 and the retention index: 0,55. The branch support values correspond to bootstrap % obtained with 100 000 replicates (factory settings except for no swapping and addition sequence : asis). The asterix indicates BS< 50%. At: *Arabidopsis thaliana*; Os: rice; CLEGCYC: *Cadia CYC*-like gene (legume); LLEGCYC: *Lupinus CYC*-like gene (legume); NICYC: tobacco *CYC*-like gene; *PETCYC*: petunia *CYC*-like gene; *SCHCYC*: *Schizanthus wisotonensis CYC*-like gene; Lv: *Linaria vulgaris*; *CYCLOIDEA* (*A. majus*); *DICHOTOMA* (*A. majus*).

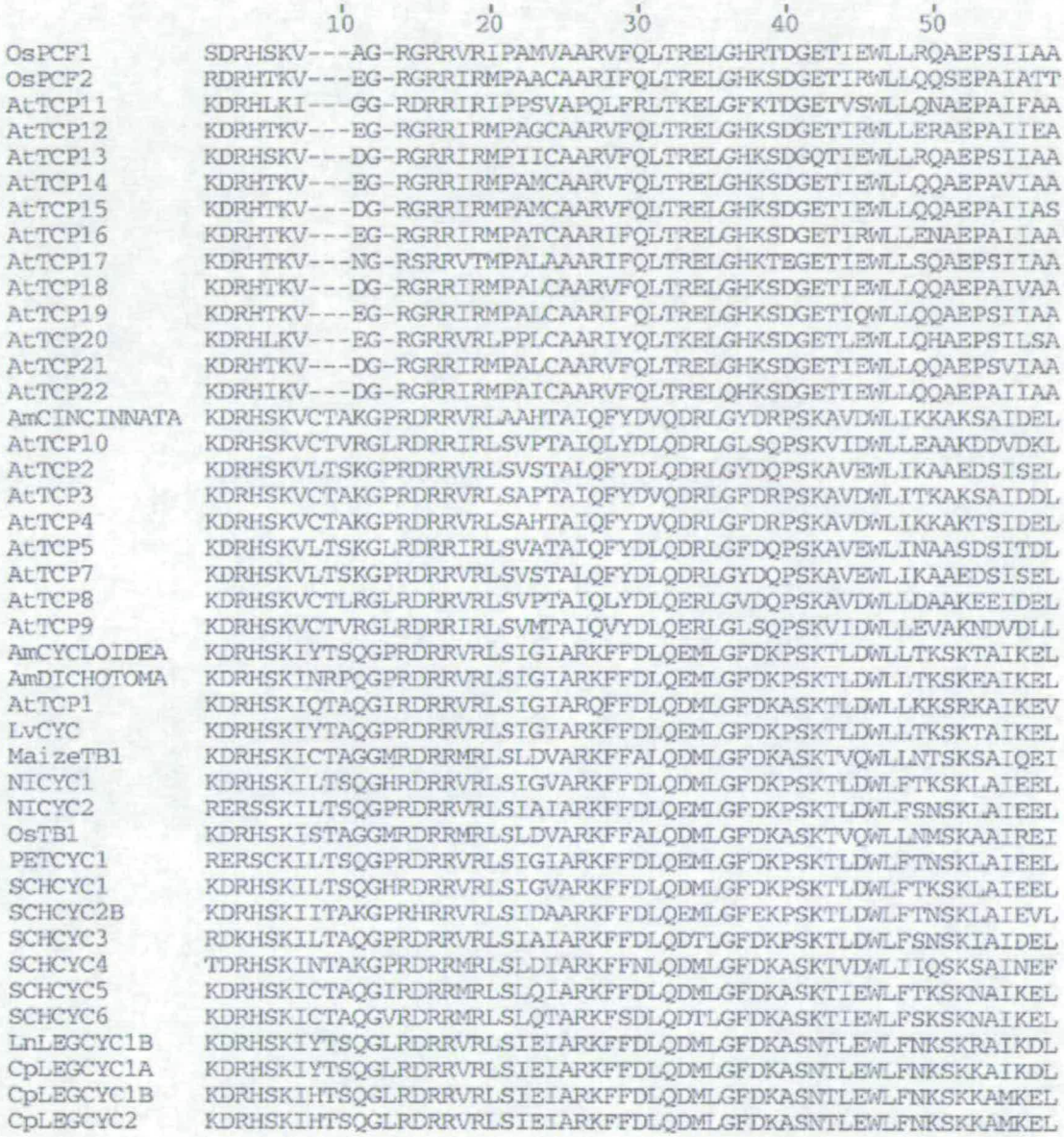

Appendix IV.37: Protein matrix M1

At: *Arabidopsis thaliana*; Os: rice; CLEGCYC: *Cadia CYC*-like gene (legume); LLEGCYC: *Lupinus CYC*-like gene (legume); NICYC: tobacco *CYC*-like gene; *PETCYC*: petunia *CYC*-like gene; *SCHCYC*: *Schizanthus wisotonensis CYC*-like gene; Lv: *Linaria vulgaris*; *Am: Antirrhinum majus.*

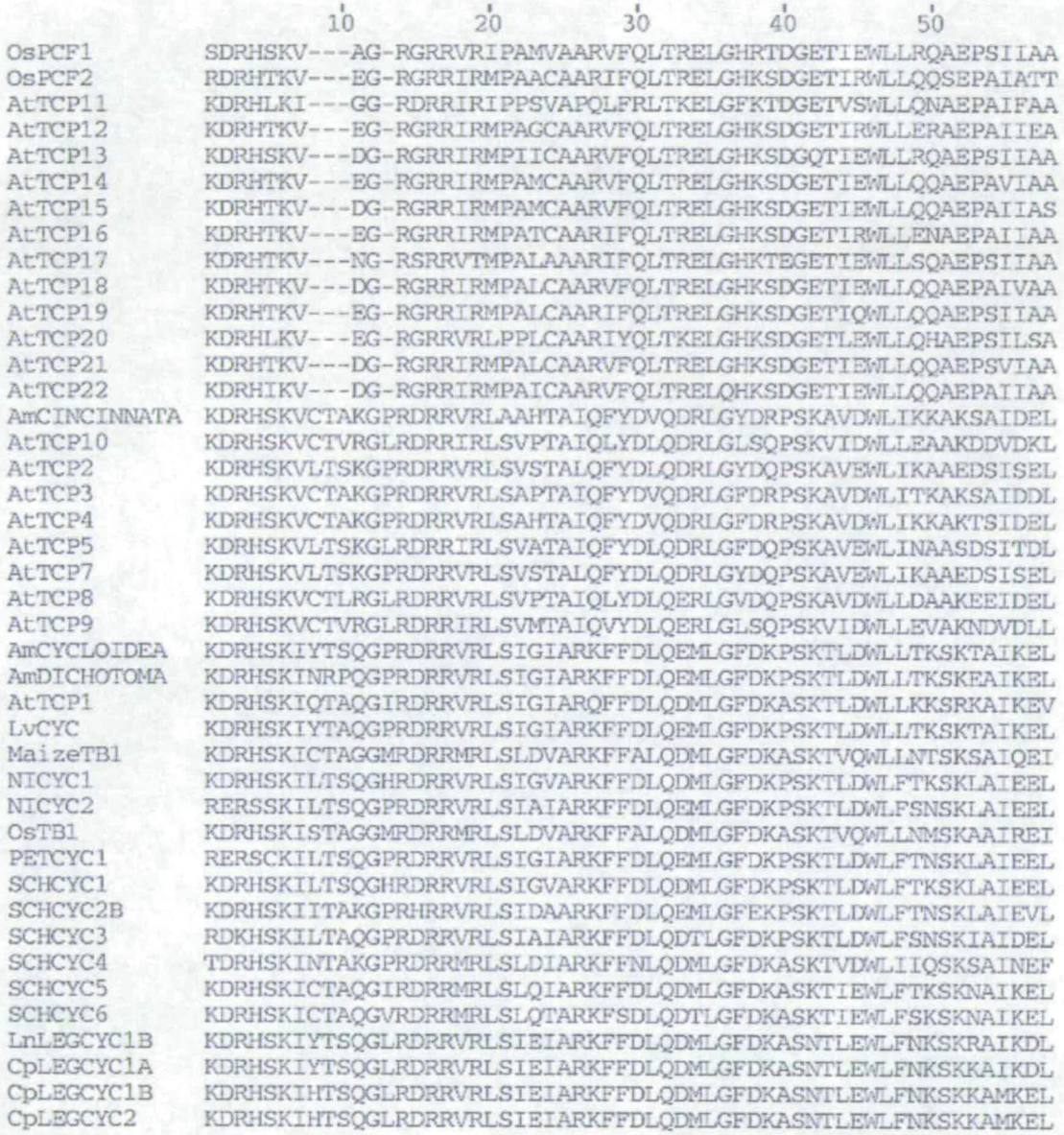

Appendix IV.37: Protein matrix M1

At: *Arabidopsis thaliana*; Os: rice; CLEGCYC: *Cadia CYC*-like gene (legume); LLEGCYC: *Lupinus CYC*-like gene (legume); NICYC: tobacco *CYC*-like gene; *PETCYC*: petunia *CYC*-like gene; *SCHCYC*: *Schizanthus wisotonensis CYC*-like gene; Lv: *Linaria vulgaris*; *Am: Antirrhinum majus.*

```
                  10        20        30        40        50
CYCLOIDEA         KDRHSKIYTSQGPRDRRVRLSIGIARKFFDLQEMLGFDKPSKTLDWLLTKSKTAIKEL
DICHOTOMA         KDRHSKINRPQGPRDRRVRLSIGIARKFFDLQEMLGFDKPSKTLDWLLTKSKEAIKEL
AtTCP1            KDRHSKIQTAQGIRDRRVRLSIGIARQFFDLQDMLGFDKASKTLDWLLKKSRKAIKEV
LvCYC             KDRHSKIYTAQGPRDRRVRLSIGIARKFFDLQEMLGFDKPSKTLDWLLTKSKTAIKEL
MaizeTB1          KDRHSKICTAGGMRDRRMRLSLDVARKFFALQDMLGFDKASKTVQWLLNTSKSAIQEI
NICYC1            KDRHSKILTSQGHRDRRVRLSIGVARKFFDLQDMLGFDKPSKTLDWLFTKSKLAIEEL
NICYC2            RERSSKILTSQGPRDRRVRLSIAIARKFFDLQEMLGFDKPSKTLDWLFSNSKLAIEEL
OsTB1             KDRHSKISTAGGMRDRRMRLSLDVARKFFALQDMLGFDKASKTVQWLLNMSKAAIREI
PETCYC1           RERSCKILTSQGPRDRRVRLSIGIARKFFDLQEMLGFDKPSKTLDWLFTNSKLAIEEL
SCHCYC1           KDRHSKILTSQGHRDRRVRLSIGVARKFFDLQDMLGFDKPSKTLDWLFTKSKLAIEEL
SCHCYC2B          KDRHSKIITAKGPRHRRVRLSIDAARKFFDLQEMLGFEKPSKTLDWLFTNSKLAIEVL
SCHCYC3           RDKHSKILTAQGPRDRRVRLSIAIARKFFDLQDTLGFDKPSKTLDWLFSNSKIAIDEL
SCHCYC4           TDRHSKINTAKGPRDRRMRLSLDIARKFFNLQDMLGFDKASKTVDWLIIQSKSAINEF
SCHCYC5           KDRHSKICTAQGIRDRRMRLSLQIARKFFDLQDMLGFDKASKTIEWLFTKSKNAIKEL
SCHCYC6           KDRHSKICTAQGVRDRRMRLSLQTARKFSDLQDTLGFDKASKTIEWLFSKSKNAIKEL
CpLEGCYC1A        KDRHSKIYTSQGLRDRRVRLSIEIARKFFDLQDMLGFDKASNTLEWLFNKSKKAIKDL
CpLEGCYC1B        KDRHSKIHTSQGLRDRRVRLSIEIARKFFDLQDMLGFDKASNTLEWLFNKSKKAMKEL
CpLEGCYC2         KDRHSKIHTSQGLRDRRVRLSIEIARKFFDLQDMLGFDKASNTLEWLFNKSKKAMKEL
LnLEGCYC1B        KDRHSKIYTSQGLRDRRVRLSIEIARKFFDLQDMLGFDKASNTLEWLFNKSKRAIKDL
```

Appendix IV.38: Protein matrix M2

At: *Arabidopsis thaliana*; Os: rice; CLEGCYC: *Cadia CYC*-like gene (legume); LLEGCYC: *Lupinus CYC*-like gene (legume); NICYC: tobacco *CYC*-like gene; *PETCYC*: petunia *CYC*-like gene; *SCHCYC*: *Schizanthus wisotonensis CYC*-like gene; Lv: *Linaria vulgaris*; *CYC*: *CYCLOIDEA* (*A. majus*); *DICH*: *DICHOTOMA* (*A. majus*).

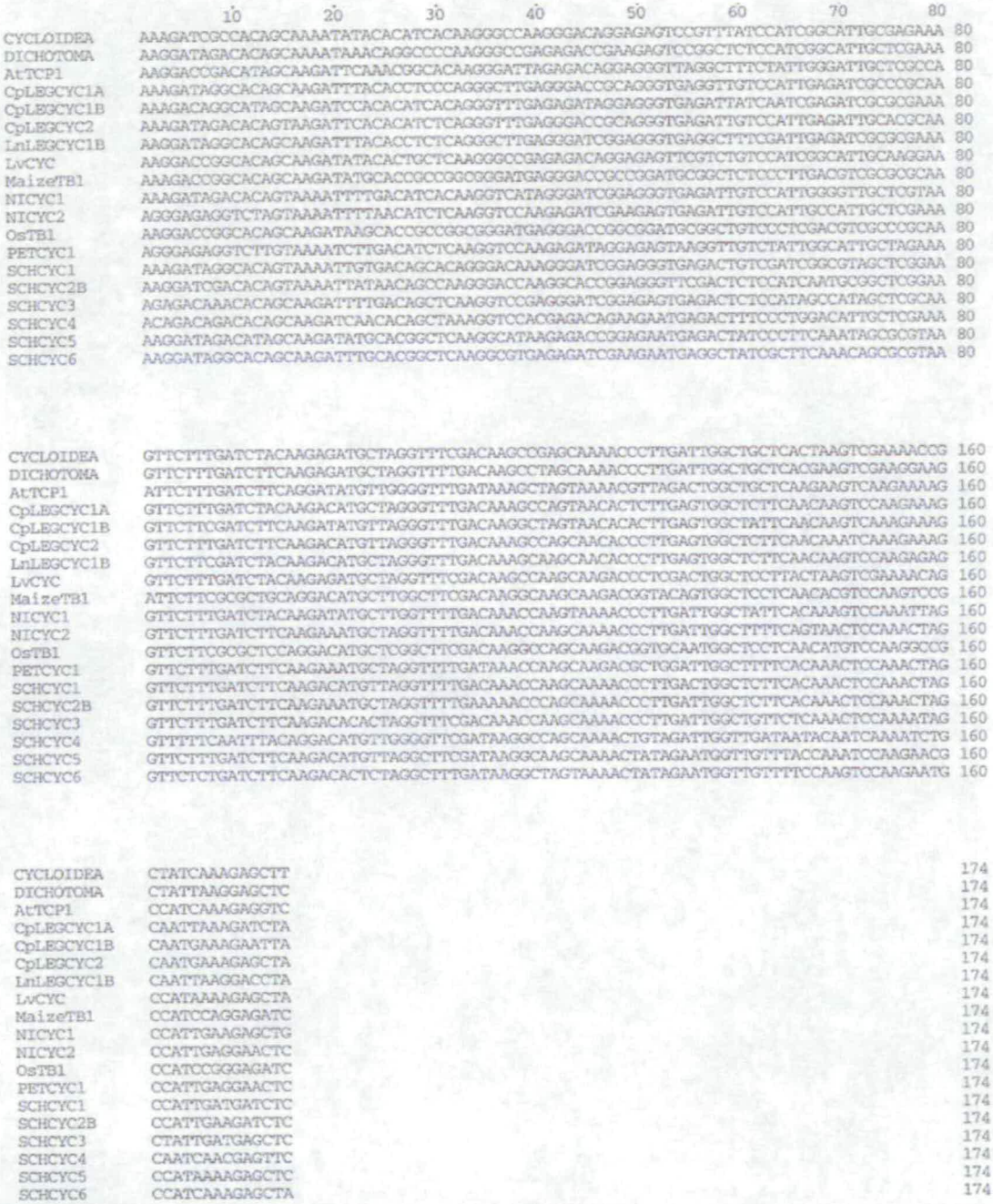

Appendix IV.39: Nucleotide matrix M3

At: *Arabidopsis thaliana*; Os: rice; CLEGCYC: *Cadia CYC*-like gene (legume); LLEGCYC: *Lupinus CYC*-like gene (legume); NICYC: tobacco *CYC*-like gene; *PETCYC*: petunia *CYC*-like gene; *SCHCYC*: *Schizanthus wisotonensis CYC*-like gene; Lv: *Linaria vulgaris*; *CYC*: *CYCLOIDEA* (*A. majus*); *DICH*: *DICHOTOMA* (*A. majus*).

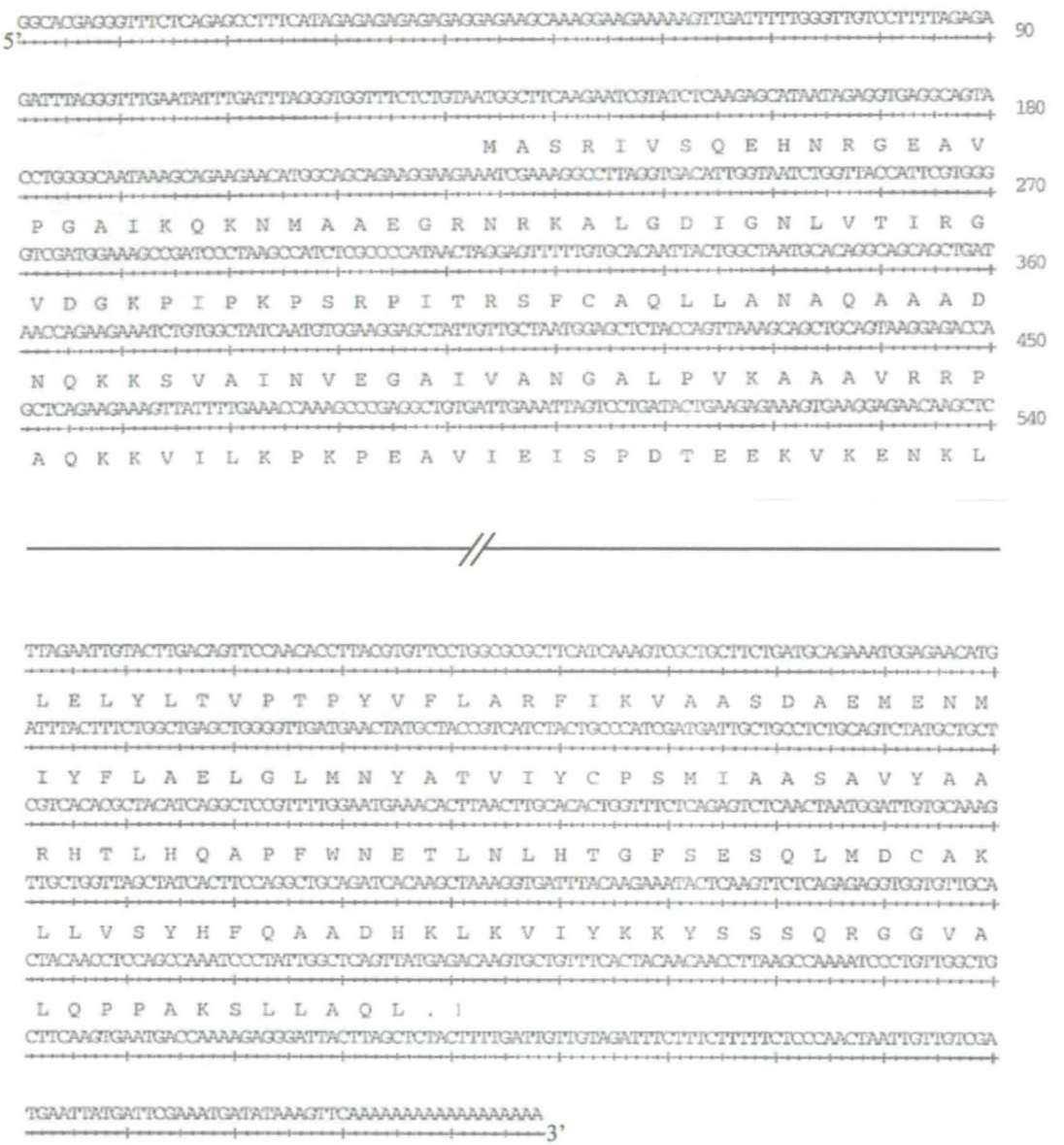

Appendix V.1: Partial cDNA of *SwCYCLINB1*

The predicted protein sequence is shown under the nucleotide sequence. The sequence of the 5' end and the 3' end of the *SwCYCLINB1* cDNA did not overlap which indicates that the sequencing was unable to recover the middle region of the cDNA (here indicated as a black line).

Appendix V.2: Partial cDNA sequence of *SwLFY1*

The predicted protein sequence is indicated under the nucleotide sequence. The red arrows indicate the position of the forward and reverse primers. The red triangles indicate the position of putative introns as deducted by a comparison with *ALF*, the *LEAFY*-like gene in *Petunia*.